June 2024

The Asymmetric Total Synthesis of Membranolide and Efforts Towards the Oxeatamides

Sean Bradley
University of South Florida

The Asymmetric Total Synthesis of Membranolide and Efforts Towards the Oxeatamides

by

Sean Bradley

A dissertation submitted in partial fulfilment
of the requirements for the degree of
Doctor of Philosophy
Department of Chemistry
College of Arts and Sciences
University of South Florida

Major Professor: James W. Leahy, Ph.D.
Bill Baker, Ph.D.
Kirpal Bisht, Ph.D.
Danielle Gulick, Ph.D.

Date of Approval:
June 20, 2024

Keywords: Total synthesis, MRSA, biofilms, natural products, drug discovery.

Dedication

To my mom, Elizabeth Stewart-Bradley

Acknowledgments

I can't believe that this chapter of my life is officially coming to an end. Over the past six years, I have undoubtedly experienced the highest of highs, as well as the lowest of lows. There have been so many people with me along this journey that have helped shape me into the chemist, but most importantly the person that I am today. I first want to say thank you to my PI, Dr. Leahy, for everything that he has done for me since I started working in his lab. Whether it's talking about synthetic strategy, or talking about football scores on a Monday morning, it's always a positive and welcoming environment when Dr. Leahy is around. I am appreciative for the support he has given me over the past six years, and I look forward to having him as a lifelong mentor. I would also like to thank my committee members: Dr. Baker, Dr. Turos, Dr. Gulick and Dr. Bisht. You all have helped me grow into the chemist that I am by challenging me during committee meetings and partaking in thoughtful discussions. Thank you all!

Next, I would like to thank all the lab mates that I have been fortunate to work with during my time at USF. Linda, Andrea, Elena, Jeanine, Grant, Jamie, Aaron, Robbie, Cameron, Angie, Gabriella, Kunjan, Maegan, and Meet – I enjoyed all the discussions we've had, both chemistry-related, or whatever else we may be talking about. Having to spend so much time together, I'm grateful to be surrounded by others that have an enthusiasm for chemistry and are overall genuine people. I would like to thank Brian Knight, who has spent countless hours sharing his expertise of organometallic chemistry with me and always partaking in insightful conversations. I would also like to thank Zac Shultz, who has been one of my main chemistry mentors since my first day in the Leahy lab. I appreciate your willingness to always be eager to talk about our current work,

while enjoying some local IPA's. Finally, I would like to thank Greg, Josh, Osama, Nichole and John; it was a pleasure to mentor you all in the lab. You were all so helpful and I hope you were able to learn as much as possible and gain a deeper appreciation for organic chemistry.

I would also like to thank Dr. Laurent Calcul and the entire CPAS facility for always keeping instruments functioning, allowing me to succeed as an organic chemist. I'm also very grateful for the education that Laurent, as well as his TA's, have given me on the basics of LCMS, GCMS, HRMS, HPLC, etc. Also, I would like to thank the NMR facility and the dedicated TA's who are always around to help and ensure that we get reliable data. Lastly, I would like to thank the X-ray facility for assisting us with some of our crystalline compounds.

Next, I would like to thank my friends and extended family, who are so important to me and always look out for me. Rob and Sharon, I have enjoyed our friendship, love of SCUBA diving and Eagles fandom for the past six years. I look forward to many more memories, both in Chicago and in Florida. Sara, Lizzie and the Patel family, you have brought me in and treated me like family since the first day I met all of you. I can't wait to continue eating great food, drinking bourbon and singing karaoke while watching someone fall into the koi pond soon. Pete, Omi and the southside Karlovics crew, you all have been so welcoming, and I can't wait to spend many more holidays with you all and make more memories once Steph and I move to Chicago. Although I don't understand all the SpongeBob jokes, you all still tolerate my casual fandom and treat me like family. There are too many people to individually name, but I wouldn't be who I am today without the love and support of friends and family.

I would also like to thank the Karchers, Wuillermans and Aunt Ruth for always being great people and caring family members. We have all experienced so much together and I appreciate the

love and support that you all show daily for one another. I cherish all the holidays we spent together and the future memories that we will share.

Steph, I don't know where I would be without you. You are my rock. You have been there with me for my best memories, as well as the darkest times in my life. I admire how hard you work and the care you give to your students. I wouldn't have been able to make it through graduate school without you. You always cheer me on and help me through my problems; we are a team and I hope you know that I would do the same for you. Your students call you "Ms. K", but I'm going to start calling you "Dr. K", because you deserve this PhD just as much as I do. I look forward to cheering you on in your career and being your number 1 fan if you choose to pursue graduate school for education. Now that our Florida chapter is closing and our Chicago chapter is almost here, the best is yet to come and I'm excited to continue making lifelong memories with you.

Dad, you have always been a family man and actively make decisions that are best for everyone. You and mom made it possible for me to go to Eckerd and have always been my biggest supporters. I cherish our weekly phone calls, catching up on whatever has happened the past week. You've gone through so much over the past few years, but you continue to always push forward and have a positive outlook. Your hard work doesn't go unnoticed and us boys are all proud of everything that you've overcome. I'm looking forward to you visiting Chicago and continuing to make more memories with you and Corey.

Bob, you're the hardest working person I know. Your work hours are relentless, yet you still enjoy long phone calls with everyone and help everyone in the family. I cherish our sports talks, beer reviews and hearing about your time in Austin. You deserve more from your work, and I know you'll get that soon. Your passion is something that is going to take you so far in life;

continue to believe in yourself and big things will happen. You and Cecelia have always been so supportive, and I love to keep up to date with all the adventures you two go on. I'm still looking forward to visiting Austin and trying all your favorite brisket recommendations.

Corey, I admire how disciplined you are and how passionate you are about the things that you love. You always put family first and always make decisions that will set you up for success. You were forced to grow up so quickly and your maturity really shows. Just know that Bob, Dad and I will always be there for you, and we can't wait to see you continue to accomplish great things. It's been 10 years since we lived in the same house, but I'm so happy that you decided to go to Elmhurst; we have tons of memories to continue to make in this new chapter for both of us. I will make up all the wrestling matches I've missed over the past six years and hope to be an honorary member of the Elmhurst wrestling team.

Mom, I don't even know where to begin. I'm still figuring out how to navigate life without you. I'll always cherish our love for animals, as well as for delicious food. You always put others before yourself, whether it was opening our home to members of the community in need, or mentoring employees that were destined for a career in pet care or grooming. I didn't always appreciate it, but every single decision you ever made was to benefit Bobby, Corey and me. You were so selfless and so hard-working. I am incredibly grateful that you always believed in me and pushed me with regards to education. I never understood why you were so hard on me, starting from kindergarten, all the way through graduate school, but your actions helped to shape me into the scientist and student that I am today. It meant the world to me when I recently found one of my AP Biology lab reports from the 11th grade on your living room table; I don't know if you were reading it but knowing that you had it within an arm's reach meant the world to me. Even though you can't be with us for my dissertation defense in a few weeks, I hope to continue to make you

proud. I hope to someday come close to being the person that you were. All my best qualities come directly from you, and that is something that I will hold onto and cherish forever.

Table of Contents

List of Figures

Abstract

Total synthesis is a discipline within organic chemistry that is a constant force that propels the field forward. In our lab, we have immersed ourselves within the field of total synthesis to gain access to complex natural products, perform SAR studies, as well as highlight interesting methodology. Within these endeavors, we have completed the first asymmetric total synthesis of membranolide. This has allowed us to synthesize potential biofilm eradication agents in our efforts to combat multi-drug resistant ESKAPE pathogens. We have also begun to pursue the first asymmetric total synthesis of the oxeatamides. By utilizing our previous methods, we plan to evaluate the oxeatamides as potential biofilm eradication agents, as well as confirm their structural assignments.

Chapter 1: The Art of Total Synthesis

1.1 Introduction

The field of organic chemistry is constantly progressing and crucial to many other areas of chemistry. Synthetic organic chemistry allows access to simple molecules, as well as exceedingly complex molecules through strategic planning and execution. The versatility of chemical synthesis is paramount, leading to development of new bioactive molecules, novel materials and polymers, dyes, and catalysts.[1] The continued exploration of chemical synthesis has led to many advancements within the field of chemistry, as well as the entire scientific community.

Total synthesis, a topic within the field of synthetic organic chemistry, is the complete and comprehensive synthesis of a complex molecule, which is typically a natural product. There are many reasons why research groups perform a total synthesis. One reason is that it can enable access to a complex scaffold that is otherwise difficult to achieve. Many biologically relevant natural products can't be isolated on a scale that can be utilized medicinally, so synthesis may allow access to appreciable amounts of a desired molecule. Total synthesis often allows for screening of complex molecules for drug discovery purposes; the use of synthesis may also allow rapid analog development of these scaffolds, expediting SAR studies.

Another common application of total synthesis is the development of synthetic methods. When labs develop a new synthetic method, it is common to utilize that method towards the synthesis of a natural product. Since these total synthesis targets are typically quite complex, the utilization of a given method towards the synthesis of a natural product may show how robust and

versatile the method is, especially in the presence of other functionality. In addition to this, some groups may already be pursuing a total synthesis for any given reason but can't gain access to an advanced scaffold. The appearance of a challenge like this may catalyze the development of new synthetic methods, giving access to complex scaffolds. Whether the method is originally implemented into a total synthesis, or later designed to achieve a total synthesis, total synthesis is a constant driver in the development of novel synthetic methodology.

It's impossible to merely emphasize the importance of total synthesis through a brief discussion. To follow is a discussion of the history of total synthesis, which highlights landmark achievements, justification and necessity of total synthesis and current advances to the field of synthetic organic chemistry, due to total synthesis efforts.

1.2 History

1.2.1 The Early Days

The first example of total synthesis was demonstrated in the Wöhler laboratory in 1828.[2] Wöhler's successful synthesis of urea from ammonium cyanate showed that the saying "the business of nature and nature's alone" wasn't accurate, therefore sparking the era of natural product total synthesis. This accomplishment had directly impacted the course of scientific discovery and helped to shape the current field of total synthesis, as well as synthetic organic chemistry.

In the early days of total synthesis, the main purpose was for structural confirmation and configuration of natural products.[3] In the mid-19th century through the early parts of the 20th century, the analytical methods required for thorough characterization of complex molecules weren't very advanced, so structural determination could be difficult. Many structural confirmations came by way of degradation studies and partial synthesis; however, a landmark use

of total synthesis for structural elucidation was demonstrated by Komppa' synthesis of camphoric acid, which aided in the elucidation of the of camphor's ring structure in 1903 (**Figure 1**).[4] Shortly after, Perkin also completed a synthesis of camphor.[4] With modern X-ray techniques, as well as mass spectrometry and NMR spectroscopy, characterization of natural products is much simpler. Because of this, modern total synthesis isn't quite used for structural elucidation and confirmation as it used to be but can be a helpful tool for stereochemical and regiochemical confirmation.

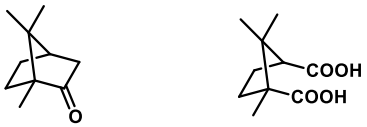

Camphor Camphoric acid

Figure 1.1: Structures of Camphor and Camphoric Acid

Many years after the total synthesis camphor, synthetic and analytical techniques improved to allow for the synthesis of much more complex molecules. The "Stone Age" of organic synthesis ended around 1930,[2] dawning upon a new age of achievements. Around this time, Eschenmoser stated that "natural product synthesis was freed from the chains to be structure-proof and could develop to a creative field of chemistry in its own right," which was the start of total synthesis being used for other purposes.[2]

1.2.2 A New Era

In 1944, Woodward completed his historic total synthesis of quinine.[5] Quinine is a natural product isolated from the bark of a cinchona tree, which had been used to treat malaria and babesiosis. Previous partial syntheses by Rabe[6] and Prelog[7] have been reported in 1918 and 1943, respectively. These syntheses involved the degradation of quinine to quinotoxine, followed by the subsequent synthesis of quinine. Woodward's synthesis (**Scheme 1.1**)[5] starts off with commercially available **1** to which was converted to **2** in a handful of steps. The conversion from **2** to **3**, which

was the crucial part of Woodward's synthesis, was performed by a clever ring cleavage carried out by ethyl nitrate. The resulting oxime was reduced, followed by elimination to eventually lead to **3**. Next, a Claisen Condensation was utilized, followed by decarboxylation, which led to quinotoxine **5**, which was easily converted into quinine **6**. The work that Woodward had demonstrated was well before its time and demonstrated fantastic synthetic utility. More recently, quinine has been synthesized by Stork[8] and Williams[9] in 2001 and 2008, respectively. Their pursuits were for different reasons than Woodward's but goes to show the synthetic novelty that can be achieved through a synthesis of quinine, as well as the precedent that Woodward has established in the field of total synthesis. In addition to quinine, Woodward has also accomplished the feats of synthesizing cephalosporin C, vitamin B_{12}, and erythromycin A, among many others.

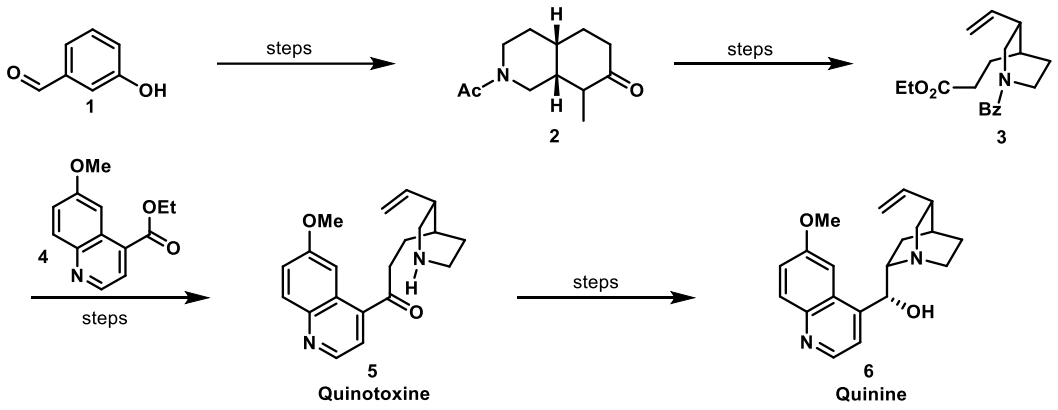

Scheme 1.1: Woodward's Synthesis of Quinine

Another monumental synthesis around this time was Corey's synthesis of longifolene in 1961.[10] Longifolene is a natural product isolated from pine resins[11] and has been a synthetic goal for many, due to its obscure ring structure and lack of heteroatoms. Prior to Corey's synthesis, previous degradation studies had been performed to confirm its structure. Unfortunately, there had been some debate about the structure of longifolene, and Corey stated that "…at present, the chemical facts alone do not constitute proof of structure," so Corey decided to settle the debate

and synthesize longifolene. Corey's synthesis started with Wieland-Miescher Ketone **7**, which underwent a ketal protection, olefination, then oxidation to yield **8**. Next, this was utilized to perform a ring expansion, leading to **9**. At this point, the ketal was deprotected and the double bond on the 7-membered ring isomerized to form an α,β-unsaturated ketone. This new intermediate was reactive, causing a carbon-carbon bond to form between the α-carbon of the 6-membered ring and the β-carbon of the 7-membered ring through a conjugate addition, forming tricyclic compound **10**. Finally, after a chemo selective manipulation of the more reactive ketone and an olefination of the remaining ketone, Corey arrived at **11**.[10] Along with this elegant synthetic achievement, Corey was also able to confirm the correct structure of longifolene. Due to the synthetic desire to many, longifolene has also been synthesized by McMurry,[12] Oppolzer[13] and others.

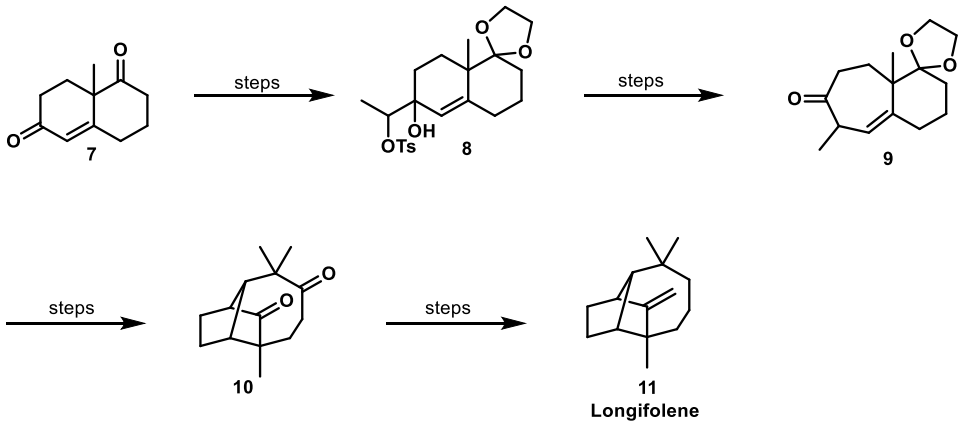

Scheme 1.2: Corey's Synthesis of Longifolene

In addition to these two natural products, there were strenuous efforts to synthesize other complex natural products to further demonstrate synthetic utility and to gain access to these intricate scaffolds. Some other popular synthetic targets during this time were strychnine, monensin, amphotericin B and many others. The chemists that pursued these challenges were truly pioneers in the art of total synthesis and paved the way for future endeavors, setting high expectations for generations to come.

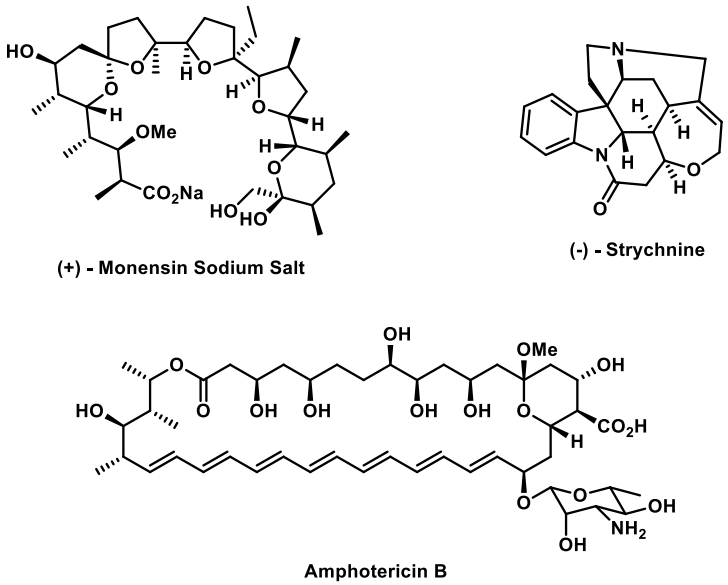

Figure 1.2: Structures of Selected Total Synthesis Targets

1.2.3 Modern Total Syntheses

The bar has been set high for complex total synthesis endeavors. The previously described syntheses helped to lay the groundwork for the next generation of synthetic efforts and achievements. Now, with even more tools and established methodologies, the sky is the limit for accessing complex scaffolds and highly sought after natural products.

Due to the increase in synthetic techniques and newer synthetic strategies, complex scaffolds that took an extensive number of steps in the past have proven to be much more accessible. In 1979, Kishi successfully synthesis austamide over 29 steps, which was a fantastic feat and a monumental synthesis.[14] A few decades later, Baran and Corey took on the challenge of synthesizing austamide, but with a C-H functionalization strategy.[15] Corey utilized (S)-tryptophan **12** and performed a reductive amination, followed by amidation to synthesize **13**. Next, **13** underwent a Pd-catalyzed C-H functionalization to selective activate C-2 of the indole, allowing for the formation of the core 8-membered ring, forming **14**. This key step gave rapid access to this

complex scaffold, ultimately allowing for this synthesis to proceed so quickly. Next, **14** underwent removal of the Fmoc protecting group, causing a ring closure to synthesize **15.** Finally, **15** underwent an oxidation, followed by elimination to yield (+)-austamide in only 5 steps (**Scheme 1.3**). Corey demonstrated that the development of novel methods aimed at complex scaffolds can gain rapid access to natural products, like **16**, but can further be extrapolated to an array of other structurally complex molecules.

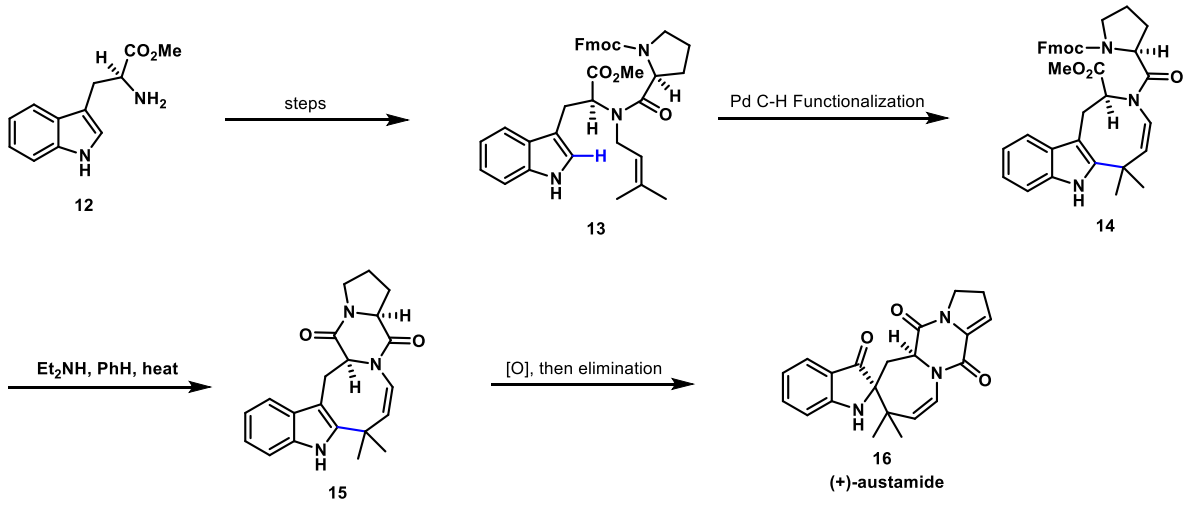

Scheme 1.3: Corey's Synthesis of (+)-Austamide

Later on, an elegant synthesis that demonstrates the power of strategic C-O bond construction was demonstrated by Reisman's 2016 synthesis of (+)-ryanodol.[16] Reisman's synthesis begins with commercially available (S)-pulegone **17**, which undergoes treatment with the Davis reagent to perform multiple oxidations in a single synthetic step. Next, the alcohols that were just formed undergo a protection as benzyloxymethyl ethers, followed by strategic grignard additions to form **18**. With **18** in hand, the next goal was to perform an intramolecular Pauson-Khand reaction. With optimization, Reisman was able to greatly enhance the diastereoselectivity and overall yield of this reaction, gaining rapid access to **19**. Next, SeO_2 was utilized to perform

three crafty site-selective oxidations, converting **19** to **20.** Finally, **20** was converted into (+)-ryanodol **21** over an additional six steps, which included a Stille coupling, a stereoselective reduction and a reductive cyclization, leading to (+)-ryanodol in a mere 15 steps (**Scheme 1.4**). This synthesis continues to pioneer and foster a new approach to total synthesis, with an emphasis on multiple conversions in a single synthetic step and strategic bond construction.

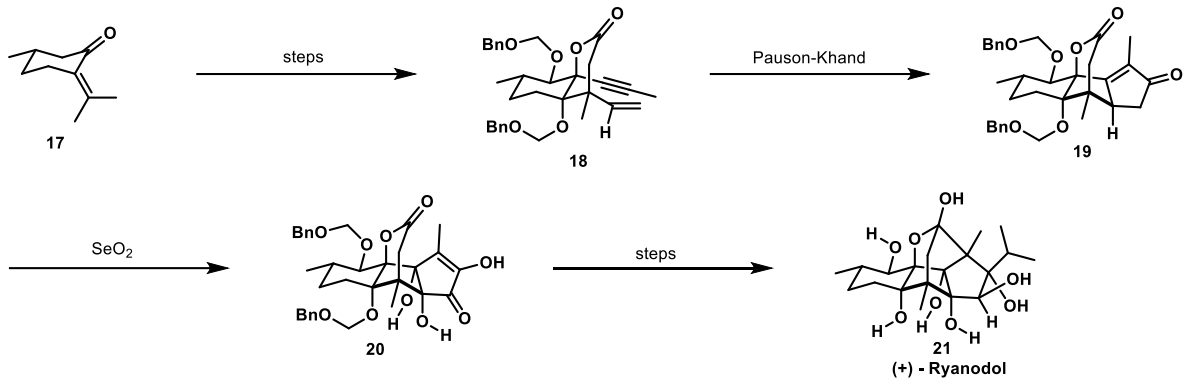

Scheme 1.4: Reisman's Synthesis of (+)-Ryanodol

These are just a few of the distinguished total synthesis efforts from recent history. In addition to these, there are other synthetic targets, like taxol and tetrodotoxin (**Figure 1.3**), which are significant due to their bioactivities, but also due to their structural complexity and the synthetic novelty that comes through pursuing a synthesis of them. It's apparent that total synthesis is a key driver in the development of novel synthetic methods, which can be used for an array of synthetic fields. The evolution of the field of total synthesis is fascinating, from the early days of synthesizing camphor, all the way to where we currently are; the best is yet to come and many synthetic chemists are contributing to this new wave of total synthesis.

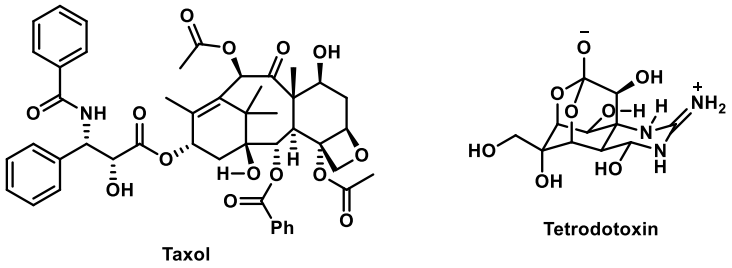

Figure 1.3: Structures of Taxol and Tetrodotoxin

1.3 One Final Thought

Finally, and perhaps the most overlooked purpose of total synthesis, is its ability to train synthetic chemists. As stated above, total synthesis can aid in structure confirmation/elucidation, method development and gaining access to biologically active compounds, but the tangible and intangible skills that total synthesis researchers gain may be of the highest significance. The well-rounded knowledge and skillset needed for total synthesis efforts results in the development of skilled and versatile chemists, as well as overall scientists.

Due to the nature of total synthesis and the complexity of synthetic targets, the synthetic planning required for these endeavors are very meticulous. This forces chemists to adopt a more holistic approach, accounting for clashing functionality that may be encountered along the route. Also, these synthetic plans don't typically work out as planned initially, so this forces chemists to truly dissect these reactions and think critically about the transformations occurring. The exposure to many different transformations and functionality allows synthetic chemists to continue adding tools to their toolbox and continue their development as a scientist.

Because of the broad and well-rounded skillset of total synthesis chemists, they are typically highly sought after in the industrial setting. The skillset and mindset of a chemist with total synthesis work can commonly crossover well to other disciplines, like translational chemistry

or method development. Although total synthesis efforts can be rather lengthy and arduous, the skills and experiences gained throughout these processes are unparalleled.

Chapter 2: The Asymmetric Total Synthesis of Membranolide

2.1 Antibiotics: A Brief History

The discovery and advancements of antibiotics has drastically enhanced the lifespan of humans and overall quality of life. Antibiotics function through their specificity to certain pathogens, as well as their lethality. The term antibiotic is derived from the word "antibiose," which describes the contrast of symbiosis, therefore describing their ability to negatively impact pathogens.[17] Later, the term antibiotic was used to describe secondary metabolites that were isolated from bacteria and fungi.[17] These secondary metabolites could act in ways that were bacteriostatic, which would interfere with a cellular process that prevented bacterial growth.[17] They could also be defined as bactericidal, which would interfere with a crucial pathway that is needed for the longevity of certain bacteria.[17] As time went on, the term antibiotic became more broad and described molecules that were active against bacteria and fungi, but also included synthetic molecules.[17]

In 1893, Italian physician and microbiologist Bartolomeo Gosio isolated a small molecule called mycophenolic acid from *Penicillium glaucum* **(Figure 2.1).**[17] This was the first example of an antibiotic that was discovered from nature, showing activity that inhibited the growth of *Bacillus anthracis*.[17] To date, mycophenolic acid has shown antitumor, antiviral and antifungal activity.[17] In the US, a mycophenolic acid analog is currently an FDA approved drug that is used to prevent organ transplant rejection.

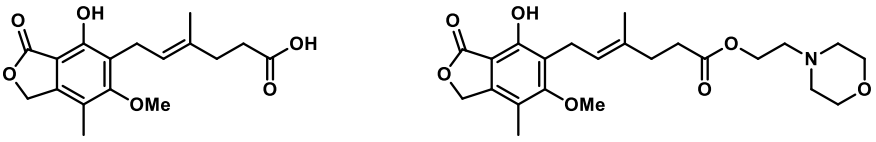

Figure 2.1: Structures of Mycophenolic Acid and FDA Approved Mycophenolate Mofetil

Roughly 20 years after the discovery of mycophenolic acid, Alfred Bertheim synthesized arsphenamine, being the first known synthetic antibiotic.[17] Interestingly, the structure of arsphenamine wasn't elucidated until roughly 2005, which was performed by Ronimus through extensive mass spectrometry analysis.[18] Shortly after Bertheim's synthesis of arsphenamine, it was quickly discovered that this molecule was particularly active in irradicating syphilis infections.[17] For the following 40 years arsphenamine, also known as Salvarsan, was the market standard for the treatment of syphilis, but began to be further derivatized to lessen side effects and improve the overall quality of the drug.[17] The story of Salvarsan's discovery and the idea of a "magic bullet"[17] has shown to be crucial for modern drug discovery.

A more well-known story is the discovery of penicillin. In 1928, Alexander Fleming returned to his lab and found a sample of *Staphylococcus aureus* had been contaminated with the fungus *Penicillium notatum*. Instead of discarding the sample, Fleming noticed that the bacteria that were close to the fungus were killed, but the bacteria that weren't in the nearby vicinity remained unaffected.[17] Based on this observation, Fleming grew a pure culture of the fungus and was able to observe its bioactivity against *Staphylococci*, as well as other Gram-positive bacteria.[17] In 1929, Fleming named the active compound from the fungus penicillin (**Figure 2.2**).[17] Over a decade later, there was a major push to obtain large amounts of penicillin to treat infection during World War 2.[17] In 1957, Sheehan completed the first total synthesis of penicillin V, achieving this feat in five linear steps.[19] Although this wasn't an efficient way to produce penicillin for industrial

use, it certainly provided an avenue for antibiotic analog development. The impact that penicillin has had on humanity is astonishing and paved the way for new classes of antibiotics.

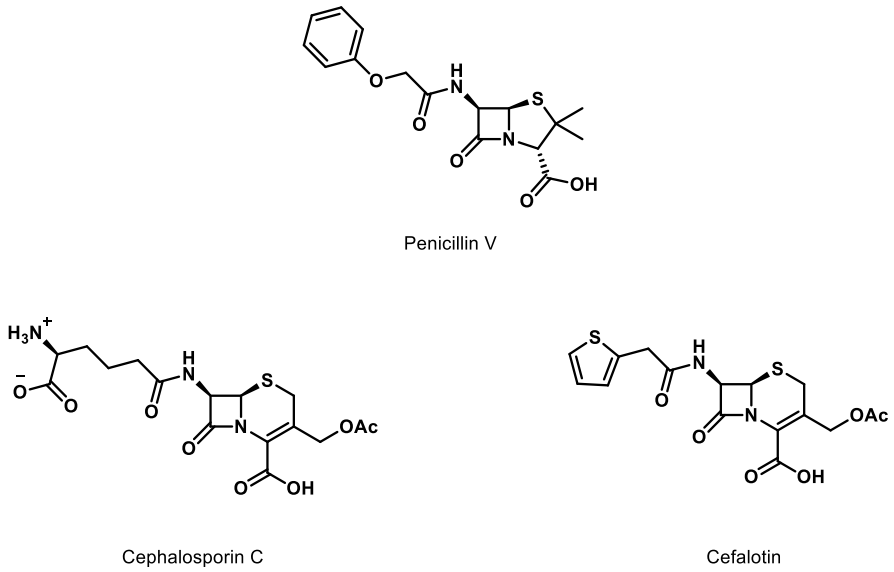

Figure 2.2: Structures of Penicillin V and Selected Cephalosporins

Following the discovery of penicillin, a class of antibiotics called the cephalosporins was discovered (**Figure 2.2**). Cephalosporin C, initially discovered in 1945, functions through the same mode of action as penicillin.[17] Cephalosporin C's structure was elucidated in 1961 through a series of crystallography experiments and degradation studies,[20,21] then was first synthesized by Woodward in 1965.[22] Cephalosporin C was never an approved drug, but it inspired the synthesis of many analogs, including cefalotin, which is a broad-spectrum antibiotic.[23]

Another exceedingly valuable class of antibiotics is the sulfonamides. The story of the sulfonamides began in 1932 when a group of scientists at Bayer synthesized sulfamidochrysoidin, now known as Prontosil, while attempting to synthesize dyes.[17] Shortly after discovering its bioactivity, sulfonamide drugs were commonly used during World War II to prevent infection of wounded soldiers.[17] Sulfonamide drugs (**Figure 2.3**) function as broad spectrum antibiotics and are bacteriostatic through the inhibition of folic acid biosynthesis.[24]

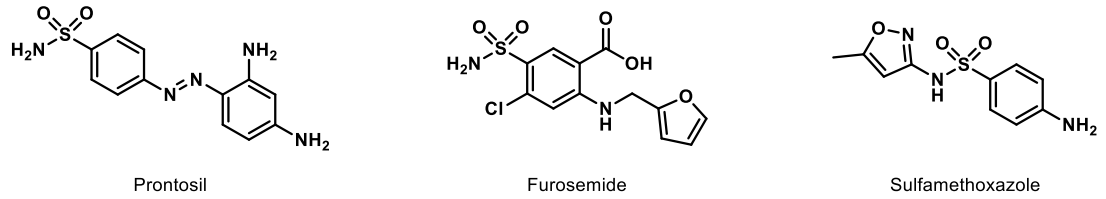

Figure 2.3: Selected Sulfonamide Structures

The discovery of these antibiotics paved the way towards our current treatments and further development of antibiotics. Currently, we have an immense library of accessible antibiotics that can be used for both mild and severe infections.[17] Some of these common antibiotics include ciprofloxacin, tigecycline and amoxicillin (**Figure 2.4**). As a last line of defense, we can also utilize antibiotics like vancomycin, linezolid and colistin.[17] The race to develop safer and more effective antibiotics is a strenuous one with continuous obstacles along the way.

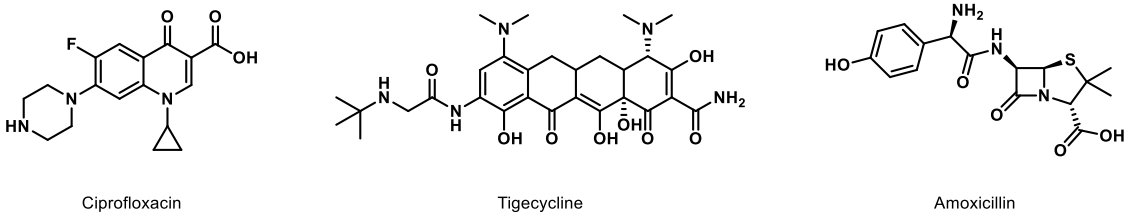

Figure 2.4: Commonly Utilized Antibacterial Drugs

2.2 Antibiotic Resistance

As we develop new antibiotics, bacteria also develop mechanisms of resistance to these therapeutics, which is an ongoing and never-ending battle. Long before the discovery and use of antibiotics, bacteria were at war with each other, essentially developing resistance mechanisms to enhance their own survival.[25] This is called primary resistance, which also can explain why there are both Gram-positive and Gram-negative bacteria; bacterial resistance to our modern antibiotics started long before antibiotics were utilized by humans.[25] Secondary resistance, which is typically what we're referring to when talking about bacterial resistance, is the ability of bacteria to gain the means to no longer be susceptible to an antibiotic treatment that was once effective.[17] These

resistance mechanisms can occur in many ways, making the task to overcome these mechanisms rather arduous.

One common resistance mechanism is drug inactivation.[26] This occurs when a drug that was once effective becomes modified by the bacteria, therefore making it ineffective. A common example of this is shown by the presence of β-lactamases. β-lactamases can selectively hydrolyze β-lactam containing-molecules, thus making drugs like penicillins, cephalosporins and any other structurally related therapeutics ineffective.[27] These β-lactamases are extremely common, so the use of β-lactam drugs has significantly decreased, but this has also inspired research into developing β-lactamase inhibitors.

Another common resistance mechanism employed by bacteria is the modification of drug binding sites. A common example of this is the mutation in a gene that encodes for Penicillin-Binding Proteins (PBPs), which is a protein that is needed for the cell wall assembly.[26] PBPs are common targets for β-lactam drugs, but the most common PBP in Methicillin-Resistant *Staphylococcus aureus* (MRSA) strains is PBP2a.[28] PBP2a has an extremely low affinity for all β-lactam drugs, which makes these therapies very ineffective, thus providing MRSA a crafty resistance mechanism.[26] Besides PBPs, there are many other modifications to drug binding sites that offer advantageous resistance.

In addition to this, efflux pumps are often associated with antibiotic resistance. Efflux pumps are active transporters that remove antibiotics from the cell, which helps to keep intracellular drug-accumulation low.[26] Due to this low concentration of a given antibiotic within the cells, it's extremely difficult to evoke the desired antibacterial activity. Efflux pumps are becoming exceedingly common in *Enterobacter aerogenes* and *K. pneumoniae* strains, contributing to multidrug resistance.[26]

2.3 Biofilms

A resistance mechanism that is becoming increasingly prominent is the formation of biofilms. Biofilms are complex communities of microbes, with the main biomass being the extracellular polymeric substance (EPS).[29] EPS is made up of lipids, proteins, polysaccharides, and extracellular DNA from the microbes within the biofilm.[29] There are three phases to biofilm formation (**Figure 2.5**).[30,31] The first phase is the attachment phase, which is when favorable environmental conditions cue planktonic bacteria to adhere to a surface.[30] Next is the growth phase, which is when the EPS is produced, and the full biofilm is formed. At this point, the bacteria within the biofilm are well protected from antibiotic treatment, immune responses, and other forces.[30] The final stage is the detachment phase. This can be performed through two pathways: active detachment and passive detachment. Active detachment occurs when environmental conditions are favorable; these bacteria can communicate through quorum sensing, thus initiating an enzymatic degradation of the biofilm. This can also be achieved by passive detachment, which is caused by some sort of outside force like human intervention or fluid shear.[30]

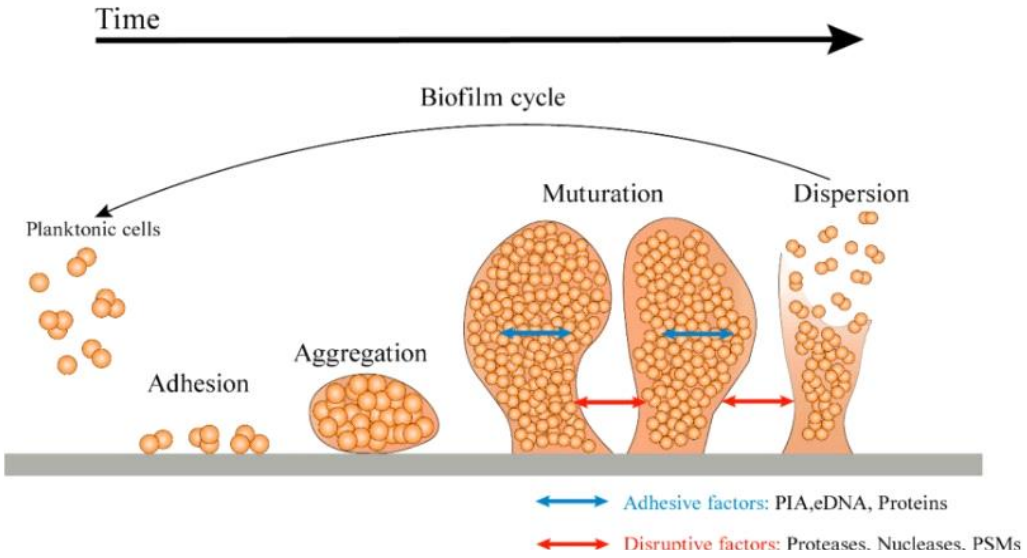

Figure 2.5: Phases in Biofilm Formation[31]

Biofilms essentially act as a biochemical shield, protecting the bacteria from environmental conditions and immune responses, thus providing a unique mechanism of antibiotic resistance.[26] These biofilms can form on biotic surfaces, causing infections that can lead to open wounds or lesions. Biofilms can also form on abiotic surfaces, most commonly observed on medical devices or in a medical setting.[26] There are many instances where pacemakers with biofilms on their surfaces are implanted into humans, unintentionally spreading these bacterially colonies.[26] Interestingly, cells that are deep within a biofilm can become metabolically inactive, making them very difficult to kill, even if the biofilm is eradicated.[32] These bacteria gain back their susceptibility to antibiotic intervention once they're no longer in a biofilm, but this makes it very difficult to eradicate the entire biofilm community.[32] Biofilms are an extremely common defense mechanism for bacteria that make our efforts to combat antibiotic resistance even harder.

To date, there are some efforts towards the development of therapeutics to combat biofilms. One of the major strategies is to develop biofilm inhibition agents. These agents are used to prevent the early stages of biofilm formation, but they can't eradicate biofilms once they're already formed.[33] This strategy is useful for surfaces that commonly observe biofilm formation, like on medical devices and hospital vents.[33] This can be done by imprinting 3D patterns on the surface, making it difficult for the bacteria to attach.[34] Another strategy is to treat the surface with molecules, like surfactants (Triton X-100 and Tween 80), which inhibit adherence of the bacteria.[33,35]

The other approach is to develop biofilm dispersal agents. These agents work by eradicating biofilms but would need to be used in tandem with an agent that can eradicate the bacteria. One example of this strategy is the use of anti-quorum sensing agents. Quorum sensing is crucial for the longevity of biofilms, so molecules like hordenine have been shown to be effective

in decreasing signaling within *P. aeruginosa* biofilms, which also decreased the biofilm production.[36] Both of these strategies provide potential therapies to help combat biofilms, but most antibacterial research is focused on planktonic bacteria, rather than biofilm communities, limiting the amount of discoveries to be made. To continue our efforts to combat biofilms, more research needs to be devoted to understanding how these complex communities' function, therefore providing answers on how to easily eradicate them.

2.4 ESKAPE and MRSA

ESKAPE is an acronym that describes a group of pathogens that exhibit multi-drug resistance: *Enterococcus faecium, Staphylococcus aureus, Klebsiella pneumoniae, Acinetobacter baumannii, Pseudomonas aeruginosa* and *Enterobacter*.[26] In addition to being multi-drug resistant, ESKAPE pathogens are the leading cause of nosocomial infections globally.[26] These ESKAPE pathogens make use of an array of resistance mechanisms, which were described above. Many of these instances of multi-drug resistance can be attributed to the overuse of antibiotics and substandard medical care.[37] ESKAPE pathogens are such a problem clinically that the World Health Organization (WHO) listed ESKAPE pathogens on a list of 12 bacteria in which new antibiotics are desperately needed for treatment.[38]

One of these ESKAPE pathogens, MRSA, is a significant cause of both hospital-acquired infections (HAI's) and community-acquired infections (CAI's).[39] Besides being very difficult to treat, MRSA can cause sepsis, cerebral abscesses, osteomyelitis and pneumonia, causing a large economic burden and potential mortality.[40] MRSA has been known to show resistance against β-lactam drugs due to its ability to generate and utilize β-lactamase enzymes.[41] Considered a less traditional resistance mechanism, MRSA is also able to exist within a biofilm community, substantially protecting it from its host's immune response, as well as antibiotic treatments.[39]

Because of these mechanisms, MRSA is an incredibly difficult infection to irradicate; the WHO and Centers for Disease Control (CDC) have marked MRSA as a grave and substantial danger on the virulent bacteria target list.[41]

2.5 Marine Natural Products

Marine Natural Products (MNPs) are a rich source of biologically relevant molecules that can be used to treat an array of diseases.[42] Marine habitats and ecosystems encompass roughly 75% of the earth's surface and are home to roughly 80% of the earth's animal and plant species, allowing for continued discovery of novel therapeutics.[43] Many MNPs are known for their bioactivity pertaining to anti-cancer, anti-inflammatory and antibacterial properties.[42, 44] As of 2017, more than roughly 27,000 marine natural products were known, with 8 of those being marketed drugs, mostly for cancer.[45] The continued exploration and discovery of MNPs could readily lead to the uncovering of many new bioactive compounds and potential therapeutics.

At the early stages of discovering marine natural products, SCUBA wasn't an available resource, so scientists relied on the studies of soft corals, sponges and red algae.[44] Overall, sponges have contributed to roughly 30% of all MNPs to date.[46] In the 1950s, the discovery of spongouridine and spongothymidine (**Figure 2.6**) demonstrated the initial significance and role that MNPs could have on human health.[46] Since then, sponges have contributed to MNP drug discovery by the isolation and utilization of natural products like clathric acid, which is active against MRSA and vancomycin-resistant *Staphylococcus aureus* (VRSA) and metachromin A, which is bioactive against Hepatitis B.[43] The field of MNP chemistry continues to grow and provide a starting point for many novel therapeutics that we utilize today.

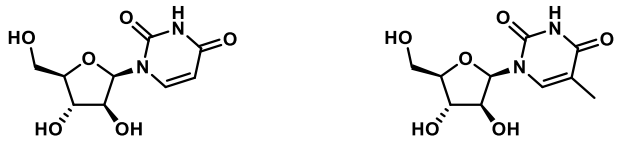

Spongouridine Spongothymidine

Figure 2.6: Structures of Spongouridine and Spongothymidine

Antarctica is home to diverse marine life and a rich source of bioactive MNPs. An exceedingly significant MNP that was discovered from the waters of Antarctica is palmerolide A, a polyketide MNP that was isolated from the tunicate *Synoicum adareanum* by the Baker group (**Figure 2.7**).[47] Palmerolide A contains a 20-membered macrocycle and is potent and selective against melanoma, likely through the inhibition of V-ATPase.[47] Many other natural products from the vicinity of Palmer Station have been discovered, further continuing the search for MNPs and scaffolds that can become successful therapeutics.

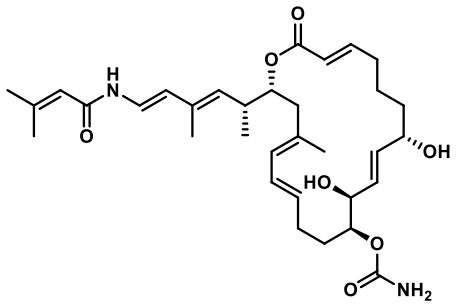

Figure 2.7: Structure of Palmerolide A

Another rich source of MNPs come from sponges, which are sessile invertebrates that can be found in tropical regions, as well as polar and temperate regions.[43] An intriguing cactus sponge also found in the vicinity of Palmer Station, *Dendrilla membranosa*, has been a rich source of MNPs. Many diterpene natural products (NPs) have been isolated from this cactus sponge (**Figure 2.8**), some of which have promising bioactivities. Another MNP of interest, darwinolide, showed promising activity against MRSA.[48] Interestingly, darwinolide displayed a 4-fold selectivity

against MRSA biofilms, compared to planktonic MRSA.[48] Another study found biofilm inhibitors that were more potent than darwinolide, but they didn't show an increased selectivity for biofilms over planktonic cells.[49] This provides an extremely fascinating platform for the development of an anti-biofilm agent. The ability to selectively target the biofilm allows for the possibility to overcome this resistance mechanism, causing the cells that were once within the biofilm to then become susceptible to standard treatment. This approach is more ideal than a therapy that eradicates both the biofilm and planktonic cells, as this would be a harsher approach that could cause an extreme immune response.

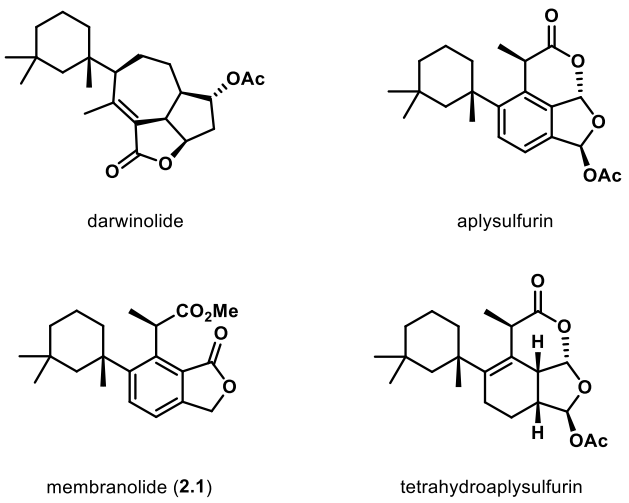

Figure 2.8: Selected Structures of MNPs Isolated from *Dendrilla membranosa*

Although darwinolide is a MNP with promising anti-biofilm properties, it's quite structurally complex and wouldn't necessarily result in a good drug candidate. The Baker and Shaw groups collaborated to conduct assays of "darwinolide cousins" to further evaluate these MNPs and related compounds as biofilm eradication agents. Each compound was tested against a multi-drug resistant MRSA strain at 3 different concentrations (**Figure 2.9**).[50]

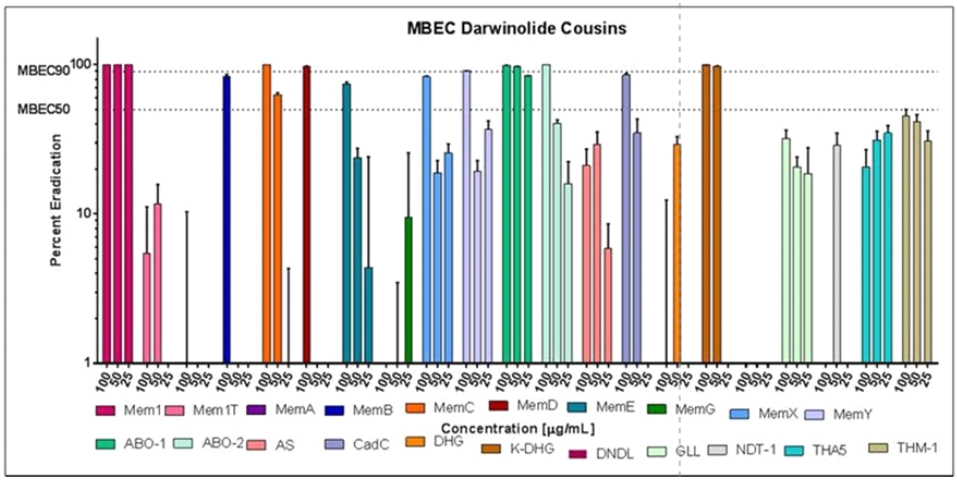

Figure 2.9: Evaluation of Darwinolide Cousins Against MRSA Biofilms (Patent Number: US 11547691)[50]

At the far left of **Figure 2.9**, there is a notably active compound in eradicating these MRSA biofilms called "Mem1". Mem1 is a MNP called membranolide, a diterpene NP isolated from *Dendrilla membranosa*.[51,52] Membranolide is more "drug-like," based off of Lipinski's Rule of 5 (RO5).[53] Given membranolide's demonstrated efficacy against MRSA biofilms and its structural simplicity compared to darwinolide, we believed that performing the first asymmetric total synthesis of this MNP would be exceedingly impactful. We also envisioned that we could create a synthesis that would allow for rapid analog development, therefore being able to perform SAR studies and discover new molecules with high efficacy in eradicating MRSA biofilms.

2.6 Research Goal

Our lab has been fascinated by the exploration of marine natural products and their biological utility. By utilizing chemical synthesis, we hope to successfully synthesize many marine natural products to further evaluate them for their potential biofilm eradication properties. It is known that membranolide has promising bioactivity with regards to biofilm eradication, so our eminent goal was to perform the first asymmetric total synthesis of membranolide. By achieving this goal, we figured this would allow us to easily pursue the synthesis of many analogs of

membranolide, as well as synthesize other related natural products. Upon the successful synthesis of these molecules, they could be examined for their efficacy in biofilm eradication. Finally, the biological target and mechanism of action of membranolide's anti-biofilm activity is unknown, so we wanted to pursue the synthesis of a biological tool that could help us answer these questions. By elucidating this mechanism, future efforts to synthesize biofilm eradication agents can be much more streamlined and directed.

2.7 Racemic Synthesis

To date, there is only one known synthesis of membranolide.[54] In 1990, the Yi group completed a racemic synthesis of membranolide, motivated by membranolide's ability to inhibit the growth of *Bacillus subtilis* and *Staphylococcus aureus*. Their efforts began with the 1,4-addition of aryl grignard **2.3** into isophorone **2.2**. This addition resulted in the formation of a chiral center, which was racemic mixture (**Scheme 2.1**); at this point, there wasn't a way for the Yi group to perform this synthesis asymmetrically.

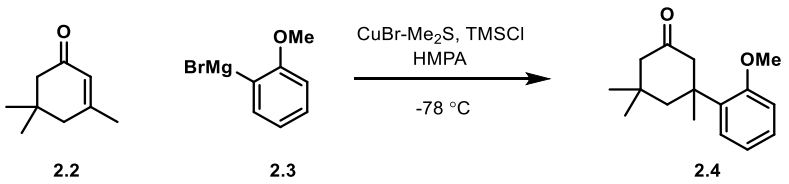

Scheme 2.1: Grignard Addition to Isophorone

With the quaternary carbon formed, their next efforts were to functionalize the arene further. They did this via Wolff-Kishner reduction of the ketone **2.4**, followed by *ortho*-lithiation, quenching with CO_2 and further functionalization of the arene to synthesize an oxazoline moiety **2.5** (**Scheme 2.2**).

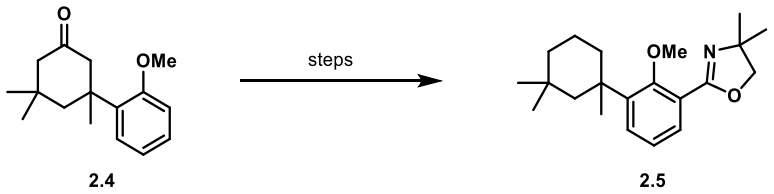

Scheme 2.2: Synthesis of Oxazoline Functionality

After a few more steps, they were able to convert the oxazoline functionality into a phthalide core, establishing the major scaffold of membranolide (**Scheme 2.3**).

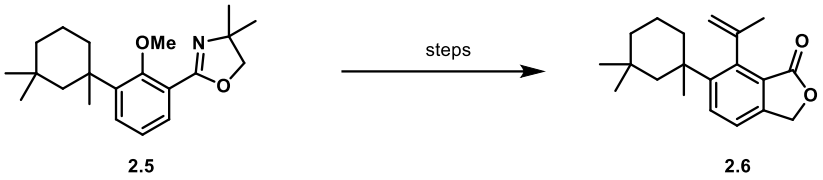

Scheme 2.3: Synthesis of Phthalide Core

With alkene **2.6**, they performed two oxidations, followed by an esterification to access their advanced ester intermediate **2.7** (**Scheme 2.4**).

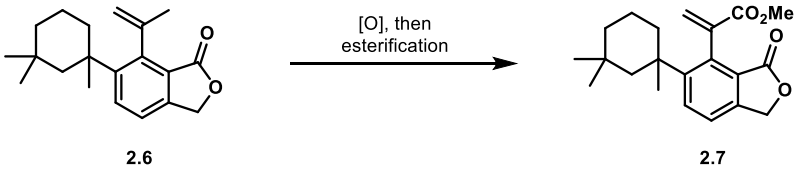

Scheme 2.4: Synthesis of Ester Intermediate

Interestingly, upon reduction of alkene **2.7**, they observed a 3:1 mixture of diastereomers, with the major diastereomer being membranolide **2.1** (**Scheme 2.5**).

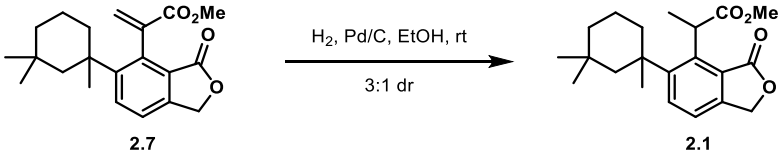

Scheme 2.5: Reduction Leading to Membranolide (Racemic)

This showed that due to the existing functionality of the molecule, there was a facial preference for the delivery of H_2, likely due to sterics and overall accessibility. This was a spectacular feat to synthesize membranolide in a relatively short step count. This route, unfortunately, doesn't enable an asymmetric synthesis to be incorporated and doesn't lend itself to much analog development. We wanted to use this previous effort as motivation and guide our strategy towards the asymmetric total synthesis of membranolide.

2.8 Retrosynthetic Analysis

The synthesis of membranolide **2.1**, containing a highly substituted arene core, could be pursued in many ways. Our retrosynthetic strategy (**Scheme 2.6**) starts with the dissociation of the arene core from the ester functionality, which we presumed could be installed through a cross-coupling reaction. To pursue this approach, we would need to couple a propionate equivalent with the corresponding aryl halide **2.25** or **2.26**. There are many combinations of coupling partners we could explore, but it was necessary to be able to synthesize the aryl halide. Our next retrosynthetic step and a major transformation of this sequence is the synthesis of the highly substituted phthalide core. Tom Hoye at the University of Minnesota has been a pioneer in developing the Hexadehydro Diels Alder (HDDA) reaction, which was an appealing approach for us in the pursuit of this phthalide. Using this chemistry, our next retrosynthetic step takes us to **2.23**, a triyne molecule that is the precursor to the HDDA reaction. This could be synthesized from the Steglich Esterification of diyne **2.21** and carboxylic acid **2.22**. Next, to synthesize the unsymmetric diyne **2.21**, we envisioned a Cadiot-Chodkiewicz reaction would be ideal, as reactions like Glaser couplings would result in symmetric diynes. This alkyne **2.19** could be synthesized from the corresponding aldehyde **2.17**, which is derived from α-hydroxy acid **2.16.** This α-hydroxy acid is crucial, as the quaternary carbon stereocenter is set in this step. **2.16** would be synthesized via an Ireland-Claisen

rearrangement of ester **2.10.** This ester could be made through the esterification of readily synthesized carboxylic acid **2.9** and enantioenriched isophorol **(S)-2.8**. There are developed methods utilizing an enzymatic resolution to enhance racemic isophorol **2.8** to greater than 98% ee of both enantiomers. Finally, racemic isophorol **2.8** can be obtained with the reduction of isophorone **2.2** under Luche conditions.

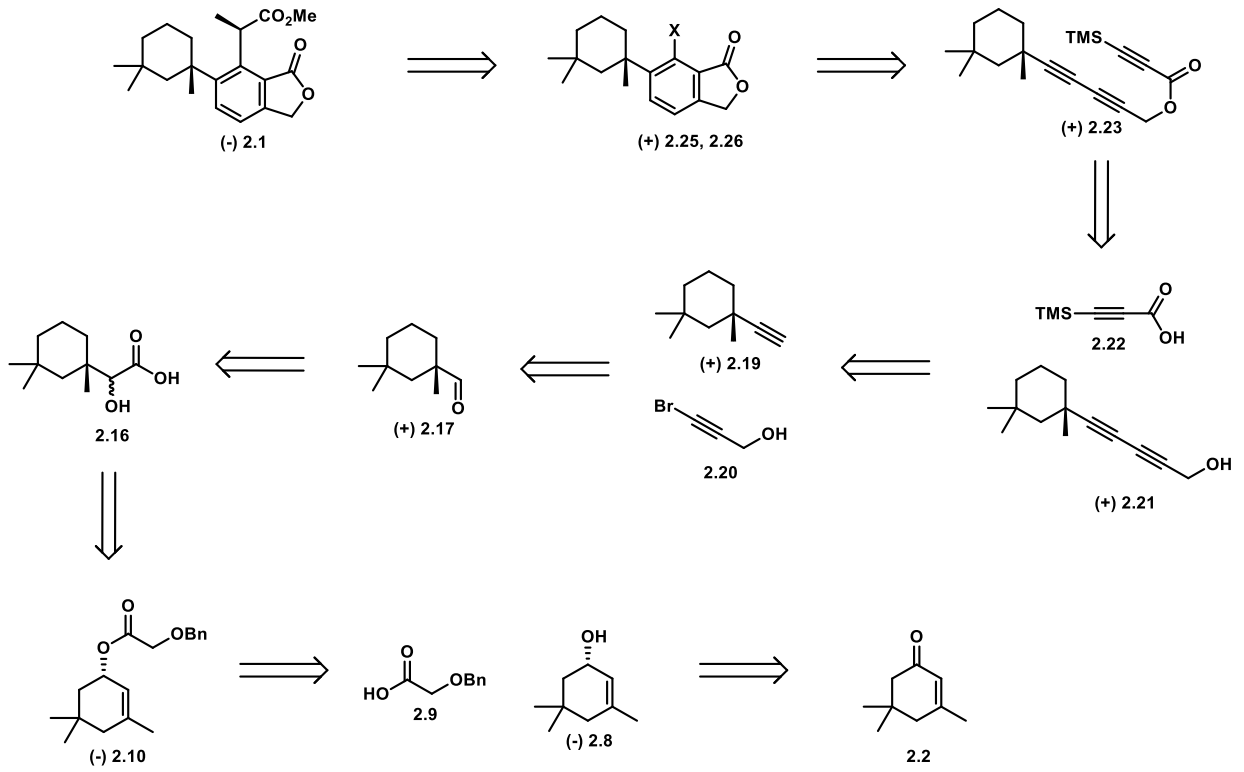

Scheme 2.6: Retrosynthesis of Membranolide

2.9 Membranolide Initial Synthetic Efforts

Now that we had our synthetic plan, it was time to execute this strategy. First, we performed a large-scale reduction of isophorone under Luche conditions to afford racemic allylic alcohol **2.8** (**Scheme 2.7**). This was an extremely clean reaction that didn't require chromatographic purification.

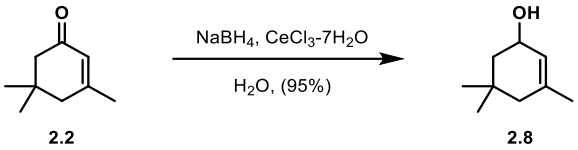

Scheme 2.7: Reduction of 2.2

With this racemic allylic alcohol **2.8** in hand, our next goal was to increase the % ee of **2.8** to >98%. There are many known asymmetric reductions of ketones that can result in the formation of enantioenriched alcohols, but we decided to pursue a different approach. An Enzymatic Kinetic Resolution (EKR) is a crafty technique that allows enantiomers to be transformed at different rates. Exploiting this reactivity makes it possible for extremely high enantioenrichment of one alcohol in the presence of the other (**Scheme 2.8**).[55]

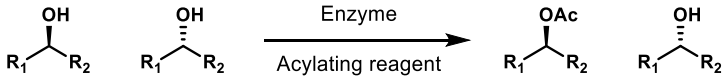

Scheme 2.8: Enzymatic Kinetic Resolution

Although this is an extremely desirable transformation, EKR's do have some limitations. One limitation is that the maximum yield is only 50% since the starting materials are a racemic mixture of enantiomers. Also, the scope of substrates can be somewhat limited and require rigorous screening efforts of enzymes and acylating reagents. Dynamic Kinetic Resolutions (DKR) have been developed to alleviate the problem of low yields that are associated with EKR's.[55] A DKR functions similarly to an EKR, but a DKR allows for the continuous isomerization of the starting materials, allowing for much higher conversion to the desired product of a given enantiomer (**Scheme 2.9**).[55]

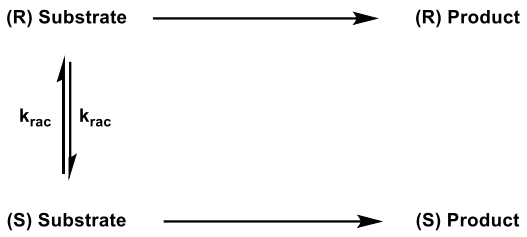

Scheme 2.9: Dynamic Kinetic Resolution

We were successful in following a known procedure in pursuit of enantioenriched (S)-**2.8** (**Scheme 2.10**). Through the use of a lipase from *Candida rugosa*, we were able to achieve 98% ee, but observed a roughly 20% yield over the 3 rounds of resolution. The yields weren't all that surprising since the theoretical maximum is a yield of 50%. Also, this process takes roughly two weeks to fully enhance the ee, so it is quite time consuming. Due to both limitations, we pursued the screening of other enzymes and acyl donors, but ultimately found that our initial conditions were most advantageous.

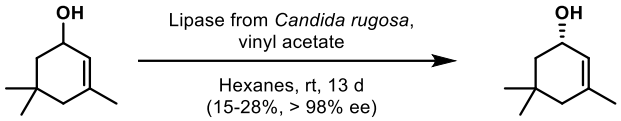

Scheme 2.10: Enzymatic Resolution of 2.8

Now with enantioenriched (-) **2.8**, we could continue with our synthesis. (-) **2.8** was successfully coupled with commercially available and readily prepared **2.9** to furnish ester **2.10** (**Scheme 2.11**).

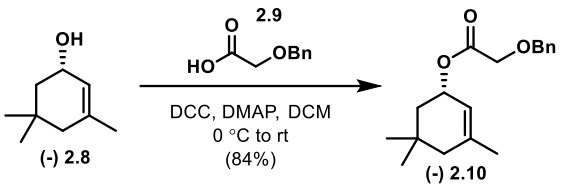

Scheme 2.11: DCC Coupling to Afford 2.10

After the synthesis of **2.10**, we now approached a crucial transformation in our synthesis, which involves the chirality transfer from our established stereocenter to create a new stereocenter. Upon enolate formation, then subsequent trapping of the enolate as a silyl enol ether, we were able to observe a sigmatropic rearrangement: an Ireland-Claisen Rearrangement (**Scheme 2.12**).[56] Since the stereochemistry is already set, this sigmatropic rearrangement occurs on the bottom face of the molecule, allowing for the quaternary stereocenter to be established enantiospecifically. We observed a 2:1 mixture of diastereomers via ^{1}H NMR, which can be explained through a mixture of enolate geometries present upon treatment with LiHMDS.[56] Although we observed a mixture of diastereomers, this wasn't an issue to us because we planned to remove this newly generated α-stereocenter in the upcoming transformations.

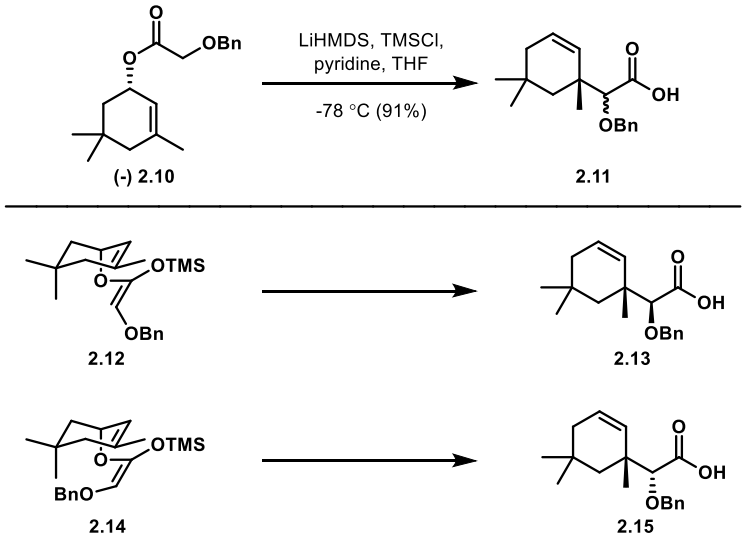

Scheme 2.12: Ireland Claisen Rearrangement and Rationale for Diastereomers

Next, we treated **2.11** with Pd/C and H_2 to reduce the alkene, as well as deprotect the benzyl ether. This transformation affords α-hydroxy acid **2.16,** which was then oxidized with $NaIO_4$ to afford aldehyde **2.17**. This aldehyde was extremely volatile, so extra care had to be taken to prevent the undesired evaporation of **2.17** when removing solvent under reduced pressure. Next, we performed

a Seyferth-Gilbert Homologation to create alkyne **2.19**, which was also extremely volatile and had to be handled carefully. Following this transformation, we performed a Cadiot-Chodkiewicz coupling of **2.19** and bromoalkyne **2.20** to afford unsymmetric diyne **2.21**. Finally, **2.21** was converted into triyne **2.23** through a DCC coupling with carboxylic acid **2.22** (**Scheme 2.13**).

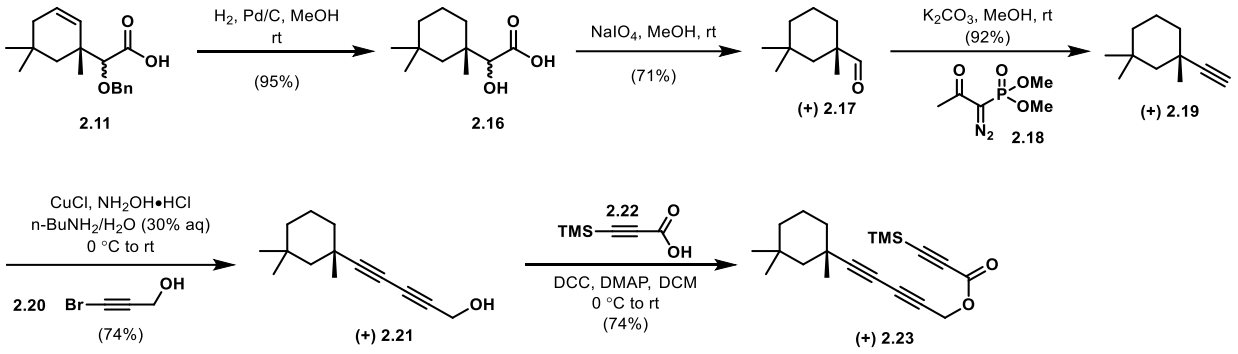

Scheme 2.13: Synthesis of Triyne 2.23

With triyne **2.23** in hand, we were now able to pursue an HDDA reaction to synthesize our phthalide core. Tom Hoye has performed extensive studies elucidating the mechanism of the HDDA reaction,[57] as well as furthering developing the scope and utility of the reaction. Hoye performed a series of HDDA reactions, as well as Diels-Alder (DA) reactions, with varying substituents on the diyneophilic alkyne (for the HDDA reaction) and dienophilic alkyne (for the DA reaction). Hoye found that changing the electronic substituents improved the rate of one reaction but hurt the rate of the other.[57] Groups that improved radical stability generally increased the rate of the HDDA reaction, whereas electron-withdrawing effects didn't encourage the reaction proceed quicker.[57] Based on these findings, Hoye concluded that this transformation must proceed through a stepwise mechanism (**Scheme 2.14**).[57]

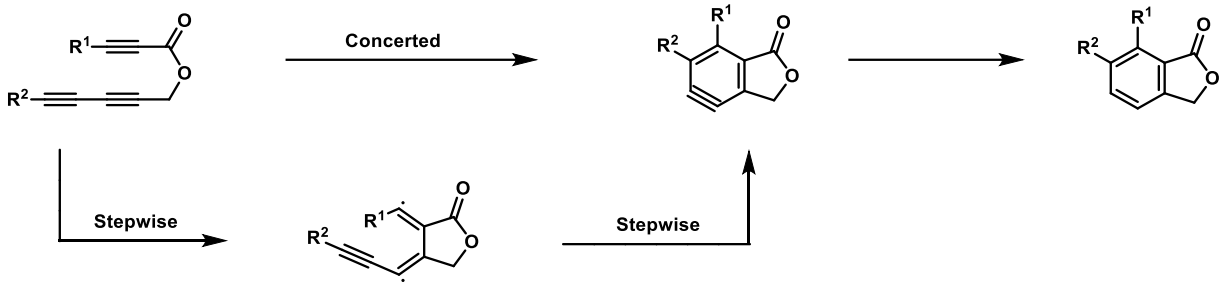

Scheme 2.14: Proposed HDDA Mechanisms

Through reaction optimization, we were able to successfully perform an HDDA reaction on **2.23**, synthesizing phthalide **2.24**. We found that it was crucial to freshly distill, then degas the cyclooctane prior to the reaction. With this arene in hand, our next sight was to convert the aryl silyl group into an aryl halide. Fortunately, we were able to treat this arene with NBS to synthesize aryl bromide **2.25**, as well as treat the arene with Selectfluor^{TM} and I_2 to synthesize aryl iodide **2.26 (Scheme 2.15)**.

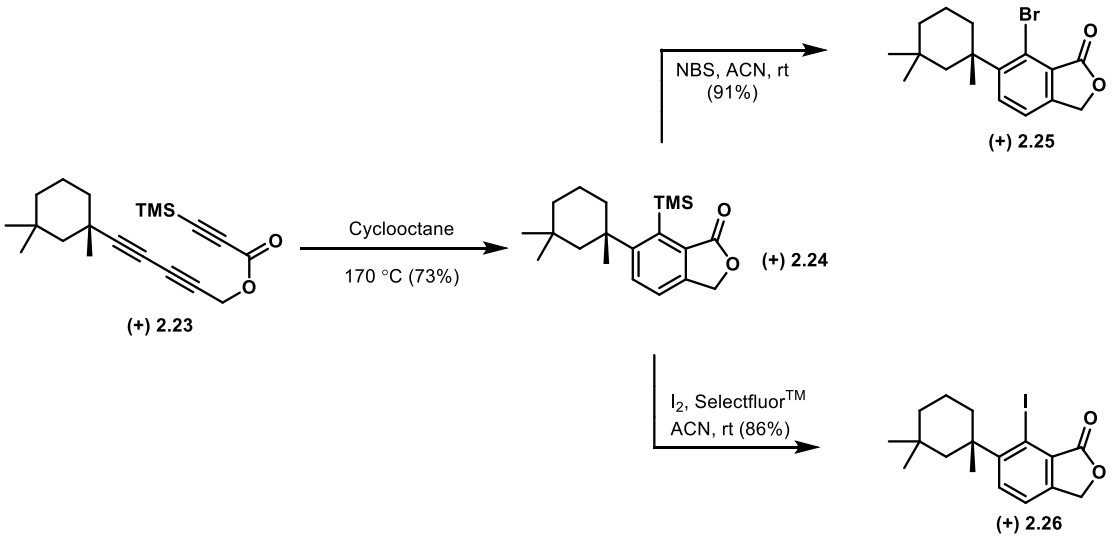

Scheme 2.15: Synthesis of Aryl Halides 2.25 and 2.26

Both aryl halides are capable of being used for cross-coupling reactions, so the versatility of having these aryl halides at our disposal is significant. In addition to the success of these reactions, we were delighted to obtain aryl bromide **2.25** as a crystalline solid. This enabled us to

obtain a crystal structure of aryl bromide **2.25** with the help of Dr. Lukasz Wojtas. The presence of a heavy atom, like bromine, allowed us to confirm the absolute stereochemistry of **2.25** (**Figure 2.10**).

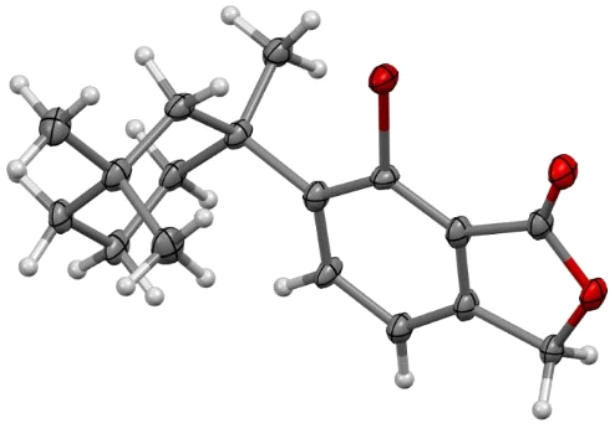

Figure 2.10: Crystal Structure of 2.25

With the success that we had pursuing this route, our sights were on the finish line. The next order of business was to conduct a cross-coupling to furnish the northern functionality of the arene, thus completing our synthesis of membranolide. Due to the observed facial selectivity that was demonstrated in Yi's racemic synthesis upon reduction of the advanced alkene intermediate,[54] we were intrigued to see if the coupling of either aryl halide with silyl ketene acetal (SKA) **2.27** would result in any amount of favorable diastereoselectivity. Given the unique axial conformation of the phthalide group and the existing chirality on the trimethylcyclohexyl group, this was a journey we were excited to pursue. Even without favorable selectivity, we figured we could explore chiral ligands to induce the desired asymmetry. Previous work by Yamamoto had shown the ability to perform α-arylations with aryl halides and SKA's asymmetrically by utilizing chiral ligands, like Josiphos.[58]

Before attempting to perform this transformation with our sights set on high selectivity, it was paramount to first demonstrate that the cross-coupling would be successful. Unfortunately, our attempts at coupling aryl bromide **2.25** with SKA **2.27** resulted in no observable formation of membranolide **2.1**. We observed that one of the major products formed was the protodemetalation product **2.28**. The steric strain of the aryl bromide after oxidative addition likely stalled the catalytic cycle, allowing protodemetalation to occur quicker than the desired nucleophilic termination, coming by way of SKA **2.27**. We also observed the formation of the Heck-like product **2.29**; this is likely due to the isomerization of SKA **2.27** in situ to form methyl acrylate, which easily underwent a Heck coupling with **2.25** (**Scheme 2.16**). We observed the same reactivity when utilizing aryl halide **2.26**.

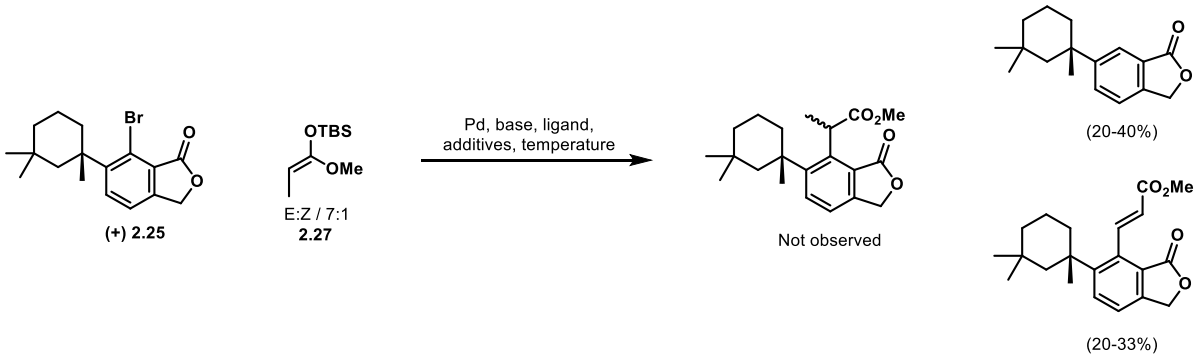

Scheme 2.16: Initial Attempt to Synthesize 2.1 Through Coupling with SKA 2.27

Due to the unforeseen shortcomings of our cross-coupling attempt with SKA **2.27**, we thought it would be worthwhile to pursue a simpler approach. Had this previous cross-coupling worked, this would have been our "homerun" attempt, but we decided to pursue a similar transformation with SKA **2.30** instead. Without the extra methyl group, we wouldn't expect to see any isomerization of the SKA, thus preventing the formation of the Heck-like product. Also, the lack of an extra methyl group ever so slightly decreases the steric constraints of our palladium

complex, thus making the transformation easier to perform. To do this, we screened an array of palladium catalysts, ligands, bases, and solvents; fortunately, we were able to successfully perform this cross-coupling and synthesize normembranolide **2.31** (**Scheme 2.17**). We found that the use of TlOAc was required for this transformation. Tl^+ likely helps to facilitate the oxidative addition step,[58] which is likely to already be slow because of the overall steric hinderance. This increased rate is likely due to the formation of insoluble thallium salts, which drives the catalytic cycle forward.[58] Thallium compounds are highly toxic, so we attempted to develop a coupling that wouldn't require the use of TlOAc, but we weren't able to produce the same results by utilizing other bases. We had to continue using this method, but of course, with extreme caution.

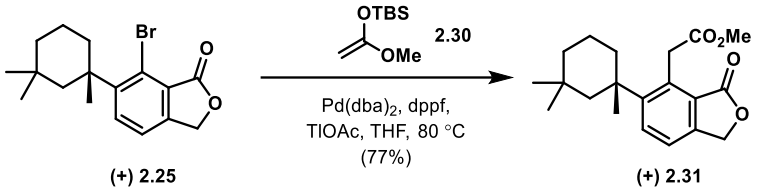

Scheme 2.17: Synthesis of 2.31

With normembranolide **2.31** in hand, all that was left to do was perform a methylation, thus yielding membranolide **2.1**. Initial attempts involved the formation of an enolate under kinetic conditions, followed by quenching of the enolate with MeI. In this alkylation, we noticed a 3:1 mixture of diastereomers form via ^{1}H NMR, however, we ended up forming the undesired diastereomer as the major product (**Scheme 2.18**). Initial attempts to salvage this undesired diastereoselectivity was an epimerization strategy. This is not an attractive strategy to close out a total synthesis, but we were curious to see if we could flip the selectivity in a 3:1 ratio, in favor of the natural product. Upon reformation of the enolate and quenching with various proton sources, the best we were able to obtain was a 1:1 mixture of diastereomers, which was obviously not sufficient.

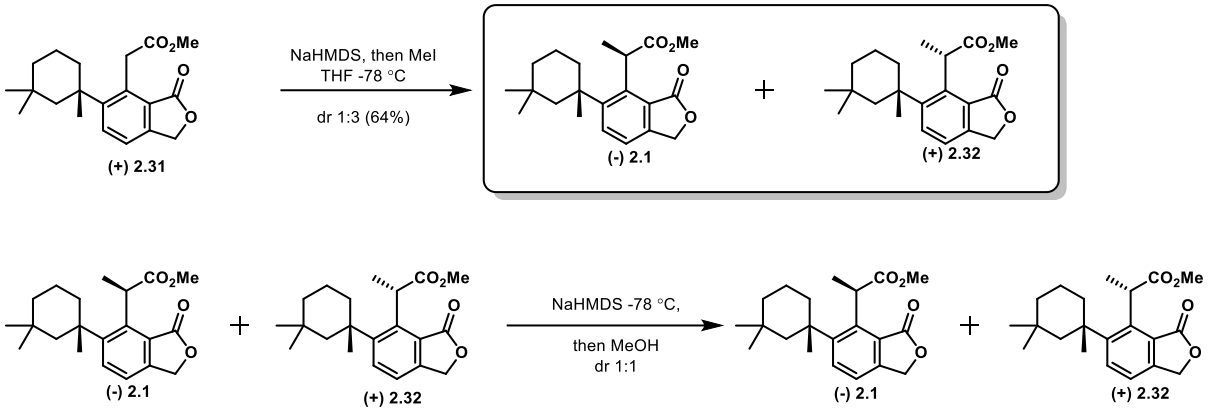

Scheme 2.18: Alkylation of 2.31 and Epimerization

Based on the existing chirality of the trimethylcyclohexyl moiety and the unique axial conformation of our arene, it's not all that surprising to observe facial selectivity during this methylation. It's likely that the front face of this molecule is more hindered due to the blocking from the geminal dimethyl groups. Because of this, the back face of this molecule is more accessible, allowing methylation to occur from the backside more easily (**Scheme 2.19**).

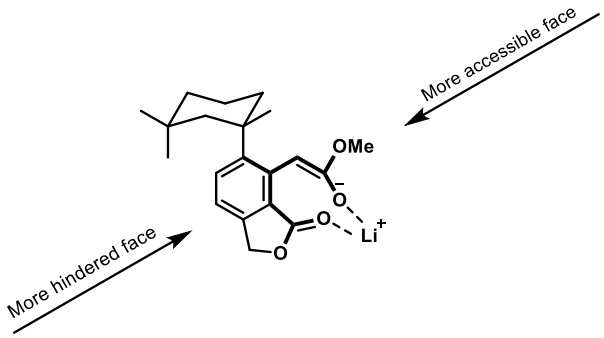

Scheme 2.19: Rationale for Undesired Diastereoselectivity

To move forward, we decided that it would be useful to exploit the observed facial selectivity by intercepting the late-stage intermediate that the Yi group utilized: alkene **2.7** that, upon reduction, yielded membranolide.[54] Based on our observed 3:1 ratio upon methylation and Yi's 3:1 ratio upon reduction of the alkene, it stands to reason that the argument for facial selectivity is the same. In both cases, the back face is more accessible, which is why we observed

a higher instance of methylation occurring from the backside. This would also explain why Yi observed a favorable ratio, given that the backside is more accessible, allowing for H_2 to be more easily delivered from the back face and forcing the methyl group forward. This analysis led us to assume that Yi's intermediate existed in an extremely similar conformation to **2.31** (**Scheme 2.20**).

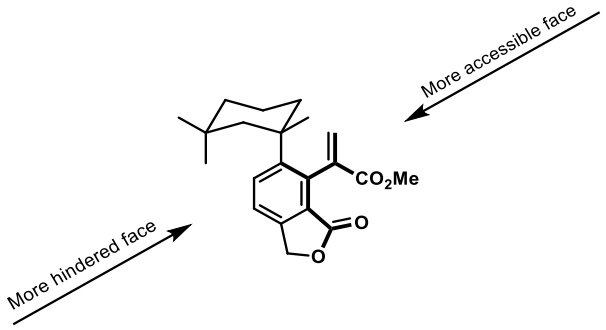

Scheme 2.20: Proposed Confirmation of 2.7

To pursue this strategy, we first had to install an alkene at the α-carbon of **2.31**. Our initial attempt was to utilize Eschenmoser's Salt, but we were unable to successfully complete this transformation (**Scheme 2.21**).[59] We were able to previously methylate this position, but the slightly bulkier reagent that Eschenmoser developed couldn't be successfully attacked by our enolate.

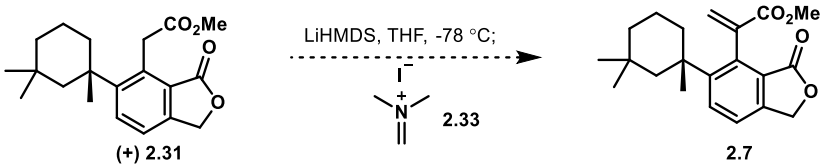

Scheme 2.21: Failed Attempt with Eschenmoser's Salt

We were still hoping to intercept this alkene intermediate **2.7**, so we next tried an array of cross-couplings to install the entire acrylate portion. To do this, we wanted to utilize aryl bromide **2.25** or aryl iodide **2.26** with an appropriate coupling partner. Our initial thought was to pursue a Suzuki coupling. To do this, it would be necessary to synthesize the corresponding boronic ester

2.35. First, we brominated methyl acrylate **2.34** with Br_2, followed by treatment with NEt_3 to afford α-brominated methyl acrylate. Our next effort was to convert this vinyl bromide into the vinyl boronic ester by utilizing a Miyaura borylation. We noticed that the vinyl bromide was quite unstable and decomposed readily, so it couldn't withstand the reaction conditions that are required for a Miyaura borylation. Because of the inability to synthesize **2.35** we had to abandon this Suzuki coupling approach (**Scheme 2.22**).

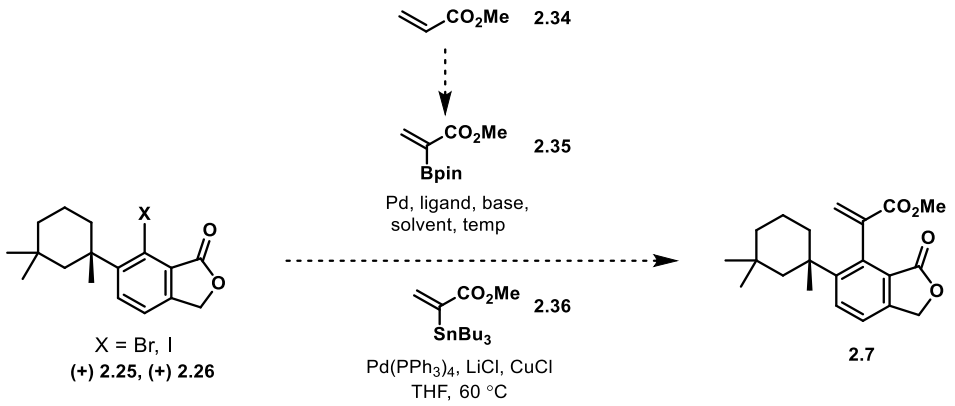

Scheme 2.22: Attempted Suzuki and Stille Routes to Install Branched Acrylate

This led us to pursue a different approach that would result in the same desired product. Utilizing a known procedure, we were able to react methyl propiolate and tributyltin hydride, along with a palladium catalyst to synthesize our vinyl tributyltin species **2.36**. With this, we explored many conditions to cross couple vinyl tributyltin species **2.36** with both of our aryl halides, but none of these efforts were successful. Again, we observed the overwhelming power involving the steric constraints of these late-stage intermediates, making the path to membranolide **2.1** extremely difficult.

With these failures, we decided that we needed to move away from this route and explore new strategies. Although we fell short, this was by no means a failure. We were able to collect so much information and gain insight into how these molecules exist and behave. With this

knowledge, we can be even more strategic in our upcoming attempts and successfully perform the first asymmetric total synthesis of membranolide **2.1**.

2.10 Acetonide Approach

Due to the shortcomings of our initial route, we envisioned a synthetic strategy that would avoid sterically hindered cross couplings, as well as late-stage functionalization of sterically encumbered molecules. Our next approach involved the synthesis of an arene containing an acetonide, which could be rapidly converted into membranolide (**Scheme 2.23**).

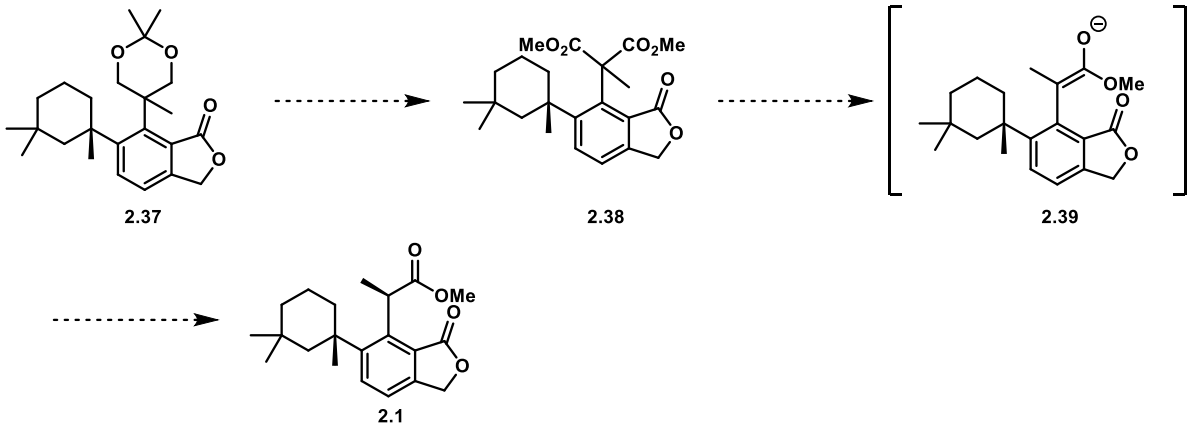

Scheme 2.23: Justification for Acetonide Approach

Upon the successful synthesis of compound **2.37**, we envisioned that we could deprotect the acetonide, creating a 1,3-diol. This diol could then be oxidized, followed by esterification to create malonate **2.38**. Finally, this malonate could be decarboxylated via Krapcho decarboxylation, which would go through enol-intermediate **2.39**. Based on our initial efforts on the methylation of normembranolide **2.31**, we noticed that the back face was more accessible for the addition of a methyl group. Using this same rationale, we hoped that intermediate **2.39** would be more likely to protonate from the back face, thus correctly setting the second stereocenter in a highly diastereoselective manner.

This proposed approach involves significant changes from our initial efforts, so we decided to utilize a model system. This model system would allow us to test out many reaction conditions, without having to consume our chiral and highly valuable trimethylcyclohexyl-containing compounds. We decided that a phenyl moiety would be a good substitute for the trimethylcyclohexyl moiety. Both moieties are rather hydrophobic, so they should share some similar properties. Also, a phenyl group is fairly simple, so we envisioned that the methods that we developed for the model compounds would also be compatible with the trimethylcyclohexyl compounds.

We envisioned that phenyl acetylene would function as a cheap starting material for our model system. Starting with phenyl acetylene would also allow us to bypass many steps in the proposed synthesis, which would expedite our pursuit of this strategy. We were aware that this would not give us any information on the diastereoselectivity of the installation of our alpha stereocenter, but we wanted to perform a proof-of-concept study to ensure that we could form all the necessary bonds.

To start this endeavor, we utilized triol **2.40** and easily converted it into acetonide **2.41**. The primary alcohol was then oxidized with TEMPO and BAIB, forming aldehyde **2.42**. This aldehyde was then converted into the corresponding dibromo alkene **2.43** via a Corey-Fuchs reaction. This dibromo alkene was then treated with n-BuLi, which formed an acetylide, which was then quenched with methyl chloroformate to synthesize alkynoate **2.45** (**Scheme 2.24**).

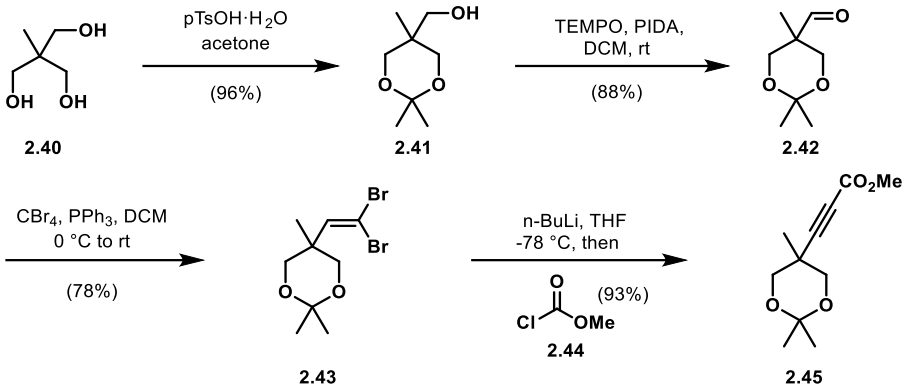

Scheme 2.24: Synthesis of Acetonide Intermediate 2.45

With alkynoate **2.45** in hand, we next had to hydrolyze the ester so we could couple it with our diyne. This hydrolysis had to be performed under basic conditions, due to the acid-labile acetonide group. This protecting group made it difficult to isolate the protonated carboxylic acid, so we ultimately utilized the potassium carboxylate **2.46** in the next step (**Scheme 2.25**).

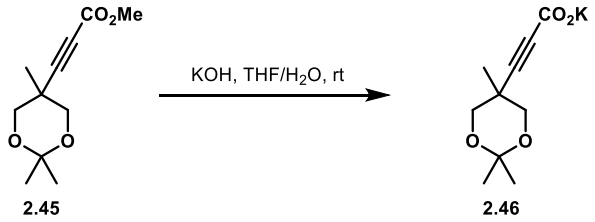

Scheme 2.25: Synthesis of Potassium Carboxylate 2.46

Having completed the synthesis of our advanced acetonide intermediate **2.46**, our attention now focused on the synthesis of its coupling partner. First, we performed a Cadiot-Chodkiewicz coupling of phenyl acetylene **2.118** and bromoalkyne **2.20** to synthesize diyne **2.47**. This was then reacted with MsCl and NEt_3 to produce mesylate **2.48**, which could be used without the need of chromatographic purification. This mesylate was then easily coupled with acetonide **2.46** to produce our crucial triyne **2.49**. This triyne then underwent a successful HDDA reaction to form our advanced arene **2.50** (**Scheme 2.26**). Due to the sterically hindered quaternary carbon of our

acetonide portion, we had reservations about the success of this cyclization. Fortunately, the cyclization went without trouble, and we were able to further our studies with this model system.

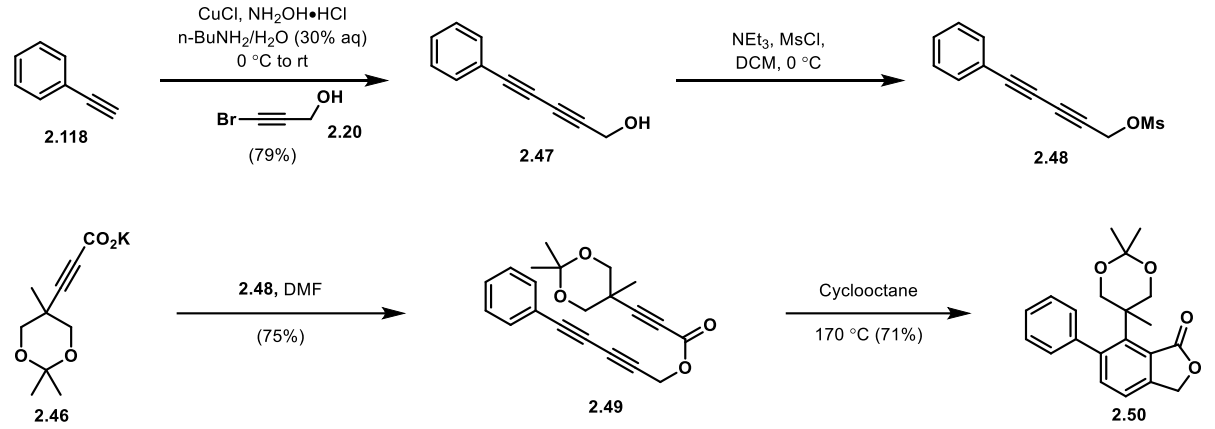

Scheme 2.26: Synthesis of Acetonide 2.50

Now that arene **2.50** was synthesized, all that was left to perform was the deprotection of the acetonide, followed by a subsequent oxidation and esterification, which would leave us one step away from phenyl-membranolide. Initial attempts to deprotect the acetonide led to rapid and complete consumption of starting material, but we did not observe the intended product. Upon deprotection of the acetonide under acidic conditions, the 5-membered lactone **2.51** underwent a subsequent acid-catalyzed rearrangement to form a new 6-membered lactone **2.52** (**Scheme 2.27**), which was undesired and detrimental to our efforts**.**

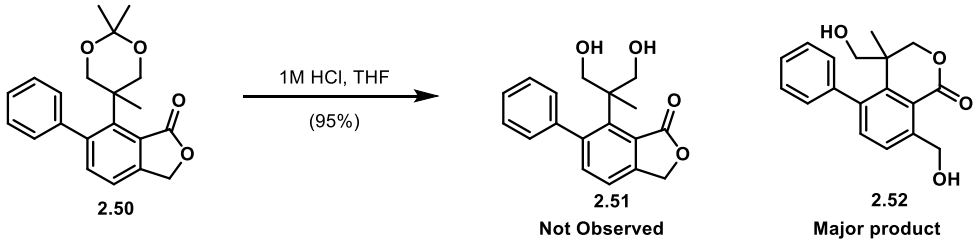

Scheme 2.27: Observed 6-Membered Lactone Formation

To salvage this route, we first explored the possibility of driving the equilibrium towards the 5-membered lactone; unfortunately, these efforts did not show any promise. Our initial attempts

to deprotect acetonide **2.50** utilized excess HCl at room temperature, which was stirred overnight. Our first efforts to fix this reaction involved decreasing the reaction time, performing the reaction at lower temperature, and even using weaker acids. Unfortunately, these efforts did not allow for any amount of the 5-membered lactone **2.51** to be isolated. We observed complete recovery of the starting material if the conditions were too mild, or complete formation of the 6-membered lactone **2.52** if the reaction conditions were too harsh. Unfortunately, we weren't able to discover conditions that would give access to **2.51**.

Due to these shortcomings, we unfortunately had to abandon our acetonide approach. Although we could not pursue this approach any further, it did provide us with some valuable information. First, this approach showed that we were able to perform an HDDA reaction without an alkynyl-silicon group, which opens the possibility of completing this total synthesis without the reliance on an extremely hindered cross-coupling reaction. Also, this synthetic strategy is convergent, allowing for fewer linear steps and larger output of material. With this information, we were eager to develop new strategies in our pursuit towards **2.1**.

2.11 Meldrum's Acid Approach

Based on the late-stage issues of our previous approach, we wanted to use this knowledge to try and develop a more successful route to membranolide **2.1**. Our next approach encompassed the same idea of performing a decarboxylation, followed by a potentially selective protonation step of an enol/enolate intermediate **2.39**, which would ultimately furnish our second stereocenter. Our previous attempt showed that we could not prevent an intramolecular rearrangement from occurring in the presence of our diol moiety. This led us to pursue an approach utilizing Meldrum's acid, rather than an acetonide protecting group (**Scheme 2.28**).

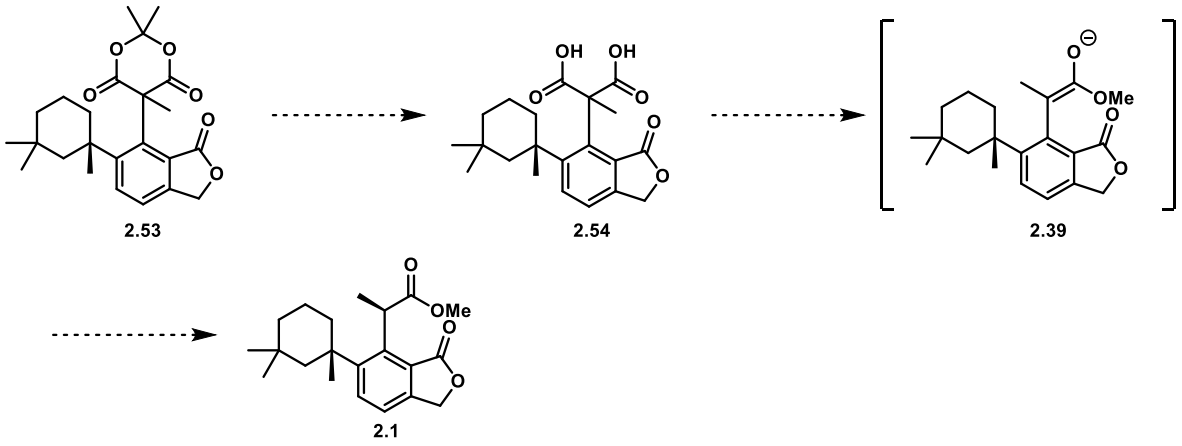

Scheme 2.28: Justification for Meldrum's Acid Approach

With the Meldrum's acid functionality, the carboxylic acid that would be liberated upon deprotection would be far less nucleophilic than the alcohol that was formed upon deprotection of the acetonide. With this rationale, we were hopeful that we could continue with the same approach as before but avoid the formation of a 6-membered lactone intermediate. To test out this idea, we envisioned that it would be logical to start with phenyl acetylene as a model system, which could be coupled with a Meldrum's acid intermediate (**Scheme 2.29**)

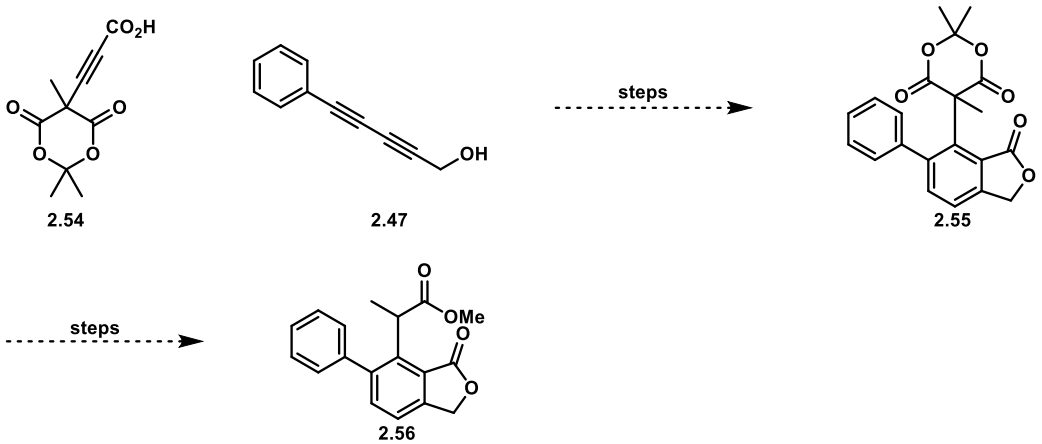

Scheme 2.29: Proposed Route to 2.56

To begin to explore this idea, it was necessary to synthesize the derivatized Meldrum's acid coupling partner. Our initial thought was to take methyl Meldrum's acid and perform a formylation

at the alpha position. We then presumed that we could perform a Seyferth-Gilbert homologation to convert the aldehyde into a terminal alkyne, but we weren't able to perform the formylation in any sort of appreciable yield (**Scheme 2.30**).

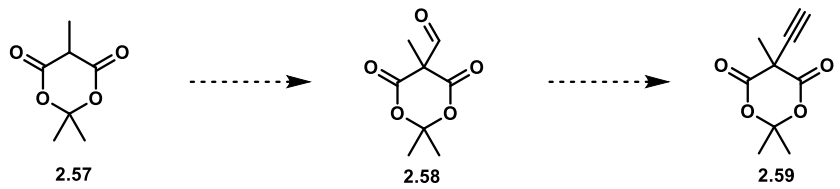

Scheme 2.30: Initial Approach to Alkyne Intermediate

Due to the lack of success of the previous approach, we continued to browse the literature for inspiration. We were inspired by the work of Jerome Waser, which led us to a completely different approach. We decided that we could exploit the installation of the terminal alkyne through umpolung chemistry. Waser has developed many reagents and shown vast scope of utilizing hypervalent-iodine reagents to perform electrophilic alkynylations.[60] With this inspiration, we sought to first synthesize TMS-EBX. To synthesize this, we performed a sodium periodate-mediated oxidation of 2-iodobenzoic acid **2.60** to synthesize **2.61**. This could then be treated with TMS-OTf and bis(trimethylsilyl) acetylene to successfully synthesize TMS-EBX **2.62**. This route provided TMS-EBX in high yields, without the need for column chromatography (**Scheme 2.31**).

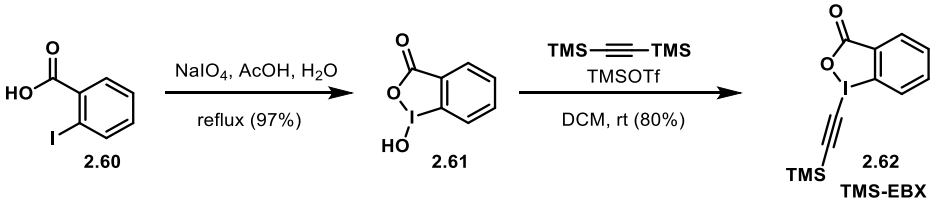

Scheme 2.31: Preparation of TMS-EBX

With TMS-EBX in hand, our next step was to perform an electrophilic alkynylation of methyl Meldrum's Acid **2.57**. Initial attempts using TBAF as a base, as well as to deprotect the TMS group, were unsuccessful. This led us to other literature procedures that utilized K-OtBu to

be used as a base for this type of transformation. We were happy to observe that this worked in high yields to install the alkyne, as well as deprotect the TMS group. Next, we sought to install a carboxylic acid functionality so that we could couple it with the phenyl coupling partner **2.47**. Initial attempts to carboxylate the alkyne involved the formation of the acetylide with LiHMDS, followed by quenching with CO_2. Unfortunately, this method led to complete decomposition of our starting material and no observable product formation. Next, we altered the bases that we used, employing NaHMDS, KHMDS, NaH, n-BuLi and even freshly preparing NaHMDS from HMDS and NaH. Unfortunately, none of these attempts were successful.

We hypothesized that the acetylide was too reactive and was likely reacting with the carbonyl of another molecule **2.63**. Because of this, our next approach dealt with shortening the amount of time that the acetylide was present. To do this, we treated our alkyne with base, then altered the amount of time for deprotonation before bubbling in CO_2. Our most extreme attempt only allowed the deprotonation to occur for five minutes prior to bubbling in CO_2, but we were still unable to prevent the decomposition of our material. Because of the continued failure, we next explored milder palladium and copper-catalyzed carboxylation chemistry,[61,62] but none of our efforts afforded any of the desired product (**Scheme 2.32**).

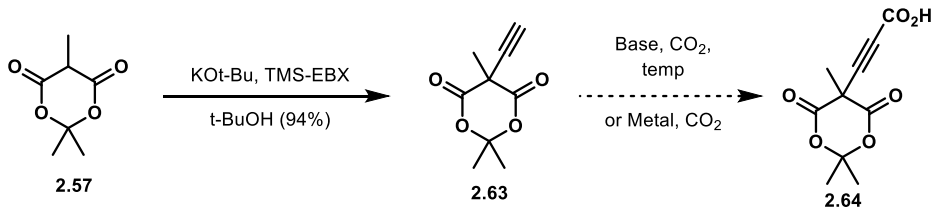

Scheme 2.32: Attempt to Synthesize Functionalized Meldrum's Acid Component

At this stage, we had to abandon our Meldrum's acid approach because we couldn't synthesize the desired intermediate **2.64** to continue our studies. Although the carbonyls were possibly the reason we couldn't continue, we were still drawn to the idea of having an arene that

had a 1,3-dicarbonyl functionality. We believed that this would prevent any intramolecular rearrangement from occurring towards the end of our synthesis, so we were determined to continue with this strategy. That being said, Meldrum's acid wouldn't give us access to the desired advanced intermediate, so we were forced to go back to the drawing board.

2.12 Malonate Approach

Inspired by our shortcomings from our previous efforts, we developed a new strategy in the pursuit of synthesizing membranolide. As we observed earlier, the acetonide deprotection resulted in a rearrangement that couldn't be controlled, and the Meldrum's acid approach came up short due to the highly reactive carbonyl functionality of our intermediates. Our next approach was similar, as we still pursued a decarboxylation in the final step, which would hopefully set our final stereocenter in high selectivity. This led us to pursue a synthetic route involving a late-stage malonate moiety. This did cause some concern, however, due to the malonate likely having reactivity that is similar to Meldrum's acid; our approach involved the synthesis of a "masked" malonate, that could furnish a malonate later in the synthesis. We envisioned that the product from a Birch reduction could be an acceptable surrogate to a malonate (**Scheme 2.33**).

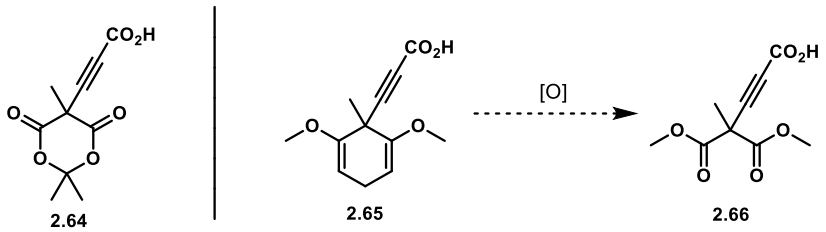

Scheme 2.33: Meldrum's Acid Idea and Proposed Synthesis of Malonate Moiety

To pursue this route, we started with commercially available 2,6-dimethoxybenzoic acid **2.67** and performed a Fischer esterification, converting our carboxylic acid to methyl ester **2.68** in high yields. Next, we sought to optimize a Birch reduction of **2.68**; the presence of the ester was

crucial for the Birch reduction to provide the desired regioselectivity. Upon optimization, we were able to successfully perform a Birch reduction, followed by a methylation, ultimately creating our valuable quaternary center (**Scheme 2.34**).

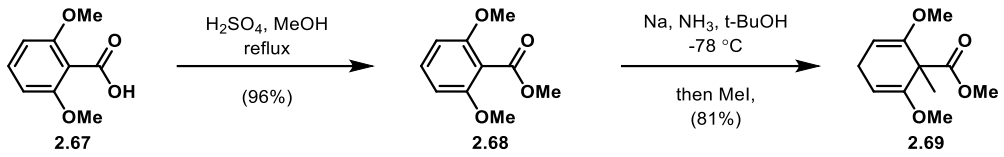

Scheme 2.34: Esterification and Birch Reduction

With this product in hand, our next efforts were aimed at converting methyl ester **2.69** into an alkyne, which could then be carboxylated. To do this, we converted methyl ester **2.69** into a Weinreb amide **2.72** by treating the ester with lithiated-Weinreb amine **2.71**. This easily furnished the Weinreb amide product in 88% yield, which was then selectively reduced with LAH to produce aldehyde intermediate **2.73**. Similar to previous approaches, we next performed a Seyferth-Gilbert homologation to rapidly convert this aldehyde into terminal alkyne **2.74**. Next, we were able to convert the alkyne into an acetylide, which was used as a nucleophile to attack methyl chloroformate. Finally, this newly formed methyl ester **2.75** could be saponified, producing our desired carboxylic acid intermediate **2.76**. Extreme caution had to be taken during this step due to the sensitivity of our vinyl ethers functionality. Vinyl ethers are very prone to hydrolysis under acidic conditions, but we were able to carefully work up the reaction to obtain the carboxylic acid, while avoiding the hydrolysis of the vinyl ethers (**Scheme 2.35**).

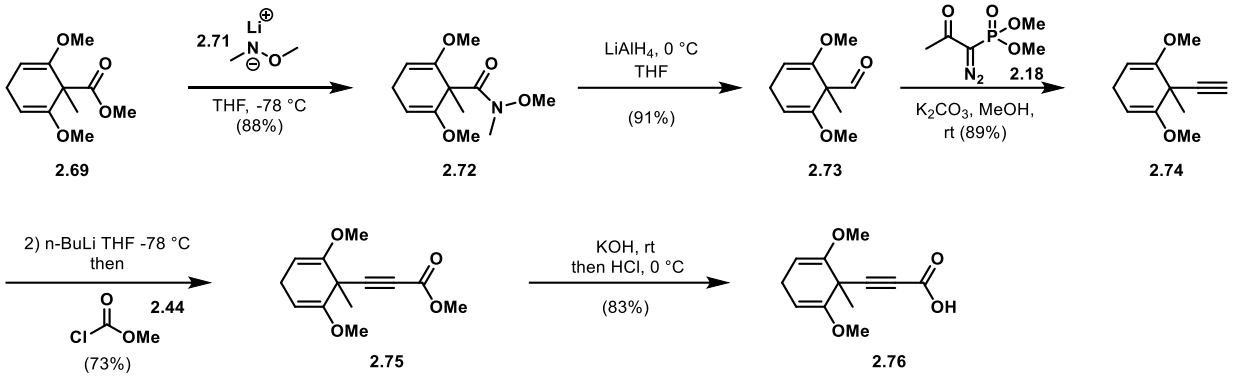

Route 2.35: Route to Malonate Precursor 2.76

To this point, the optimization of these reactions went relatively smoothly and without issue. The next step, however, took quite a bit of optimization. Now that we had intermediate **2.76** in hand, it was crucial to oxidatively cleave the ring, liberating our masked malonate functionality. The issue is that there is an alkyne present, which is also prone to oxidative cleavage. Due to the electron-rich property of the vinyl ethers, we hypothesized that they should be oxidatively cleaved more quickly than the relatively electron-poor alkyne. Upon our initial attempts, we weren't able to observe any isolatable product. Our initial attempts included a Lemieux-Johnson oxidation, as well as a variation using $RuCl_3$. Due to the lack of success with both strategies, we next pursued conditions utilizing Oxone, but these efforts also failed to produce any product. Finally, we moved on to using ozone as our oxidant. Initial attempts with ozone were not successful, but we were ultimately able to optimize the reaction by altering many reaction parameters. We altered solvents, reaction temperature, reaction time, work up conditions, as well as other parameters. After roughly 40 attempts, we were able to optimize our yield of **2.77** to 36% (**Scheme 2.36**).

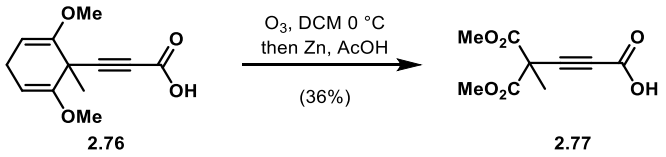

Scheme 2.36: Ozonolysis to Create Malonate Intermediate 2.77

This yield was far from ideal, but we were ultimately satisfied because the synthesis of this malonate intermediate was crucial to continue our efforts. The most valuable intermediates in our synthesis are those that possess chirality, so it was fortunate that our low-yielding process, described above, was on a molecule that did not contain any chiral centers. With this advanced intermediate **2.77** in hand, we next coupled it to alcohol **2.47**, forming our triyne intermediate, which further underwent an HDDA reaction (**Scheme 2.37**).

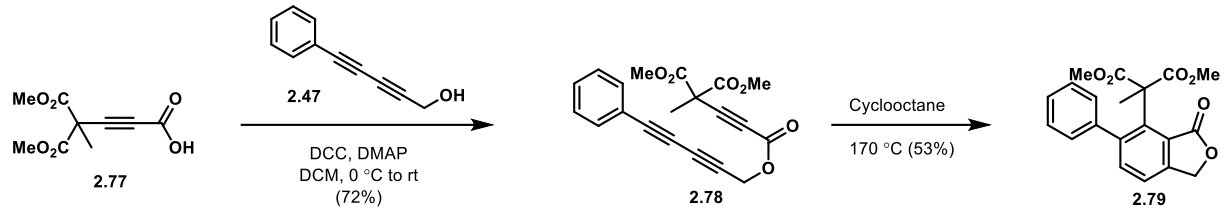

Scheme 2.37: Synthesis of Malonate Intermediate 2.79

With arene **2.79** in hand, we were able to attempt a Krapcho decarboxylation. With a small amount of reaction modification, we were delighted to synthesize our phenyl analog of membranolide **2.56**. The yield for this transformation wasn't optimized, but we were ecstatic to see a new approach yield an analog of membranolide, thus completing the synthesis of our model system (**Scheme 2.38**).

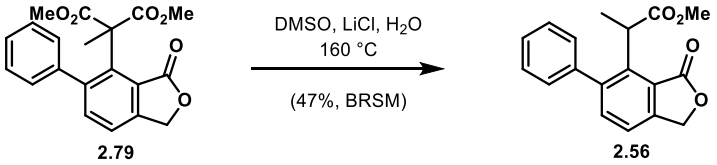

Scheme 2.38: Synthesis of 2.56

With the success of synthesizing the phenyl analog **2.56** with our malonate approach, we next sought to utilize this strategy to synthesize membranolide **2.1**. We started by coupling our previously synthesized alcohol **2.21** with our recently synthesized malonate handle **2.77**. Upon the successful coupling of these two components to create **2.80**, we attempted to perform an HDDA

reaction. Unfortunately, we were not able to observe any of the desired product upon initial attempts. Further attempts to optimize this reaction included modifications in reaction time, temperature, reaction molarity and even solvent choice, but none of these were successful; we noticed full decomposition of the reaction substrates, or no consumption of starting material. We hypothesize that the steric hinderance created by the proximity of the two quaternary carbons was too high to overcome (**Scheme 2.39**).

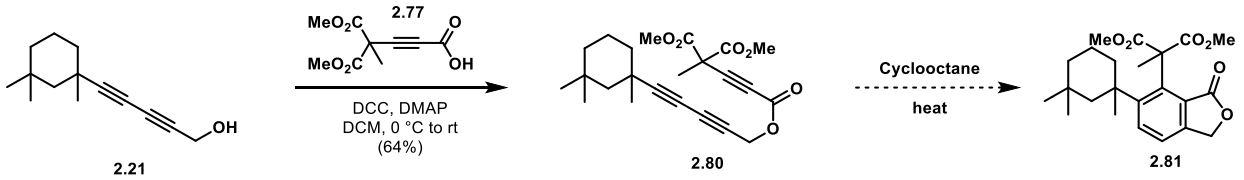

Scheme 2.39: Malonate Attempt for Membranolide Synthesis

Because of this failure, we came to the realization that it would be unlikely to successfully perform an HDDA reaction in the presence of extremely functionalized and bulky groups. We also learned that although the phenyl handle provides a model scaffold that allowed us to expedite the exploration of reaction conditions, the phenyl moiety doesn't remotely demonstrate the sterically encumbered characteristics of our trimethylcyclohexyl moiety. This observation, although very time-consuming, was crucial to understanding the characteristics and behavior of our advanced intermediates. This information will be crucial to our understanding and future approaches to synthesize membranolide **2.1**.

2.13 A New Model System

Although we had shortcomings with our previous model system (phenyl), we still saw value in utilizing model systems. The use of a model system allows us to start at our terminal alkyne advanced intermediate, which greatly cuts down on our linear step count. It also allows us to test reaction conditions on something that is achiral, preventing us from consuming valuable

material that was enantioenriched. This led us to pursue a new model system, starting with t-Bu acetylene **2.83.** Based on our past experiences, the quaternary carbon of the trimethylcyclohexyl moiety was likely part of the equation regarding our steric hinderance problem. We envisioned that replacing this crucial moiety with a t-Bu moiety would still allow us to pursue synthetic ideas from an advanced part of the synthetic route, as well as provide much more reliable information about the steric component of our intermediates, compared to the phenyl system (**Scheme 2.40**).

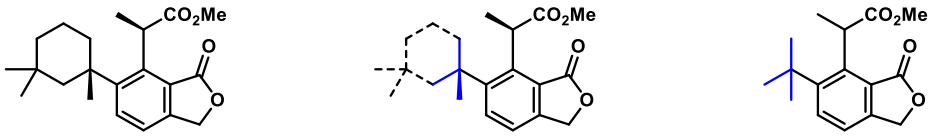

Scheme 2.40: New Model System Rationale

To develop and test out new synthetic strategies, we first sought to synthesize a new model compound. To do this, we started with t-Bu acetylene **2.83** and performed a Cadiot-Chodkiewicz coupling with bromo alkyne **2.20** to furnish propargylic alcohol **2.84**. With this, we then performed a Steglich esterification with readily synthesized carboxylic acid **2.22** to easily synthesize ester **2.85**. This ester smoothly underwent an HDDA reaction to yield arene **2.86**, which was swiftly iodinated to synthesize aryl iodide **2.87** (**Scheme 2.41**).

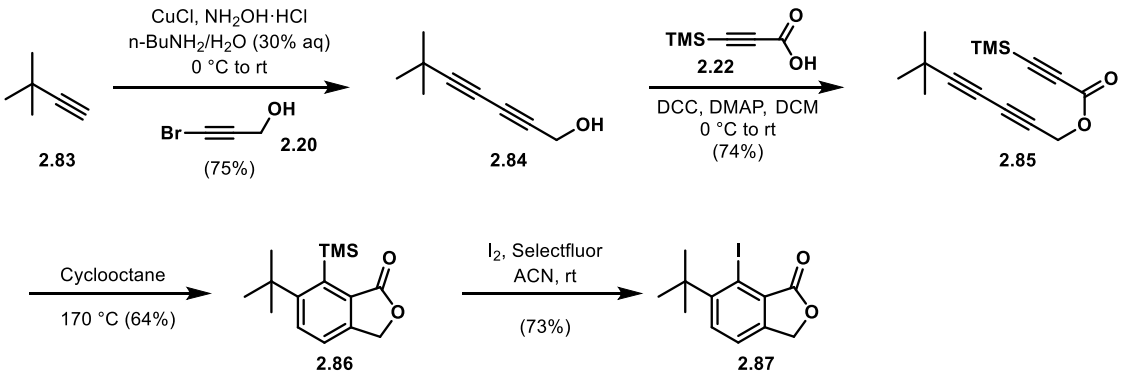

Scheme 2.41: Synthesis of tBu Aryl Iodide

2.14 Revisiting Cross-Coupling Reactions

With aryl iodide **2.87** in hand, we were now able to explore new strategies. In our early efforts, we experienced many shortcomings with the palladium-catalyzed cross-coupling reactions we attempted. We mostly explored well developed α-arylation chemistry, which didn't provide access to the desired scaffolds. Now that we presumably had a model system that represents the steric environment of the natural product, we decided to explore some additional cross-coupling methods. Rather than trying to install the entire northern-piece of the natural product from a single cross-coupling reaction, we were eager to explore cross-couplings with simpler coupling partners, in hopes to then further functionalize these intermediates and gain access to membranolide **2.1**. We also were drawn to explore more cross-coupling strategies to finish this synthesis because of the vast number of chiral ligands that can be purchased or synthesized, which could be utilized to enhance the stereoselectivity of the α-stereocenter.

2.14.1 Suzuki Strategy

With hopes of discovering a new route to membranolide, we decided to explore the possibility of utilizing a Suzuki Coupling. We envisioned that we could perform a cross-coupling with an allyl boronic ester coupling partner, which would hopefully proceed smoothly under our highly strained system. Upon the success of this idea, we were hoping to oxidatively cleave the alkene, which could be oxidized to a carboxylic acid. This could then be further esterified to furnish the methyl ester that is present in membranolide. We also envisioned that we could screen chiral ligands that would provide high diastereoselectivity in this overall transformation (**Scheme 2.42**).

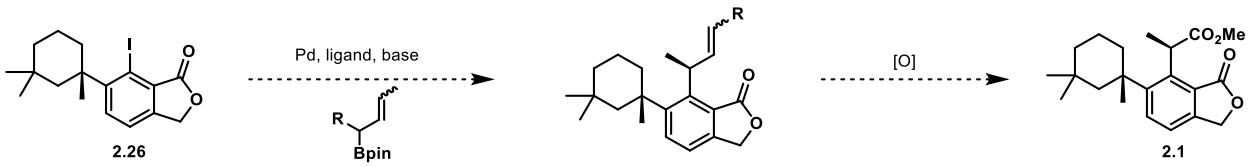

Scheme 2.42: Ideal Suzuki Coupling

When performing a Suzuki coupling with an allyl coupling partner, the coupling partner forms an η-3 complex with the palladium species after transmetallation occurs. This η-3 complex represents the isomerization of a C-Pd bond of the α and γ carbons. If this isomerization is able to proceed forward and backward, the rate of reductive elimination of either species would determine which regioisomer would be the major product.[63] There are well-established ways to activate either of these carbons in an η-3 complex, typically due to steric or electronic effects of the coupling partner and arene, and we were hopeful that we could use this to our advantage (**Scheme 2.43**).

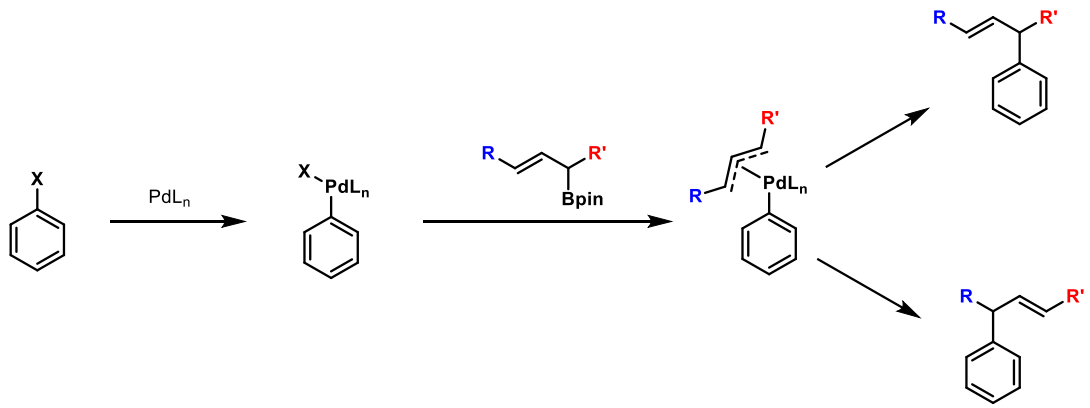

Scheme 2.43: Proposed Rationale for Both Potential Regioisomers

Utilizing this strategy, our next goal was to synthesize the corresponding coupling partner to achieve this transformation. We envisioned that a crotyl coupling partner would be necessary, which could be a symmetric coupling partner **2.88** or an unsymmetric coupling partner **2.89**. If symmetric **2.88** was used, either α or γ product would lead to the desired outcome. We were worried that the synthesis of this coupling partner would be difficult due to its volatility, so we decided to first start with the synthesis of **2.89**. Although **2.89** isn't symmetric, the steric

environment of this transformation should lead to the α-product, which is desired for this transformation (**Scheme 2.44).**

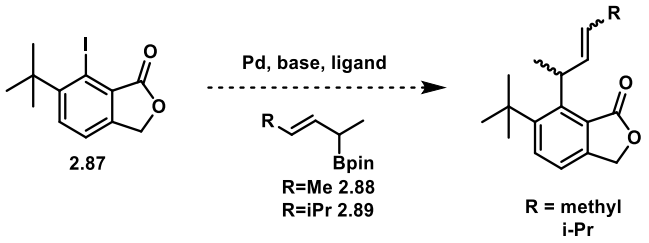

Scheme 2.44: Proposed Suzuki Strategy

We pursued this effort by starting with readily accessible crotyl carbonate **2.91** and converted it into crotyl boronic ester **2.89** (**Scheme 2.45**). For the next step, we were aware that a mixture of regioselectivity could be observed, so we made sure to proceed with caution. Demonstrated in Hall's work,[64] it was apparent that the electronic character of the palladium complex could dictate the regioselectivity of the transformation. Upon transmetallation, we would observe a Pd (II) species, which is already fairly electron poor. If electron poor ligands are also utilized, the complex is even more electron poor, which would increase the rate of reductive elimination. If reductive elimination happens quickly, there is less time for the isomerization between the α and γ carbons to occur, most likely leading to one product. If we use electron rich ligands, this will stabilize the Pd (II) species and allow isomerization to occur; we believed that this was favorable in our system, allowing the sterics of the coupling partner to dictate when reductive elimination occurs and therefore give the desired regioselectivity. Based on this, we decided to first utilize electron rich ligands, like XPhos, for this effort to synthesis **2.91**. Unfortunately, we recovered most of the starting material and were unable to observe any formation of **2.91** (**Scheme 2.45).** We believed that the Pd (II) complex was extremely sterically hindered, which prevented transmetallation from occurring.

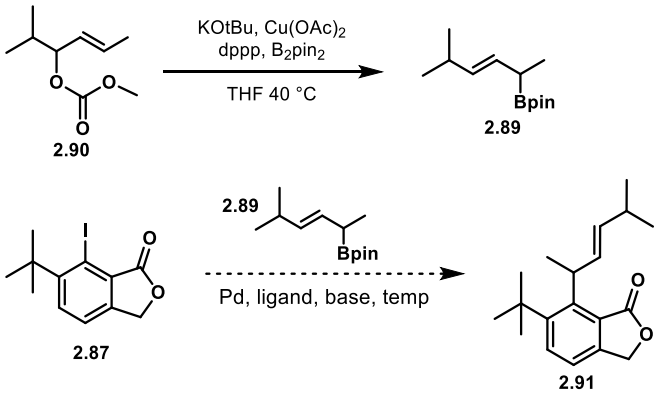

Scheme 2.45: Suzuki Attempt with 2.89

One possible way to solve this would be to convert **2.89** into a boronic acid, which is known to enhance transmetallation. Although this would be reasonable to pursue, we decided to devote our time into utilizing **2.88**, which should also allow us to access our desired intermediate. To do this, we converted crotyl carbonate **2.92** into crotyl boronic ester **2.88.** We then pursued many different conditions to couple **2.87** and **2.88**, but we were ultimately unsuccessful (**Scheme 2.46**).

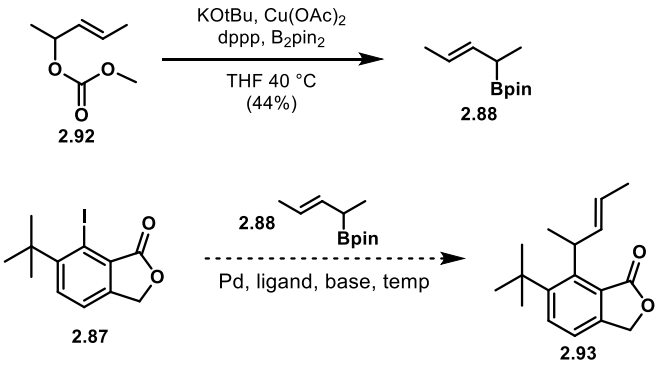

Scheme 2.46: Suzuki Attempt with 2.88

We tried various mono and bidentate phosphine ligands, as well as many different bases and solvents, but still came up short. We hypothesized that the bulky Pd (II) complex was either slowing down the rate of transmetallation or reductive elimination. In order to try to increase the rate of reductive elimination, we utilized ligands with large bite angles,[65] like Xantphos, but weren't able to solve the problem. Again, the next reasonable attempt would be to convert **2.88** to

a boronic acid to enhance the rate of transmetallation, but we didn't think this was worthwhile. We envisioned that the bulkiness of these crotyl coupling partner were too extreme, making it very difficult to achieve the desired carbon-carbon bond formation. At this point, we decided it was worthwhile to focus our efforts elsewhere.

2.14.2 Sonogashira Strategy

Due to the unfortunate attempts utilizing Suzuki couplings, we concluded that it would be extremely difficult to form the desired sp^2-sp^3 bond. A common theme of our work is that steric hinderance has created major roadblocks in our pursuit of membranolide. We envisioned that the use of a small and flat coupling partner was desired, which led us to pursue a Sonogashira coupling. There are many developed methods to convert aryl acetylenes into aryl acrylates, which we decided to explore in hopes to wrap up our synthesis (**Scheme 2.47**). The Zhou group has developed a mild hydrocarboxylation method utilizing formic acid and acetic anhydride.[66] They observed that mono-substituted aryl acetylenes predominantly formed α-substituted acrylic acid products, both in high yield and regioselectivity.[66] We were optimistic that we could utilize this strategy in our synthetic efforts towards **2.1**.

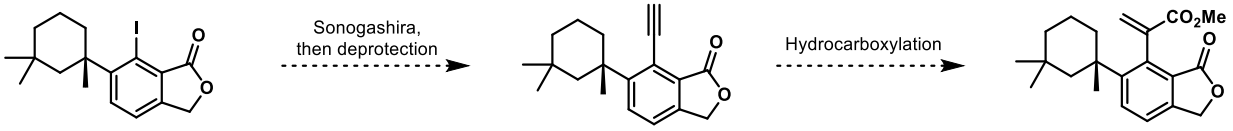

Scheme 2.47: Proposed Route Utilizing Sonogashira Coupling

To see if this approach could work, we started by taking our tBu aryl iodide **2.87** and performed a Sonogashira coupling with TMS-acetylene **2.94**. With minimal screening of solvent, base and palladium catalyst, we were able to rapidly synthesize our aryl acetylene **2.95**. This could rapidly be desilylated upon treatment with K_2CO_3 and methanol to afford the desired terminal alkyne **2.96** in modest yields (**Scheme 2.48**).

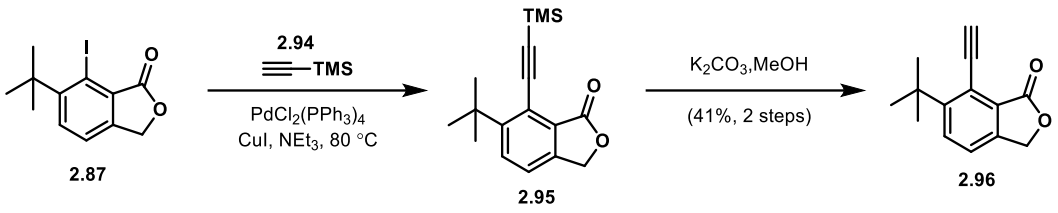

Scheme 2.48: Sonogashira Route to 2.95

With **2.96** in hand, we were now able to utilize Zhou's hydrocarboxylation method. To our delight, we were successful in the synthesis of this acrylic acid, which was then immediately esterified with TMS-diazomethane to afford methyl acrylate **2.97** in 75% yield. All that was left to do was reduce the double bond, which would afford our tBu version of membranolide **2.82**. We were hopeful that the reduction would proceed effortlessly, but we unfortunately didn't have that luxury. Initial attempts to reduce the alkene were with Pd/C, 1 atm of H_2 (balloon) and methanol as our solvent. The reaction was quite difficult to monitor by TLC due to similar retention times of the starting material and product, so we mainly utilized NMR to monitor this transformation. After only observing a portion of the starting material getting consumed, we screened other palladium catalysts, which didn't improve our results at all. Because of this issue, we decided that our next efforts had to be a bit harsher. We were fortunate to utilize a hydrogenator that belonged to USF's CPAS core facility (thanks to Dr. Laurent Calcul), which allowed us to successfully reduce the alkene and form our final product **2.82**. After some brief screening, we found that Pd/C, methanol and H_2 (60 psi) were sufficient to fully reduce the alkene (**Scheme 2.49**)**.** With the successful synthesis of our tBu membranolide **2.82**, our next endeavor would utilize these conditions in pursuit of **2.1**.

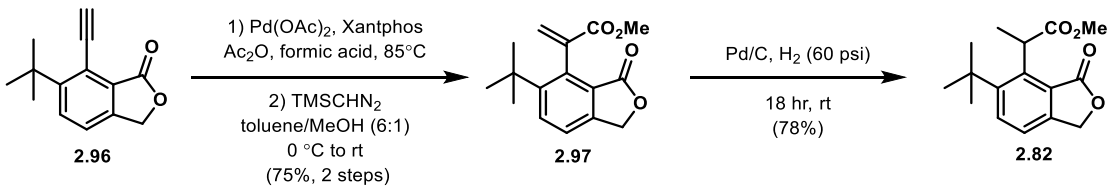

Scheme 2.49: Synthesis of 2.82

To continue with this strategy, were performed a Sonogashira coupling on **2.26** and TMS-acetylene **2.94.** To our delight, we successfully performed the cross coupling to synthesize the desired aryl acetylene, which was then easily desilylated upon treatment with K_2CO_3 and methanol to afford **2.99** (**Scheme 2.50**). This success was a huge relief because of our past difficulties performing cross couplings with **2.26**. The difficulty of our Suzuki strategy compared to the quick success of our Sonogashira strategy was instant confirmation that it was logical to abandon our Suzuki strategy.

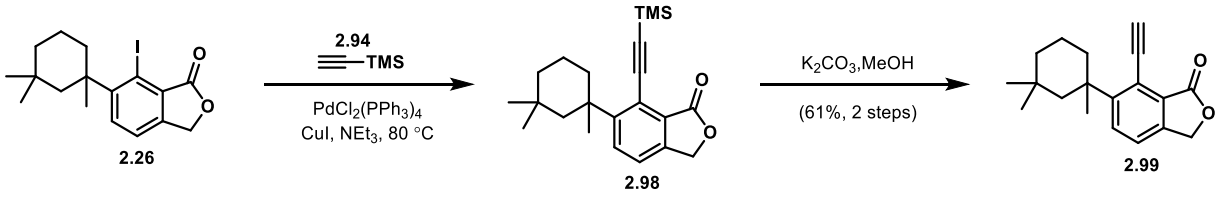

Scheme 2.50: Sonogashira Route to 2.99

With **2.99** in our grasp, our next effort was to perform a hydrocarboxylation to further functionalize this acetylene. Utilizing Zhou's method, followed by esterification, we were successful in our synthesis of **2.7**, but this was unfortunately a minor product, with its regioisomer **2.105** being the major product (**Scheme 2.51**).

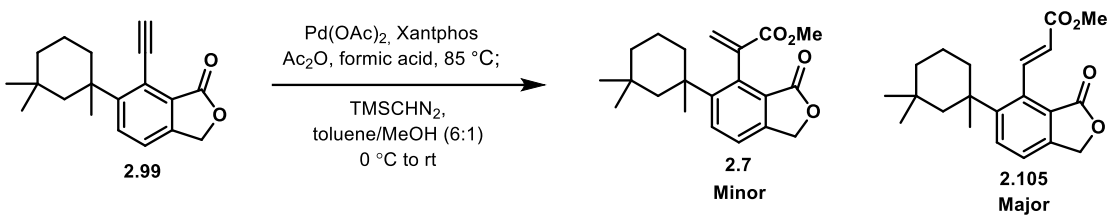

Scheme 2.51: Attempted Hydrocarboxylation of 2.99

It's likely that, again, the steric constraints of this scaffold led to the failure of the desired transformation. It's likely that this catalytic cycle begins with the activation of the alkyne upon coordination with the Pd (0) complex. Next, this complex reacts with formic acid to create **2.102**. The congested character of this palladium complex forces the carbon-palladium bond to be formed at the terminal end; we didn't observe this reactivity with **2.96**, which goes to show how much more hindered the trimethylcyclohexyl moiety is, compared to the tBu moiety. Next, carbon monoxide (which is generated in situ from Ac_2O and formic acid) inserts selectively between the palladium-carbon bond, forming **2.103**. The intermediate undergoes a reductive elimination step, reforming a Pd (0) complex and releasing **2.104**, which readily decomposes into acrylate **2.101** (**Scheme 2.52**).[66]

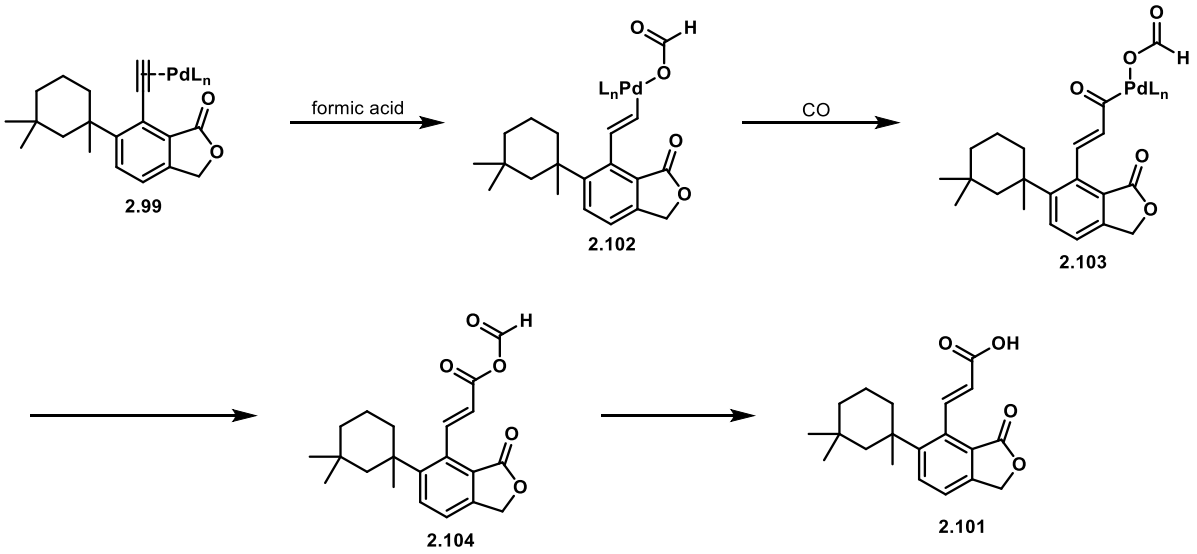

Scheme 2.52: Proposed Route to Undesired Regioisomer 2.101[49]

Unfortunately, we observed that this strategy couldn't enable the synthesis of **2.1**. Although utilizing the tBu model system is useful, we clearly see that it's not a perfect representation of the complex scaffold of **2.1**. Below (**Scheme 2.53**) is a summary of many of the strategies we pursued in our efforts toward **2.1**. Strategies A through D have all been discussed; strategy E was quickly explored, before discovering that this strategy wouldn't work for our system. We were hoping to highlight a nickel-catalyzed reductive cross-coupling (RCC), which has been extensively used by the likes of Reisman, Baran and others.[67,68] This strategy had the possibility to expedite the synthesis of **2.1**, as well as lend itself to the possibility of being pursued asymmetrically. There is a large library of known chiral ligands that have been utilized extensively in nickel-catalyzed RCC reactions. Based on these continued shortcomings, we continue to use these observations as motivation to develop a tactical strategy to finally achieve the asymmetric synthesis of **2.1**.

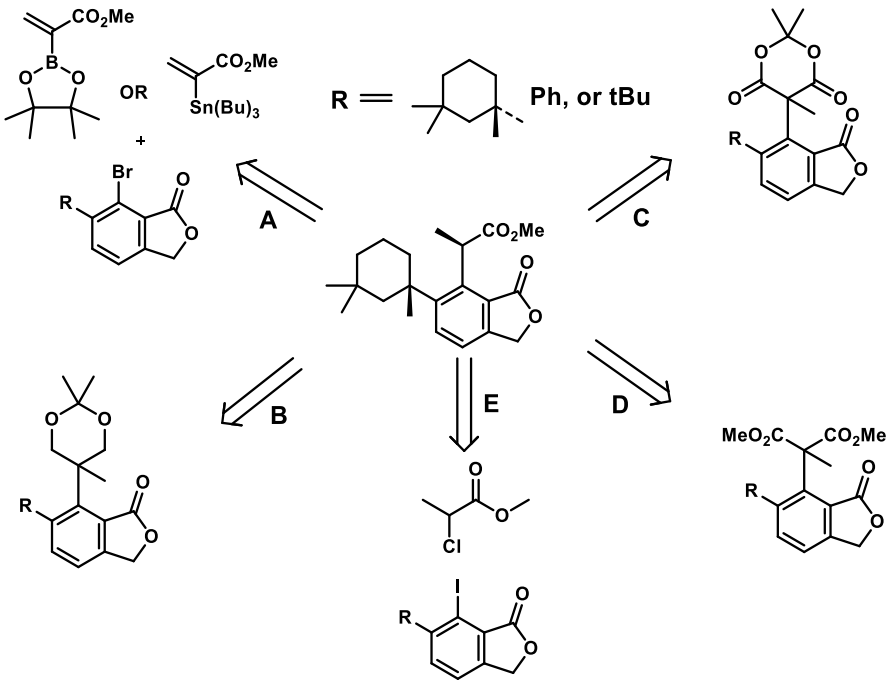

Scheme 2.53: Failed Strategies to Synthesize 2.1

2.15 Simplified Suzuki Attempt

Unfortunately, we still had been unsuccessful in synthesizing membranolide asymmetrically, so we decided to revisit the drawing board. The idea of functionalizing an arene with an allyl group was desired because it could be oxidatively cleaved and quickly converted into an ester. As we witnessed, our initial Suzuki couplings didn't succeed due to overwhelming steric constraints. Based on these efforts, we were intrigued by the possibility of performing a Suzuki coupling with allyl boronic ester **2.106**. This was ideal because the allyl group provides symmetry; if we observed α or γ selectivity, it wouldn't matter because both of those regiochemical outcomes would result in the same product (**Scheme 2.54**)**.** Also, this is a slightly smaller coupling partner, potentially making the reaction easier to perform. Although this strategy is intriguing, it won't allow us to install the second stereocenter during the cross coupling, eliminating any chance of utilizing chiral ligands to achieve high selectivity. Through this route, however, it does allow us to install the methyl group in a different way, compared to our original synthesis. This can possibly provide a new route enabling the asymmetric synthesis of membranolide.

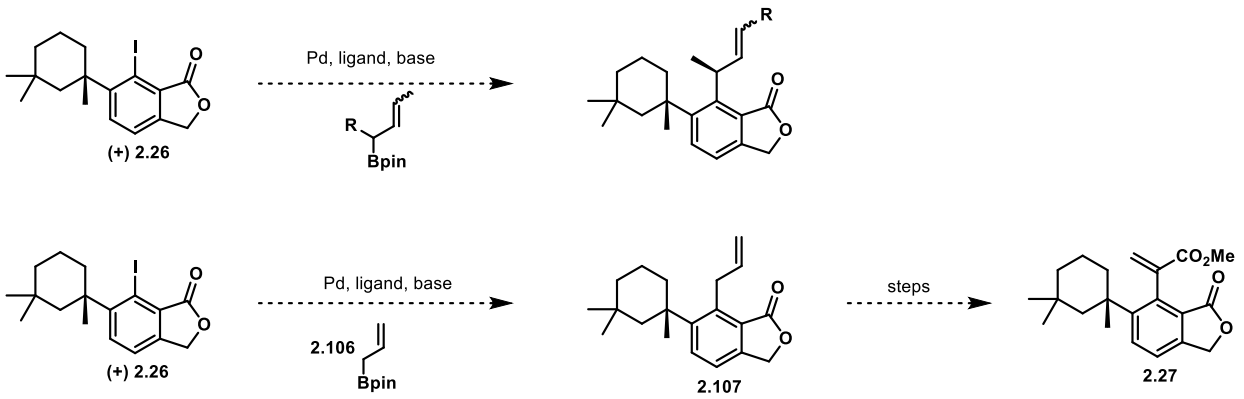

Scheme 2.54: Previous (top) and New (bottom) Approach via Suzuki Coupling

To test out this strategy, we decided it would be beneficial to utilize our tBu model scaffold, to prove that this strategy could be effective. To do this, we started by taking aryl iodide **2.87** and

briefly screened conditions to optimize the desired Suzuki coupling. The reaction proceeded extremely well, but there was a minor amount of protodemetalation product that was inseparable, so we were forced to proceed with the next step with mostly pure material. The next step was an ozonolysis, followed by a reductive work up with Zn^0 and AcOH, which yielded **2.110** in 77% over 2 steps from aryl iodide **2.87** (**Scheme 2.55**).

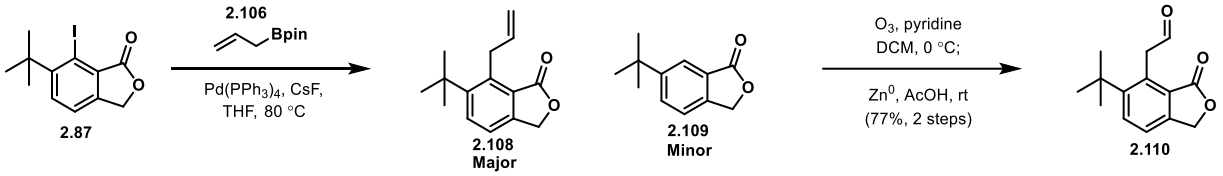

Scheme 2.55: Optimized Suzuki Coupling and Ozonolysis for tBu Model

After synthesizing aldehyde **2.110**, we were now in an interesting situation because we were able to install the final methyl group in a way that is unique to anything else we have tried. In our initial route, we tried to functionalize the α-carbon of a methyl ester, so we were stuck with mostly pursuing enolate chemistry, whether that was a direct methylation or Eschenmoser's alkylation. None of these were successful, so our next efforts were focused on having the methyl group already installed, relying on a decarboxylation step to furnish our desired functionality, shown in the malonate and acetonide approaches. Now, having an aldehyde, we can explore milder reaction conditions through enamine chemistry. We wanted to install an alkene at the α-carbon, so we needed to create an enamine, followed by treatment with a single carbon electrophile. This led us to utilize a system with AcOH, pyrrolidine and formaldehyde (37% aq.), which gave us access to alkene **2.111** in 70% yield. This aldehyde was then easily oxidized to the carboxylic acid through a Pinnick oxidation in high yields. Compound **2.112** was then esterified with TMS-diazomethane to furnish methyl ester **2.97**, which was previously obtained through our Sonogashira efforts. As

previously demonstrated, this alkene could be reduced with Pd/C and H_2 (60 psi) to furnish tBu membranolide **2.82** (**Scheme 2.56**).

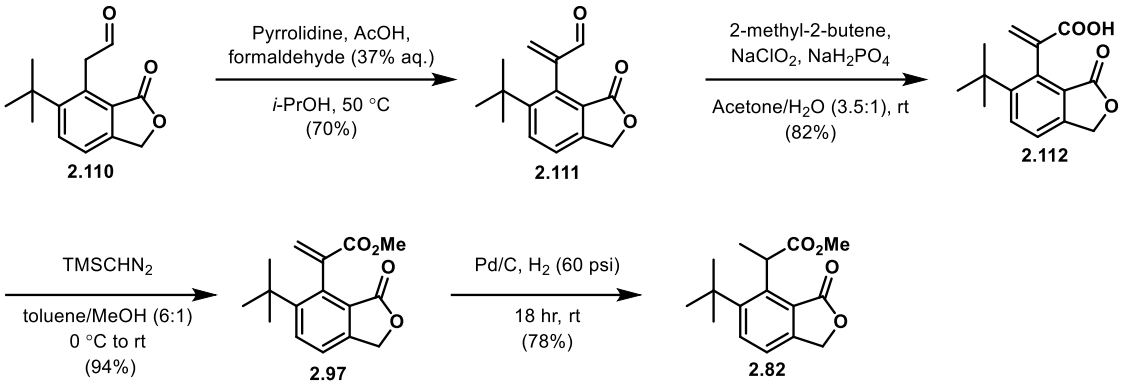

Scheme 2.56: Successful Suzuki Approach to 2.82

Now that we showed this strategy was able to achieve the synthesis of tBu membranolide **2.82**, our next efforts were to use this same strategy to synthesize the desired natural product. We had success with our Sonogashira attempt on the tBu system, which clearly didn't pan out for the synthesis of the natural product. This time, we are hopeful that this route would be more successful for the synthesis of the natural product because many of the transformations are milder. Also, we don't have any late-stage palladium functionalizations (hydrocarboxylation), which was our downfall for the Sonogashira route.

To test these efforts, we started with chiral aryl iodide **2.26** and performed a Suzuki coupling with the allyl boronic ester coupling partner. Even with some reaction optimization, we weren't able to prevent the protodemetalation product from forming. We also, similarly to the model system, couldn't separate the protodemetalation product from our desired product, so we moved forward with both products. We were able to ozonolyze this mixture, yielding our desired aldehyde **2.113** in 62% yield over two steps. (**Scheme 2.57**).

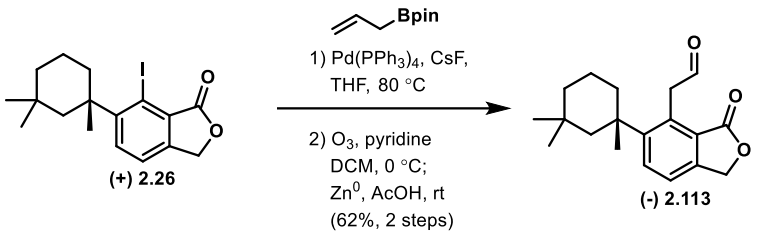

Scheme 2.57: Synthesis of Aldehyde 2.113

Our next goal was to successfully install the alkene on the α-carbon, utilizing enamine chemistry. We attempted this transformation with the conditions that worked well on the tBu system, and we were delighted to see that the reaction proceeded smoothly. We checked the reaction via TLC and saw full consumption of starting material and a clear, major spot that formed. Initial LCMS data showed that it was likely that the major spot was the desired product, but our initial analysis via NMR didn't go as expected. From all sources, what appeared to be a clean and typical transformation ended up providing quite messy ^{1}H and ^{13}C spectra. At this point, we were quite worried that we invested significant time and effort into a route that wouldn't pan out. Fortunately, we were able to crystallize the peculiar molecule, allowing us to obtain a crystal structure (**Scheme 2.58**).

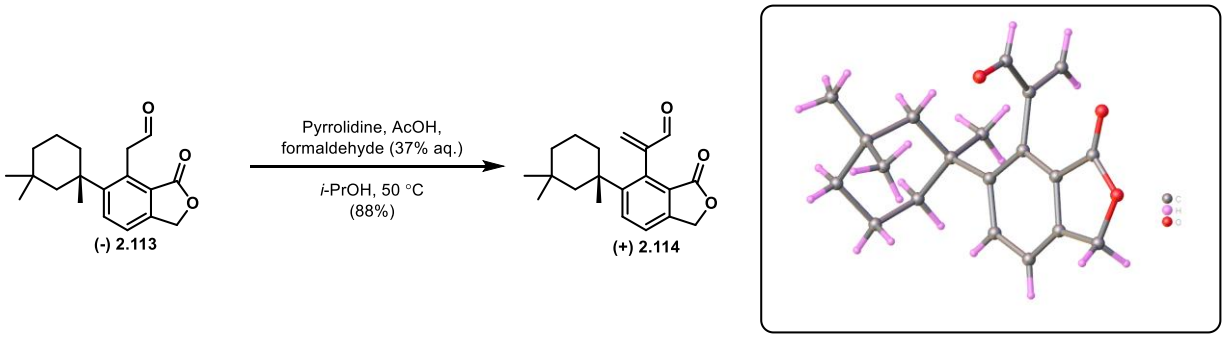

Scheme 2.58: Synthesis and Crystal Structure of 2.114

Through these efforts, we hypothesized that what we were observing was atropisomerism (**Scheme 2.59**). We already had observed that the functionalization of the northern hemisphere of

these scaffolds is difficult, due to their steric constraints. We have also witnessed through multiple crystal structures that the arene group sits in the axial position, which is not what would be expected. The installation of this alkene must have increased the overall steric strain of the molecule enough, that it now forced the molecule to sit in two unique conformations. This strain was sufficient to prohibit free rotation of the molecule. Although this made our NMRs look messy, we were fortunately able to confirm that we successfully synthesized **2.114** and could continue with our efforts.

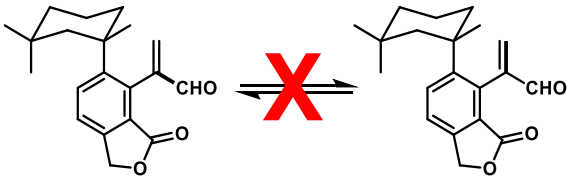

Scheme 2.59: Proposed Atropisomer Conformations of 2.114

After the successful synthesis of **2.114**, we then performed a Pinnick oxidation to furnish acrylic acid **2.115**. When characterizing **2.115**, we also observed atropisomerism, which wasn't unexpected because we wouldn't predict this oxidation to relieve any strain. Next, we esterified **2.115** with TMS-diazomethane to furnish methyl ester **2.7** (**Scheme 2.60**). Unsurprisingly, **2.7** also displayed atropisomerism.

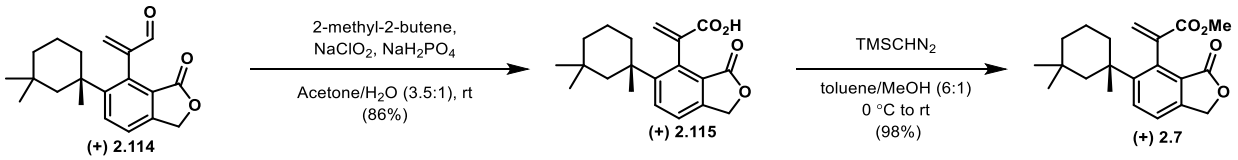

Scheme 2.60: Synthesis of 2.7

Now that we successfully synthesized **2.7**, we were hoping to gain more insight into the energy barrier desired to overcome the observed atropisomerism. We wanted to attempt the final reduction on a system that was fully equilibrated, rather than on a molecule that was stuck in two

confirmations. Our thought was that the reduction would be cleaner if we had complete rotation for all the bonds throughout the molecule. We also figured that it would be easier to rationalize any observations regarding diastereoselectivity if the molecule wasn't stuck in two different conformations throughout the reaction. To test this, we decided to utilize a variable temperature NMR experiment (**Figure 2.11**)**.** In this figure, **A** represents our initial ^{1}H NMR spectrum of **2.7** in $CDCl_3$. To determine if these experiments overcome the energy barrier, we are specifically looking at the peaks for the methyl ester (in the blue box), which is magnified in **B**. If we do not observe full rotation, then we should see two distinct peaks for the methyl ester, with each peak representing a different conformation. If heating our sample allows us to overcome this energy barrier, we should see these peaks turn into one peak. **C** represents our first experiment, which was performed in CD_3CN at 70 °C. Here, we don't see those two peaks converge, telling us that we haven't yet overcome the barrier. **D** and **E** were performed at 75 °C and 79 °C, respectively and both were in CD_3CN. It's clear in both attempts that we are still seeing two distinct methyl ester peaks, showing limited bond rotation up to 79 °C. At this point, we decided to not further pursue more variable temperature NMR experiments; although it would be interesting to learn at what temperature we observe the disappearance of this atropisomerism, temperatures above 79 °C aren't practical for our final reduction because they are typically performed in protic solvents with lower boiling points (methanol, ethanol, etc.) Also, the Yi group performed their final step by utilizing ethanol,[54] so we were hopeful that we could find a set of reaction conditions that would work in our hands.

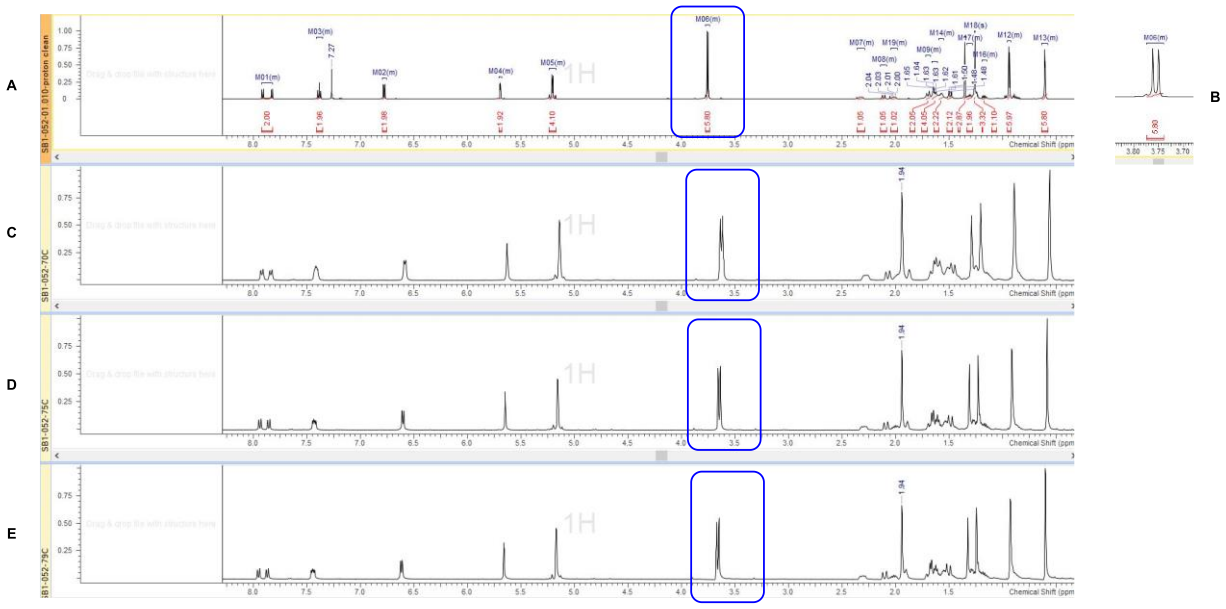

Figure 2.11: Variable Temperature NMR of 2.7

With compound **2.7** in hand and our variable temperature NMR experiments behind us, we were eager to perform the final reduction, which would yield us membranolide **2.1**. First and foremost, we wanted to prove that we were able to reduce this double bond and see what diastereoselectivity we would observe. As mentioned earlier, the Yi group performed a racemic synthesis of membranolide, which intercepted intermediate **2.7**. They observed a 3:1 mixture of diastereomers upon reduction of the double bond and were able to perform this reduction under mild conditions.[54] We were hopeful that we would observe a 3:1 selectivity in favor of the natural product, which could potentially be optimized with the use of an asymmetric reduction catalyst.

To reduce this crucial double bond, our attempts started with mild conditions, consisting of Pd/C, H_2 (1 atm) in methanol. Unfortunately, we observed little to no consumption of our starting material. This wasn't all that surprising because of the issues that we encountered with our previous efforts to reduce the alkene of **2.97**. Next, we decided to utilize the procedure that the Yi group used to obtain membranolide, which was Pd/C, H_2 in ethanol at room temperature. There

wasn't a specific pressure of H_2 listed, so we decided to first try 1 atm. Unfortunately, we also observed little to no consumption of the starting material. Again, this wasn't too surprising, but it was certainly frustrating. After this attempt, we utilized the attempt that was successful for our previous model system. Upon treatment of **2.7** with Pd/C at 60 psi of H_2, we were able to increase the consumption of our starting material slightly, but there wasn't a significant amount of product forming. We also utilized this method with Perlman's catalyst, but it didn't show any significant increase to the reaction rate. Unfortunately, all our initial attempts at this final reduction fell short.

This led us to more harsh methods, utilizing elevated temperatures and pressures. After a brief screen, we found that utilizing a screw cap vial and excess ammonium formate allowed us to observe noticeably higher rates of conversion. Upon treatment with Pd/C, ammonium formate (20 eq) in methanol at 75 °C for 4 days resulted in more than 50% conversion of **2.7** to **2.1**. This material was further treated with the same reaction conditions for 3 days, fully consuming the rest of the starting material, synthesizing membranolide as a 3:2 mixture with its diastereomer **2.32** (via NMR) in 80% yield (**Scheme 2.61**). Now that the alkene was reduced, this transformation decreased enough strain, preventing us from observing any atropisomerism. Noticing that this reaction took 7 days total, we set up the reaction under the same conditions and let it stir for 7 days. We noticed that roughly the same amount of material converted compared to letting the reaction run for 4 days, suggesting that the reaction was stalling out. Although we weren't thrilled with the necessary reaction conditions, we were ecstatic that we finally synthesized membranolide in a favored, although modest selectivity.

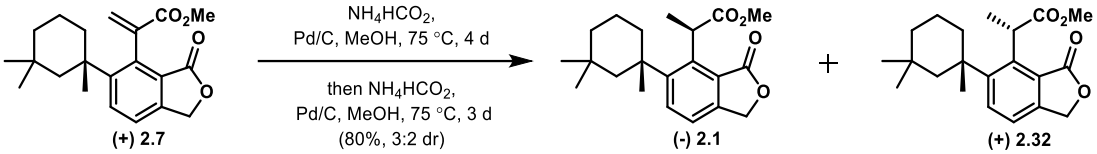

Scheme 2.61: Synthesis of Membranolide

We were able to observe a 3:2 mixture of diastereomers based on our NMR spectra, but we were delighted to be able to easily separate membranolide **2.1** from its diastereomer **2.32** via preparatory TLC (**Figure 2.12**).

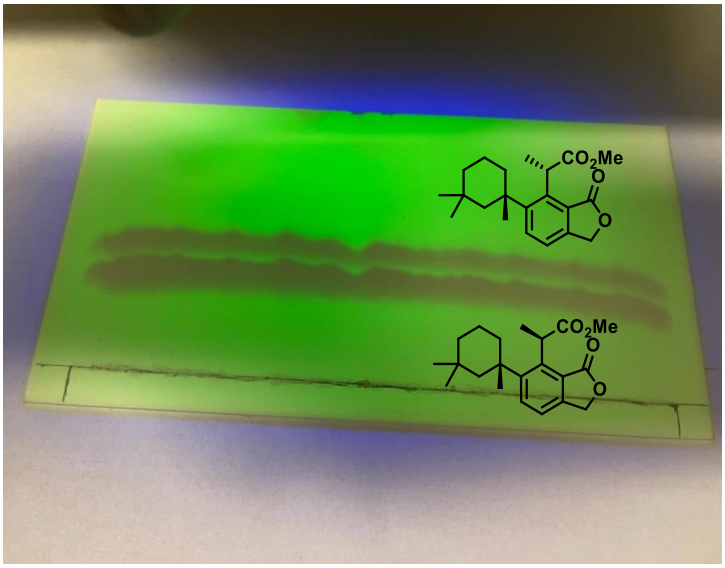

Figure 2.12: Preparatory TLC of Membranolide 2.1 and Diastereomer 2.32

Upon separation of these two diastereomers, we then were successfully able to grow membranolide as a crystal, further confirming the success of our synthesis (**Figure 2.13**), which was the icing on the cake for our efforts.

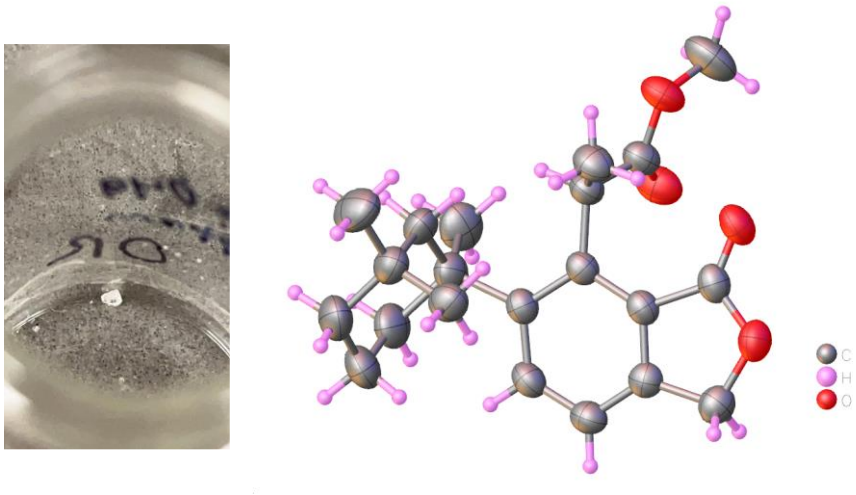

Figure 2.13: Membranolide Crystal and Observed XRD Structure

Now that we have successfully shown that we were able to reduce this capricious alkene, we briefly set our efforts towards asymmetric reductions, with hopes to increase the overall diastereoselectivity. Our initial attempts were with Crabtree's Catalyst. Although Crabtree's Catalyst is achiral, there are many examples of it being used to perform directed reductions of molecules that have existing chirality through chelation of the catalyst.[69,70] After a brief effort, we observed that we were unable to reduce this alkene with Crabtree's Catalyst. We also have investigated alternative reduction methods, specifically utilizing radical HAT chemistry, which would also be achiral;[71] this wouldn't necessarily help our diastereoselectivity issue but could certainly help make our reduction conditions milder.

2.16 Biological Evaluation

As we were pursuing the asymmetric synthesis of **2.1**, we were also able to perform SAR studies against MRSA biofilms. We wanted to study certain functionality that is rather difficult to install and see if it's necessary for bioactivity. One portion of this molecule that complicates our synthetic route is the trimethylcyclohexyl group (highlighted in red), shown in **Figure 2.14**; we

wanted to explore the importance of this group for biofilm eradication. We also wanted to explore the necessity of the chiral methyl group (highlighted in blue) for bioactivity, due to the many challenges we faced installing it, as well as the modest diastereoselectivity observed upon installation of this methyl group.

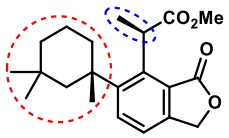

Figure 2.14: Functionality of Interest for SAR Studies of 2.1

The trimethylcyclohexyl moiety is rather greasy, so we envisioned that it was likely sitting in a hydrophobic pocket within its target enzyme. Based off this thinking, we believed that other hydrophobic groups may play the same role as the trimethylcyclohexyl group but be much easier to install. As we saw with our model systems, we can access both phenyl and tBu analogs of **2.1**. Before pursuing the evaluation of these compounds, we wanted to see if it was even necessary to have a hydrophobic group there. Truncated analog **2.116** showed no bioactivity, indicating that the trimethylcyclohexyl moiety is likely important for biofilm eradication. Based on this, we moved on to pursuing the evaluation of other accessible analogs (**Figure 2.15**).

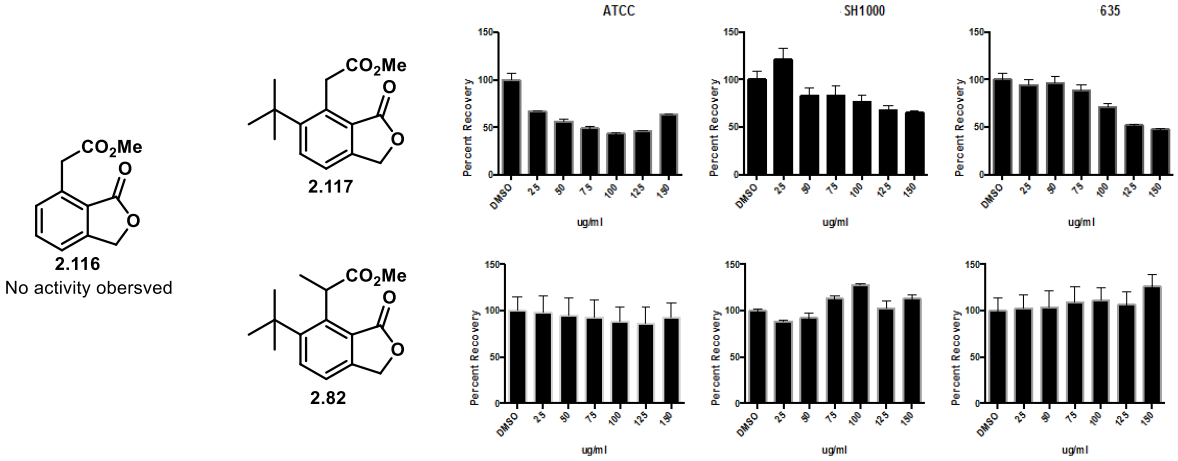

Figure 2.15: SAR Data of tBu Analogs

We went on to explore the replacement of the trimethylcyclohexyl group with other hydrophobic groups, leading us to the evaluation of tBu analogs **2.117** and **2.82**. Something interesting to note was that **2.117** showed higher biofilm eradication against ATCC, compared to **2.82**. This was very exciting because it showed that the α-methyl group may not be required for biofilm eradication, greatly simplifying analog development. Based on this data, we decided to further evaluate **2.117** and **2.1** against a SH1000 strain (**Figure 2.16**). Unfortunately, we observed higher biofilm eradication upon treatment with **2.1**. We were hopeful that structurally simple **2.117** would be more active because it's much easier to access; however, we still have gained valuable insight as to what functionality may be required for biofilm eradication. Our next interest would be to evaluate **2.31** against a MRSA biofilm strain to probe if the α-methyl is beneficial or detrimental to bioactivity. **2.31** is much easier to obtain synthetically than **2.1**, so we are very intrigued by the potential biofilm eradication properties of **2.31**.

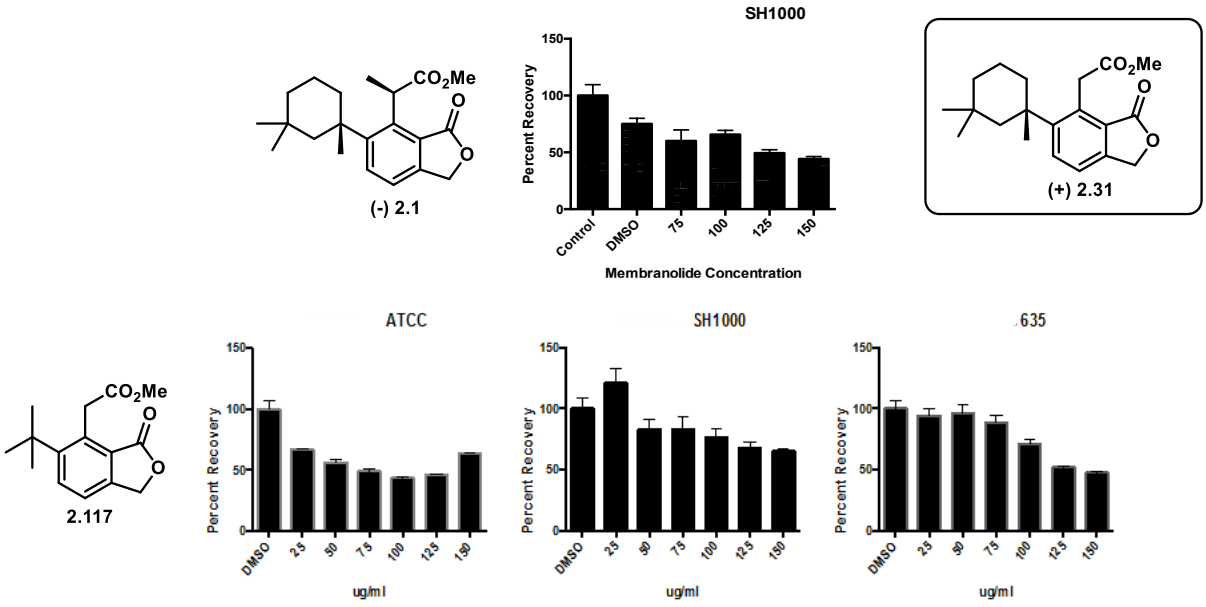

Figure 2.16: Bioactivity of 2.1 and 2.117

2.17 Conclusion and Future Directions

Our group is ecstatic to be the first to achieve an asymmetric total synthesis of **2.1**. Our synthetic route utilized an Ireland-Claisen Rearrangement, an HDDA reaction, as well as an extremely hindered Suzuki cross-coupling reaction. This journey involved the execution of many synthetic strategies, most of which turned out to be unsuccessful. Nonetheless, we continued to persevere and think critically, enabling us to be victorious in our pursuit of **2.1**.

In tandem with our total synthesis efforts, we were able to biologically evaluate **2.1**, as well as other synthetic analogs. We observed that the trimethylcyclohexyl group is required for biofilm eradication, based on the lack of activity of truncated analog **2.116**. We also observed that the α-methyl group may not be required for biofilm eradication, which could greatly alleviate the difficulty to access bioactive analogs. We would like to continue to synthesize and test more analogs to further probe the SAR of **2.1** and its biological activity against MRSA biofilms.

Although we were able to perform SAR studies of **2.1**, we still aren't aware of the mechanism of action of **2.1** against MRSA biofilms. To study this further, we want to synthesize a molecular tool that can help us explore this mechanism of action. By utilizing a photoaffinity probe, we can gain insight into what membranolide's (or similar analogs) biological target is.[72] The desired photoaffinity probe (**Figure 2.17)** consists of functionality that is similar **2.1**, so that it would bind to the same target as **2.1**. In addition to that, it would also contain a diazirine (shown in blue), which covalently crosslinks the probe to the biological target upon UV radiation. The probe would also contain an alkyne (shown in red), which can undergo a click reaction with biotin azide; biotin has a high affinity for avidin, which aids in the isolation of the complex. Finally, we could perform proteomic studies to characterize its biological target. The identification of this target can give us insight into the mechanism of membranolide's anti-biofilm properties, as well as guide the synthesis and evaluation of new small molecules.

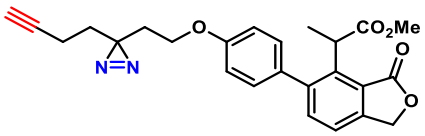

Figure 2.17: Potential Photoaffinity Probe

2.18 Chapter 2 Experimental Procedures

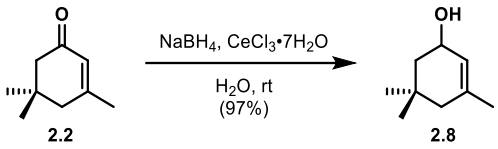

Cerium (III) chloride heptahydrate (9.95 g, 26.7 mmol) was dissolved in H_2O (534 mL). Next, **2.2** (40.0 ml, 267 mmol) was added and was allowed to stir vigorously. Next, sodium borohydride (20.21 g, 534 mmol) was added portion wise to the solution at room temperature, then was allowed to stir at room temperature overnight. Upon completion, the reaction was extracted with CH_2Cl_2

(3 x 300 mL). Next, the organic layer was dried over sodium sulfate, filtered, and concentrated under reduced pressure to yield **2.8** (36.5 g, 260 mmol, 97% yield) as a colorless oil. ^{1}H NMR (500 MHz, $CDCl_3$) δ 5.41 (br s, 1 H), 4.16 - 4.29 (m, 1 H), 1.84 (br d, *J*=17.24 Hz, 1 H), 1.75 (ddd, *J*=12.44, 5.99, 0.95 Hz, 1 H), 1.67 (s, 3 H), 1.60 (br d, *J*=17.30 Hz, 1 H), 1.48 (br s, 1 H), 1.22 (dd, *J*=12.35, 9.11 Hz, 1 H), 0.98 (s, 3 H), 0.87 (s, 3 H) ppm. ^{13}C NMR (126 MHz, $CDCl_3$) δ 136.0, 123.6, 66.8, 45.2, 44.1, 31.2, 31.0, 26.2, 23.5 ppm.

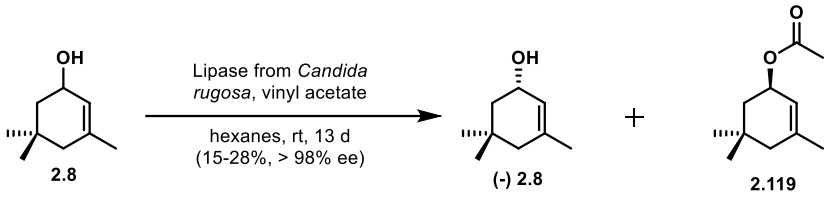

2.8 (35.6 mL, 233 mmol) and vinyl acetate (117 mL, 127 mmol) were dissolved in hexanes (233 mL). The reaction was stirred, then Lipase from *Candida rugosa* (7 g, 20% wt.) was added and the reaction continued to stir at room temperature and under argon for 72 hours. Next, the reaction was filtered through a pad of Celite, then the filtrate was concentrated under reduced pressure. The crude mixture was purified via column chromatography using hexanes/acetone (9:1) to yield **(*S*)-2.8** (17.5 g, 125 mmol, 53.5% yield) with >50% ee. The % ee was increased by subjecting enantio-enriched **(*S*)-2.8** to the same reaction and purification procedures. Round one = 3 days, round 2 = 10 days, round 3 = 3-5days. After a third round of resolution **(*S*)-2.8** (9.21 g, 65.6 mmol, 28% overall yield) was obtained as a clear colorless oil with >98% ee. ^{1}H NMR (500 MHz, $CDCl_3$) δ 5.38-5.45 (m, 1 H), 4.19-4.26 (m, 1 H), 1.84 (br d, *J*=17.24 Hz, 1 H), 1.75 (br dd, *J*=5.96, 12.44 Hz, 1 H), 1.67 (s, 3 H), 1.60 (br d, *J*=17.30 Hz, 1 H), 1.46 (br s, 1 H), 1.22 (dd, *J*=9.11, 12.35 Hz, 1 H), 0.99 (s, 3 H), 0.88 (s, 3 H) ppm. ^{13}C NMR (126 MHz, $CDCl_3$) δ 136.0, 123.6, 66.8, 45.2, 44.1, 31.2, 31.0, 26.2, 23.5 ppm. $[\alpha]^{20}_{D}$ = -23.2 (c = 1, $CHCl_3$). Enantiopurity determination by GCMS using a chiral column (120-Alphadex-chiral) RT: minor = 25 min, r.t. major = 25.4 min.

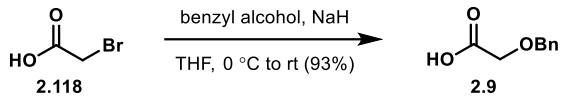

NaH (21.4 g, 534 mmol, 60 wt.%) was suspended in THF (534 mL) and cooled to 0 °C. Benzyl alcohol (28.8 mL, 277 mmol) was added dropwise to the cold solution. The solution was stirred at 0 °C for 30 minutes, then a solution of **2.118** (19.3 g, 139 mmol) in THF (66.7 mL) was added dropwise. The resulting reaction mixture was warmed to room temperature and stirred overnight. Upon completion, the reaction was carefully quenched with water (250 mL) then transferred to a separatory funnel. Saturated aq. $NaHCO_3$ (250 mL) was added, and the aqueous layer was washed with Et_2O (200 mL x 2). The organic layer was discarded, then the aq. layer was acidified using 2M HCl to pH 2. The acidic aq. layer was extracted with Et_2O (250 mL x 3). The organic layer was dried over $MgSO_4$, filtered and concentrated to give **2.9** (21.5 g, 129 mmol, 93% yield) as a light-yellow oil, which was used without further purification. Our data corresponds with the reported literature data.[73] 1H NMR (400 MHz, CDCl3) δ 7.27-7.43 (m, 5 H), 4.65 (s, 2 H), 4.06-4.18 (m, 2 H) ppm.

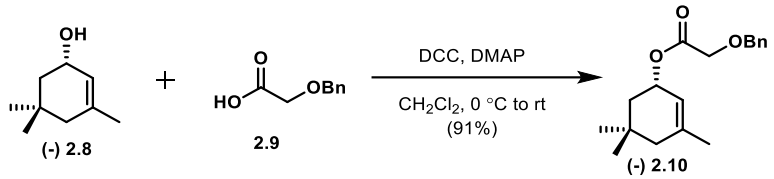

2.9 (10.2 g, 61.2 mmol) was dissolved in CH_2Cl_2 (371 mL). The solution was cooled to 0 °C and (***S***)**-2.8** (7.81 g, 55.6 mmol) was added along with DCC (12.6 g, 61.2 mmol) and DMAP (0.680 g, 5.56 mmol). The reaction was allowed to stir for one hour at 0 °C, then was warmed to room temperature and stirred overnight. Upon completion, the reaction mixture was filtered through celite and rinsed with CH_2Cl_2 (200 mL). The filtrate was concentrated under reduced pressure, then the crude mixture was purified via column chromatography using hexanes/EtOAc (20:1) to

give **2.10** (14.6 g, 50.6 mmol, 91% yield) as a clear colorless oil. ^{1}H NMR (400 MHz, $CDCl_3$): δ 7.27-7.38 (m, 5H), 5.40-5.47 (m, 1H), 5.38 (br s, 1H), 4.62 (s, 2H), 4.05 (s, 2H), 1.82-1.89 (m, 1H), 1.75 (dd, *J* = 12.9, 6.1 Hz, 1H), 1.67 (s, 3H), 1.63-1.70 (m, 1H), 1.40 (dd, *J* = 12.9, 7.9 Hz, 1H), 0.97 (s, 3H), 0.92 (s, 3H) ppm. ^{13}C NMR (101 MHz, $CDCl_3$): δ 170.2, 138.8, 137.2, 128.4, 128.0, 127.9, 118.8, 73.3, 70.8, 67.4, 44.0, 40.6, 30.6, 30.3, 27.0, 23.6 ppm. HRMS m/z: $[M + Na]^+$ Calcd for $C_{18}H_{24}O_3Na$ 311.1618; found 311.1612. $[\alpha]^{20}_D$ = -66.6 (c = 1, $CHCl_3$).

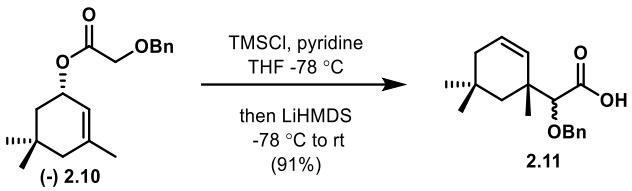

2.10 (9.98 g, 34.7 mmol) was added to a three-neck round bottom flask, then was dissolved in anhydrous THF (510 mL). The reaction was cooled to -78 °C, then TMSCl (40.7 mL, 312 mmol) and pyridine (12.6 mL, 156 mmol) were added via syringe. Next, LiHMDS (173 mL, 173 mmol, 1 M in THF/ethylbenzene) was added dropwise via addition funnel to the solution at -78 °C. Once the addition was complete, the reaction mixture became clear with a yellow tint. The reaction continued to stir at -78 °C for one hour, then was allowed to warm to room temperature and continued to stir overnight. Upon completion, the reaction was quenched with aq. 1M HCl (100 mL) then the THF was removed under reduced pressure. The crude mixture was acidified with aq. 6M HCl to a pH of 2, then extracted with Et_2O (3 x 300 mL). The organic layer was dried over $MgSO_4$, filtered, and concentrated under reduced pressure. The crude oil was purified via column chromatography using hexanes/EtOAc (9:1-2:1) to give **2.11** (9.12 g, 31.6 mmol, 91% yield) as a yellow oil. ^{1}H NMR (400 MHz, $CDCl_3$) δ 7.27-7.36 (m, 5H), 5.66-5.76 (m, 1H), 5.44-5.65 (m, 1H), 4.65 (dd, *J* = 11.5, 3.6 Hz, 1H), 4.44 (dd, *J* = 11.5, 3.0 Hz, 1H), 3.69-3.72 (m, 1H), 1.75-1.83 (m, 2H), 1.67-1.74 (m, 1H), 1.26 (br d, *J* = 14.1 Hz, 1H), 1.14 (s, 3H), 0.95 (s, 3H), 0.89-0.94 (m,

3H) ppm. ^{13}C NMR (101 MHz, $CDCl_3$) δ 174.6, 136.8, 130.4, 128.4, 128.1, 126.9, 126.5, 85.6, 73.4, 43.7, 39.6, 38.4, 31.6, 29.7, 28.7, 23.9 ppm. HRMS m/z: $[M + Na]^+$ Calcd for $C_{18}H_{24}O_3Na$ 311.1618; found 311.1612.

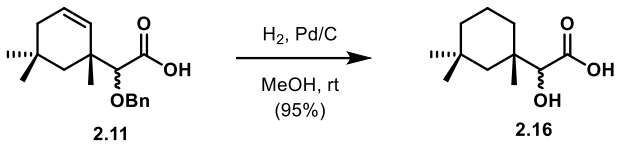

2.11 (7.11 g, 24.6 mmol) and Pd/C (2.62 g, 0.10 eq, 10% wt.) were added to a flask, which was placed under an argon atmosphere. Next, MeOH (123 mL) was added to the flask under argon. The flask was then evacuated and purged with argon two additional times. The flask was then evacuated and replaced with an atmosphere of hydrogen gas via balloon. The reaction mixture was allowed to stir for 24 hours at room temperature. Upon completion, the flask was evacuated and replaced with an atmosphere of argon. Next, the reaction was vacuum filtered through a pad of Celite and rinsed with EtOAc (200 mL). The filtrate was concentrated under reduced pressure to give **2.16** (mixture of diastereomers that were not assigned) (4.71 g, 23.5 mmol, 95% yield) as a yellowish solid that was used without further purification. Purification via column chromatography using hexanes/EtOAc (4:1-2:1) can be used if needed. ^{1}H NMR (400 MHz, $CDCl_3$): δ 6.20 (br s, 2H, COOH and OH), 3.91-3.96 (m, 1H), 1.39-1.54 (m, 3H), 1.31-1.38 (m, 3H), 1.06-1.22 (m, 2H), 0.97-1.01 (m, 3H), 0.95-0.97 (m, 3H), 0.92-0.94 (m, 3H) ppm. ^{13}C NMR (101 MHz, $CDCl_3$): δ 178.5, 78.8, 46.5, 39.2, 38.5, 33.9, 33.3, 30.6, 28.9, 20.8, 18.6 ppm. HRMS m/z: $[M + Na]^+$ Calcd for $C_{11}H_{20}O_3Na$ 223.1305; found 223.1299.

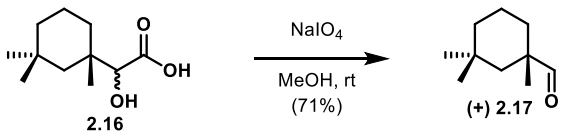

2.16 (2.81 g, 13.9 mmol) was dissolved in degassed methanol (254 mL), then the flask was wrapped with aluminum foil. Next, sodium periodate (2.99 g, 13.9 mmol) was added, and the reaction stirred at room temperature for 12 h. Upon completion, the reaction was quenched with a 1N aq. sodium sulfite solution (35 mL), then poured into a separatory funnel with brine (300 mL). The aq. layer was extracted with Et_2O (3 x 50 mL). The combined organic layers were washed with water (2 x 50 mL), dried over $MgSO_4$, filtered, and very carefully concentrated under reduced pressure to give a crude liquid containing residual solvent. The crude liquid was purified via column chromatography using hexanes/Et_2O (20:1) to give **2.17** (1.52 g, 9.85 mmol, 71% yield) as a clear colorless oil. ^{1}H NMR (500 MHz, $CDCl_3$) δ 9.46 (s, 1H), 2.00-2.09 (m, 1H), 1.73-1.81 (m, 1H), 1.41-1.50 (m, 2H), 1.27-1.35 (m, 1H), 1.14 (d, J = 14.1 Hz, 1H), 1.04-1.11 (m, 1H), 0.95-1.03 (m, 1H), 0.92 (s, 3H), 0.91 (s, 3H), 0.75 (s, 3H) ppm. ^{13}C NMR (126 MHz, $CDCl_3$): δ 206.4, 47.3, 46.3, 38.5, 33.1, 31.5, 30.9, 26.0, 24.9, 19.2 ppm. HRMS m/z: $[M + H]^+$ Calcd for $C_{10}H_{19}O$ 155.1430; found 155.1431. $[\alpha]^{20}_D$ = +14.9 (c = 1, $CHCl_3$).

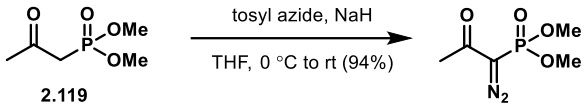

2.119 2.18

2.119 (6.39 mL, 46.2 mmol) was dissolved in anhydrous THF (154 mL) at 0 °C. NaH (2.2 g, 55 mmol, 60% wt.) was then added portion wise and the reaction stirred at 0 °C for 1 h. A solution of tosyl azide (8.20 g, 41.6 mmol) in anhydrous THF (77 mL) was added dropwise to the reaction mixture and the reaction was warmed to room temperature where it stirred for 15 hours. Hexanes (150 mL) was added, and the precipitate was filtered through a pad of Celite. The filter cake was washed with ether (150 mL x 3) and the filtrate was concentrated under reduced pressure to give a crude oil. Further purification via column chromatography using hexanes/EtOAc (2:1 - 1:1.5)

provided **2.18** (7.5 g, 39 mmol, 94% yield) as a bright yellow oil. Our data corresponds with the reported literature data.[74] ^{1}H NMR (400 MHz, CDCl3): δ 3.81 (s, 3H), 3.78 (s, 3H), 2.21 (s, 3H) ppm. ^{13}C NMR (101 MHz, CDCl3): δ 189.7, 53.5, 53.5, 27.1 ppm.

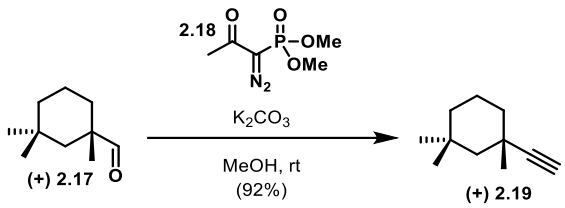

2.17 (2.02 g, 13.1 mmol) was dissolved in degassed MeOH (131 mL), then K_2CO_3 (3.62 g, 26.2 mmol) and **2.18** (3.02 g, 15.7 mmol) were added at room temperature. The reaction was allowed to stir at room temperature overnight. Upon completion, the clear yellow solution was quenched with 5% aqueous $NaHCO_3$ (30 mL), then extracted with ether (4 x 50 mL). The combined organic layers were then washed with brine (30 mL), dried over $MgSO_4$, filtered, and carefully concentrated under reduced pressure to give **2.19** (1.81 g, 12.1 mmol, 92% yield) as a clear colorless oil. The product from the work-up was sufficiently pure and was used without further purification. ^{1}H NMR (400 MHz, $CDCl_3$): δ 2.06 (s, 1H), 1.78 (br d, J = 11.3 Hz, 2H), 1.60 (br d, J = 13.5 Hz, 1H), 1.44-1.51 (m, 1H), 1.39 (br d, J = 13.1 Hz, 1H), 1.19 (s, 3H), 1.14 (s, 3H), 0.96-1.09 (m, 3H), 0.85 (s, 3H) ppm. ^{13}C NMR (101 MHz, $CDCl_3$): δ 92.6, 68.6, 50.6, 39.8, 39.2, 34.4, 32.7, 31.3, 31.0, 26.2, 20.1 ppm. HRMS m/z: $[M - H]^-$ Calcd for $C_{11}H_{17}$ 149.1336; found 149.1334. $[\alpha]^{20}_D$ = +7.2 (c = 1, $CHCl_3$).

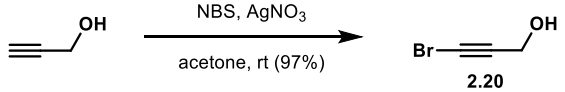

Propargyl alcohol (4.11 g, 73.3 mmol) was dissolved in acetone (146 mL) at room temperature. Next, NBS (15.6 g, 88.1 mmol) and $AgNO_3$ (1.24 g, 7.31 mmol) were added, and the reaction was

stirred at room temperature for two hours. Upon completion, the solvent was evaporated under reduced pressure. The crude oil was adsorbed onto silica gel and purified by silica gel column chromatography using a gradient of hexanes/EtOAc (20:1-5:1) to give **2.20** (9.58 g, 71.0 mmol, 97% yield) as a light-yellow oil. Our data corresponds with the reported literature data.[75] ^{1}H NMR ($CDCl_3$, 400 MHz): δ 4.27 (s, 2 H), 1.86 (s, 1 H) ppm. ^{13}C NMR ($CDCl_3$, 101 MHz): δ 78.2, 51.8, 45.8 ppm.

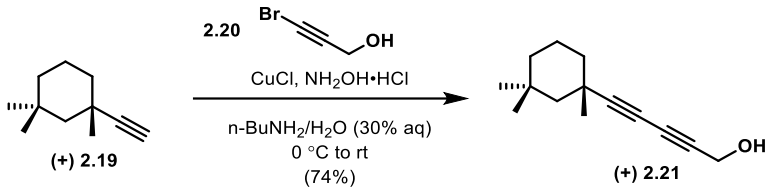

CuCl (9.4 mg, 0.095 mmol, 0.020 eq.) was added to a flask, then was suspended in 30% aq. n-butylamine (11 mL). The solution turned blue, and the flask was stirred until most of the CuCl had dissolved. Next, a spatula tip of $NH_2OH{\cdot}HCl$ was added, and the solution turned clear and colorless. The mixture was then cooled to 0 °C and put under an argon atmosphere, followed by the addition of a cold solution of **2.19** (0.711 g, 4.73 mmol) in THF (2 mL). The reaction mixture turned bright yellow, and a precipitate formed. After 2 minutes, **2.20** (0.766 g, 0.403 mL, 5.68 mmol) was added in one portion along with another small scoop of $NH_2OH{\cdot}HCl$. The reaction continued to stir at 0 °C. Whenever the reaction turned blue or green in color, a small amount of $NH_2OH{\cdot}HCl$ was added, which turned the reaction yellow again. The reaction was completed once the mixture turned amber in color. Upon completion the reaction mixture was quenched with saturated aq. NH_4Cl (30 mL), then was extracted with ether (3 x 25 mL). The combined organic layers were dried over $MgSO_4$, filtered, and concentrated under reduced pressure to give a crude oil. The crude was purified via column chromatography using hexanes/EtOAc (5:1) to give **2.21** (0.712 g, 3.48 mmol, 74% yield) as a yellow oil. ^{1}H NMR (400 MHz, $CDCl_3$): δ 4.32 (s, 2H), 1.79-

1.87 (m, 1H), 1.67-1.78 (m, 1H), 1.62 (br d, J = 13.6 Hz, 1H), 1.47-1.53 (m, 1H), 1.41 (br dd, J = 13.2, 1.5 Hz, 1H), 1.21 (s, 3H), 1.13 (s, 3H), 0.97-1.11 (m, 4H), 0.87 (s, 3H) ppm. ^{13}C NMR (101 MHz, $CDCl_3$): δ 89.0, 74.3, 71.0, 65.0, 51.6, 50.6, 39.6, 39.0, 34.2, 32.0, 31.9, 31.2, 26.0, 20.3 ppm. HRMS m/z: $[M + K]^+$ Calcd for $C_{14}H_{20}OK$ 243.1146; found 243.1151. $[\alpha]^{20}_D$ = +16.0 (c = 1, $CHCl_3$).

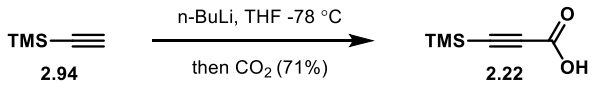

In a 250 mL round-bottomed flask equipped with a stir bar was added **2.94** (5.81 mL, 40.7 mmol) in anhydrous THF (100 mL) at -78 °C. n-BuLi (25.5 mL, 40.7 mmol, 1.6 M in hexanes) was added dropwise and the cold solution stirred for 30 min at -78 °C. The cooling bath was removed, and the CO_2 bubbled through the solution for 30 min. The reaction mixture continued to stir for 30 min at room temperature then Et_2O (80 mL) was added along with water (90 mL) and 1 N HCl (45 mL). The layers were separated, and the aqueous layer was extracted with Et_2O (3 x 50 mL). The combined organic layers were dried over $MgSO_4$, filtered and concentrated to give a thick yellow oil. Further purification via column chromatography using hexanes/EtOAc (2:1) provided **2.22** (4.2 g, 29 mmol, 71% yield) as a thick opaque oil. Our data corresponds with the reported literature data.[76] ^{1}H NMR (400 MHz, $CDCl_3$): δ 9.54 (br s, 1H), 0.24 (s, 9H) ppm.

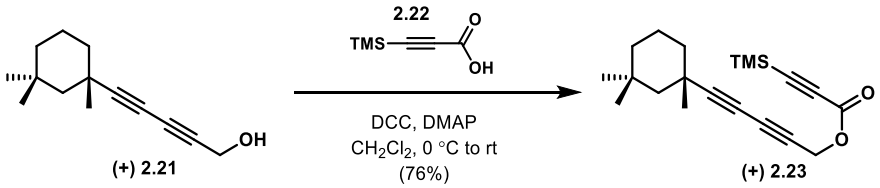

2.22 (0.398 mL, 3.08 mmol) was dissolved in CH_2Cl_2 (25.6 mL), then the mixture was cooled to 0 °C. Next, **2.21** (0.484 g, 2.37 mmol), DCC (0.551 g, 2.67 mmol) and DMAP (0.0131 g, 0.103 mmol) were added, and the reaction was stirred at 0 °C for 30 minutes. The reaction was then

warmed to room temperature and stirred overnight. Upon completion, the reaction was filtered through a fritted funnel and rinsed with CH_2Cl_2 (15 mL). The filtrate was then concentrated under reduced pressure to give an oily solid that was further purified via column chromatography using hexanes/EtOAc (25:1) to give **2.23** (0.592 g, 1.80 mmol, 76% yield) as a clear light-yellow oil. ^{1}H NMR (400 MHz, $CDCl_3$): δ 4.80 (s, 2H), 1.81 (br d, *J* = 13.0 Hz, 1H), 1.65-1.77 (m, 1H), 1.61 (br d, *J* = 13.5 Hz, 1H), 1.46-1.54 (m, 1H), 1.40 (br d, *J* = 13.1 Hz, 1H), 1.19 (s, 3H), 1.11 (s, 3H), 0.98-1.09 (m, 3H), 0.86 (s, 3H), 0.24 (s, 9H) ppm. ^{13}C NMR (101 MHz, $CDCl_3$): δ 152.0, 95.7, 93.6, 89.7, 72.6, 68.7, 64.8, 53.9, 50.6, 39.5, 39.0, 34.1, 32.0, 31.9, 31.2, 26.0, 20.2, -1.0 ppm. HRMS m/z: $[M + H]^+$ Calcd for $C_{20}H_{29}O_2Si$ 329.1931; found 329.1928. $[\alpha]^{20}_D$ = +44.9 (c = 0.91, $CHCl_3$).

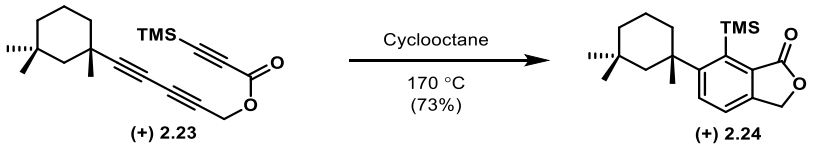

2.23 (0.198 g, 0.603 mmol) was dissolved in freshly distilled and degassed cyclooctane (121 mL) in a reaction vial. The reaction mixture was purged with argon and capped tightly. The reaction was heated to 170 °C and allowed to stir for 72 hours. Upon completion, the reaction was cooled to room temperature and filtered through a pad of silica gel. The silica plug was rinsed with hexanes to elute off any additional cyclooctane. Next, EtOAc was used to elute the remainder of the reaction mixture, which was then concentrated under reduced pressure. The crude was purified via column chromatography using hexanes/EtOAc (20:1) to give **2.24** (0.145 g, 0.439 mmol, 73% yield) as a yellow oil. ^{1}H NMR (400 MHz, $CDCl_3$): δ 7.72 (d, *J* = 8.2 Hz, 1H), 7.31 (d, *J* = 8.2 Hz, 1H), 5.22 (s, 2H), 2.32 (br d, *J* = 7.2 Hz, 1H), 2.24 (br d, *J* = 13.9 Hz, 1H), 1.45-1.55 (m, 4H), 1.40 (s, 3H), 1.15-1.25 (m, 2H), 0.88 (s, 3H), 0.53 (s, 9H), 0.12 (s, 3H) ppm. ^{13}C NMR (101 MHz, $CDCl_3$): δ 171.8, 157.3, 144.2, 143.1, 132.1, 131.1, 121.2, 68.3, 53.9, 40.3, 40.0, 39.5, 35.3, 33.2,

31.6, 27.4, 19.7, 5.8 ppm. HRMS m/z: $[M + H]^+$ Calcd for $C_{20}H_{31}O_2Si$ 331.2088; found 331.2093. $[\alpha]^{20}_D = +16$ (c = 1, $CHCl_3$).

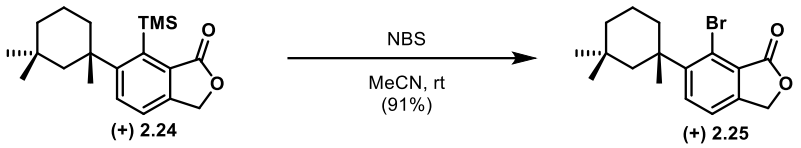

2.24 (0.0512 g, 0.154 mmol) was added to a scintillation vial, then dissolved in ACN (2.2 mL) at room temperature. The vial was wrapped with aluminum foil, then NBS (0.055 g, 0.31 mmol) was added to the solution. The reaction was purged with argon and allowed to stir at room temperature for 24 hours. Upon completion, the solvent was removed under reduced pressure and the crude solid was purified via column chromatography (Hex/EtOAc, 6:1) to give **2.25** (0.048 g, 0.14 mmol, 91% yield) as a white solid. ^{1}H NMR (400 MHz, $CDCl_3$): δ 7.79 (d, *J* = 8.2 Hz, 1H), 7.37 (d, *J* = 8.2 Hz, 1H), 5.18 (s, 2H), 3.28 (br d, *J* = 14.3 Hz, 1H), 2.31-2.42 (m, 1H), 1.67 (br dd, *J* = 9.3, 4.4 Hz, 2H), 1.46 (s, 3H), 1.18-1.36 (m, 4H), 0.90 (s, 3H), 0.36 (s, 3H) ppm. ^{13}C NMR (101 MHz, $CDCl_3$): δ 168.9, 148.6, 146.3, 134.5, 125.7, 121.9, 120.6, 66.5, 47.0, 40.8, 40.3, 39.5, 33.1, 31.4, 30.3, 25.8, 19.8 ppm. HRMS m/z: $[M + H]^+$ Calcd for $C_{17}H_{22}O_2Br$ 337.0798; found 337.0803. $[\alpha]^{20}_D = +23$ (c = 1, $CHCl_3$). MP = 141-142 °C.

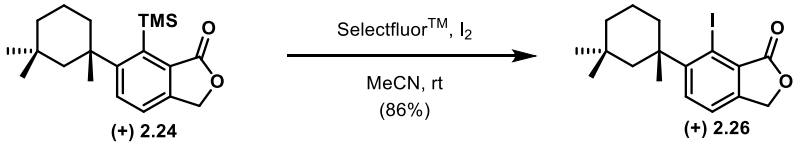

2.24 (0.015 g, 0.045 mmol) was added to a scintillation vial, then was dissolved in acetonitrile (0.5 mL) at room temperature. Next, Selectfluor™ (0.032 g, 0.091 mmol) and I_2 (0.012 g, 0.045 mmol) were added, then the vial was purged with argon and stirred at room temperature for 2 hours. Upon completion, the reaction was quenched with saturated aq. $Na_2S_2O_3$ and extracted with EtOAc (3 x

20 mL). The combined organic layers were dried over $MgSO_4$, filtered, and concentrated under reduced pressure. The crude oil was purified via column chromatography using hexanes/EtOAc (8:1) to give **2.26** (0.015 g, 0.039 mmol, 86% yield) as a yellow oil. ^{1}H NMR (400 MHz, $CDCl_3$): δ 7.74 (d, *J* = 8.2 Hz, 1H), 7.38 (d, *J* = 8.2 Hz, 1H), 5.11 (s, 2H), 3.53 (br d, *J* = 14.5 Hz, 1H), 2.38 (br d, *J* = 15.1 Hz, 1H), 1.62-1.72 (m, 2H), 1.52 (s, 3H), 1.22-1.32 (m, 4H), 0.90 (s, 3H), 0.33 (s, 3H) ppm. ^{13}C NMR (101 MHz, $CDCl_3$): δ 169.9, 151.0, 146.0, 133.8, 128.4, 121.4, 94.2, 65.7, 46.6, 41.4, 40.8, 39.7, 32.9, 31.5, 30.5, 26.0, 19.9 ppm. HRMS m/z: $[M + Na]^+$ Calcd for $C_{17}H_{22}O_2INa$ 407.0478; found 407.0478. $[\alpha]^{20}_D = +21$ (c = 1, $CHCl_3$).

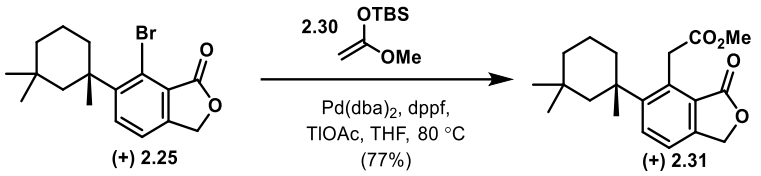

$Pd(dba)_2$ (2.53 mg, 4.41 μmol), dppf (4.89 mg, 8.82 μmol) and thallium (I) acetate (0.029 g, 0.11 mmol) were added to a reaction vial, then suspended in anhydrous and degassed THF (0.25 mL). The mixture was allowed to stir for 5 minutes at room temperature, then a solution of **2.25** (0.019 g, 0.055 mmol) and **2.30** (0.032 g, 0.17 mmol) in anhydrous and degassed THF (0.25 mL) was added to the reaction mixture. The reaction was then purged with argon, capped tightly, and heated to 80 °C for 15 hours. Upon completion, the reaction was cooled to room temperature, then diluted with Et_2O (20 mL) and filtered through a pad of Celite. The filtrate was concentrated under reduced pressure, then was purified via column chromatography using hexanes/EtOAc (6:1) to give **2.31** (0.014 g, 0.042 mmol, 77% yield) as a pale-yellow oil. ^{1}H NMR (400 MHz, $CDCl_3$) δ 7.76 (d, *J* = 8.2 Hz, 1H), 5.20 (s, 2H), 4.47 (br d, *J* = 7.1 Hz, 2H), 3.70 (s, 3H), 2.23 (br d, *J* = 14.0 Hz, 1H), 2.01 (br d, *J* = 13.8 Hz, 1H), 1.61-1.82 (m, 2H), 1.48 (br d, *J* = 13.8 Hz, 2H), 1.30 (s, 3H), 1.26 (br d, *J* = 7.5 Hz, 3H), 0.88 (s, 3H), 0.38 (s, 3H) ppm. ^{13}C NMR (101 MHz, $CDCl_3$): δ 171.3, 171.2,

148.9, 144.6, 134.1, 132.7, 126.0, 120.5, 68.1, 52.0, 50.9, 40.1, 39.2, 35.2, 32.4, 31.9, 31.5, 29.7, 27.6, 19.8 ppm. HRMS m/z: $[M + Na]^+$ Calcd for $C_{20}H_{26}O_4Na$ 353.1723; found 353.1721. $[\alpha]^{20}_D$= +2.3 (c = 1, $CHCl_3$).

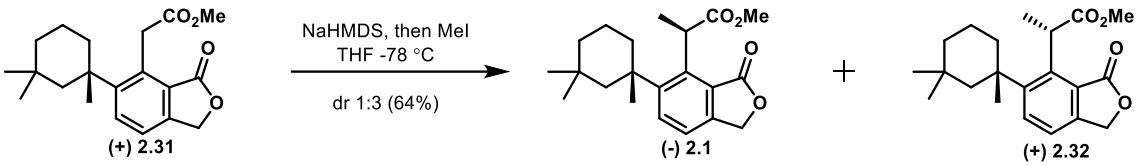

2.99 (0.012 g, 0.036 mmol) was added to a flask, then was dissolved in anhydrous THF (0.4 mL) and cooled to -78 °C. Next, NaHMDS (0.054 mL, 0.044 mmol, 0.8 M) was added dropwise and then the reaction was allowed to stir for 1 hour at -78 °C. Next, MeI (2.95 µL, 0.0471 mmol) was added and the reaction was allowed to stir for 1 hour at -78 °C, then was warmed to room temperature and allowed to stir for an additional for 2 hours. Upon completion, the reaction was quenched with saturated aq. NH_4Cl (5 mL) and water (3 mL). The aqueous phase was extracted with Et_2O (4 x 10 mL), dried over $MgSO_4$, filtered, and concentrated under reduced pressure to give a crude oil that was further purified via column chromatography using hexanes/EtOAc (10:1) to give **2.1** and **2.32** (8.05 mg, 0.023 mmol, 64% yield) as a mixture of diastereomers (1:3 based on crude NMR). Full experimental data for **2.1** and **2.32** are listed later in this experimental section.

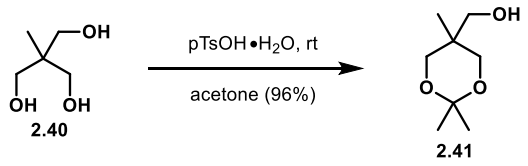

2.40 (5.0 g, 42 mmol) and a small scoop of pTsOH-H_2O (catalytic) were dissolved in Acetone (78 mL) and the solution was stirred at room temperature overnight. Upon completion, the reaction mixture was neutralized with sodium carbonate (0.115 g, 1.08 mmol), then sodium sulfate was added. The reaction mixture was filtered, then concentrated under reduced pressure. The crude was

then purified via column chromatography using hexanes/EtOAc (1:1) to give **2.41** (6.4 g, 40 mmol, 96% yield) as a clear oil. ^{1}H NMR (600 MHz, $CDCl_3$): δ 3.70 (s, 2H), 3.7-3.7 (d, *J*=12.0 Hz, 2H), 3.6-3.6 (d, *J*=12.0 Hz, 2H), 1.94 (br s, 1H), 1.45 (s, 3H), 1.40 (s, 3H), 0.83 (s, 3H) ppm. ^{13}C NMR (151 MHz, $CDCl_3$): δ 98.0, 66.4, 66.1, 34.7, 31.0, 27.3, 20.1, 17.6 ppm. HRMS m/z: $[M + Na]^+$ Calcd for $C_8H_{16}O_3Na$ 183.0992; found 183.0988.

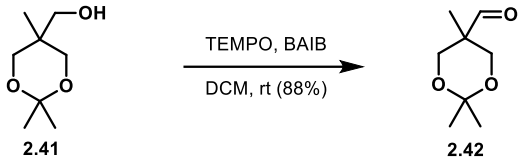

2.41 2.42

2.41 (6.2 g, 39 mmol) was dissolved in DCM (148 mL), then TEMPO (0.302 g, 1.94 mmol) and BAIB (13.7 g, 42.6 mmol) were added to the solution at room temperature. The solution was purged with argon and allowed to stir overnight. Sodium bicarbonate (4.88 g, 58.0 mmol) was added, and the reaction was stirred for 10 minutes. The reaction was filtered, then concentrated under reduced pressure. The crude was then purified via column chromatography using hexanes/EtOAc (20:1) to give **2.42** (5.4 g, 34 mmol, 88% yield) as a clear oil. ^{1}H NMR (600 MHz, $CDCl_3$): δ 9.77 (s, 1H), 4.08 (d, *J*=12.0 Hz, 2H), 3.75 (d, *J*=12.7 Hz, 2H), 1.45 (s, 3H), 1.33 (s, 3H), 0.85 (s, 3H) ppm. ^{13}C NMR (151 MHz, $CDCl_3$): δ 204.5, 98.1, 65.0, 45.2, 27.6, 19.4, 14.8 ppm. HRMS m/z: $[M + Na]^+$ Calcd for $C_8H_{14}O_3Na$ 181.0835; found 181.0813.

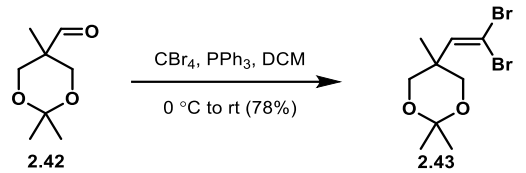

2.42 2.43

PPh_3 (14.1 g, 53.6 mmol) was dissolved in DCM (38.9 mL), then cooled to 0 °C. Next, CBr_4 (8.89 g, 26.8 mmol) was added to the solution and stirred at 0 °C for 10 minutes. Next. **2.42** (2.12 g, 13.4 mmol) in DCM (3.89 mL) was added dropwise at 0 °C, then the reaction was warmed to room

temperature. The solution was stirred for three hours, then diluted with hexanes (100 mL), forming a precipitate. The mixture was filtered, then the filtrate was concentrated under reduced pressure. The crude was then purified via column chromatography using hexanes/EtOAc (20:1) to give **2.43** (3.27 g, 10.4 mmol, 78% yield) as a clear oil. ^{1}H NMR (600 MHz, $CDCl_3$): δ 6.70 (s, 1H), 3.94 (d, *J*=11.6 Hz, 2H), 3.64 (d, *J*=11.6 Hz, 2H), 1.43 (s, 3H), 1.41 (s, 3H), 1.24 (s, 3H) ppm. ^{13}C NMR (151 MHz, $CDCl_3$): δ 141.2, 98.0, 87.9, 68.0, 38.3, 25.1, 22.3, 17.8 ppm. HRMS m/z: $[M + Na]^+$ Calcd for $C_9H_{14}O_2Br_2Na$ 334.9253; found 334.9246.

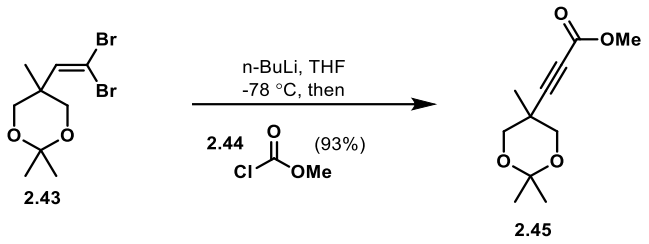

2.43 (0.501 g, 1.59 mmol) was dissolved in THF (9.20 mL) and cooled to -78 °C. Next, n-BuLi (3.72 mL, 5.57 mmol 1.5 M in hexanes) was added to the reaction dropwise. The reaction was stirred at -78 °C. for 20 minutes, then was warmed up to room temperature and stirred for an additional 15 minutes. Next, the solution was cooled back down to -78 °C and **2.44** (0.617 mL, 7.96 mmol) was added dropwise. The solution was stirred for 45 minutes at -78 °C, then was warmed to room temperature and stirred for an additional hour. Upon completion, the reaction was diluted with water and extracted with EtOAc (3 x 50 mL). The organic layer was washed with brine, dried over Na_2SO_4, filtered, and concentrated under reduced pressure. The crude was then purified via column chromatography using hexanes/EtOAc (20:1) to give **2.45** (0.315 g, 1.48 mmol, 93% yield) as a clear oil. ^{1}H NMR (600 MHz, $CDCl_3$): δ 3.85 (d, *J*=12.0 Hz, 2H), 3.64 (s, 3H), 3.51 (d, *J*=12.4 Hz, 2H), 1.33 (s, 3H), 1.29 (s, 3H), 1.26 (s, 3H) ppm. ^{13}C NMR (151 MHz, $CDCl_3$): δ 153.9, 98.3, 90.1, 74.4, 67.7, 52.7, 31.1, 25.4, 21.6, 20.5 ppm. HRMS m/z: $[M + Na]^+$

Calcd for $C_{11}H_{16}O_4Na$ 235.094; found 235.0935.

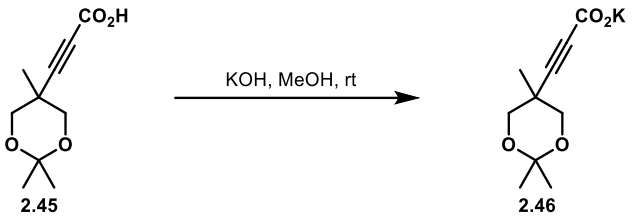

2.45 2.46

2.45 (1.8 g, 8.48 mmol) was dissolved in MeOH (9.94 mL), then KOH (0.952 g, 16.9 mmol) was added. The reaction was stirred at room temperature overnight. Upon completion, the reaction was cooled to 0 °C, then was carefully neutralized to pH 8 by dropwise addition of 6M HCl. Next, the solution was concentrated under reduced pressure to yield potassium **2.46**, which was sufficiently pure and used in the next step without further purification. ^{1}H NMR (DMSO-d_6, 400 MHz) δ 3.76 (d, *J*=11.0 Hz, 2H), 3.47 (d, *J*=11.8 Hz, 2H), 1.35 (s, 3H), 1.29 (s, 3H), 1.22 (s, 3H) ppm. ^{13}C NMR (DMSO-d_6, 101 MHz) δ 156.2, 97.8, 84.5, 77.1, 68.1, 30.3, 27.0, 21.8, 21.1 ppm.

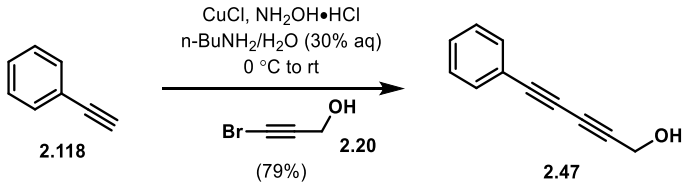

2.118 2.20 (79%) 2.47

CuCl (0.097 g, 0.98 mmol) was added to a flask and suspended in 30% aq. n-butylamine (45.5 mL) to give a blue solution. A small scoop of $NH_2OH{\cdot}HCl$ was added, then the solution became clear and colorless. The reaction was purged with argon, then **2.118** (2.15 mL, 19.6 mmol) was added and the reaction mixture was cooled to 0 °C. The reaction was allowed to stir for 2 minutes, then a solution of **2.20** (1.66 mL, 23.5 mmol) in THF (5 mL) was added. The reaction was allowed to stir at 0 °C for 15 minutes, then was warmed to room temperature. Whenever the solution turned blue/green in color another small scoop of $NH_2OH{\cdot}HCl$ was added. After 1 hour, the reaction turned amber in color. The reaction was quenched with saturated aq. NH_4Cl (50 mL) and extracted

with Et_2O (3 x 30 mL). The combined organic layers were dried over $MgSO_4$, filtered, and concentrated under reduced pressure to give a crude oil. The crude was then purified via column chromatography using hexanes/EtOAc (5:1) to give **2.47** (2.42 g, 15.5 mmol, 79% yield) as an amber oil. Our data corresponds with the reported literature data.[77] ^1H NMR (400 MHz, $CDCl_3$): δ7.43-7.50 (m, 2H), 7.25-7.37 (m, 3H), 4.39 (s, 2H), 2.23 (br s, 1H) ppm.

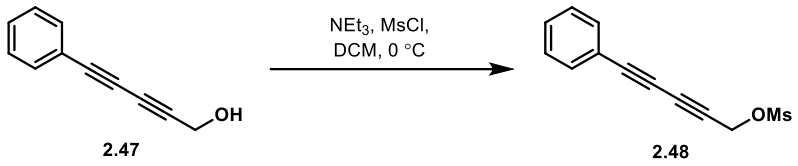

2.47 2.48

2.47 (1.90 g, 12.2 mmol) and NEt_3 (2.20 mL, 15.8 mmol) were dissolved in DCM (148 mL). Next, the solution was cooled to 0 °C and MsCl (1.412 mL, 18.25 mmol) was added dropwise. The reaction was stirred for five minutes, then warmed to room temperature; the reaction was stirred overnight and monitored by TLC. After the reaction was completed, the reaction was quenched with NH_4Cl (20 mL) and extracted with DCM (3 x 50 mL). The organic layer was washed with a brine solution (50 mL) and dried with Na_2SO_4. The product was filtered, then concentrated under reduced pressure. The crude mixture was purified using column chromatography (Hex/EtOAc 4:1) to yield **2.48** as a clear oil.

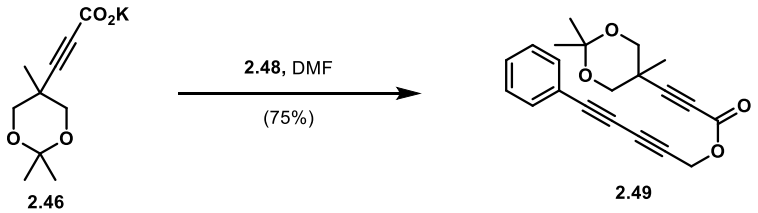

2.46 2.49

2.46 (0.78 g, 3.3 mmol) and **2.48** (0.60 g, 2.6 mmol) were dissolved in DMF (12.8 mL) and allowed to stir at room temperature overnight. Upon completion, the reaction mixture was diluted with water and extracted with EtOAc (3 x 40 mL). The organic layer was then washed with water (3 x

30 mL) and then with brine. The organic layer was dried over Na_2SO_4, filtered, and concentrated under reduced pressure. The crude was then purified via column chromatography using hexanes/EtOAc (10:1) to give **2.47** (0.644 g, 1.91 mmol, 75% yield). ^{1}H NMR (600 MHz, $CDCl_3$): δ 7.5-7.5 (m, 2H), 7.4-7.4 (m, 1H), 7.3-7.4 (m, 2H), 4.90 (s, 2H), 3.99 (d, *J*=11.3 Hz, 2H), 3.65 (d, *J*=11.3 Hz, 2H), 1.47 (s, 3H), 1.43 (s, 3H), 1.40 (s, 3H) ppm. ^{13}C NMR (151 MHz, $CDCl_3$): δ 152.4, 132.7, 129.6, 128.5, 121.1, 98.4, 91.6, 79.3, 74.9, 73.8, 72.9, 72.0, 67.6, 53.8, 31.2, 25.3, 21.8, 20.4 ppm. HRMS m/z: $[M + Na]^+$ Calcd for $C_{21}H_{20}O_4Na$ 359.1254; found 359.1262.

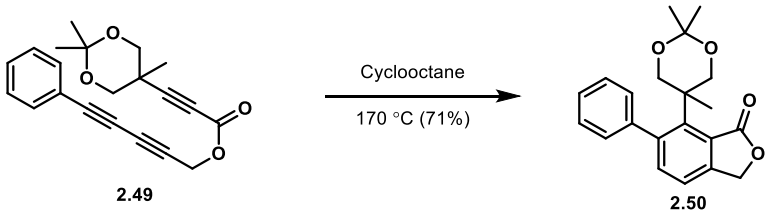

2.49 **2.50**

2.49 (0.15 g, 0.45 mmol) was added to a reaction vial, then was dissolved in freshly distilled and degassed Cyclooctane (149 mL). The reaction was heated to 170 °C for 24 hours and monitored by TLC. Upon completion, the crude was rinsed through a silica plug with hexanes (100 mL) to remove cyclooctane. Next, the silica plug was rinsed with EtOAc (100 mL) to elute the reaction mixture. The EtOAc filtrate was concentrated under reduced pressure. The crude was then purified via column chromatography using hexanes/EtOAc (15:1) to give **2.50** (0.107 g, 0.316 mmol, 71% yield) as an amorphous yellow solid. ^{1}H NMR (600 MHz, $CDCl_3$): δ 7.3-7.4 (m, 4H), 7.2-7.3 (m, 3H), 5.25 (s, 2H), 3.87 (d, *J*=12.0 Hz, 2H), 3.56 (d, *J*=12.0 Hz, 2H), 1.70 (s, 3H), 1.27 (s, 3H), 1.12 (s, 3H) ppm. ^{13}C NMR (151 MHz, $CDCl_3$): δ 148.7, 143.6, 143.5, 138.9, 129.5, 127.9, 127.7, 124.6, 119.3, 98.2, 69.9, 68.1, 42.0, 23.8, 23.3, 22.9 ppm. HRMS m/z: $[M + Na]^+$ Calcd for $C_{21}H_{22}O_4Na$ 361.1410; found 361.1410.

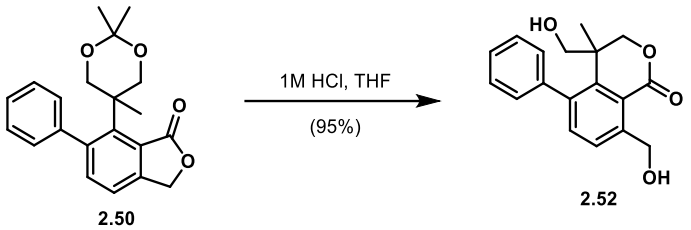

2.50 2.52

2.50 (0.049 g, 0.15 mmol) was dissolved in THF (0.965 mL), then 1M aq. HCl (1.014 ml, 1.014 mmol) was added, and the reaction was allowed to stir at room temperature overnight. Upon completion, the mixture was diluted with water (10 mL) and extracted with DCM (3 x 20 mL). The organic layer was dried over Na_2SO_4, filtered, and concentrated under reduced pressure. The crude was then purified via column chromatography using hexanes/EtOAc (4:1) to give **2.50** (0.041 g, 0.14 mmol, 95% yield) as a white solid. ^{1}H NMR (600 MHz, $CDCl_3$): δ 7.48 (d, *J*=8.0 Hz, 1H), 7.4-7.4 (m, 3H), 7.37 (d, *J*=8.0 Hz, 1H), 7.3 (m, 1H), 7.2 (m, 1H), 4.8 (m, 2H), 4.43 (d, *J*=10.9 Hz, 1H), 4.17 (br s, 1H), 4.04 (d, *J*=9.4 Hz, 1H), 3.6 (m, 2H), 1.89 (br s, 1H), 0.93 (s, 3H) ppm. HRMS m/z: $[M + H]^+$ Calcd for $C_{18}H_{19}O_4$ 299.1278; found 299.1273.

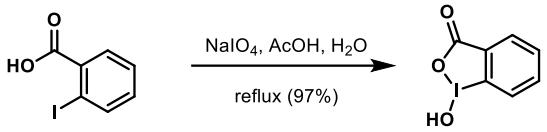

2.60 2.61

2.60 (4.0 g, 16 mmol) and sodium periodate (3.62 g, 16.9 mmol) were dissolved in acetic acid (7.22 mL) and water (16.9 mL). The reaction was stirred vigorously and refluxed for 4 hours. Upon completion, the mixture was diluted with cold water (90 mL) and cooled to room temperature in the absence of light for one hour. The product was filtered, then washed with cold water (3 x 10 mL), then finally washed with acetone (3 x 10 mL). The crude product was air-dried in the dark to yield **2.61** (4.1 g, 16 mmol, 97% yield) as a white solid. Our data corresponds with the reported literature data.[78] ^{1}H NMR (DMSO-d_6, 600 MHz) δ 8.06 (br s, 1H), 8.01 (d, *J*=7.6 Hz, 1H), 7.96 (t,

J=6.9 Hz, 1H), 7.84 (d, *J*=8.0 Hz, 1H), 7.70 (t, *J*=6.9 Hz, 1H) ppm. ^{13}C NMR (DMSO-d_6, 151 MHz) δ 167.7, 134.5, 131.5, 131.1, 130.4, 126.3, 120.4 ppm.

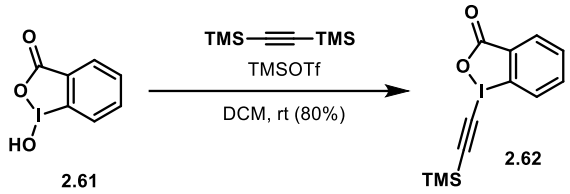

2.61 2.62

TMSOTf (3.01 ml, 16.7 mmol) was added to a solution of **2.61** (4.0 g, 15 mmol) in DCM (46 mL) at room temperature. The mixture was stirred for one hour, then bis(trimethylsilyl)acetylene (3.74 ml, 16.7 mmol) was slowly added and the mixture stirred overnight, and a white solid formed. Saturated aq. $NaHCO_3$ (30 mL) was added and stirred until the white solid dissolved. The two layers were then separated and extracted with DCM (3 x 25 mL). The organic layers were combined, washed with saturated aq. $NaHCO_3$, which was then dried with Na_2SO_4, filtered and concentrated under reduced pressure. The crude was recrystallized with acetonitrile (2 mL) to yield **2.62** (4.2 g, 12 mmol, 80% yield) as a white solid. Our data corresponds with the reported literature data.[78] ^{1}H NMR (600 MHz, $CDCl_3$): δ 8.42 (dd, *J*=1.0, 7.3 Hz, 1H), 8.2 (m, 1H), 7.8 (m, 2H), 0.32 (s, 9H) ppm. ^{13}C NMR (151 MHz, $CDCl_3$): δ 166.8, 135.3, 132.9, 132.0, 131.7, 126.5, 117.6, 115.8, 64.5, 0.0 ppm.

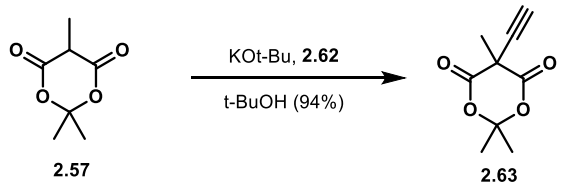

2.57 2.63

2.57 (0.0750 g, 0.474 mmol) was dissolved in tBuOH (3.70 mL), then KOt-Bu (0.0640 g, 0.569 mmol) was added. The solution was stirred for 15 minutes at room temp. Next, **2.62** (0.196 g, 0.569 mmol) was added in one portion and the solution stirred at room temperature for three hours.

The reaction mixture was then concentrated under reduced pressure and the crude was purified via column chromatography using hexanes/EtOAc (15:1) to yield **2.63** (0.081 g, 0.45 mmol, 94% yield) as an amorphous yellow solid. ^{1}H NMR (600 MHz, $CDCl_3$): δ 2.56 (s, 1H), 1.97 (s, 3H), 1.90 (s, 3H), 1.75 (s, 3H) ppm. ^{13}C NMR (151 MHz, $CDCl_3$): δ 164.6, 106.2, 78.3, 74.5, 43.1, 28.3, 27.9, 25.0 ppm. HRMS m/z: $[M + H]^+$ Calcd for $C_9H_{11}O_4$ 183.0652; found 183.0682.

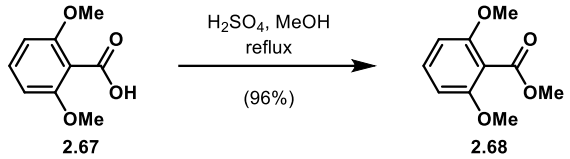

2.67 (10 g, 55 mmol) was dissolved in methanol (183 mL), then H_2SO_4 (2.93 mL, 54.9 mmol) was added. The reaction was refluxed for 12 hours. Upon completion, the mixture was concentrated under reduced pressure, then the crude was dissolved in EtOAc and washed with saturated aq. NaHCO3 (50 mL). The organic layer was washed with brine, dried over Na2SO4, filtered and concentrated under reduced pressure to yield **2.68** (10.6 g, 53.9 mmol, 98% yield) as a clear oil. ^{1}H NMR (600 MHz, $CDCl_3$): δ 7.18 (t, *J*=8.4 Hz, 1H), 6.43 (d, *J*=8.0 Hz, 2H), 3.81 (s, 3H), 3.70 (s, 6H) ppm. ^{13}C NMR (151 MHz, $CDCl_3$): δ 167.1, 157.3, 131.1, 112.9, 103.9, 56.0, 52.4 ppm.

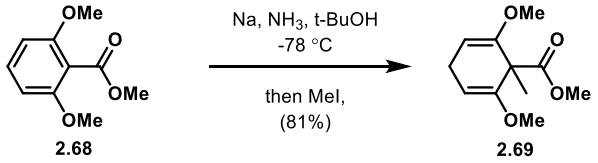

2.68 (4.90 g, 24.9 mmol) was dissolved in t-BuOH (2.39 mL, 25.0 mmol) and THF (49.9 mL), then was cooled to -78 °C. Next, ammonia (200 mL) was condensed into the flask, followed by the addition of small pieces of sodium metal (1.28 g, 55.7 mmol). Once the solution remained blue for 15 minutes, MeI (4.68 ml, 74.9 mmol) was slowly added, and the solution became clear. The solution stirred at -78 °C for an additional 30 minutes, then was warmed to room temperature and

the ammonia was evaporated overnight. Next, the mixture was dissolved in water (50 mL), then extracted with EtOAC (3 x 75 mL). The organic layer was dried over Na_2SO_4, filtered and concentrated under reduced pressure. The crude was purified via column chromatography using hexanes/EtOAc (20:1) to yield **2.69** (4.30 g, 20.3 mmol, 81% yield) as an amorphous white solid. ^{1}H NMR (600 MHz, $CDCl_3$): δ 4.69 (t, *J*=3.6 Hz, 2H), 3.61 (s, 3H), 3.46 (s, 6H), 2.81 (m, 2H), 1.43 (s, 3H) ppm. ^{13}C NMR (151 MHz, $CDCl_3$): δ 173.3, 154.8, 91.1, 54.8, 52.5, 50.6, 23.9, 21.3 ppm. HRMS m/z: $[M + H]^+$ Calcd for $C_{11}H_{17}O_4$ 213.1121; found 213.1116.

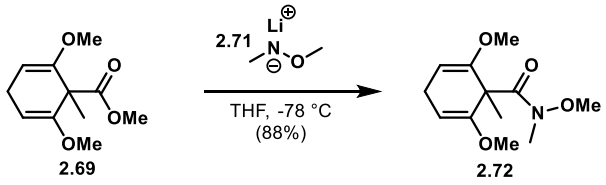

N,O-Dimethylhydroxylamine hydrochloride (2.76 g, 28.3 mmol) was suspended in THF (26.6 mL), then cooled to -78 °C. Next, n-BuLi (35.3 mL, 56.5 mmol, 1.6 M in hexanes) was added dropwise and the solution stirred for 15 minutes, then was warmed to room temperature and stirred for an additional 20 minutes. The reaction was cooled to -78 °C and **2.69** (1.50 g, 7.07 mmol) in THF (10.22 mL) was added dropwise to the solution. The reaction stirred at -78 °C for 30 minutes, then was warmed to room temperature and stirred for an additional 30 minutes. Upon completion, the reaction was quenched with saturated aq. NH_4Cl (30 mL) and was vigorously stirred for 5 minutes. The biphasic mixture was separated and extracted with ether (3 x 30 mL). The organic layer was washed with brine, dried over $MgSO_4$, filtered and concentrated under reduced pressure. The crude was purified via column chromatography using hexanes/EtOAc (4:1) to yield **2.72** (1.5 g, 6.2 mmol, 88% yield). ^{1}H NMR (600 MHz, $CDCl_3$): δ 4.50 (t, *J*=3.6 Hz, 2H), 3.38 (s, 6H), 3.36 (s, 3H), 3.02 (s, 3H), 2.72 (m, 2H), 1.4 (m, 3H) ppm. ^{13}C NMR (151 MHz, $CDCl_3$): δ 171.8, 155.3, 89.3, 60.3, 54.5, 50.2, 33.8, 24.4, 24.1 ppm. HRMS m/z: $[M + H]^+$ Calcd for$C_{12}H_{20}NO_4$ 242.1387;

found 242.1384.

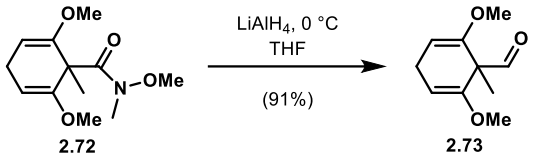

2.72 (0.507 g, 2.10 mmol) was dissolved in THF (6.31 mL) and cooled to 0 °C. $LiAlH_4$ (2.311 ml, 2.311 mmol, 1M in THF) was added dropwise, and the solution was allowed to stir for two hours. Upon completion, the reaction was carefully quenched with water (20 mL) and extracted with ether (3 x 30 mL). The organic layer was dried over $MgSO_4$, filtered and concentrated under reduced pressure. The crude was purified via flash chromatography using hexanes/EtOAc (30:1) to yield **2.73** (0.35 g, 1.9 mmol, 91 % yield). ^{1}H NMR (600 MHz, $CDCl_3$): δ 9.38 (s, 1H), 4.66 (t, *J*=3.6 Hz, 2H) 3.52 (s, 6H), 2.92 (m, 2H), 1.41 (s, 3H) ppm. ^{13}C NMR (151 MHz, $CDCl_3$): δ 198.3, 152.3, 93.5, 55.7, 54.8, 24.1, 16.2 ppm. HRMS m/z: $[M + H]^+$ Calcd for $C_{10}H_{15}O_3$ 183.1016; found 183.1011.

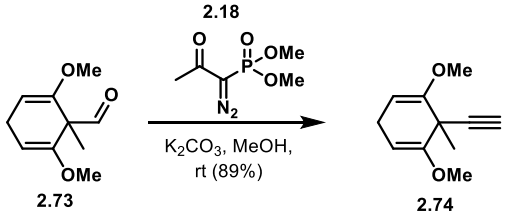

2.73 (0.713 g, 3.91 mmol) was dissolved in MeOH (39.1 mL), then K_2CO_3 (1.08 g, 7.83 mmol) and **2.18** (0.902 g, 4.70 mmol) were added. The reaction was stirred overnight. Upon completion, the clear yellow solution was quenched with 5% aq. $NaHCO_3$ (50 mL) and extracted with ether (3 x 50 mL). The combined organic layers were washed with brine, dried over $MgSO_4$, filtered and concentrated under reduced pressure. The crude was purified via column chromatography using hexanes/EtOAc (30:1) to yield **2.74** (0.623 g, 3.50 mmol, 89% yield) as an amorphous white solid.

^{1}H NMR (600 MHz, $CDCl_3$): δ 4.64 (t, *J*=3.6 Hz, 2H), 3.56 (s, 6H), 2.9 (m, 2H), 2.13 (s, 1H), 1.53 (s, 3H) ppm. ^{13}C NMR (151 MHz, $CDCl_3$): δ 154.2, 90.7, 87.0, 67.6, 55.1, 38.4, 25.7, 23.8 ppm.

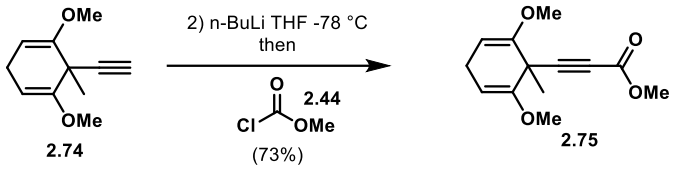

2.74 (0.697 g, 3.91 mmol) was dissolved in THF (19.6 mL) and cooled to -78 °C. Next, n-BuLi (2.93 mL, 4.69 mmol, 1.6 M in hexanes) was added dropwise, and the solution stirred at -78 °C for 20 minutes, then was allowed to stir at room temperature for 10 minutes. The reaction was cooled back down to -78 °C and **2.44** (0.454 ml, 5.87 mmol) was added dropwise. The solution stirred at -78 °C for 30 minutes, then was warmed to room temperature and stirred for an additional 30 minutes. Upon completion, the reaction was quenched with water (30 mL) and extracted with EtOAc (3 x 30 mL). The organic layer was washed with brine, dried over Na_2SO_4, filtered and concentrated under reduced pressure. The crude was purified via column chromatography using hexanes/EtOAc (10:1) to yield **2.75** (0.680 g, 2.88 mmol, 73% yield) as a clear oil. ^{1}H NMR (600 MHz, $CDCl_3$): δ 4.70 (t, *J*=4.0 Hz, 2H), 3.72 (s, 3H), 3.59 (s, 6H), 2.79 (m, 2H), 1.60 (s, 3H) ppm. ^{13}C NMR (151 MHz, $CDCl_3$): δ 154.3, 152.9, 91.3, 91.1, 71.5, 55.1, 52.4, 38.9, 24.9, 23.7 ppm. HRMS m/z: $[M + H]^+$ Calcd for $C_{13}H_{17}O_4$ 237.1121; found 237.1120.

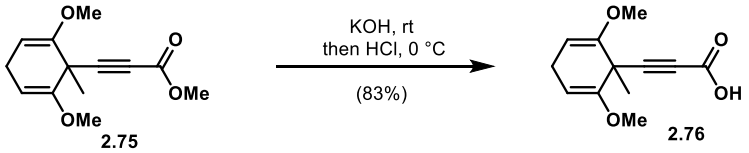

2.75 (1.63 g, 6.90 mmol) was dissolved in THF (33.2 mL) and cooled to 0 °C. Next, KOH (0.774 g, 13.8 mmol) in water (11.1 mL) was added to the solution, which stirred at 0 °C for 30 minutes, then stirred at room temperature overnight. Upon completion, the reaction was cooled to 0 °C and

the solution was neutralized to pH 7 by dropwise addition of 1M HCl. Next, the solution was concentrated under reduced pressure to yield **2.76** (1.28 g, 5.76 mmol, 83% yield) as a clear oil, which was used in the next step without further purification. ^{1}H NMR (600 MHz, $CDCl_3$): δ 4.6-4.7 (m, 2H), 3.5-3.6 (m, 6H), 2.7-2.8 (m, 2H), 1.5-1.6 (m, 3H) ppm. ^{13}C NMR (151 MHz, $CDCl_3$): δ 155.5, 152.8, 91.7, 91.5, 72.0, 55.1, 38.9, 23.7, 18.2 ppm.

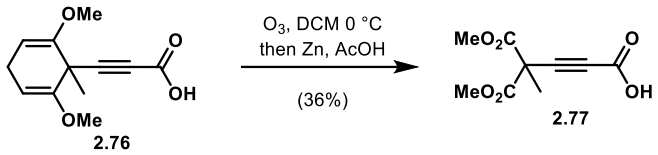

2.76 (0.132 g, 0.594 mmol) was dissolved in DCM (8.49 mL), then pyridine (0.192 mL, 2.38 mmol) was added. Next, ozone (600 mg/hr. output, air as feed gas) was bubbled into the solution at 0 °C until the starting material was fully consumed (roughly 45 minutes). More DCM was added as the solvent evaporated. Next, nitrogen was bubbled into the solution for five minutes, then zinc metal (0.155 g, 2.38 mmol) and acetic acid (0.272 mL, 4.75 mmol) were added. The solution was warmed to room temperature and allowed to stir for 2 hours. Next, aq. 1M HCl (15 mL) was added, and the mixture was extracted with DCM (3 x 20 mL). The organic layer was dried over Na_2SO_4, filtered and concentrated under reduced pressure. The crude was purified via column chromatography using hexanes/EtOAc (3:1, 1% AcOH-1:1, 1% AcOH) to yield **2.77** (0.0469 g, 0.219 mmol, 36% yield) as a yellow oil. ^{1}H NMR (600 MHz, $CDCl_3$): δ 8.31 (br s, 1H), 3.82 (s, 6H), 1.77 (s, 3H) ppm. ^{13}C NMR (151 MHz, $CDCl_3$): δ 167.3, 155.8, 84.2, 76.2, 54.1, 49.8, 22.4 ppm.

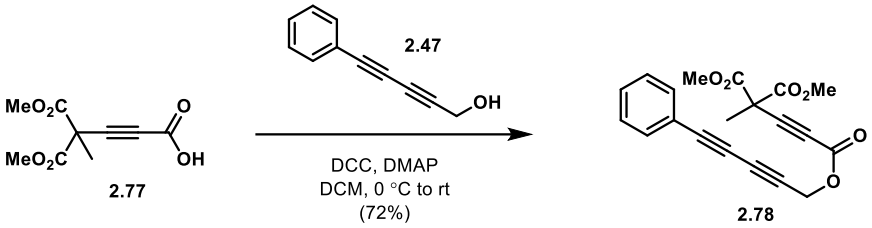

2.77 (0.069 g, 0.32 mmol) was dissolved in DCM (1.79 mL) and cooled to 0 °C, then DCC (0.066 g, 0.32 mmol) was added. The solution stirred at 0 °C for 15 minutes, then **2.47** (0.042 g, 0.27 mmol) and DMAP (3.28 mg, 0.0270 mmol) were added. The solution was stirred at 0 °C for 30 minutes, then was warmed to room temperature and allowed to stirred overnight. Upon completion, the reaction mixture was filtered through celite and rinsed with DCM. Next, the filtrate was washed with aq. 1M HCl (50 mL) and saturated aq. $NaHCO_3$ (50 mL). The organic layer was washed with brine, dried over Na_2SO_4, filtered and concentrated under reduced pressure. The crude was purified via column chromatography using hexanes/EtOAc (10:1) to yield **2.78** (0.0678 g, 0.192 mmol, 72% yield) as a colorless oil. ^{1}H NMR (600 MHz, $CDCl_3$): δ 7.50 (d, *J*=7.6 Hz, 2H), 7.3-7.4 (m, 3H), 4.92 (s, 2H), 3.84 (s, 6H), 1.80 (s, 3H) ppm. ^{13}C NMR (151 MHz, $CDCl_3$): δ 167.1, 152.1, 132.7, 129.7, 128.5, 128.4, 84.0, 79.3, 75.5, 74.7, 72.8, 72.2, 54.0, 51.7, 49.7, 22.5 ppm.

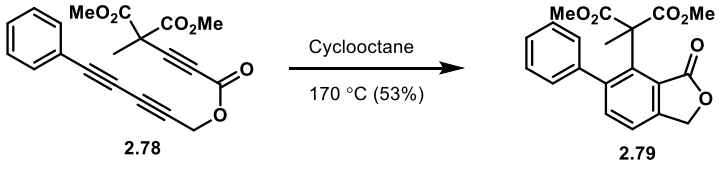

2.79 (0.0381 g, 0.108 mmol) was added to a reaction vial then dissolved in freshly distilled and degassed Cyclooctane (36 mL). The reaction mixture was purged with argon and capped with a screw cap, then heated at 170 °C for 48 hours. The reaction mixture was then cooled and filtered through silica gel, then rinsed with hexanes to remove the remaining cyclooctane. The compound

was eluted with EtOAc, then the filtrate was concentrated under reduced pressure. The crude was purified via column chromatography using hexanes/EtOAc (10:1) to yield **2.79** (0.020 g, 0.057 mmol, 53 % yield) as an amorphous white solid. ^{1}H NMR (600 MHz, $CDCl_3$): δ 7.38 (m, 1H), 7.3-7.3 (m, 4H), 7.2-7.2 (m, 2H), 5.23 (s, 2H), 3.31 (s, 6H), 2.00 (s, 3H) ppm. ^{13}C NMR (151 MHz, $CDCl_3$): δ 170.6, 170.4, 147.2, 142.7, 139.7, 139.0, 138.6, 130.3, 127.9, 127.8, 124.8, 120.6, 68.5, 58.9, 52.8, 24.2 ppm.

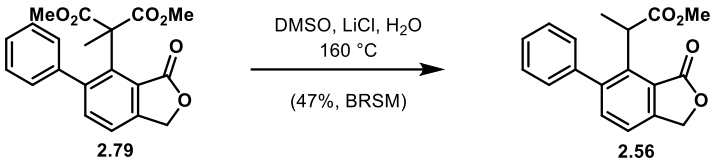

2.79 (0.0421 g, 0.129 mmol) and LiCl (0.015 g, 0.36 mmol) were dissolved in DMSO (0.210 mL) and water (5.25 µL). The reaction was stirred at 160 °C overnight. Upon completion, the reaction mixture was diluted with water (30 mL), then extracted with DCM (3 x 50 mL). The organic layer was dried over Na_2SO_4, filtered and concentrated under reduced pressure. The crude was purified via flash chromatography using hexanes/EtOAc (6:1) to yield **2.56** (0.012 g, 0.040 mmol, 34% yield). The yield based off recovered starting material (BRSM) was 47%. ^{1}H NMR (600 MHz, $CDCl_3$): δ 7.56 (d, *J*=8.0 Hz, 1H), 7.4-7.5 (m, 3H), 7.41 (d, *J*=8.0 Hz, 1H), 7.3-7.3 (m, 2H), 5.33 (s, 2H), 4.14 (q, *J*=6.9 Hz, 1H), 3.65 (s, 3H), 1.51 (d, *J*=7.3 Hz, 3H) ppm. ^{13}C NMR (151 MHz, $CDCl_3$): δ 173.7, 170.5, 147.3, 143.2, 140.0, 139.5, 136.1, 129.3, 128.5, 127.9, 123.3, 120.2, 68.9, 52.1, 40.0, 17.5 ppm.

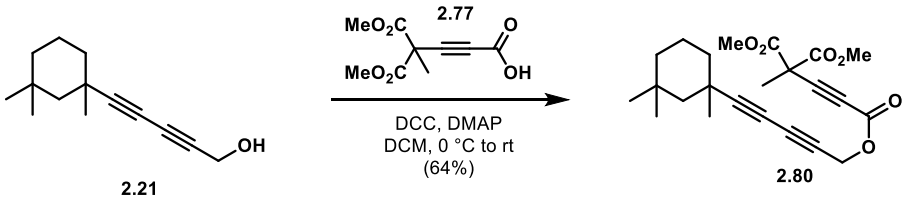

2.21 (0.0234 g, 0.115 mmol) and **2.77** (0.0319 g, 0.149 mmol) were dissolved in DCM (1.43 mL) and cooled to 0 °C. Next, DCC was added (0.031 g, 0.15 mmol), followed by the addition of DMAP (3.5 mg, 0.029 mmol) at 0 °C. The reaction mixture stirred at 0 °C for 30 min before warming to room temperature where it continued to stir for 8 hours. At this time the reaction was filtered through a frit funnel and concentrated under reduced pressure to give an oily solid that was further purified by silica gel column chromatography using hexanes/EtOAc (25:1) to give **2.80** (0.0295 g, 0.0740 mmol, 64% yield) as a clear light-yellow oil. ^{1}H NMR (600 MHz, $CDCl_3$): δ 4.83 (s, 2H), 3.83 (s, 6H), 1.8-1.8 (m, 1H), 1.78 (s, 3H), 1.73 (td, *J*=2.9, 13.8 Hz, 1H), 1.62 (td, *J*=1.0, 13.8 Hz, 1H), 1.5-1.5 (m, 1H), 1.4-1.4 (m, 1H), 1.21 (s, 3H), 1.13 (s, 3H), 1.0-1.1 (m, 3H), 0.87 (s, 3H) ppm. ^{13}C NMR (151 MHz, $CDCl_3$): δ 167.1, 152.1, 89.9, 83.9, 75.6, 72.7, 68.6, 64.8, 54.1, 54.0, 50.6, 49.7, 39.5, 39.0, 34.1, 32.0, 31.9, 31.2, 26.1, 22.5, 20.3 ppm. HRMS m/z: $[M + Na]^+$ Calcd for $C_{23}H_{29}O_6$ 401.1959; found 401.1951.

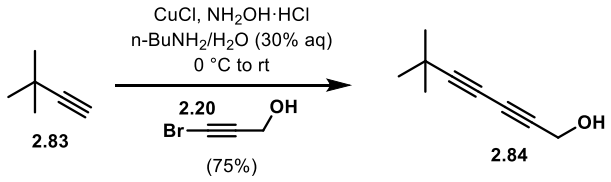

CuCl (0.121 g, 1.217 mmol) was suspended in aq. 30% n-$BuNH_2$ (56 mL), then cooled to 0 °C and purged with argon. The reaction turned blue, then the blue color was quenched with a spatula tip of hydroxylamine hydrochloride. **2.83** (3.00 mL, 24.4 mmol) was added to the reaction mixture and stirred for 5 minutes. Next, **2.20** (2.25 mL, 31.7 mmol) in THF (1 mL) was added and the reaction continued to stir at 0 °C until completion. Every few minutes a spatula tip of hydroxylamine hydrochloride was added whenever the reaction turned blue or green in color. After 2 hours, the reaction was warmed to room temperature and quenched with saturated aq. NH_4Cl (40

mL) and extracted with ether (3 x 25 mL). The combined organic layers were dried over $MgSO_4$, filtered and concentrated under reduced pressure. The crude was purified via column chromatography using hexanes/EtOAc (6:1) to **2.84** (2.51 g, 18.4 mmol, 75% yield) as pale yellow oil. ^{1}H NMR (600 MHz, $CDCl_3$): δ 4.25 (s, 2H), 2.10 (br s, 1H), 1.17 (s, 9H) ppm. ^{13}C NMR (151 MHz, $CDCl_3$): δ 89.3, 74.8, 70.6, 63.1, 51.4, 30.4, 28.0 ppm. HRMS m/z: $[M + Na]^+$ Calcd for $C_9H_{12}ONa$ 159.0780; found 159.0771.

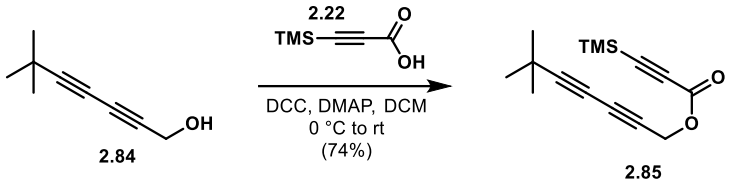

DCC (2.73 g, 13.2 mmol), DMAP (0.135 g, 1.10 mmol) and **2.84** (1.5 g, 11 mmol) were dissolved in DCM (60 mL) and cooled to 0 °C. Next, **2.22** (1.88 g, 13.2 mmol) in DCM (25 mL) was added to the reaction. The reaction was allowed to stir for 30 minutes at 0 °C, then the reaction was warmed to room temperature and stirred overnight. Upon completion, the reaction mixture was filtered through celite then rinsed with DCM. The filtrate was concentrated under reduced pressure, then the crude was purified via column chromatography using hexanes/EtOAc (20:1) to give **2.85** (2.12 g, 8.14 mmol, 74% yield) as a clear colorless oil. ^{1}H NMR (400 MHz, $CDCl_3$): δ 4.78 (s, 2H), 1.22 (s, 9H), 0.23 (s, 9H) ppm. ^{13}C NMR (101 MHz, $CDCl_3$): δ 152.0, 95.7, 93.6, 90.0, 72.3, 69.2, 62.9, 53.8, 30.3, 28.0, -1.0 ppm. HRMS m/z: $[M + Na]^+$ Calcd for $C_{15}H_{20}O_2SiNa$ 283.1125; found 283.1130.

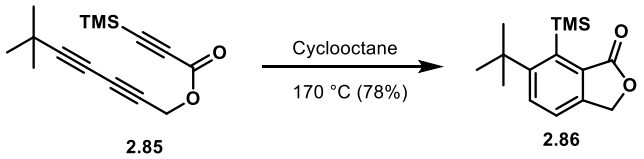

2.85 (0.125 g, 0.384 mmol) was added to a reaction vial, then freshly distilled and degassed cyclooctane (75 mL) was added. The reaction vial was purged with argon and equipped with a screw cap lid. The reaction mixture was heated for 48 hours at 170 °C. Upon completion, the reaction was cooled to room temperature and the mixture was filtered through a pad of silica gel using hexanes (100 mL) as the eluent to remove cyclooctane from the reaction mixture. The rest of the reaction mixture was eluted with EtOAc (50 mL). The EtOAC rinse was concentrated under reduced pressure, then purified via column chromatography using hexanes/EtOAc (7:1) to give **2.87** (0.0791 g, 0.301 mmol, 78% yield) as a yellow oil. ^{1}H NMR (500 MHz, $CDCl_3$): δ 7.75 (d, J = 8.2 Hz, 1H), 7.32 (d, J = 8.2 Hz, 1H), 5.21 (s, 2H), 1.46 (s, 9H), 0.53 (s, 9H) ppm. ^{13}C NMR (101 MHz, $CDCl_3$): δ 171.7, 159.2, 144.3, 142.7, 132.0, 131.0, 121.4, 68.3, 37.4, 33.5, 5.3 ppm. HRMS m/z: $[M + H]^+$ Calcd for $C_{15}H_{23}O_2Si$ 263.1462; found 263.1464.

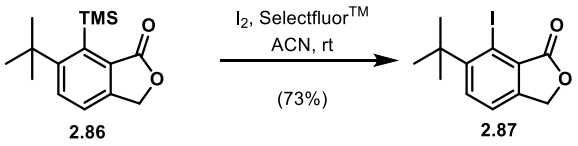

2.86 (0.032 g, 0.12 mmol) was added to a scintillation vial, then was dissolved in ACN (1.67 mL). Next, Selectfluor™ (0.086 g, 0.24 mmol) and iodine (0.031 g, 0.12 mmol) was added to the solution, then the vial was purged with argon and capped. The reaction mixture stirred at room temperature for 1 hour. Upon completion, the reaction was quenched with saturated aq. $Na_2S_2O_3$ (10 mL) and stirred for five minutes. The reaction was extracted with EtOAc (3 x 25 mL) The combined organic layers were dried over $MgSO_4$, filtered and concentrated under reduced pressure. The crude was purified via column chromatography using hexanes/EtOAc (6:1) to give **2.87** (0.028 g, 0.088 mmol) as a clear oil. ^{1}H NMR (600 MHz, $CDCl_3$): δ 7.66 (d, 1H, *J*=8.0 Hz), 7.31 (d, 1H, *J*=8.0 Hz), 5.05 (s, 2H), 1.58 (s, 9H) ppm. ^{13}C NMR (151 MHz, $CDCl_3$): δ 169.9,

152.7, 146.3, 133.0, 128.3, 121.5, 93.9, 65.8, 38.2, 30.4 ppm.

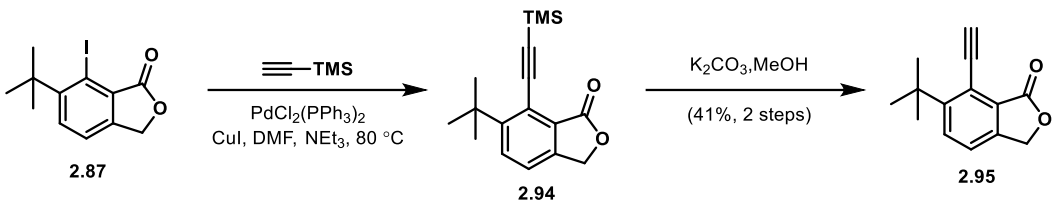

CuI (0.027 g, 0.14 mmol) and $PdCl_2(PPh_3)_2$ (0.049 g, 0.070 mmol) were added to a reaction vial under argon, then **2.87** (0.220 g, 0.696 mmol) in dry and degassed DMF (6.96 mL) was added to the vial. Next, NEt_3 (0.349 mL, 2.505 mmol) and trimethylsilyl acetylene (0.293 mL, 2.09 mmol) were added to the vial, which was then purged with argon and sealed with a screw cap. The reaction was stirred at 70 °C for 18 hours. Upon completion, the reaction was diluted with water (10 mL) and extracted with EtOAc (3 x 25 mL). The organic layer was washed with water (2 x 25 mL) and brine (25 mL). The organic layer was dried over Na_2SO_4, filtered and concentrated under reduced pressure. The crude was purified via column chromatography using hexanes/EtOAc (6:1) to yield **2.94** as a slightly crude yellow solid, which was used in the next step without further purification.

Crude **2.94** from the previous step was dissolved in methanol (6.96 mL), then K_2CO_2 (0.192 g, 1.39 mmol) was added, and the reaction stirred at room temperature overnight. Upon completion, the reaction was filtered, then diluted with water (10 mL) and extracted with DCM (3 x 10 mL). The organic layer was washed with brine (10 mL) and dried over Na_2SO_4. The organic layer was then filtered and concentrated under reduced pressure. The crude mixture was purified via column chromatography using hexanes/EtOAc (5:1) to **2.95** (0.0614 g, 0.287 mmol, 41% yield) over 2 steps as a clear oil. ^{1}H NMR (600 MHz, $CDCl_3$): δ 7.67 (d, *J*=8.4 Hz, 1H), 7.31 (d, *J*=8.4 Hz, 1H), 5.12 (s, 2H), 3.94 (s, 1H), 1.51 (s, 9H) ppm. ^{13}C NMR (151 MHz, $CDCl_3$): δ 169.3, 154.5, 145.0, 131.6, 127.7, 121.7, 119.6, 92.9, 78.7, 67.5, 36.4, 30.0 ppm.

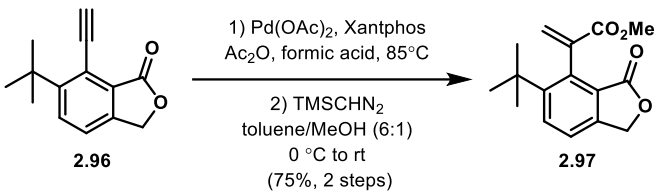

2.96 2.97

$Pd(OAc)_2$ (5.7 mg, 0.025 mmol) and Xantphos (0.029 g, 0.050 mmol) were added to a reaction vial under argon, then was suspended in toluene (0.840 mL). In a separate flask, **2.96** (0.054 g, 0.252 mmol), formic acid (0.014 mL, 0.378 mmol) and Ac_2O (4.76 µL 0.050 mmol) were dissolved in toluene (1.68 mL), which was then added to the reaction vial under argon. The reaction was stirred at 85 °C overnight. Upon completion, the reaction was cooled to room temperature and transferred to a round bottom flask. The mixture was concentrated under reduced pressure then purified via column chromatography using hexanes/EtOAc (10:1-2:1) to yield 2-(5-(tert-butyl)-3-oxo-1,3-dihydroisobenzofuran-4-yl)acrylic acid as a slightly crude solid, which was used in the next step.

2-(5-(tert-butyl)-3-oxo-1,3-dihydroisobenzofuran-4-yl)acrylic acid from the previous step was dissolved in MeOH (1.80 mL) and toluene (10.8 mL), then $TMSCHN_2$ (0.252 mL, 0.504 mmol, 2M in diethyl ether) was added. The reaction stirred at room temperature for 3 hours, then was concentrated under reduced pressure. The crude was purified via column chromatography using hexanes/EtOAc (5:1) to yield **2.97** (0.0516 g, 0.188 mmol, 75% yield) over 2 steps as an amorphous white solid. ^{1}H NMR (600 MHz, $CDCl_3$): δ 7.76 (d, *J*=8.2 Hz, 1H), 7.32 (d, *J*=8.2 Hz, 1H), 6.71 (s, 1H), 5.62 (s, 1H), 5.14 (s, 2H), 3.69 (s, 3H), 1.32 (s, 9H) ppm. ^{13}C NMR (151 MHz, $CDCl_3$): δ 170.0, 166.3, 149.7, 144.3, 138.4, 136.3, 133.1, 129.8, 125.2, 121.3, 68.0, 52.3, 37.0, 32.2 ppm. HRMS m/z: $[M + H]^+$ Calcd for $C_{16}H_{19}O_4$ 275.1278; found 275.1276.

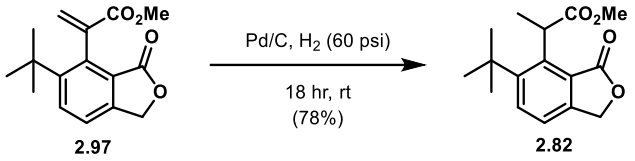

2.82 (0.052 g, 0.19 mmol) was dissolved in degassed MeOH (2.5 mL) in a Parr vial, then Pd/C (0.020 g, 0.019 mmol, 10% wt.) was added. The reaction was evacuated under vacuum, then backfilled with H_2 (60 psi). The reaction was then shaken overnight at room temperature. Upon completion, the reaction was filtered through Celite, then the filtrate was concentrated under reduced pressure. The crude was purified via column chromatography using hexanes/EtOAc (4:1) to yield **2.82** (0.041 g, 0.15 mmol, 78% yield) as a clear oil. ^{1}H NMR (600 MHz, $CDCl_3$): δ 7.77 (d, *J*=8.4 Hz, 1H), 7.31 (d, *J*=8.4 Hz, 1H), 5.23 (s, 2H), 4.60 (q, *J*=6.9 Hz, 1H), 3.71 (s, 3H), 1.67 (d, *J*=6.9 Hz, 3H), 1.49 (s, 9H) ppm. ^{13}C NMR (151 MHz, $CDCl_3$): δ 173.7, 170.8, 148.5, 146.1, 142.0, 132.7, 124.3, 120.2, 68.5, 52.2, 40.6, 36.1, 32.1, 18.0 ppm. HRMS m/z: $[M + Na]^+$ Calcd for $C_{16}H_{20}O_4Na$ 299.1254; found 299.1254.

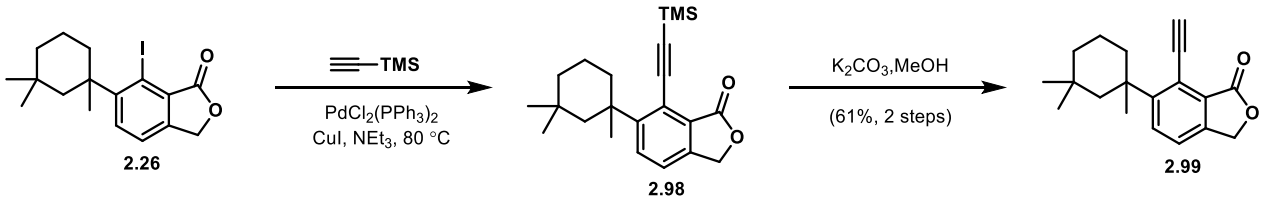

2.26 (0.007 g, 0.02 mmol), CuI (1.39 mg, 7.29 µmol) and $PdCl_2(PPh_3)_2$ (2.56 mg, 3.64 µmol) were added to a reaction vial with a septum under argon. Next, trimethylsilyl acetylene (0.013 mL, 0.091 mmol) in NEt3 (0.364 mL) were added to the vial, which was then purged with argon and sealed with a screw cap. The reaction was stirred at 80 °C for 24 hours. Upon completion, the reaction was diluted with water (10 mL) and extracted with EtOAc (3 x 25 mL). The organic layer was washed with water (2 x 25 mL) and brine (25 mL). The organic layer was dried over Na_2SO_4,

filtered and concentrated under reduced pressure. The crude was purified via column chromatography using hexanes/EtOAc (10:1-4:1) to yield **2.98** as a slightly crude oil, which was used in the next step without further purification.

2.98 (6.9 mg, 0.018 mmol) was dissolved in methanol (0.180 mL), then K_2CO_3 (7.5 mg, 0.054 mmol) was added. The reaction was stirred for two hours, then diluted with water. The reaction mixture was extracted with ether (3 x 20 mL), dried over MgSO4, filtered and concentrated under reduced pressure. The crude was purified via column chromatography using hexanes/EtOAc (4:1) to yield **2.99** (0.0031 g, 0.012 mmol, 61% yield) over 2 steps as an amorphous white solid. ^{1}H NMR (600 MHz, $CDCl_3$): δ 7.78 (d, *J*=8.0 Hz, 1H), 7.39 (d, *J*=7.6 Hz, 1H), 5.19 (s, 2H), 4.04 (s, 1H), 3.28 (br d, *J*=14.2 Hz, 1H), 2.35 (br d, *J*=13.4 Hz, 1H), 1.7-1.7 (m, 1H), 1.6-1.7 (m, 1H), 1.47 (s, 3H), 1.4-1.5 (m, 1H), 1.3-1.4 (m, 2H), 1.2-1.2 (m, 1H), 0.90 (s, 3H), 0.34 (s, 3H) ppm. ^{13}C NMR (151 MHz, $CDCl_3$): δ 168.2, 152.3, 143.6, 131.2, 126.8, 120.6, 118.8, 92.6, 77.8, 66.4, 47.3, 38.6, 38.4, 37.8, 32.1, 30.5, 30.4, 29.9, 18.7 ppm. HRMS m/z: $[M + Na]^+$ Calcd for $C_{19}H_{23}O_2Na$ 283.1693; found 283.1693.

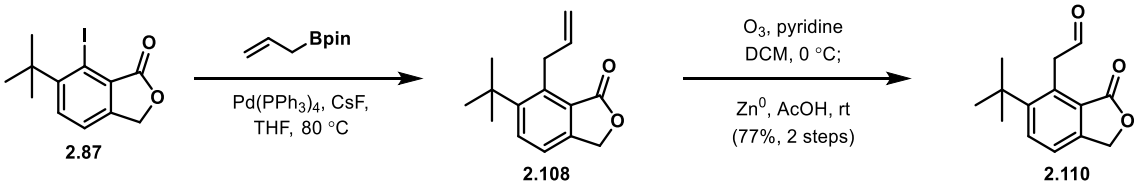

2.87 (0.115 g**,** 0.364 mmol), CsF (0.216 g, 1.42 mmol) and $Pd(PPh_3)_4$ (0.042 g, 0.036 mmol) were dissolved in dry and degassed THF (2.43 mL) and stirred for 15 minutes at room temperature. Next, allyboronic acid, pinacol ester (0.246 ml, 1.31 mmol) in THF (2.43 mL) was added and the reaction was stirred at 80 °C for 12 hours. Upon completion, the reaction was cooled to room temperature, then was diluted with water (10 mL) and. The reaction was extracted with EtOAc (3

x 20 mL), dried over $MgSO_4$, filtered and concentrated under reduced pressure. The crude was purified via column chromatography using hexanes/EtOAc (6:1) to yield **2.108** as a slightly crude yellow oil, which was used in the next step without further purification.

2.110 (0.084 g, 0.36 mmol) was dissolved in DCM (5.20 mL), then pyridine (0.088 mL, 1.1 mmol) was added. Next, ozone (600 mg/hr. output, air as feed gas) was bubbled into the solution at 0 °C until the starting material was fully consumed (roughly 45 minutes). More DCM was added as the solvent gradually evaporated. Next, nitrogen was bubbled into the solution for five minutes, then zinc metal (0.095 g, 1.5 mmol) and acetic acid (0.125 mL, 2.18 mmol) were added. The solution was warmed to room temperature and allowed to stir for 2 hours. Next, 1M HCl (15 mL) was added, and the mixture was extracted with DCM (3 x 20 mL). The organic layer was dried over Na_2SO_4, filtered and concentrated under reduced pressure. The crude was purified via column chromatography using hexanes/EtOAc (4:1) to yield **2.110** (0.065 g, 0.28 mmol, 77% yield) as an amorphous white solid. ^{1}H NMR (600 MHz, $CDCl_3$): δ 9.79 (s, 1H), 7.70 (d, *J*=8.0 Hz, 1H), 7.27 (d, *J*=8.4 Hz, 1H), 5.14 (s, 2H), 4.53 (s, 2H), 1.35 (s, 9H) ppm. ^{13}C NMR (151 MHz, $CDCl_3$): δ 198.5, 171.4, 150.4, 145.0, 132.9, 132.6, 125.0, 120.7, 68.2, 44.6, 35.8, 31.8 ppm.

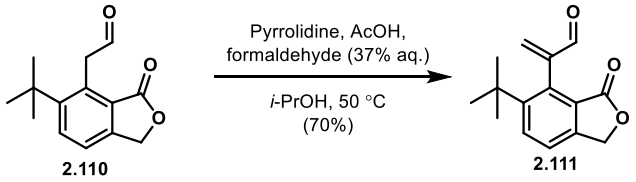

2.110 (0.023 g, 0.099 mmol) was dissolved in i-PrOH (0.99 mL) at room temperature, then formaldehyde (0.040 g, 0.50 mmol) was added, followed by the addition of acetic acid (6.0 mg, 0.099 mmol) and pyrrolidine (7.1 mg, 0.099 mmol). The reaction was stirred at 50 °C overnight. Upon completion, the reaction was diluted with saturated aq. $NaHCO_3$ and extracted with DCM

(3 x 20 mL). The organic layer was dried over $MgSO_4$, filtered and concentrated under reduced pressure. The crude was purified via column chromatography using hexanes/EtOAc (4:1) to yield **2.111** (0.017 g, 0.070 mmol, 70% yield) as an amorphous white solid. ^{1}H NMR (600 MHz, $CDCl_3$): δ 9.78 (s, 1H), 7.78 (d, *J*=8.4 Hz, 1H), 7.34 (d, *J*=8.4 Hz, 1H), 6.53 (s, 1H), 6.33 (s, 1H), 5.12 (s, 2H), 1.29 (s, 9H) ppm. ^{13}C NMR (151 MHz, $CDCl_3$): δ 192.9, 169.7, 150.4, 148.2, 144.6, 136.5, 133.8, 133.1, 124.7, 121.7, 67.9, 36.9, 32.3 ppm.

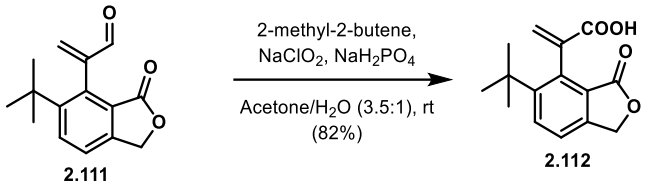

2.111 (0.039 g, 0.16 mmol) was dissolved in t-BuOH (1.24 mL) and water (0.36 mL) at room temperature. Next, 2-methyl-2-butene (0.085 mL, 0.80 mmol), sodium dihydrogen phosphate (0.044 g, 0.37 mmol) and sodium chlorite (0.036 g, 0.32 mmol) were added sequentially at 0 °C. The reaction was warmed to room temperature and stirred for four hours. Upon completion, the reaction was concentrated under reduced pressure. The crude was diluted with saturated aq. $NaHCO_3$ (10 mL) and DCM (10 mL). The organic layer was discarded, then the aq. Layer was acidified to pH 2 with 1M HCl. The aq. layer was extracted with DCM (3 x 20 mL), then the crude was dried over $MgSO_4$, filtered and concentrated under reduced pressure to yield **2.112** (0.034 g, 0.13 mmol) as an amorphous white solid, which was sufficiently pure.

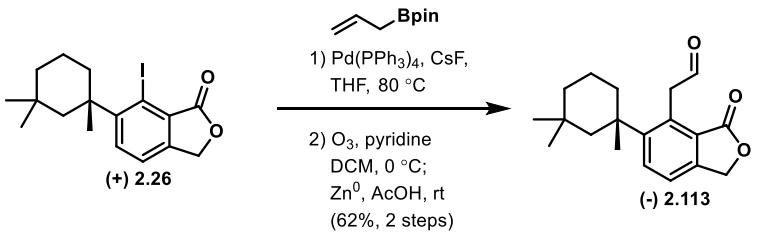

2.26 (0.269 g, 0.700 mmol), CsF (0.415 g, 2.73 mmol) and $Pd(PPh_3)_4$ (0.081 g, 0.070 mmol) were dissolved in dry and degassed THF (7.00 mL) and stirred for 15 minutes at room temperature. Next, allylboronic acid, pinacol ester (0.473 ml, 2.52 mmol) in THF (7.00 mL) was added dropwise and the reaction was stirred at 80 °C for 18 hours. Upon completion, the reaction was diluted with water and extracted with EtOAc (3 x 20 mL). The organic layer was dried over $MgSO_4$, filtered and concentrated under reduced pressure. The crude was purified via column chromatography using hexanes/EtOAc (6:1) to yield a crude arene intermediate, which was used in the next step without further purification.

The crude intermediate from the previous step was dissolved in DCM (10 mL), then pyridine (0.170 mL, 2.10 mmol) was added. Next, ozone (600 mg/hr. output, air as feed gas) was bubbled into the solution at 0 °C until the starting material was fully consumed; more DCM was added upon evaporation of solvent. Next, zinc metal (0.183 g, 2.80 mmol) and acetic acid (0.240 ml, 4.20 mmol) were added. The solution was warmed to room temperature and allowed to stir for 2 hours. Next, aq. 1M HCl (15 mL) was added, and the mixture was extracted with DCM (3 x 20 mL). The organic layer was dried over Na_2SO_4, filtered and concentrated under reduced pressure. The crude was purified via column chromatography using hexanes/EtOAc (4:1) to yield **2.113** (0.130 g, 0.433 mmol, 62% yield) as an amorphous white solid. ^1H NMR (600 MHz, $CDCl_3$): δ 9.84 (s, 1H), 7.82 (d, *J*=8.4 Hz, 1H), 7.37 (d, *J*=8.4 Hz, 1H), 5.2-5.3 (m, 2H), 4.60 (s, 2H), 2.3-2.3 (m, 1H), 2.0-2.1 (m, 1H), 1.7-1.8 (m, 1H), 1.7-1.7 (m, 1H), 1.5-1.5 (m, 2H), 1.3-1.3 (m, 5H), 0.90 (s, 3H), 0.36 (s, 3H) ppm. ^{13}C NMR (151 MHz, $CDCl_3$): 198.5, 171.5, 149.5, 144.8, 133.1, 125.2, 120.6, 68.2, 50.9, 44.9, 40.2, 39.3, 39.1, 32.6, 32.3, 31.6, 27.4, 19.9 ppm. HRMS m/z: $[M + Na]^+$ Calcd for $C_{19}H_{24}O_3Na$ 323.1618; found 323.1621. $[\alpha]^{20}_D$ = -17.7 (c = 1, $CHCl_3$).

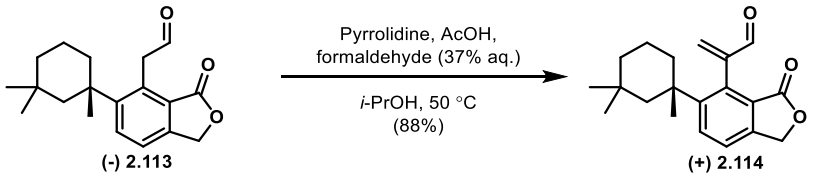

2.113 (0.085 g, 0.28 mmol) was dissolved in i-PrOH (2.83 mL), then formaldehyde (0.211 mL, 2.83 mmol, 37% aq.) was added, followed by the addition of acetic acid (0.016 mL, 0.28 mmol) and pyrrolidine (0.023 mL, 0.28 mmol). The reaction was stirred under argon at 50 °C overnight. Upon completion, the reaction was diluted with saturated aq. $NaHCO_3$ and extracted with DCM (3 x 20 mL). The organic layer was dried over $MgSO_4$, filtered and concentrated under reduced pressure. The crude was purified via column chromatography using hexanes/EtOAc (4:1) to yield **2.114** (0.078 g, 0.25 mmol, 88% yield) as an amorphous white solid, which existed as a mixture of atropisomers. ^{1}H NMR (600 MHz, $CDCl_3$): δ 9.8-9.9 (m, 2H), 7.9-7.9 (m, 2H), 7.4-7.4 (m, 2H), 6.6-6.6 (m, 2H), 6.4-6.4 (m, 2H), 5.2-5.2 (m, 4H), 2.2-2.3 (m, 1H), 2.11 (br d, 1H, *J*=1.5 Hz), 1.7-1.8 (m, 2H), 1.6-1.6 (m, 6H), 1.5-1.5 (m, 3H), 1.35 (s, 3H), 1.2-1.3 (m, 6H), 0.94 (s, 3H), 0.89 (s, 3H), 0.61 (s, 3H), 0.53 (s, 3H) ppm. ^{13}C NMR (151 MHz, $CDCl_3$): δ 192.6, 192.5, 169.7, 169.7, 150.7, 150.0, 148.2, 147.8, 144.4, 144.3, 136.9, 136.9, 133.8, 133.7, 133.7, 133.1, 124.8, 121.6, 121.4, 67.8, 67.7, 51.9, 49.9, 40.6, 40.3, 39.4, 39.4, 39.2, 38.3, 32.1, 31.6, 31.6, 31.5, 31.1, 29.8, 19.9, 19.7 ppm. HRMS m/z: $[M + Na]^+$ Calcd for $C_{20}H_{24}O_3Na$ 335.1618; found 335.1621. $[\alpha]^{20}_D$ = +2.4 (c = 1, $CHCl_3$).

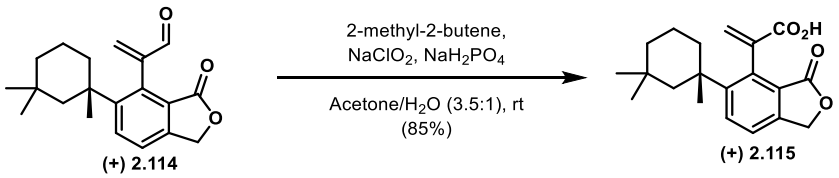

2.114 (0.056 g, 0.18 mmol) was dissolved in acetone (1.40 mL) and water (0.398 mL) at room

temperature. Next, 2-methyl-2-butene (0.095 ml, 0.90 mmol), sodium dihydrogen phosphate (0.049 g, 0.41 mmol) and sodium chlorite (0.041 g, 0.36 mmol) were added sequentially, and the reaction stirred at room temperature overnight. Upon completion, the reaction was diluted with saturated aq. $NaHCO_3$ and extracted with DCM (20 mL). The organic layer was discarded, then the aq. layer was acidified to pH 2 with 1M HCl and extracted with DCM (3 x 20 mL). The acidified organic layer was dried over $MgSO_4$, filtered and concentrated under reduced pressure. The crude was purified via column chromatography using hexanes/EtOAc (2:1) to yield **2.115** (0.0501 g, 0.15 mmol, 85% yield) as an amorphous white solid, which existed as a mixture of atropisomers. ^{1}H NMR (600 MHz, $CDCl_3$): δ 7.8-7.9 (m, 2H), 7.4-7.4 (m, 2H), 6.8-6.9 (m, 2H), 5.8-5.8 (m, 2H), 5.2-5.2 (m, 4H), 2.3-2.3 (m, 1H), 2.1-2.1 (m, 1H), 1.7-1.8 (m, 2H), 1.4-1.7 (m, 9H), 1.34 (s, 3H), 1.3-1.3 (m, 2H), 1.28 (s, 3H), 1.2-1.2 (m, 1H), 0.94 (s, 6H), 0.6-0.6 (m, 6H) ppm. ^{13}C NMR (151 MHz, $CDCl_3$): δ 170.6, 170.4, 169.9, 169.9, 150.9, 149.6, 144.2, 144.2, 138.0, 137.6, 135.4, 135.2, 133.9, 133.1, 131.8, 131.7, 125.4, 125.3, 121.5, 121.2, 67.9, 67.8, 52.0, 49.7, 40.7, 40.5, 39.5, 39.3, 39.0, 38.3, 32.0, 31.8, 31.7, 31.6, 31.5, 30.5, 29.9, 19.8, 19.8 ppm. HRMS m/z: $[M + Na]^+$ Calcd for $C_{20}H_{24}O_4Na$ 351.1567; found 351.1574. $[\alpha]^{20}_D = +7.1$ (c = 1, $CHCl_3$).

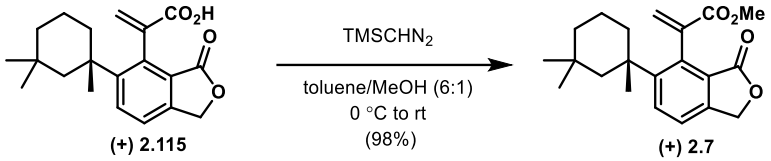

2.115 (0.040 g, 0.12 mmol) was dissolved in MeOH (0.870 mL) and toluene (5.22 mL), then $TMSCHN_2$ (0.12 ml, 0.24 mmol, 2M in diethyl ether) was added. The reaction stirred at room temperature for 3 hours, then was concentrated under reduced pressure. The crude was purified via column chromatography using hexanes/EtOAc (5:1) to yield **2.7** (0.041 g, 0.12 mmol, 98% yield) as an amorphous white solid, which existed as a mixture of atropisomers. ^{1}H NMR (600

MHz, $CDCl_3$): δ 7.8-7.9 (m, 2H), 7.4-7.4 (m, 2H), 6.8-6.8 (m, 2H), 5.7-5.7 (m, 2H), 5.2-5.2 (m, 4H), 3.7-3.8 (m, 6H), 2.3-2.4 (m, 1H), 2.1-2.1 (m, 1H), 2.0-2.0 (m, 1H), 1.7-1.7 (m, 2H), 1.6-1.7 (m, 4H), 1.6-1.6 (m, 2H), 1.5-1.5 (m, 2H), 1.35 (s, 3H), 1.3-1.3 (m, 2H), 1.26 (s, 3H), 1.1-1.2 (m, 1H), 0.9-1.0 (m, 6H), 0.6-0.6 (m, 6H) ppm. ^{13}C NMR (151 MHz, $CDCl_3$): δ 170.0, 170.0, 166.3, 166.2, 150.9, 149.3, 144.2, 144.1, 138.5, 138.2, 136.1, 134.0, 132.8, 130.0, 125.5, 125.4, 121.3, 120.9, 67.9, 67.8, 52.3, 52.2, 52.0, 49.3, 40.8, 40.3, 39.7, 39.3, 39.2, 38.2, 34.7, 32.0, 31.7, 31.4, 30.3, 29.8, 25.3, 19.8, 19.7 ppm. HRMS m/z: $[M + Na]^+$ Calcd for $C_{21}H_{26}O_4Na$ 365.1723; found 365.1732. $[\alpha]^{20}_D = +2.7$ (c = 1, $CHCl_3$).

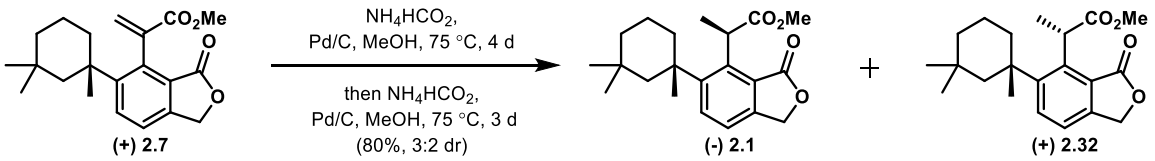

2.7 (0.026 g, 0.076 mmol) and Pd/C (8.08 mg, 7.59 μmol, 10% wt.) were added to a reaction vial under argon. Next, degassed methanol (1.52 mL) was added, followed by the addition of ammonium formate (0.120 g, 1.90 mmol). The reaction was sealed with a screw cap and heated at 75 °C for 4 days. The reaction was cooled to room temperature, filtered through celite, then concentrated under reduced pressure into a screw cap vial. Pd/C (8.08 mg, 7.59 μmol 10% wt.) was added to the vial, followed by degassed methanol (1.52 mL). Next, ammonium formate (0.120 g, 1.90 mmol) was added, and the reaction was sealed and stirred at 75 °C for an additional 3 days. Upon completion, the reaction was cooled to room temperature and carefully opened. The reaction was filtered through celite and concentrated under reduced pressure. The crude was purified via column chromatography using hexanes/EtOAc (3:1) to yield a diastereomeric mixture of **2.1** and **2.32** (0.021 g, 0.061 mmol, 3:2 dr.) which were separable by preparatory TLC using hexanes/EtOAc (5:1). **2.1** was isolated as a crystalline solid. Data for **2.1** ^1H NMR (600 MHz,

$CDCl_3$): δ 7.81 (d, *J*=8.4 Hz, 1H), 7.30 (d, *J*=8.4 Hz, 1H), 5.20 (s, 2H), 4.61 (q, *J*=6.9 Hz, 1H), 3.67 (s, 3H), 2.28 (br d, *J*=14.5 Hz, 1H), 2.08 (br d, *J*=13.8 Hz, 1H), 1.8-1.9 (m, 1H), 1.75 (d, *J*=6.9 Hz, 3H), 1.7-1.7 (m, 1H), 1.5-1.5 (m, 1H), 1.5-1.5 (m, 1H), 1.37 (s, 3H), 1.3-1.3 (m, 1H), 1.2-1.3 (m, 1H), 0.93 (s, 3H), 0.47 (s, 3H) ppm. ^{13}C NMR (151 MHz, $CDCl_3$): δ 173.8, 170.8, 148.1, 145.9, 141.9, 133.0, 124.7, 120.3, 68.4, 52.1, 50.9, 40.9, 40.5, 39.6, 39.4, 32.7, 31.8, 27.5, 20.1, 17.7 ppm. HRMS m/z: $[M + Na]^+$ Calcd for $C_{21}H_{28}O_4Na$ 367.1880; found 367.1884. $[\alpha]^{20}_D$ = -24.4 (c = 1, $CHCl_3$). MP = 154-156 °C. Our spectra corresponds to the reported literature data.[52]

Data for **2.32** ^1H NMR (600 MHz, $CDCl_3$): δ 7.80 (d, *J*=8.4 Hz, 1H), 7.30 (d, *J*=8.4 Hz, 1H), 5.22 (s, 2H), 4.64 (q, *J*=7.3 Hz, 1H), 3.71 (s, 3H), 2.33 (br d, *J*=14.2 Hz, 1H), 2.11 (br d, *J*=14.2 Hz, 1H), 1.8-1.8 (m, 1H), 1.7-1.7 (m, 1H), 1.61 (d, *J*=6.9 Hz, 3H), 1.5-1.5 (m, 1H), 1.4-1.5 (m, 1H), 1.40 (s, 3H), 1.3-1.3 (m, 1H), 1.3-1.3 (m, 1H), 0.86 (s, 3H), 0.39 (s, 3H) ppm. ^{13}C NMR (151 MHz, $CDCl_3$): δ 173.5, 170.8, 147.5, 145.9, 142.1, 133.1, 124.5, 119.9, 68.3, 51.9, 51.0, 41.0, 40.7, 39.3, 39.2, 32.8, 32.6, 31.5, 26.6, 20.0, 18.4 ppm. HRMS m/z: $[M + Na]^+$ Calcd for $C_{21}H_{28}O_4Na$ 367.1880; found 367.1886. $[\alpha]^{20}_D$ = +6.2 (c = 1, $CHCl_3$).

Chapter 3: Efforts Towards the Asymmetric Total Synthesis of the Oxeatamides

3.1 The Oxeatamides and Research Goal

The oxeatamides are a class of nitrogenous spongian diterpene natural products that were isolated from the New Zealand sponge *Darwinella oxeata* (**Figure 3.1**).[79] It's likely that the nitrogen in these natural products are derived from amino acids, which is quite rare to find among terpenoids derived from sponges.[79,80]

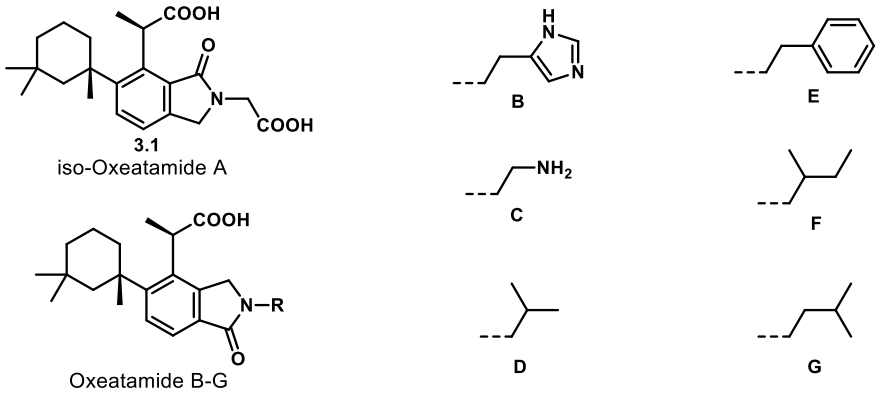

Figure 3.1: Structures of Selected Oxeatamide Natural Products

The oxeatamides were a desirable synthetic goal of ours for many reasons. First, they are structurally related to **2.1**, which we successfully synthesized asymmetrically. Due to the structural similarities, we were excited to explore these natural products as potential biofilm eradication agents. Also, our synthetic route to **2.**1 lends well to the oxeatamides scaffold, so we found this as a feasible synthetic challenge.

In addition to this, we were intrigued by the structural similarities and differences between **2.1** and the oxeatamide natural products. All of these natural products contain an arene substituted

with a trimethylcyclohexyl moiety, as well as the same two chiral centers. The major difference between many of these natural products is the inconsistent oxidation patterns (**Figure 3.2**). As shown, the lactone moiety of **2.1** demonstrates the same oxidation pattern as the lactam moiety of **3.1**. Interestingly, most of the other oxeatamides natural products contain oxidation on the other side of the lactam moiety. It's interesting to speculate why the sponge would demonstrate different oxidation patterns for extremely similar natural products, so we were eager to pursue the synthesis of these natural products to further confirm their structural assignments.

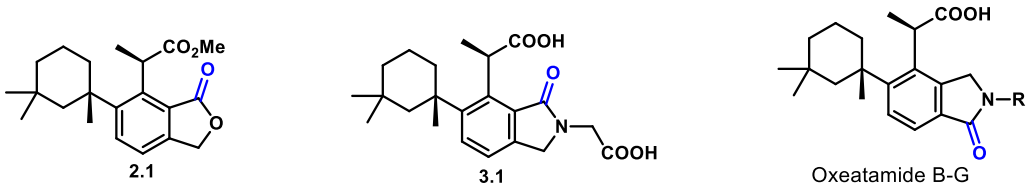

Figure 3.2: Inconsistent Oxidation Pattern of 2.1 and the Oxeatamides

In addition to the synthesis of these natural products, we are eager to perform SAR studies due to the ability to rapidly functionalize the group directly attached to the lactam ring. With this in mind, our synthetic strategy to these natural products was built around our already established synthesis of **2.1** but will also account for the ability to rapidly produce analogs and further our drug discovery efforts.

3.2 Synthetic Strategy

To expedite our efforts towards the synthesis of the oxeatamides, it's paramount that we utilize our previous synthesis as much as possible. As mentioned above, the oxeatamides demonstrate differential oxidation patterns, so there is a point where we need to diverge our synthesis, dependent upon which natural product we are currently pursuing. Our strategy utilizes

alcohol **2.21** as an advanced intermediate that can provide access to these natural products containing either oxidation pattern (**Scheme 3.1**).

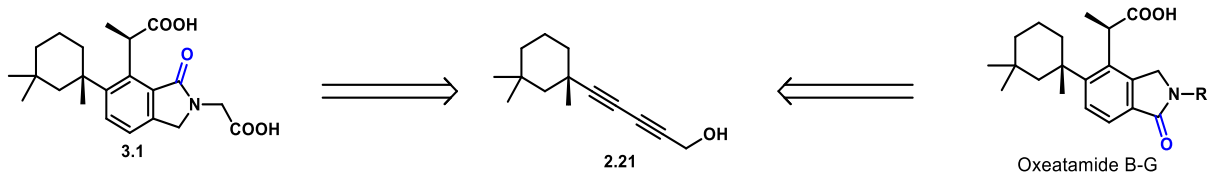

Scheme 3.1: Strategy to Natural Products with Varying Oxidation Patterns

To pursue the synthesis of **3.1**, we would first convert the alcohol of **2.21** into a mesylate, then treat it with an appropriate amine, thus creating a propargylic amine compound. This amine could then be coupled with carboxylic acid **2.22** to achieve a new lactam compound. At this point, we would utilize the same steps that were utilized in our previous synthesis, leading us to **3.1** (**Scheme 3.2**). Of course, we are aware that issues may arise, but this was our starting strategy, and we would adjust this strategy as needed.

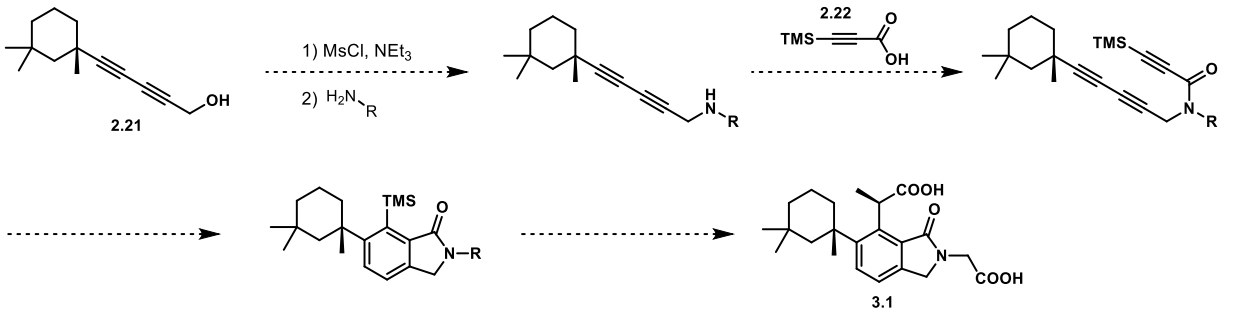

Scheme 3.2: Strategy Towards the Synthesis of 3.1

To pursue the synthesis of oxeatamides B-G, we will again start with **2.21**, but we will instead oxidize the propargylic alcohol to the carboxylic acid first. At this point, we could think about coupling many amines to provide the desired side chains of these natural products. This strategy, however, will be quite lengthy to achieve each individual natural product. An approach

that is more attractive to use is one where we install a side chain that can be removed later, therefore leading to rapid access to the rest of these natural products, as well as many analogs for future SAR studies (**Scheme 3.3**).

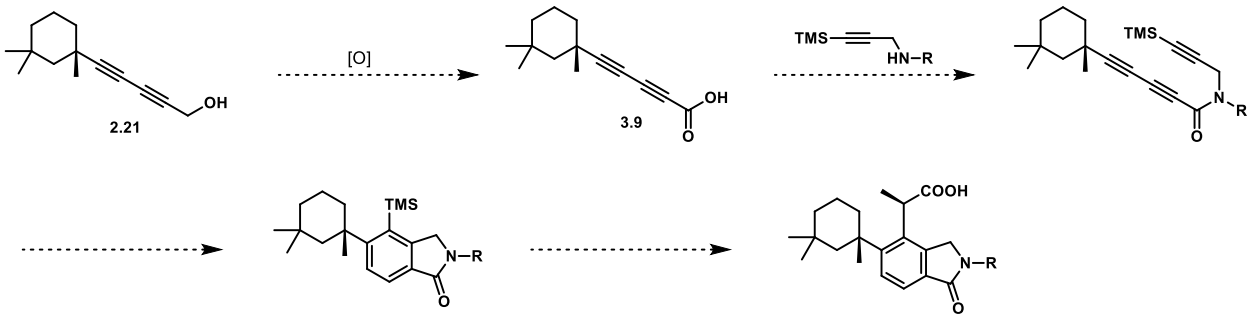

Scheme 3.3: Strategy Towards the Synthesis of Oxeatamide B-G and Other Analogs

3.3 Efforts Towards 3.1

Although we have experience working with compounds structurally similar to **3.1** and many of the intermediates we may encounter, we decided that it would be logical to utilize a model system to work out many of the reaction conditions in our synthesis. Based on previous efforts, we know that the tBu system, although not perfect, is a much better representation of the trimethylcyclohexyl moiety than phenyl. Because of this, we started with **2.83** and performed a Cadiot Chodkiewicz coupling with bromo-alkyne **2.20**, just as we had previously, to synthesize **2.84**. With **2.84** in hand, we successfully converted it into mesylate **3.2** upon treatment with MsCl and NEt_3. **3.2** was treated with **3.3** and NEt_3 to yield **3.4.** We decided to utilize the glycine benzyl ester **3.3** because the benzyl group could be removed under reducing conditions; given that we plan to go through a similar acrylate late-stage intermediate as we did during our synthesis of **2.1**, we were hopeful to reduce the alkene concurrently with the reduction of our benzyl ester. **3.4** could easily undergo an EDC coupling with **2.22** to achieve amide **3.5**, which existed as a rotameric mixture of 1.2:1.

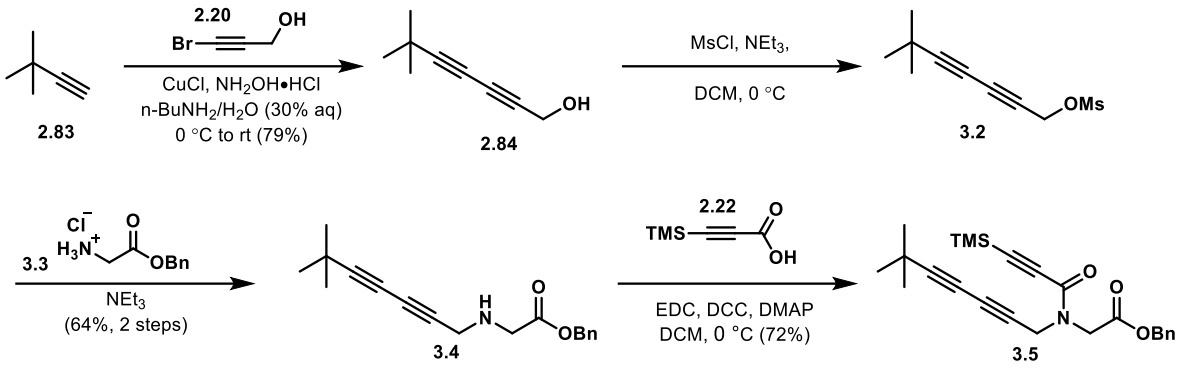

Scheme 3.4: Synthesis of 3.5

With a rotameric mixture of amides, we had some reservations about the potential success of an HDDA reaction. Fortunately, we successfully performed an HDDA reaction with **3.5**, synthesizing **3.6** in a 64% yield (**Scheme 3.5**). We are unsure what ratio of rotamers we will observe when we perform this with the trimethylcyclohexyl compounds, but based on this success, we're confident that we can achieve this transformation on the route to **3.1**.

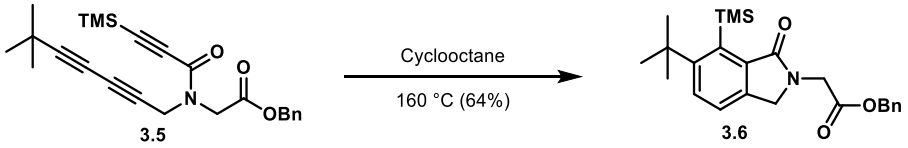

Scheme 3.5: Synthesis of 3.6 via HDDA Reaction

Unfortunately, this is the furthest we have been able to progress with this synthetic route. Based on the structural similarities and consistent oxidation pattern with **2.1**, we envision that we could proceed with the same conditions that we found success within Chapter 2. Upon completion of this synthetic route with the tBu model system, we plan to utilize these findings towards our pursuit of **3.1** Since only one of the oxeatamide natural products possesses this scaffold, this synthetic route has unfortunately received less of our attention. We are eager to further our efforts with this route and successfully synthesize **3.1**.

3.4 Efforts Towards Oxeatamide B-G

Given that oxeatamides B-G have a different oxidation pattern relative to **3.1**, as well as having various side chains, we had to take a slightly different approach to synthesize them. For the synthesis of **3.1**, we utilized a benzyl protecting group, with hopes of performing a global deprotection to yield **3.1**. For oxeatamides B-G, we envisioned that the use of an orthogonal protecting group would be ideal so that we could selectively functionalize the nitrogen-containing side chain, then reduce the alkene. Based on this thought process, we envisioned that a PMB group would be ideal because we could remove the PMB group under oxidizing conditions. We could then derivatize the N-side chain, followed by reduction of the alkene (**Scheme 3.6**).

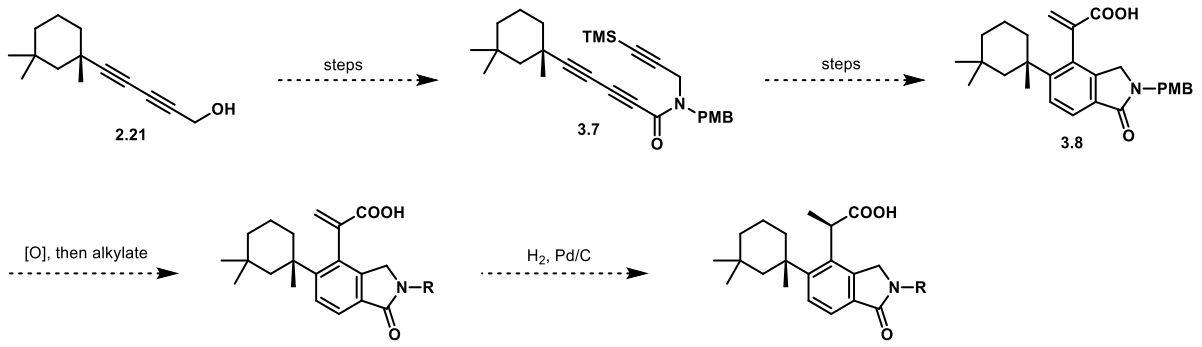

Scheme 3.6: Strategy Towards Oxeatamide B-G Using PMB

To proceed further, we decided to start with our tBu model system precursor **2.83** to synthesize **2.84** through previously established methods. Next, we were able to oxidize the propargylic alcohol cleanly and efficiently to the carboxylic acid, utilizing a system with sodium chlorite, as well as catalytic TEMPO and sodium hypochlorite. This was also a very efficient transformation because we could obtain **3.10** in high purity through an acid-base extraction. Interestingly, a very common oxidation in the presence of alkynes, the Jones oxidation, wasn't successful on our substrate. Finally, we were able to synthesize **3.11**, which could be easily coupled with **3.10** to synthesize amide **3.12**, which existed as a mixture of rotamers (**Scheme 3.7**).

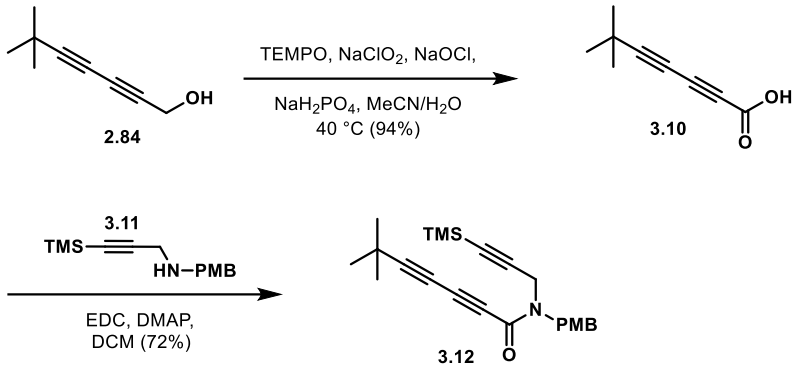

Scheme 3.7: Synthesis of 3.12

With **3.12** in hand, our sights were now set on performing a HDDA reaction and continuing this synthesis with similar methods that we have previously utilized. Fortunately, we were able to synthesize **3.13** in modest yields, which we would like to improve soon. Next, our sights were on converting the silyl group to iodide, utilizing our previous methods. Unfortunately, our initial attempts weren't successful. Based on initial mass spectrometry analysis and crude NMR data, it appears that we indeed converted the silyl group to an iodide, but we instead further iodinated **3.13**. It's reasonable to think that the electron-rich character of the PMB group allowed for an *ortho*-iodination of the PMB group, in addition to the desired iodination (**Scheme 3.8**). Attempts were made to limit the amount of I_2 in the reaction, but then we started to notice multiple products forming without full consumption of our starting material. This suggests that there most likely isn't a drastic difference in the rate of converting our aryl silyl group to an aryl iodide and potentially iodinating the PMB group. We haven't been able to further address this issue, but it is certainly a route that we would like to continue to pursue. We see a ton of value in being able to selectively liberate our lactam and further functionalize before reducing the double bond of the acrylate moiety.

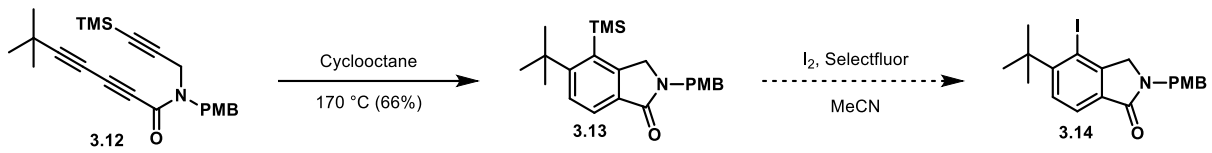

Scheme 3.8: Attempted Synthesis of 3.14

Overall, we weren't thrilled with the issues we encountered with the PMB group. As stated, we hypothesized that the extremely electron rich PMB group was being iodinated, so we wanted to attempt to continue with a similar strategy, but this time, by utilizing a side chain that wasn't as electron rich. To pursue this, we decided to use a phenethyl group as our N-functionalized side chain. We decided to use phenethyl because this would directly lead us to the tBu analog of oxeatamide E. Also, phenethyl is significantly less electron rich than PMB, so we were hopeful that we could proceed further without over iodinating our reactant. Although we wouldn't be able to remove phenethyl, like we planned to with PMB, this would still give us access to an oxeatamide E analog, as well as be used as a proof-of-concept study to that this synthetic strategy could be utilized for many of the oxeatamides.

To do this, like our most recent approach, we utilized carboxylic acid **3.10** and performed an EDC coupling with **3.15** to produce amide **3.16**, which existed as a rotameric mixture. Just like before, we were able to perform an HDDA reaction on **3.16** to synthesize arene **3.17**. With **3.17** in hand, we attempted to perform an iodination, being very careful with our reaction conditions based on our previous experiences. Based on mass spectrometry and crude NMR data, we again observed what was likely to be excessive iodination (**Scheme 3.9**). We attempted to briefly optimize the reactivity of the reaction, but we couldn't observe clean conversion to desired aryl iodide **3.18**.

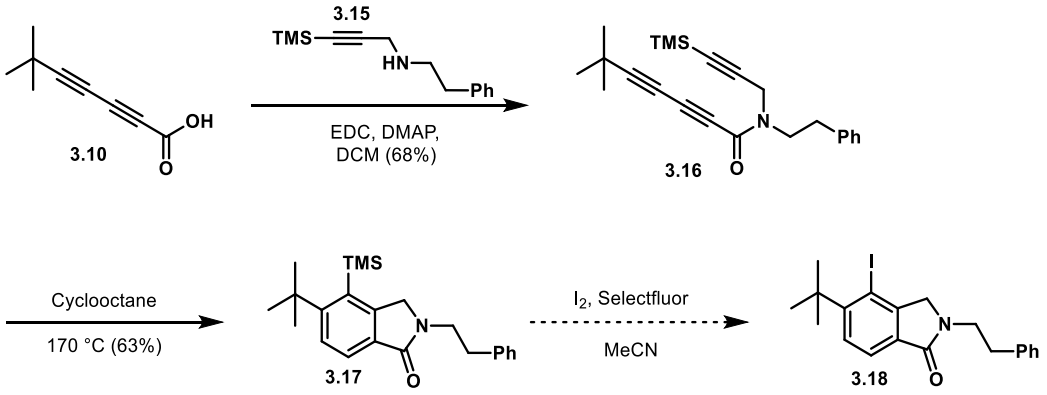

Scheme 3.9: Attempted Synthesis of 3.18

Due to the shortcomings of converting our aryl silyl compounds into aryl iodides in the presence of an aromatic ring, our next efforts will be to synthesize a model system with an aliphatic side chain, which should prevent our substrate from over iodination. Again, this approach provides low versatility because of the inability to cleave this side chain but would provide a proof-of-concept study showing that we can ultimately attain these natural products. We would like to pursue a side chain that is removable, but also electron poor, to circumvent the issue of over-iodinating our intermediate. To do this, we envisioned the use of a nosyl group, which could be deprotected without reducing the alkene of our late-stage acrylate intermediate (**Scheme 3.10**).

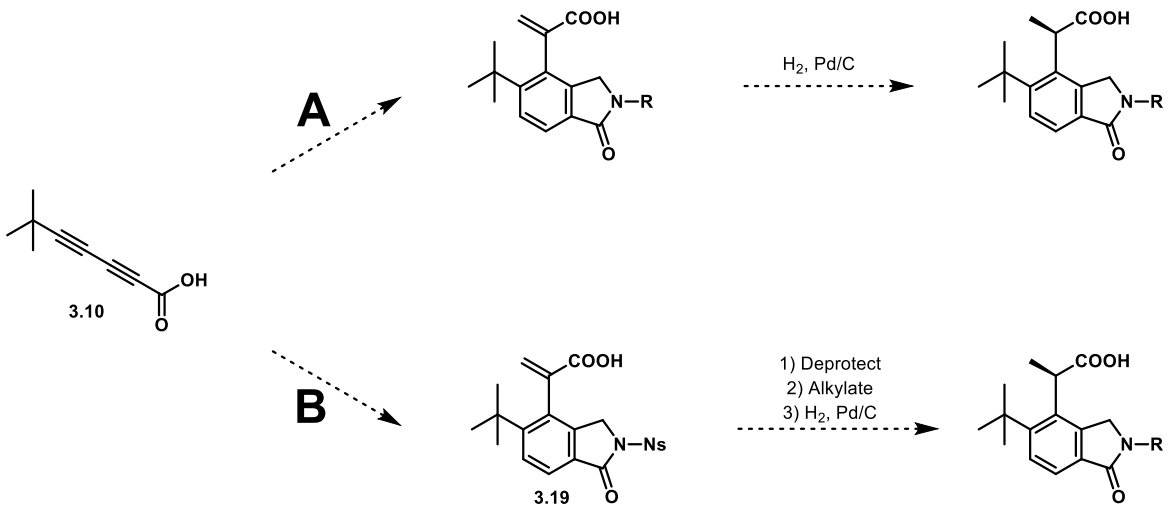

Scheme 3.10: Strategy to Obtain Oxeatamide B-G Analogs

In this scheme, path **A** demonstrates our ability to utilize a propargylamine with an already established aliphatic group, leading to a final product that contains a lactam with additional aliphatic functionality; there isn't a way to cleave this group however, so this demonstrates the less versatile pathway. Path **B** demonstrates our ability to go through a similar route, but with a nosyl protected lactam. Although this requires more steps, we would be able to deprotect the nosyl group and further functionalize the lactam with aliphatic groups, as well as other functionality. This path leads to the ability to synthesize many analogs that would allow us to achieve our total synthesis goals, as well as pursue further SAR studies for potential biofilm eradication agents. Because of this synthetic versatility, we are fascinated by the successful pursuit of path **B**.

As we were performing these studies towards **3.1**, as well as oxeatamides B-G on our tBu model system, we figured it would be a good idea to start working out conditions on our trimethylcyclohexyl scaffold. To do this, we started with racemic **2.21** and performed the same oxidation that we utilized for the synthesis of **3.10**, which yielded **3.20** in a 92% yield (**Scheme**

3.11). To our delight, **3.20** didn't require chromatographic purification to obtain a high level of purity.

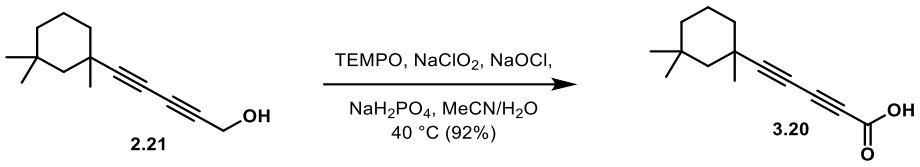

Scheme 3.11: Synthesis of 3.20

Due to our current lack of progress developing an optimal route towards oxeatamides B-G, we decided that it wouldn't be logical to move forward with **3.20**. Once we discover an ideal amine coupling partner that will grant us access to oxeatamide B-G and other analogs, we will happily move forward with our efforts.

As we start to work out these conditions more and successfully iodinate our arene, we will continue along the synthetic route by utilizing the conditions that enabled us to synthesize **2.1**. Along the way, we will certainly have new ideas and potentially pursue conditions that haven't yet been explored. One potential strategy that we're interested in is the possibility of performing a nickel catalyzed RCC to rapidly functionalize our aryl iodides. We briefly attempted this with **2.26** to yield **2.1** in a single step, but this didn't work well at all. We have found plenty of palladium catalyzed couplings with **2.26**, but we never had success with nickel catalyzed RCC's on this compound. **2.26**, as shown in **Scheme 3.12**, is extremely hindered, with bulky groups at both *ortho* positions. Our aryl iodide that we hope to gain access to on our way to oxeatamide B-G, although still very hindered, is less hindered than **2.26**. Although we still have reservations about the potential success of this due to the overall hinderance, we are eager to pursue this as an option. If we find success in this, we could easily convert the methyl ester into the carboxylic acid or utilize a different coupling partner to gain direct access to the carboxylic acid product. We are still far

from pursuing this idea, but we are excited about the possibility of pursuing new cross coupling conditions.

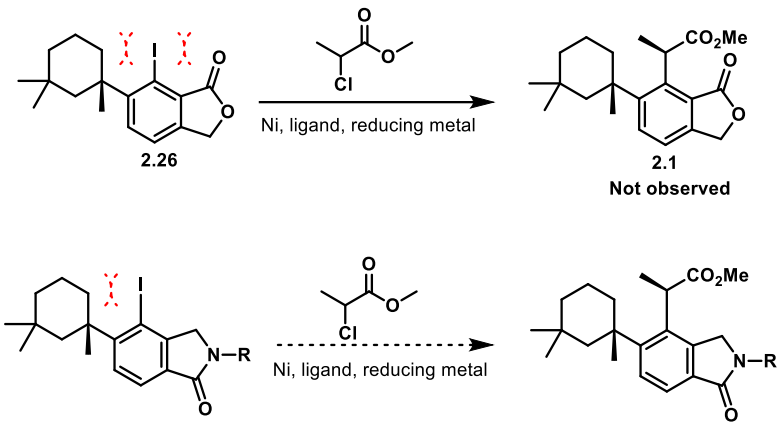

Scheme 3.12: Revisiting Nickel Catalyzed RCC

3.5 Conclusion and Future Directions

So far, we have begun studies to allow us to gain access to **3.1**, as well as oxeatamide B-G. Clearly, we still have a long way to go to achieve these synthetic efforts, but we have started to lay the groundwork for this feat. By starting with **2.83** and successfully synthesizing **3.6**, we have gained new experience working with nitrogen-containing compounds and begun our journey to synthesizing these natural products. Based on our more recent efforts, we are unsure if the iodination of **3.6** will occur without issue, due to the presence of the benzyl protecting group; immediate efforts need to be performed to determine if this protecting group will behave under these reaction conditions, or if we need to exchange it out for a different protecting group.

Although we haven't experienced much success in our efforts towards oxeatamide B-G, we've learned a great deal about the reactivity of our intermediates. Our initial efforts will be to synthesize a derivative with an N-substituted aliphatic group to prove that our overall route is

viable. Later, we will attempt to synthesize a protected lactam intermediate, which can be selectively deprotected and functionalized, diverging to many of the oxeatamide natural products.

Since Northcote's discovery and characterization of this class of natural products previously described, Berlinck has since characterized a few more natural products from *Darwinella oxeata* (**Figure 3.3**).[80] Once we successfully achieve our efforts that were previously discussed, these natural products, also being part of the oxeatamides, appear to be a feasible synthetic challenge. Upon the successful synthesis of these natural products, we would like to further evaluate them as potential biofilm eradication agents.

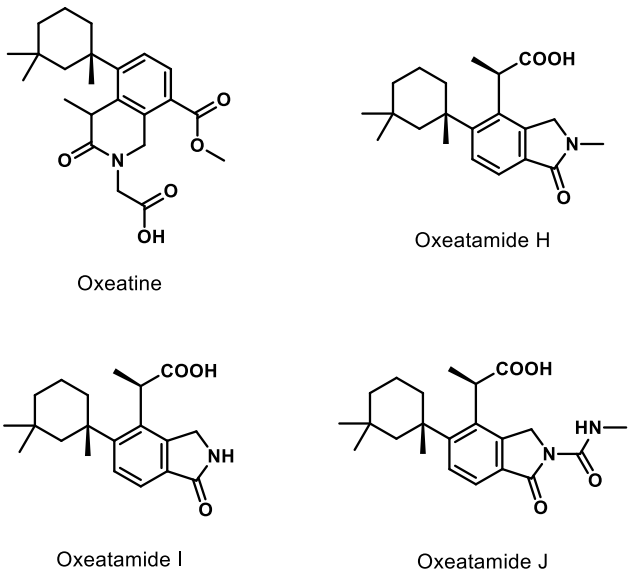

Figure 3.3: Recently Characterized Oxeatamide Natural Products

Finally, when all these methods are developed and natural products synthesized, we hope to utilize the versatility of these methods to synthesize natural product analogs that can be tested as biofilm eradication agents. Due to the access of these compounds through chemical synthesis, we expect that we can perform rapid SAR studies and further our understanding of these biofilm eradication agents.

3.6 Chapter 3 Experimental Procedures

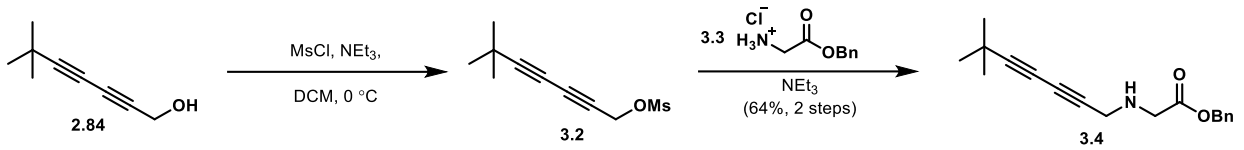

2.84 (1.2 g, 8.8 mmol) was dissolved in DCM (107 mL) and cooled to 0 °C. Next, NEt_3 (1.60 mL, 11.5 mmol) was added, followed by the dropwise addition of MsCl (0.955 mL, 12.3 mmol). The reaction was then warmed to room temperature and stirred for 2 hours. Upon completion, the reaction was quenched with saturated aq. NH_4Cl and extracted with DCM (3 x 25 mL). The organic layer was dried over $MgSO_4$, filtered and concentrated under reduced pressure to yield **3.2**, which was used in the next step without further purification.

3.2 (1.88 g, 8.77 mmol) was dissolved in MeCN (17.5 mL), followed by the addition of **3.3** (3.54 g, 17.6 mmol) and NEt_3 (3.67 mL, 26.3 mmol). The reaction was stirred at room temperature overnight. Upon completion, the reaction was diluted with water and extracted with EtOAc (3 x 50 mL). The organic layer was dried over $MgSO_4$, filtered and concentrated under reduced pressure. The crude was purified via column chromatography using hexanes/EtOAc (4:1) to yield **3.4** (1.6 g, 5.7 mmol, 64% yield) over 2 steps as a clear oil. ^1H NMR (600 MHz, $CDCl_3$): δ 7.3-7.4 (m, 5H), 5.18 (s, 2H), 3.56 (s, 4H), 1.72 (br s, 1H), 1.24 (s, 9H) ppm. ^{13}C NMR (151 MHz, $CDCl_3$): δ 171.7, 135.5, 128.6, 128.4, 87.5, 74.7, 69.0, 66.7, 63.4, 49.3, 38.4, 30.5, 28.0 ppm. HRMS m/z: $[M + Na]^+$ Calcd for $C_{18}H_{22}NO_2$ 284.1645; found 284.1642.

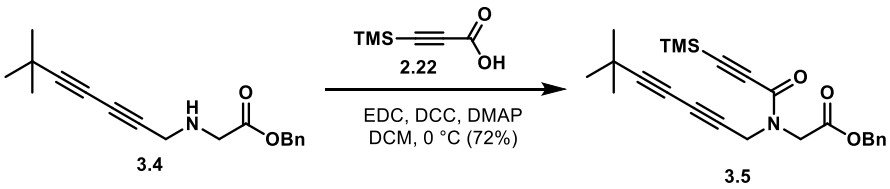

3.4 (1.3 g, 4.6 mmol) was dissolved in DCM (11.5 mL), then **2.22** (0.771 mL, 5.96 mmol) was

added. The solution was cooled to 0 °C, then EDC (1.14 g, 5.96 mmol) and DMAP (0.028 g, 0.23 mmol) were added. The reaction was warmed to room temperature and stirred overnight. Upon completion, the reaction was quenched with saturated aq. NH_4Cl (10 mL) and extracted with DCM (3 x 20 mL). The organic layer was dried over $MgSO_4$, filtered and concentrated under reduced pressure. The crude was purified via column chromatography using hexanes/EtOAc (10:1) to yield **3.5** (1.35 g, 3.30 mmol) as a clear oil, which existed as a mixture of rotamers. ^{1}H NMR (600 MHz, $CDCl_3$): δ 7.3-7.4 (m, 5H), 5.2-5.2 (m, 2H), 4.3-4.6 (m, 4H), 1.2-1.3 (m, 9H), 0.2-0.3 (m, 9H) ppm. ^{13}C NMR (151 MHz, $CDCl_3$): δ 169.2, 168.9, 154.4, 154.3, 135.9, 135.8, 129.5, 129.4, 129.4, 129.3, 129.1, 100.6, 99.9, 95.6, 95.3, 89.6, 89.0, 71.2, 71.0, 70.8, 68.2, 68.0, 63.8, 63.7, 49.8, 45.5, 40.8, 35.8, 31.2, 31.1, 28.8, 28.7, 0.0, -0.1 ppm. HRMS m/z: $[M + Na]^+$ Calcd for $C_{24}H_{29}NO_3SiNa$ 430.1809; found 430.1806.

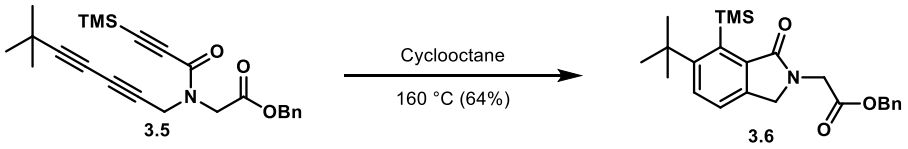

3.5 (0.209 g, 0.513 mmol) was added to a reaction vial, then was dissolved in freshly distilled and degassed cyclooctane (103 mL). The reaction was heated at 160 °C for 48 hours. Upon completion, the reaction was cooled to room temperature and filtered through a pad of silica gel. The silica plug was rinsed with hexanes to elute off any additional cyclooctane. Next, EtOAc was used to elute the remainder of the reaction mixture, which was then concentrated under reduced pressure. The crude was purified via column chromatography using hexanes/EtOAc (20:1) to give **3.6** (0.14 g, 0.33 mmol, 64% yield) as a clear oil. ^{1}H NMR (600 MHz, $CDCl_3$): δ 7.65 (d, *J*=8.7 Hz, 1H), 7.3-7.4 (m, 5H), 7.31 (d, *J*=8.0 Hz, 1H), 5.19 (s, 2H), 4.42 (s, 2H), 4.40 (s, 2H), 1.47 (s, 9H), 0.53 (s, 9H) ppm. ^{13}C NMR (151 MHz, $CDCl_3$): δ 170.5, 169.1, 158.3, 140.2, 139.1, 138.3, 135.3,

128.9, 128.6, 128.4, 128.3, 122.4, 67.1, 49.7, 44.3, 37.5, 33.5, 5.8 ppm. HRMS m/z: $[M + Na]^+$ Calcd for $C_{24}H_{31}NO_3SiNa$ 432.1965; found 432.1959.

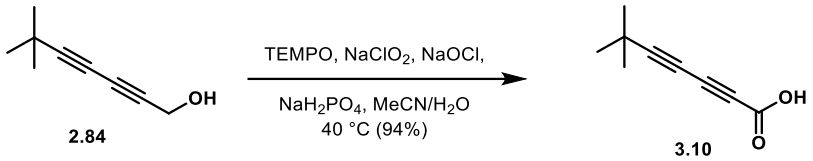

2.84 (2.36 g, 17.3 mmol) was dissolved in MeCN (85 mL) and water (63 mL). Next, sodium dihydrogen phosphate (0.042 g, 0.35 mmol) and TEMPO (0.190 g, 1.213 mmol) were added. The reaction was heated to 35 °C, then solutions of sodium chlorite (3.13 g, 34.7 mmol) in water (16.9 mL) and sodium hypochlorite (0.165 mL, 0.347 mmol, 13% available chlorine) in water (8.5 mL) were added portion wise (these solutions were added dropwise, alternating between additions of each solution. Roughly 1/3 of the first solution was added dropwise, then 1/3 of the second solution was added dropwise. This continued until all the solutions were added to the reaction). The reaction was stirred at 40 °C overnight. Upon completion, the reaction was cooled to room temperature, then basified to pH 8 with 1M NaOH. Next, 1M Na_2SO_3 (5 mL) was added, and the reaction was stirred for 10 minutes. The reaction was then poured into a separatory funnel, diluted with water (20 mL) and extracted with ether (10 mL); the organic layer was discarded. The aq. layer was acidified to pH 2 with 1M HCl, then extracted with ether (3 x 20 mL). The organic layer was dried over $MgSO_4$, filtered and concentrated under reduced pressure to yield **3.10** (2.44 g, 16.3 mmol), which was sufficiently pure and used without further purification.

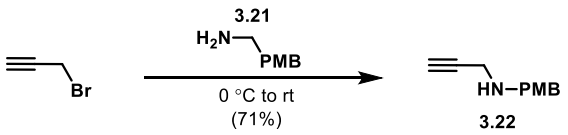

3.21 (2.1 g, 2.0 mL, 15 mmol) was added to a flask under argon and cooled to 0 °C. Next, propargyl

bromide (0.43 mL, 3.8 mmol, 80% wt. in toluene) was added dropwise. The solution was stirred at 0 °C for 30 minutes, then was warmed to room temperature and stirred overnight. Upon completion, the reaction was diluted with EtOAc (10 mL) and washed with 1M NaOH (3 x 15 mL). The organic layer was dried over $MgSO_4$, filtered and concentrated under reduced pressure. The crude was purified via column chromatography using hexanes/EtOAc (2:1) to yield **3.22** (0.49 g, 2.8 mmol, 71% yield) as a pale-yellow oil. Our data corresponds with the reported literature data.[81]

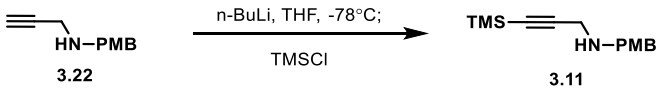

3.22 (0.598 g, 3.41 mmol) was dissolved in THF (9.75 mL), then the solution was cooled to -78 °C. Next, n-BuLi (5.33 ml, 8.53 mmol, 1.6 M in hexanes) was added dropwise and the solution stirred at -78 °C for 30 minutes. Next, TMS-Cl (0.872 ml, 6.83 mmol) was added dropwise to this solution, which was stirred at -78 °C for one hour, then warmed to room temperature and stirred for an additional hour. Upon completion, the reaction was quenched with saturated aq. NH_4Cl (20 mL) and extracted with EtOAc (3 x 20 mL). The organic layer was dried over $MgSO_4$, filtered and concentrated under reduced pressure. Crude **3.11** was obtained as a yellow oil, which was used in the next step without further purification.

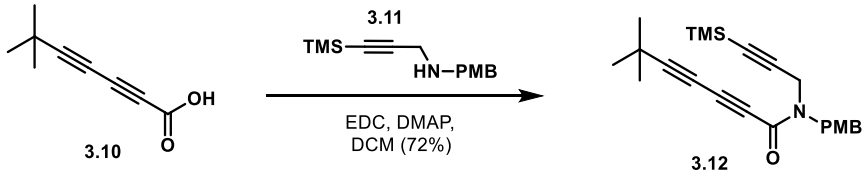

3.10 (0.104 g, 0.694 mmol) and **3.11** (0.143 g, 0.578 mmol) were dissolved in DCM (2.3 mL) and cooled to 0 °C. Next, EDC (0.144 g, 0.751 mmol) and DMAP (3.5 mg, 0.029 mmol) were added, then the reaction was warmed to room temperature and stirred overnight. Upon completion, the

reaction was quenched with saturated aq. NH_4Cl (10 mL) and extracted with DCM (3 x 20 mL). The organic layer was dried over $MgSO_4$, filtered and concentrated under reduced pressure. The crude was purified via column chromatography using hexanes/EtOAc (10:1) to yield **3.12** (0.158 g, 0.416 mmol, 72% yield), which existed as a mixture of rotamers. ^{1}H NMR (600 MHz, $CDCl_3$): δ 7.2-7.2 (m, 2H), 6.8-6.9 (m, 2H), 4.7-4.9 (m, 2H), 4.1-4.2 (m, 2H), 3.8-3.8 (m, 3H), 1.3-1.3 (m, 9H), 0.1-0.2 (m, 9H) ppm.

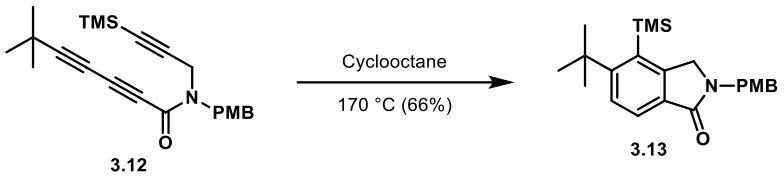

3.12 (0.048 g, 0.13 mmol) was added to a reaction vial, then was dissolved in freshly distilled and degassed cyclooctane (25.3 mL). The reaction was heated at 160 °C for 48 hours. Upon completion, the reaction was cooled to room temperature and filtered through a pad of silica gel. The silica plug was rinsed with hexanes to elute off any additional cyclooctane. Next, EtOAc was used to elute the remainder of the reaction mixture, which was then concentrated under reduced pressure. The crude was purified via column chromatography using hexanes/EtOAc (20:1) to give **3.13** (0.032 g, 0.084 mmol, 66% yield) as a clear oil. ^{1}H NMR (600 MHz, $CDCl_3$): δ 7.65 (d, *J*=8.0 Hz, 1H), 7.46 (d, *J*=7.6 Hz, 1H), 7.09 (d, *J*=7.3 Hz, 2H), 6.71 (d, *J*=7.6 Hz, 2H), 4.59 (s, 2H), 4.22 (s, 2H), 3.64 (s, 3H), 1.29 (s, 9H), 0.29 (s, 9H) ppm. ^{13}C NMR (151 MHz, $CDCl_3$): δ 168.0, 160.8, 159.1, 148.3, 134.1, 130.0, 129.4, 129.2, 125.4, 124.0, 114.1, 55.3, 52.1, 45.6, 37.3, 33.7, 5.4 ppm.

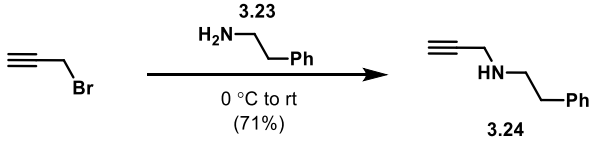

3.23 (1.9 g, 2.0 mL, 16 mmol) was added to a flask under argon and cooled to 0 °C. Next, propargyl bromide (0.44 mL, 4.0 mmol, 80% wt. in toluene) was added dropwise. The solution was stirred at 0 °C for 30 minutes, then was warmed to room temperature and stirred overnight. Upon completion, the reaction was diluted with EtOAc (10 mL) and washed with 1M NaOH (3 x 15 mL). The organic layer was dried over $MgSO_4$, filtered and concentrated under reduced pressure. The crude was purified via column chromatography using hexanes/EtOAc (2:1) to yield **3.24** (0.45 g, 2.8 mmol, 71% yield) as a pale-yellow oil. Our data corresponds with the reported literature data.[82] ^{1}H NMR (600 MHz, $CDCl_3$): δ 7.32 (t, *J* = 6.9 Hz, 2H), 7.27 - 7.22 (m, 3H), 3.44 (s, 2H), 2.99 (t, *J* = 6.9 Hz, 2H), 2.84 (t, *J* = 7.6 Hz, 2H), 2.23 (s, 1H) ppm. ^{13}C NMR (151 MHz, $CDCl_3$): δ 139.8, 128.8, 128.5, 126.2, 82.1, 71.5, 49.8, 38.1, 36.1 ppm.

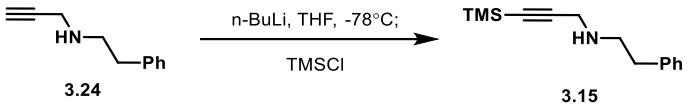

3.24 (0.598 g, 3.41 mmol) was dissolved in THF (9.75 mL), then the solution was cooled to -78 °C. Next, n-BuLi (5.33 ml, 8.53 mmol, 1.6 M in hexanes) was added dropwise and the solution stirred at -78 °C for 30 minutes. Next, TMS-Cl (0.872 ml, 6.83 mmol) was added dropwise to this solution, which was stirred at -78 °C for one hour, then warmed to room temperature and stirred for an additional hour. Upon completion, the reaction was quenched with saturated aq. NH_4Cl (20 mL) and extracted with EtOAc (3 x 20 mL). The organic layer was dried over $MgSO_4$, filtered and concentrated under reduced pressure. Crude **3.15** was obtained as a yellow oil, which was used in the next step without further purification.

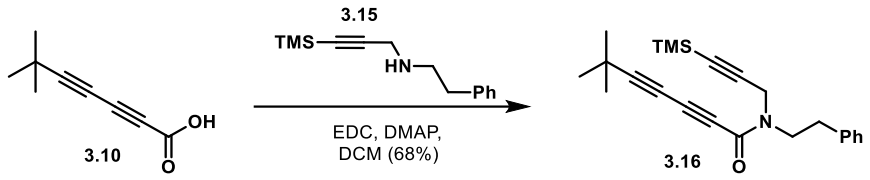

3.10 (0.084 g, 0.56 mmol) and **3.15** (0.11 g, 0.47 mmol) were dissolved in DCM (1.87 mL) and cooled to 0 °C. Next, EDC (0.116 g, 0.607 mmol) and DMAP (2.9 mg, 0.023 mmol) were added, then the reaction was warmed to room temperature and stirred overnight. Upon completion, the reaction was quenched with saturated aq. NH_4Cl (10 mL) and extracted with DCM (3 x 20 mL). The organic layer was dried over $MgSO_4$, filtered and concentrated under reduced pressure. The crude was purified via column chromatography using hexanes/EtOAc (10:1) to yield **3.16** (0.116 g, 0.318 mmol, 68% yield), which existed as a mixture of rotamers. ^{1}H NMR (600 MHz, $CDCl_3$): δ 7.1-7.2 (m, 2H), 7.0-7.1 (m, 3H), 4.1-4.1 (m, 2H), 3.5-3.7 (m, 2H), 2.7-2.8 (m, 2H), 1.1-1.1 (m, 9H), 0.0-0.0 (m, 9H) ppm.

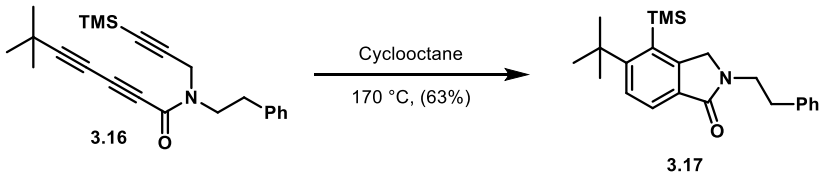

3.16 (0.052 g, 0.14 mmol) was added to a reaction vial, then was dissolved in freshly distilled and degassed cyclooctane (28.6 mL). The reaction was heated at 160 °C for 48 hours. Upon completion, the reaction was cooled to room temperature and filtered through a pad of silica gel. The silica plug was rinsed with hexanes to elute off any additional cyclooctane. Next, EtOAc was used to elute the remainder of the reaction mixture, which was then concentrated under reduced pressure. The crude was purified via column chromatography using hexanes/EtOAc (20:1) to give **3.17** (0.033 g, 0.090 mmol, 63% yield) as a clear oil. ^{1}H NMR (600 MHz, $CDCl_3$): δ 7.67 (d, *J*=8.0

Hz, 1H), 7.51 (d, *J*=8.0 Hz, 1H), 7.2-7.2 (m, 2H), 7.2-7.2 (m, 2H), 7.1-7.2 (m, 1H), 4.12 (s, 2H), 3.82 (t, *J*=6.5 Hz, 2H), 2.93 (t, *J*=6.2 Hz, 2H), 1.37 (s, 9H), 0.32 (s, 9H) ppm. ^{13}C NMR (151 MHz, $CDCl_3$): δ 168.1, 160.6, 148.2, 139.2, 133.9, 130.1, 128.8, 128.7, 126.6, 125.4, 123.7, 53.7, 44.0, 37.3, 35.2, 33.7, 5.4 ppm.

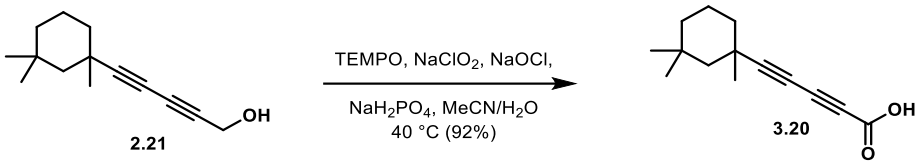

2.21 (0.217 g, 1.06 mmol) was dissolved in MeCN (5.18 mL) and water (3.89 mL) at room temperature, then sodium dihydrogen phosphate (2.6 mg, 0.021 mmol) and TEMPO (0.017 g, 0.11 mmol) were added. The reaction was stirred at 40 °C, then solutions of sodium chlorite (0.192 g, 2.12 mmol) in water (1.036 mL) and sodium hypochlorite (0.025 ml, 0.053 mmol, 13% available chlorine) in water (0.518 mL) were added (these solutions were added dropwise, alternating between additions of each solution. Roughly 1/3 of the first solution was added dropwise, then 1/3 of the second solution was added dropwise. This continued until all the solutions were added to the reaction). The reaction was stirred at 40 °C overnight. Upon completion, the reaction was cooled to room temperature, then basified to pH 8 with 1M NaOH. Next, 1M Na_2SO_3 (5 mL) was added, and the reaction was stirred for 10 minutes. The reaction was then poured into a separatory funnel, diluted with water (20 mL) and extracted with ether (10 mL); the organic layer was discarded. The aq. layer was acidified to pH 2 with 1M HCl, then extracted with ether (3 x 20 mL). The organic layer was dried over $MgSO_4$, filtered and concentrated under reduced pressure to yield **3.20** (0.214 g, 0.980 mmol, 92% yield) as a yellow oil, which was sufficiently pure and used without further purification. ^{1}H NMR (600 MHz, $CDCl_3$): δ 11.59 (br s, 1H), 1.8-1.9 (m, 1H), 1.72 (br d, *J*=13.4 Hz, 1H), 1.67 (br d, *J*=13.8 Hz, 1H), 1.5-1.6 (m, 1H), 1.4-1.5 (m, 1H), 1.25 (s, 3H),

1.0-1.1 (m, 6H), 0.89 (s, 3H) ppm. ^{13}C NMR (151 MHz, $CDCl_3$): δ 157.9, 96.8, 75.0, 65.4, 64.3, 50.4, 39.2, 38.8, 34.1, 32.3, 31.6, 31.2, 26.0, 20.2 ppm.

References

(1) Roush, W. R. Total Synthesis of Biologically Active Natural Products. *Journal of the American Chemical Society* 2008, *130* (21), 6654-6656.

(2) Nicolaou, K. C.; Rigol, S.; Yu, R. Total Synthesis Endeavors and Their Contributions to Science and Society: A Personal Account. *CCS Chemistry* 2019, *1* (1), 3-37.

(3) Hetzler, B. E.; Trauner, D.; Lawrence, A. L. Natural product anticipation through synthesis. *Nat Rev Chem* 2022, *6* (3), 170-181.

(4) Nicolaou, K. C.; Vourloumis, D.; Winssinger, N.; Baran, P. S. The Art and Science of Total Synthesis at the Dawn of the Twenty-First Century. *Angewandte Chemie International Edition* 2000, *39* (1), 44-122. DOI:

(5) Woodward, R. B.; Doering, W. E. THE TOTAL SYNTHESIS OF QUININE1. *Journal of the American Chemical Society* 1944, *66* (5), 849-849.

(6) Rabe, P.; Kindler, K. Concerning the partial sysnthesis of chinine - Information on china-alkaloids XIX. *BERICHTE DER DEUTSCHEN CHEMISCHEN GESELLSCHAFT* 1918, *51*, 466-467.

(7) Kaufman, T. S.; Rúveda, E. A. The Quest for Quinine: Those Who Won the Battles and Those Who Won the War. *Angewandte Chemie International Edition* 2005, *44* (6), 854-885.

(8) Stork, G.; Niu, D.; Fujimoto, A.; Koft, E. R.; Balkovec, J. M.; Tata, J. R.; Dake, G. R. The First Stereoselective Total Synthesis of Quinine. *Journal of the American Chemical Society* 2001, *123* (14), 3239-3242.

(9) Smith, A. C.; Williams, R. M. Rabe Rest in Peace: Confirmation of the Rabe–Kindler Conversion of d-Quinotoxine Into Quinine: Experimental Affirmation of the Woodward–Doering Formal Total Synthesis of Quinine. *Angewandte Chemie International Edition* 2008, *47* (9), 1736-1740.

(10) Corey, E. J.; Ohno, M.; Vatakencherry, P. A.; Mitra, R. B. TOTAL SYNTHESIS OF d,l-LONGIFOLENE. *Journal of the American Chemical Society* 1961, *83* (5), 1251-1253.

(11) Polanski, J. 4.26 - Chemoinformatics☆. In *Comprehensive Chemometrics (Second Edition)*, Brown, S., Tauler, R., Walczak, B. Eds.; Elsevier, 2020; pp 635-676.

(12) McMurry, J. E.; Isser, S. J. Total synthesis of longifolene. *Journal of the American Chemical Society* 1972, *94* (20), 7132-7137.

(13) Oppolzer, W.; Godel, T. A new and efficient total synthesis of (+-)-longifolene. *Journal of the American Chemical Society* 1978, *100* (8), 2583-2584.

(14) Hutchison, A. J.; Kishi, Y. Stereospecific total synthesis of dl-austamide. *Journal of the American Chemical Society* 1979, *101* (22), 6786-6788.

(15) Baran, P. S.; Corey, E. J. A Short Synthetic Route to (+)-Austamide, (+)-Deoxyisoaustamide, and (+)-Hydratoaustamide from a Common Precursor by a Novel Palladium-Mediated Indole → Dihydroindoloazocine Cyclization. *Journal of the American Chemical Society* 2002, *124* (27), 7904-7905.

(16) Chuang, K. V.; Xu, C.; Reisman, S. E. A 15-step synthesis of (+)-ryanodol. *Science* 2016, *353* (6302), 912-915.

(17) Nicolaou, K. C.; Rigol, S. A brief history of antibiotics and select advances in their synthesis. *The Journal of Antibiotics* 2018, *71* (2), 153-184.

(18) Lloyd, N. C.; Morgan, H. W.; Nicholson, B. K.; Ronimus, R. S. The Composition of Ehrlich's Salvarsan: Resolution of a Century-Old Debate. *Angewandte Chemie International Edition* 2005, *44* (6), 941-944.

(19) Sheehan, J. C.; Henery-Logan, K. R. THE TOTAL SYNTHESIS OF PENICILLIN V. *Journal of the American Chemical Society* 1957, *79* (5), 1262-1263. DOI: 10.1021/ja01562a063.

(20) Abraham, E. P.; Newton, G. G. F. The structure of cephalosporin C. *Biochemical Journal* 1961, *79* (2), 377-393.

(21) Hodgkin, D. C.; Maslen, E. N. The X-ray analysis of the structure of cephalosporin C. *Biochemical Journal* 1961, *79* (2), 393-402.

(22) Woodward, R. B.; Heusler, K.; Gosteli, J.; Naegeli, P.; Oppolzer, W.; Ramage, R.; Ranganathan, S.; Vorbrüggen, H. The Total Synthesis of Cephalosporin C1. *Journal of the American Chemical Society* 1966, *88* (4), 852-853.

(23) Hameed, T. K.; Robinson, J. L. Review of the Use of Cephalosporins in Children with Anaphylactic Reactions from Penicillins. *Canadian Journal of Infectious Diseases* 2002, *13*, 712594.

(24) Achari, A.; Somers, D. O.; Champness, J. N.; Bryant, P. K.; Rosemond, J.; Stammers, D. K. Crystal structure of the anti-bacterial sulfonamide drug target dihydropteroate synthase. *Nature Structural Biology* 1997, *4* (6), 490-497.

(25) Spellberg, B.; Bartlett John, G.; Gilbert David, N. The Future of Antibiotics and Resistance. *New England Journal of Medicine* 2013, *368* (4), 299-302.

tana, N. Mechanisms of Antimicrobial Resistance in ESKAPE Pathogens. *Biomed Res Int* 2016, *2016*, 2475067.

(27) Jacoby, G. A.; Munoz-Price, L. S. The new beta-lactamases. *N Engl J Med* 2005, *352* (4), 380-391.

(28) Pucci, M. J.; Dougherty, T. J. Direct quantitation of the numbers of individual penicillin-binding proteins per cell in Staphylococcus aureus. *J Bacteriol* 2002, *184* (2), 588-591.

(29) Sharma, G.; Rao, S.; Bansal, A.; Dang, S.; Gupta, S.; Gabrani, R. Pseudomonas aeruginosa biofilm: potential therapeutic targets. *Biologicals* 2014, *42* (1), 1-7.

(30) Laverty, G.; Gorman, S. P.; Gilmore, B. F. Biomolecular Mechanisms of Pseudomonas aeruginosa and Escherichia coli Biofilm Formation. *Pathogens* 2014, *3* (3), 596-632.

(31) Peng, Q.; Tang, X.; Dong, W.; Sun, N.; Yuan, W. A Review of Biofilm Formation of Staphylococcus aureus and Its Regulation Mechanism. In *Antibiotics*, 2023; Vol. 12.

(32) del Pozo, J. L.; Patel, R. The challenge of treating biofilm-associated bacterial infections. *Clin Pharmacol Ther* 2007, *82* (2), 204-209.

(33) Shrestha, L.; Fan, H. M.; Tao, H. R.; Huang, J. D. Recent Strategies to Combat Biofilms Using Antimicrobial Agents and Therapeutic Approaches. *Pathogens* 2022, *11* (3).

(34) Kim, S.; Jung, U. T.; Kim, S. K.; Lee, J. H.; Choi, H. S.; Kim, C. S.; Jeong, M. Y. Nanostructured multifunctional surface with antireflective and antimicrobial characteristics. *ACS Appl Mater Interfaces* 2015, *7* (1), 326-331.

(35) Allegrone, G.; Ceresa, C.; Rinaldi, M.; Fracchia, L. Diverse Effects of Natural and Synthetic Surfactants on the Inhibition of Staphylococcus aureus Biofilm. *Pharmaceutics* 2021, *13* (8).

(36) Zhou, J. W.; Luo, H. Z.; Jiang, H.; Jian, T. K.; Chen, Z. Q.; Jia, A. Q. Hordenine: A Novel Quorum Sensing Inhibitor and Antibiofilm Agent against Pseudomonas aeruginosa. *J Agric Food Chem* 2018, *66* (7), 1620-1628.

(37) Mulani, M. S.; Kamble, E. E.; Kumkar, S. N.; Tawre, M. S.; Pardesi, K. R. Emerging Strategies to Combat ESKAPE Pathogens in the Era of Antimicrobial Resistance: A Review. *Front Microbiol* 2019, *10*, 539.

(38) Tacconelli, E.; Carrara, E.; Savoldi, A.; Harbarth, S.; Mendelson, M.; Monnet, D. L.; Pulcini, C.; Kahlmeter, G.; Kluytmans, J.; Carmeli, Y.; et al. Discovery, research, and development of new antibiotics: the WHO priority list of antibiotic-resistant bacteria and tuberculosis. *Lancet Infect Dis* 2018, *18* (3), 318-327.

(39) Silva, V.; Almeida, L.; Gaio, V.; Cerca, N.; Manageiro, V.; Caniça, M.; Capelo, J. L.; Igrejas, G.; Poeta, P. Biofilm Formation of Multidrug-Resistant MRSA Strains Isolated from Different Types of Human Infections. In *Pathogens*, 2021; Vol. 10.

(40) Haysom, L.; Cross, M.; Anastasas, R.; Moore, E.; Hampton, S. Prevalence and Risk Factors for Methicillin-Resistant Staphylococcus aureus (MRSA) Infections in Custodial Populations: A Systematic Review. *Journal of Correctional Health Care* 2018, *24* (2), 197-213.

(41) Ali Alghamdi, B.; Al-Johani, I.; Al-Shamrani, J. M.; Musamed Alshamrani, H.; Al-Otaibi, B. G.; Almazmomi, K.; Yusnoraini Yusof, N. Antimicrobial resistance in methicillin-resistant staphylococcus aureus. *Saudi J Biol Sci* 2023, *30* (4), 103604.

(42) Villa, F. A.; Gerwick, L. Marine natural product drug discovery: Leads for treatment of inflammation, cancer, infections, and neurological disorders. *Immunopharmacology and Immunotoxicology* 2010, *32* (2), 228-237.

(43) Varijakzhan, D.; Loh, J. Y.; Yap, W. S.; Yusoff, K.; Seboussi, R.; Lim, S. E.; Lai, K. S.; Chong, C. M. Bioactive Compounds from Marine Sponges: Fundamentals and Applications. *Mar Drugs* 2021, *19* (5).

(44) Gerwick, William H.; Moore, Bradley S. Lessons from the Past and Charting the Future of Marine Natural Products Drug Discovery and Chemical Biology. *Chemistry & Biology* 2012, *19* (1), 85-98.

(45) Altmann, K.-H. Drugs from the Oceans: Marine Natural Products as Leads for Drug Discovery. *CHIMIA* 2017, *71* (10), 646.

(46) Begum, S. M. F. M.; Hemalatha, S. Marine Natural Products — a Vital Source of Novel Biotherapeutics. *Current Pharmacology Reports* 2022, *8* (5), 339-349.

(47) Diyabalanage, T.; Amsler, C. D.; McClintock, J. B.; Baker, B. J. Palmerolide A, a Cytotoxic Macrolide from the Antarctic Tunicate Synoicum adareanum. *Journal of the American Chemical Society* 2006, *128* (17), 5630-5631.

(48) von Salm, J. L.; Witowski, C. G.; Fleeman, R. M.; McClintock, J. B.; Amsler, C. D.; Shaw, L. N.; Baker, B. J. Darwinolide, a New Diterpene Scaffold That Inhibits Methicillin-Resistant Staphylococcus aureus Biofilm from the Antarctic Sponge Dendrilla membranosa. *Organic Letters* 2016, *18* (11), 2596-2599.

(49) Fleeman, R.; LaVoi, T. M.; Santos, R. G.; Morales, A.; Nefzi, A.; Welmaker, G. S.; Medina-Franco, J. L.; Giulianotti, M. A.; Houghten, R. A.; Shaw, L. N. Combinatorial Libraries As a Tool for the Discovery of Novel, Broad-Spectrum Antibacterial Agents Targeting the ESKAPE Pathogens. *Journal of Medicinal Chemistry* 2015, *58* (8), 3340-3355.

(50) Baker, B. J.; Shaw, L. N.; Shilling, A. J.; Bory, A. J.; Allen, J.; Amsler, C. D., Jr.; McClintock, J. B. Dendrilla membranosa derived sesquiterpene compound formulations, derivatives and antimicrobial uses thereof. US11547691, 2023.

(51) Ankisetty, S.; Amsler, C. D.; McClintock, J. B.; Baker, B. J. Further Membranolide Diterpenes from the Antarctic Sponge Dendrilla membranosa. *Journal of Natural Products* 2004, *67* (7), 1172-1174.

(52) Molinski, T. F.; Faulkner, D. J. Metabolites of the antarctic sponge Dendrilla membranosa. *The Journal of Organic Chemistry* 1987, *52* (2), 296-298.

(53) Lipinski, C. A. Drug-like properties and the causes of poor solubility and poor permeability. *Journal of Pharmacological and Toxicological Methods* 2000, *44* (1), 235-249.

(54) Yoo, S.-e.; Yi, K. Y. Total Synthesis of (±)-Membranolide. *Synlett* 1990, *1990* (11), 697-699.

(55) Persson, B. A.; Larsson, A. L. E.; Le Ray, M.; Bäckvall, J.-E. Ruthenium- and Enzyme-Catalyzed Dynamic Kinetic Resolution of Secondary Alcohols. *Journal of the American Chemical Society* 1999, *121* (8), 1645-1650.

(56) Ireland, R. E.; Wipf, P.; Armstrong, J. D., III. Stereochemical control in the ester enolate Claisen rearrangement. 1. Stereoselectivity in silyl ketene acetal formation. *The Journal of Organic Chemistry* 1991, *56* (2), 650-657.

(57) Wang, T.; Niu, D.; Hoye, T. R. The Hexadehydro-Diels–Alder Cycloisomerization Reaction Proceeds by a Stepwise Mechanism. *Journal of the American Chemical Society* 2016, *138* (25), 7832-7835.

(58) Kobayashi, K.; Yamamoto, Y.; Miyaura, N. Pd/Josiphos-Catalyzed Enantioselective α-Arylation of Silyl Ketene Acetals and Mechanistic Studies on Transmetalation and Enantioselection. *Organometallics* 2011, *30* (22), 6323-6327.

(59) Schreiber, J.; Maag, H.; Hashimoto, N.; Eschenmoser, A. Dimethyl(methylene)ammonium Iodide. *Angewandte Chemie International Edition in English* 1971, *10* (5), 330-331.

(60) Fernández González, D.; Brand, J. P.; Mondière, R.; Waser, J. Ethynylbenziodoxolones (EBX) as Reagents for the Ethynylation of Stabilized Enolates. *Advanced Synthesis & Catalysis* 2013, *355* (8), 1631-1639.

(61) Izawa, Y.; Shimizu, I.; Yamamoto, A. Palladium-Catalyzed Oxidative Carbonylation of 1-Alkynes into 2-Alkynoates with Molecular Oxygen as Oxidant. *Bulletin of the Chemical Society of Japan* 2004, *77* (11), 2033-2045.

(62) Xie, J.-N.; He, L.-N.; Fu, H.-C.; Wang, N.; Wang, M.-Y. Sodium Acetate-promoted Oxa-Michael-Aldol [3+2] Annulation Reactions: Facile Access to the Fused Heterocycle. *Current Catalysis* 2018, *7* (1), 60-64.

(63) Chausset-Boissarie, L.; Ghozati, K.; LaBine, E.; Chen, J. L. Y.; Aggarwal, V. K.; Crudden, C. M. Enantiospecific, Regioselective Cross-Coupling Reactions of Secondary Allylic Boronic Esters. *Chemistry – A European Journal* 2013, *19* (52), 17698-17701.

(64) Rybak, T.; Hall, D. G. Stereoselective and Regiodivergent Allylic Suzuki–Miyaura Cross-Coupling of 2-Ethoxydihydropyranyl Boronates: Synthesis and Confirmation of Absolute Stereochemistry of Diospongin B. *Organic Letters* 2015, *17* (17), 4156-4159.

(65) Birkholz, M.-N.; Freixa, Z.; van Leeuwen, P. W. N. M. Bite angle effects of diphosphines in C–C and C–X bond forming cross coupling reactions. *Chemical Society Reviews* 2009, *38* (4), 1099-1118, 10.1039/B806211K.

(66) Hou, J.; Xie, J.-H.; Zhou, Q.-L. Palladium-Catalyzed Hydrocarboxylation of Alkynes with Formic Acid. *Angewandte Chemie International Edition* 2015, *54* (21), 6302-6305.

(67) Poremba, K. E.; Dibrell, S. E.; Reisman, S. E. Nickel-Catalyzed Enantioselective Reductive Cross-Coupling Reactions. *ACS Catalysis* 2020, *10* (15), 8237-8246.

(68) Cornella, J.; Edwards, J. T.; Qin, T.; Kawamura, S.; Wang, J.; Pan, C.-M.; Gianatassio, R.; Schmidt, M.; Eastgate, M. D.; Baran, P. S. Practical Ni-Catalyzed Aryl–Alkyl Cross-Coupling of Secondary Redox-Active Esters. *Journal of the American Chemical Society* 2016, *138* (7), 2174-2177.

(69) Del Valle, J. R.; Goodman, M. Stereoselective Synthesis of Boc-Protected cis and trans-4-Trifluoromethylprolines by Asymmetric Hydrogenation Reactions. *Angewandte Chemie International Edition* 2002, *41* (9), 1600-1602.

(70) Zhu, Y.; Burgess, K. Filling Gaps in Asymmetric Hydrogenation Methods for Acyclic Stereocontrol: Application to Chirons for Polyketide-Derived Natural Products. *Accounts of Chemical Research* 2012, *45* (10), 1623-1636.

(71) Kattamuri, P. V.; West, J. G. Hydrogenation of Alkenes via Cooperative Hydrogen Atom Transfer. *Journal of the American Chemical Society* 2020, *142* (45), 19316-19326.

(72) Hill, J. R.; Robertson, A. A. B. Fishing for Drug Targets: A Focus on Diazirine Photoaffinity Probe Synthesis. *Journal of Medicinal Chemistry* 2018, *61* (16), 6945-6963..

(73) Dias, L. C.; Polo, E. C. Nhatrangin A: Total Syntheses of the Proposed Structure and Six of Its Diastereoisomers. *The Journal of Organic Chemistry* 2017, *82* (8), 4072-4112.

(74) Liu, Q.; Li, M.; Xiong, R.; Mo, F. Direct Carboxylation of the Diazo Group ipso-C(sp2)–H bond with Carbon Dioxide: Access to Unsymmetrical Diazomalonates and Derivatives. *Organic Letters* 2017, *19* (24), 6756-6759.

(75) Karmakar, R.; Yun, S. Y.; Chen, J.; Xia, Y.; Lee, D. Benzannulation of Triynes to Generate Functionalized Arenes by Spontaneous Incorporation of Nucleophiles. *Angewandte Chemie International Edition* 2015, *54* (22), 6582-6586.

(76) Lauber, A.; Zelenay, B.; Cvengroš, J. Asymmetric synthesis of N-stereogenic molecules: diastereoselective double aza-Michael reaction. *Chemical Communications* 2014, *50* (10), 1195-1197, 10.1039/C3CC48486F.

(77) Schmidt-Leithoff, J.; Brückner, R. Regioselective cis,vic-Dihydroxylation of α,β,γ,δ-Unsaturated Carboxylic Esters: Enhanced γ,δ-Selectivity by Employing Trifluoroethyl or Hexafluoroisopropyl Esters. *Synlett* 2006, *2006* (16), 2641-2645.

(78) Fernández González, D.; Brand, J. P.; Waser, J. Ethynyl-1,2-benziodoxol-3(1 H)-one (EBX): An Exceptional Reagent for the Ethynylation of Keto, Cyano, and Nitro Esters. *Chemistry – A European Journal* 2010, *16* (31), 9457-9461.

(79) Wojnar, J. M.; Dowle, K. O.; Northcote, P. T. The Oxeatamides: Nitrogenous Spongian Diterpenes from the New Zealand Marine Sponge Darwinella oxeata. *Journal of Natural Products* 2014, *77* (10), 2288-2295.

(80) A. Ramirez, M. C.; Williams, D. E.; Gubiani, J. R.; Parra, L. L. L.; Santos, M. F. C.; Ferreira, D. D.; Mesquita, J. T.; Tempone, A. G.; Ferreira, A. G.; Padula, V.; et al. Rearranged Terpenoids from the Marine Sponge Darwinella cf. oxeata and Its Predator, the Nudibranch Felimida grahami. *Journal of Natural Products* 2017, *80* (3), 720-725.

(81) Greenwood, P. D. G.; Grenet, E.; Waser, J. Palladium-Catalyzed Carbo-Oxygenation of Propargylic Amines using in Situ Tether Formation. *Chemistry – A European Journal* 2019, *25* (12), 3010-3013).

(82) Shiro, D.; Nagai, H.; Fujiwara, S.-i.; Tsuda, S.; Iwasaki, T.; Kuniyasu, H.; Kambe, N. Palladium-Catalyzed Decarbonylative Rearrangement of N-Allenyl Seleno- and Tellurocarbamates. *Heteroatom Chemistry* 2014, *25* (6), 518-524.

Appendices

Appendix 1: General Experimental Information

Unless otherwise noted, all materials were obtained from commercial suppliers and used without further purification. All reactions with air- and/or moisture-sensitive compounds were performed under an argon atmosphere in a flame-dried or oven-dried reaction flask, and reagents were added via syringe or cannula. Dry THF and toluene were obtained via distillation from sodium benzophenone ketyl. Preparative chromatography was carried out using Sorbtech silica gel (60 Å porosity, 40-63 m particle size) in fritted MPLC cartridges and eluted with Thomson Instrument Single Step pumps. Thin layer chromatography analyses were conducted with 200 μm precoated Sorbtech fluorescent TLC plates. Plates were visualized by UV light and by staining with a variety of stains such as acidic anisaldehyde, acidic vanillin, ceric ammonium nitrate or iodine vapor. LC-MS data was obtained using an Agilent 1100 HPLC/MSD system equipped with a diode array detector running an acetonitrile/water gradient and 0.1% formic acid. High resolution mass spectral data were obtained using an Agilent 6540 QTOF mass spectrometer. Nuclear magnetic resonance spectrometry was run on a Bruker Neo 600 MHz, Varian Inova 500 MHz or a Varian Inova 400 MHz spectrometer, and chemical shifts are listed in ppm correlated to the solvent used as an internal standard. Optical rotations were performed on a Rudolph Research Analytical Autopol IV polarimeter (λ 589) using a 700-μL cell with a path length of 1-dm. Enantiomeric excess (ee) was determined using a Varian Prostar HPLC with a 210 binary pump and a 335-diode array detector 242 or using a Agilent 7890A GC system coupled to an Agilent 7200 Accurate-Mass Q-TOF MS. IR spectra were obtained using Agilent Cary 630 FTIR. Ozonolysis reactions were performed using a household Ivation ozone generator, purchased from Home Depot (600 mg/hr output, air used as feed gas).

Appendix 2: Selected NMR Spectra

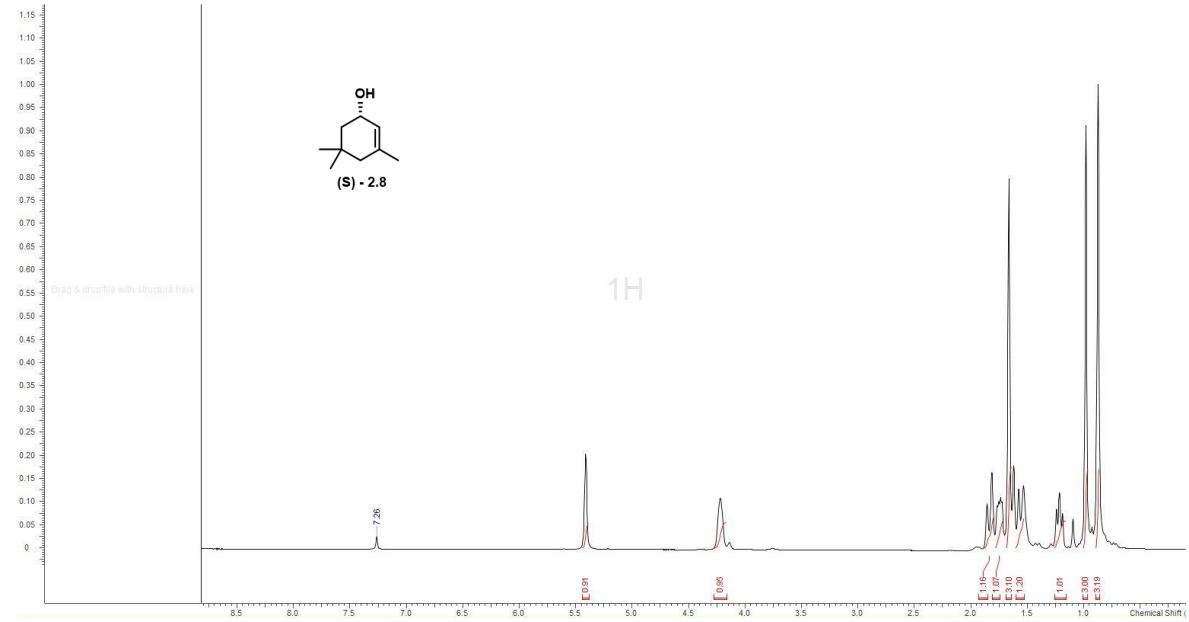

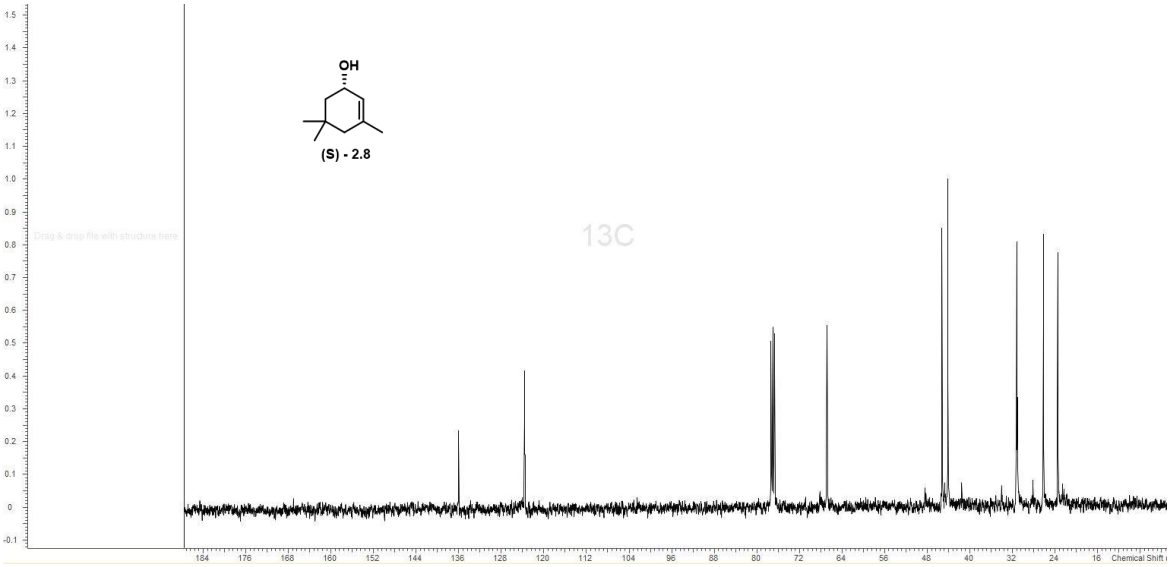

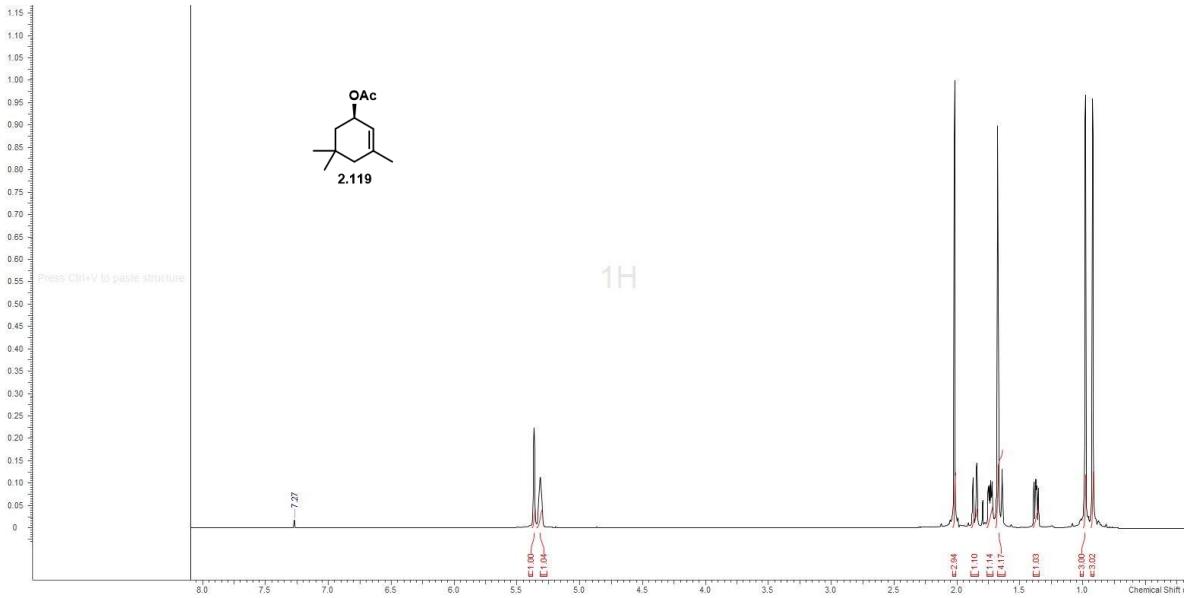
OAc
2.119
1H
7.27
1.00
1.04
2.94
1.10
1.14
4.17
1.03
3.00
3.02
Chemical Shift

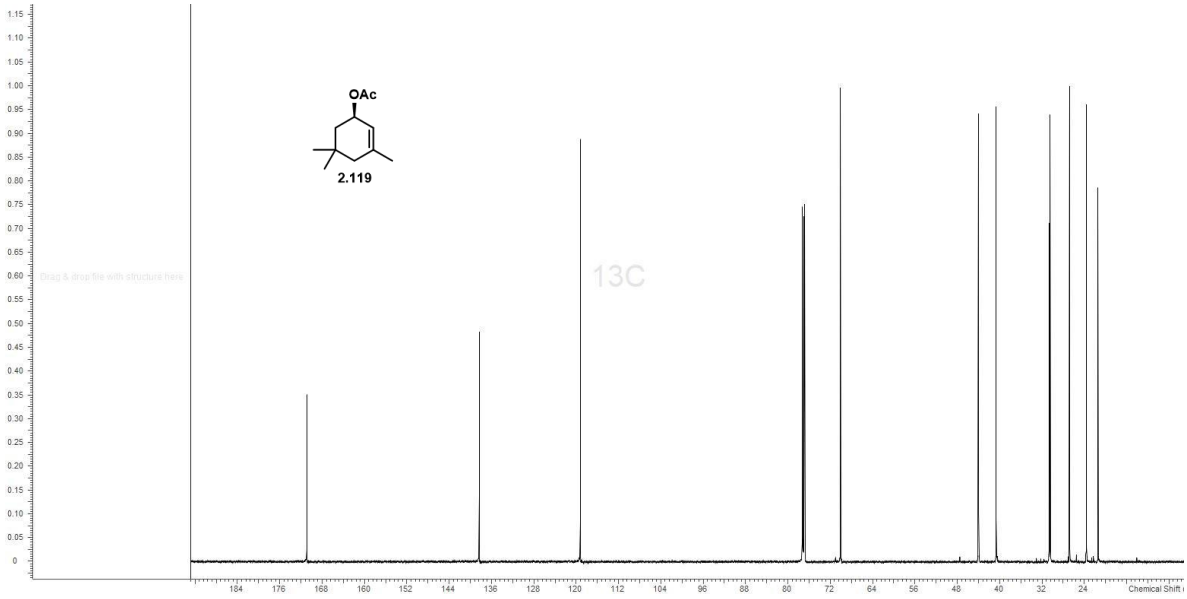
OAc
2.119
13C
Chemical Shift

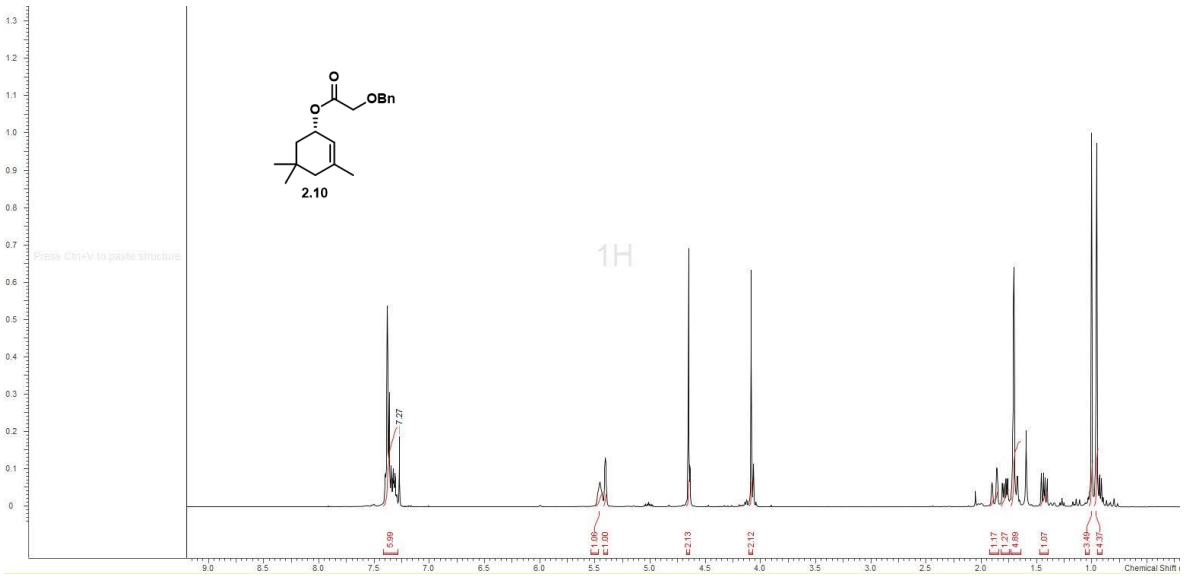
OBn
2.10
1H
7.27
5.99
1.09
1.00
2.13
2.12
1.17
1.27
4.89
1.07
3.49
4.37
Chemical Shift

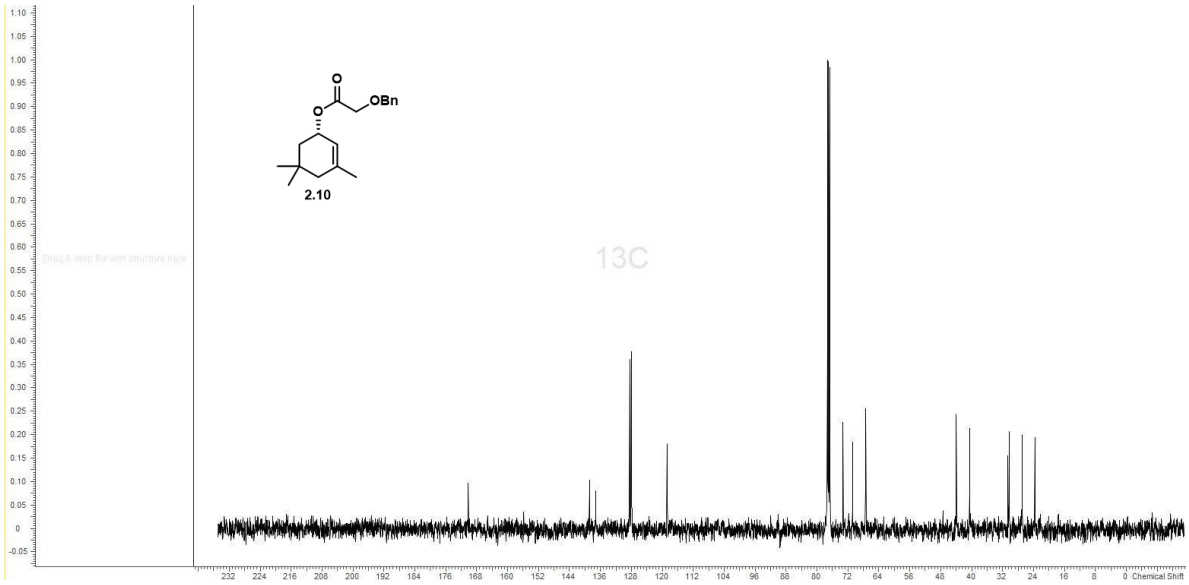
OBn
2.10
13C
Chemical Shift

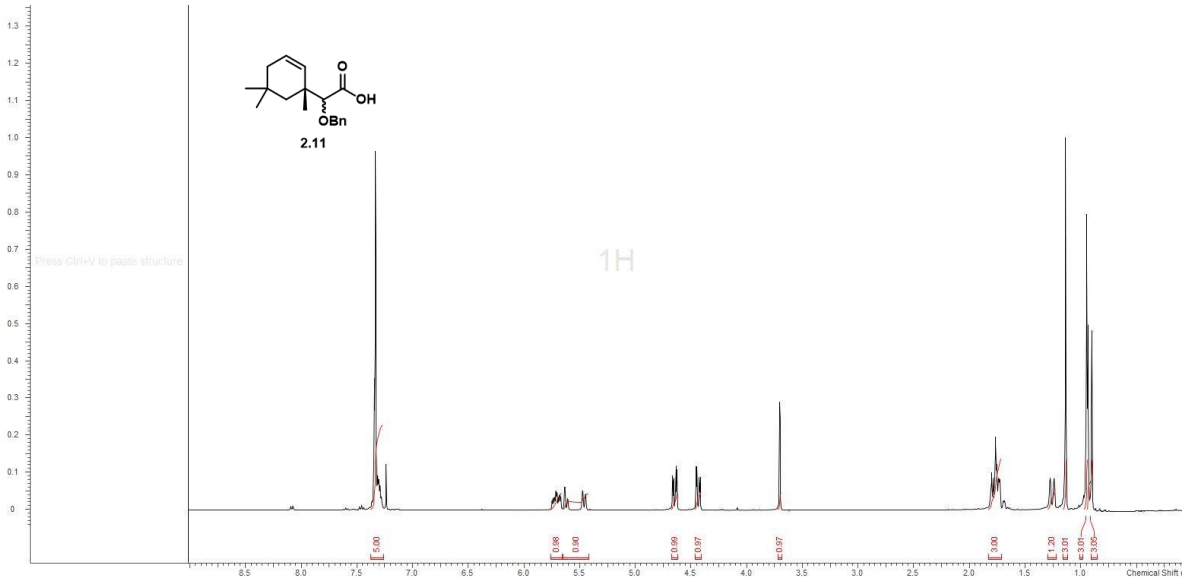
OH
OBn
2.11
Press Ctrl+V to paste structure
1H
5.00
0.98
0.90
0.99
0.97
0.97
3.00
1.20
3.01
3.00
Chemical Shift

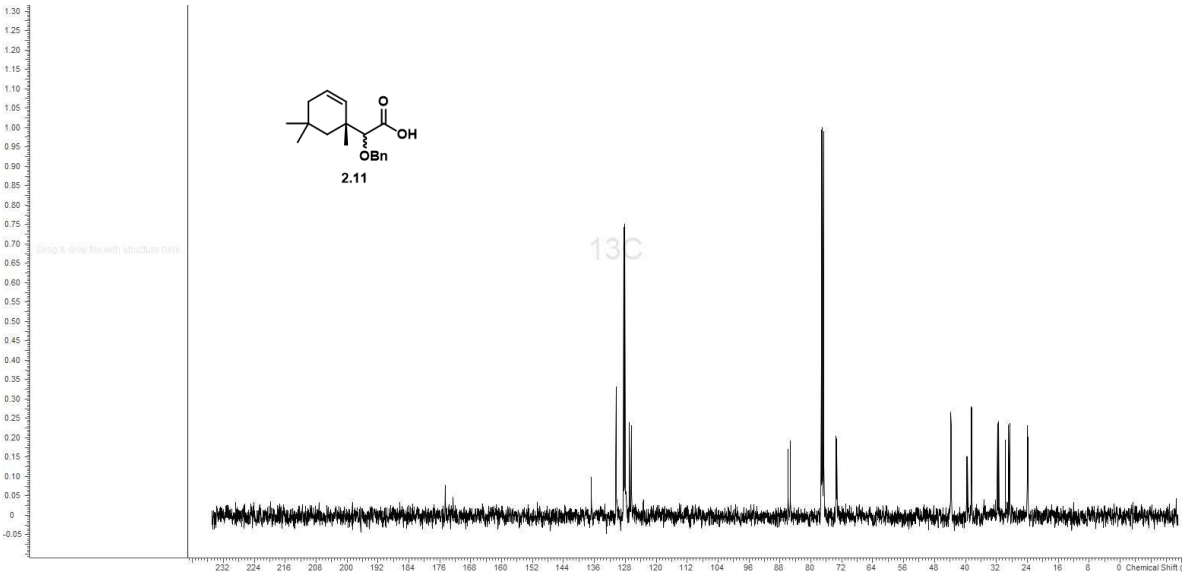
OH
OBn
2.11
Drag & drop file with structure here
13C
Chemical Shift

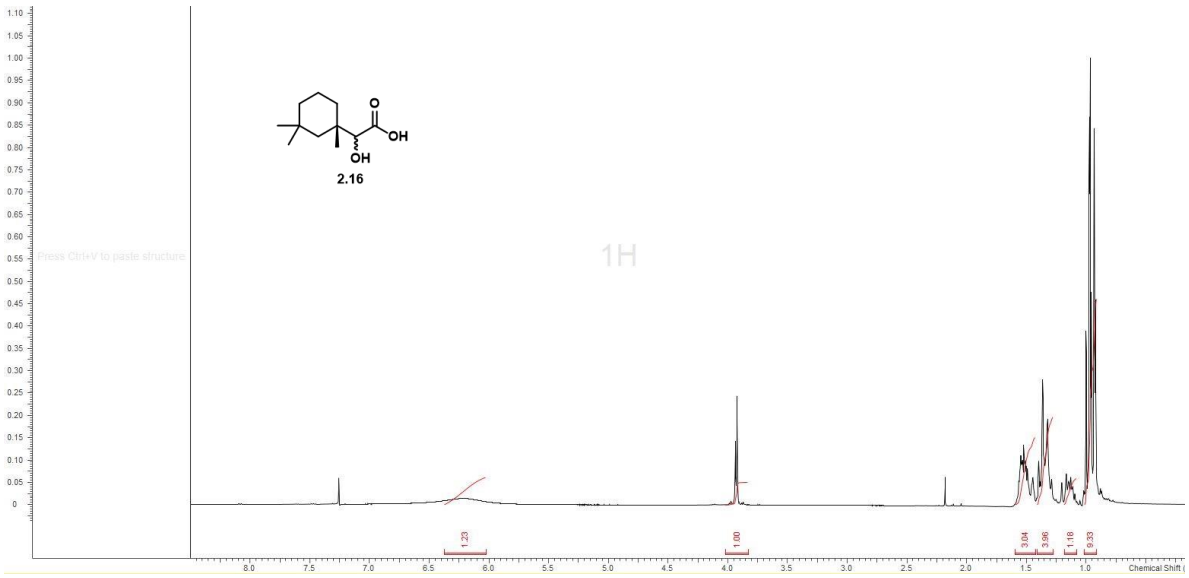
OH
OH
2.16
1H
1.23
1.00
3.04
3.96
1.16
9.33
Chemical Shift (

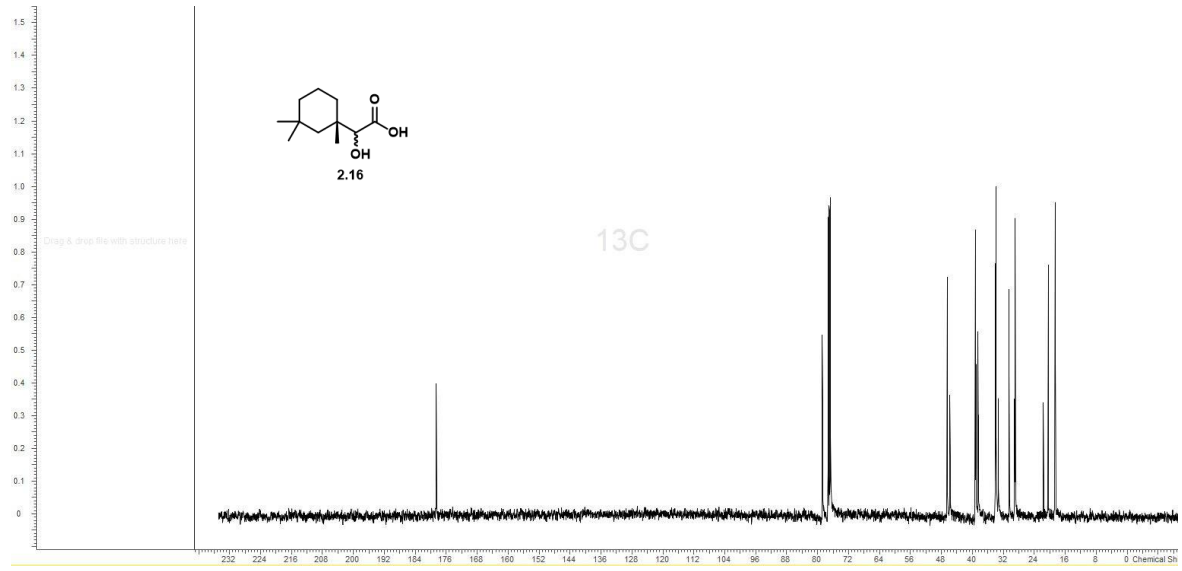
OH
OH
2.16
13C
Chemical Sh

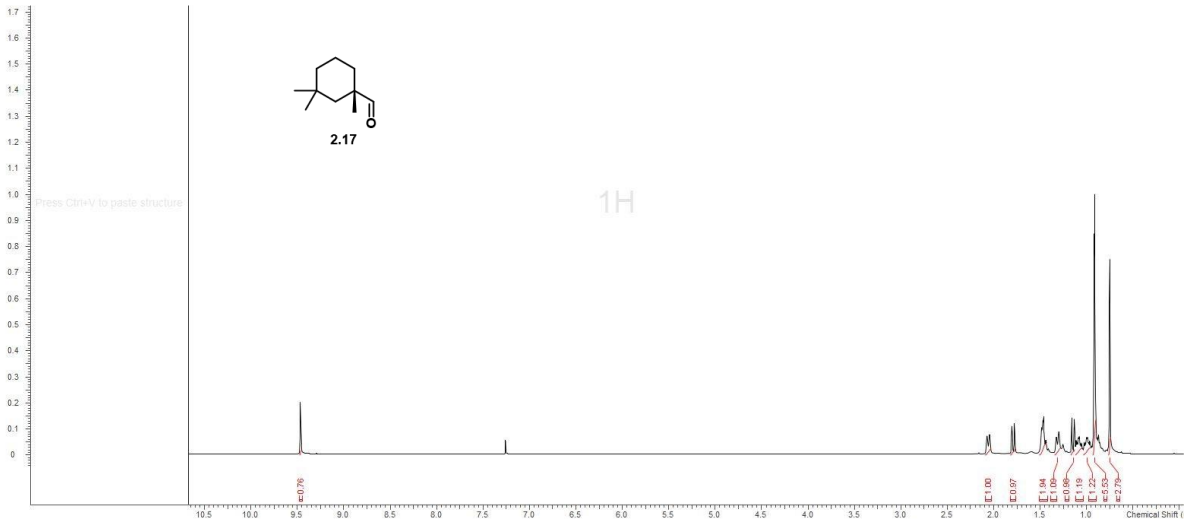
2.17
1H
Chemical Shift

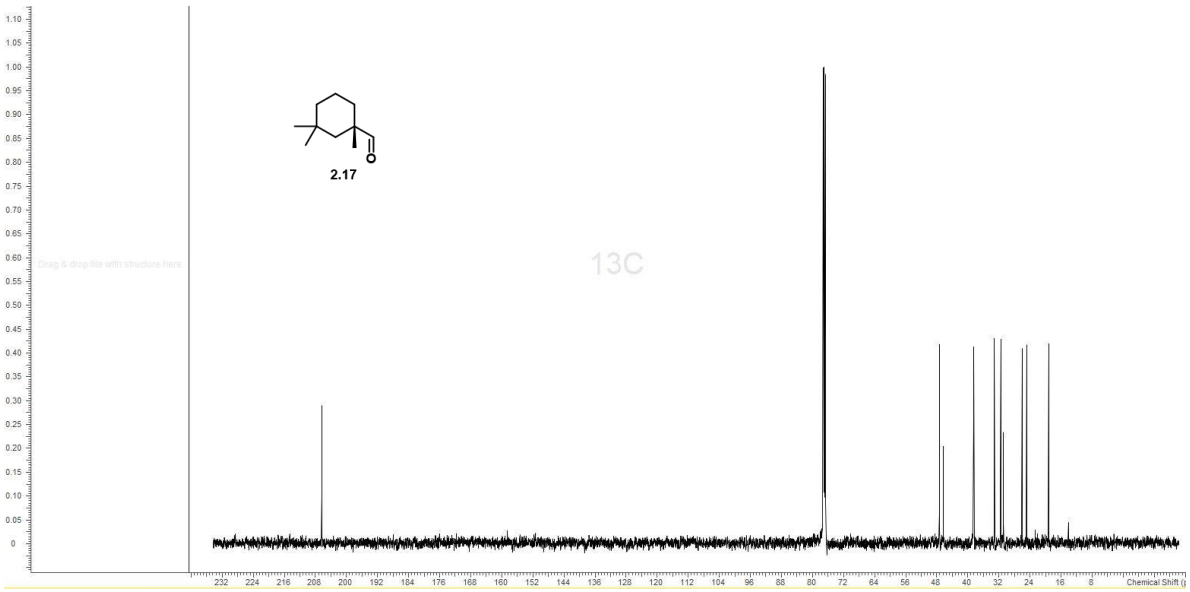
2.17
13C
Chemical Shift

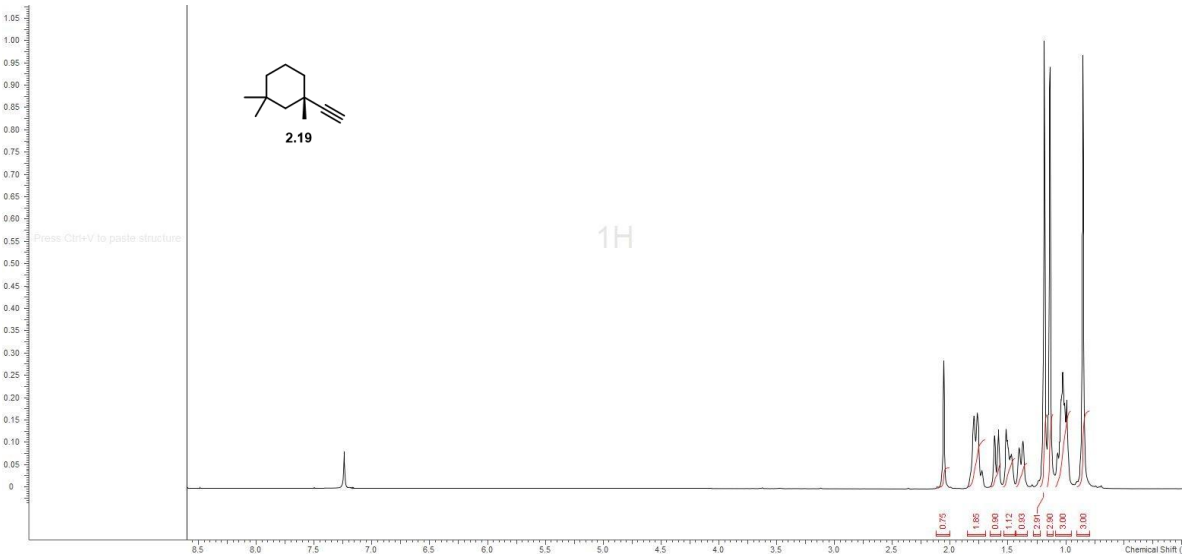
2.19
1H
0.75
1.85
0.90
1.12
0.93
2.91
2.90
3.00
3.00
Chemical Shift

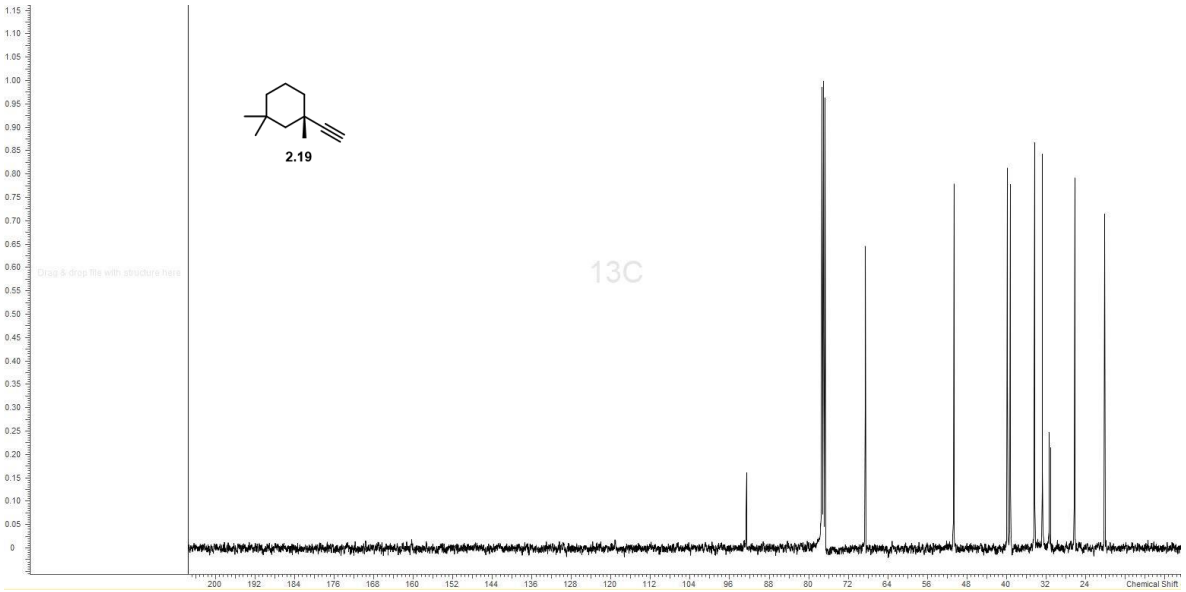
2.19
13C
Chemical Shift

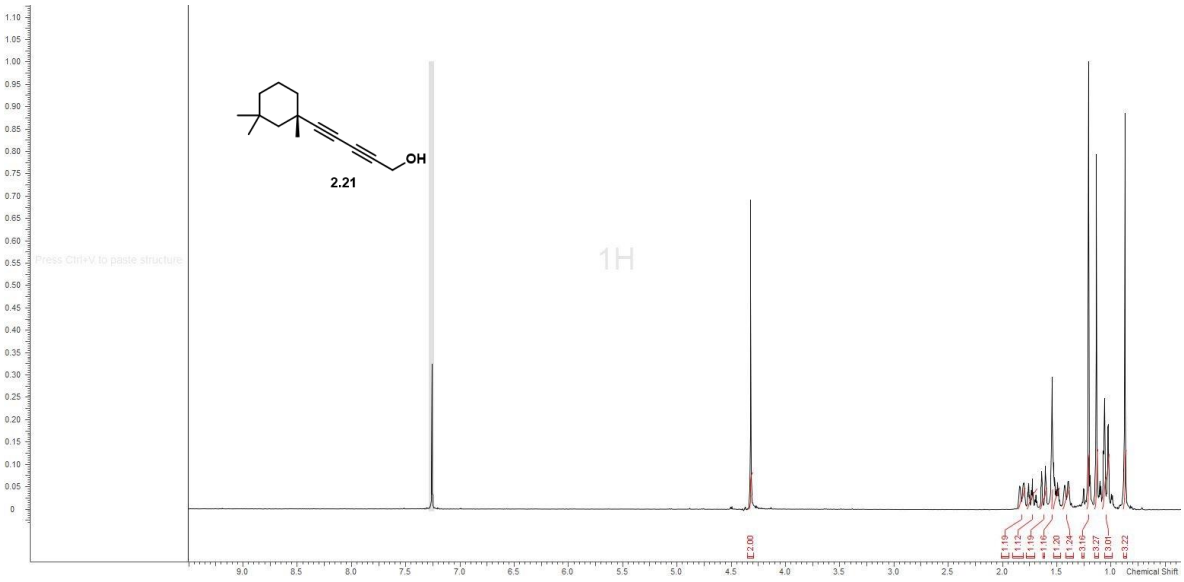
OH
2.21
1H
Chemical Shift

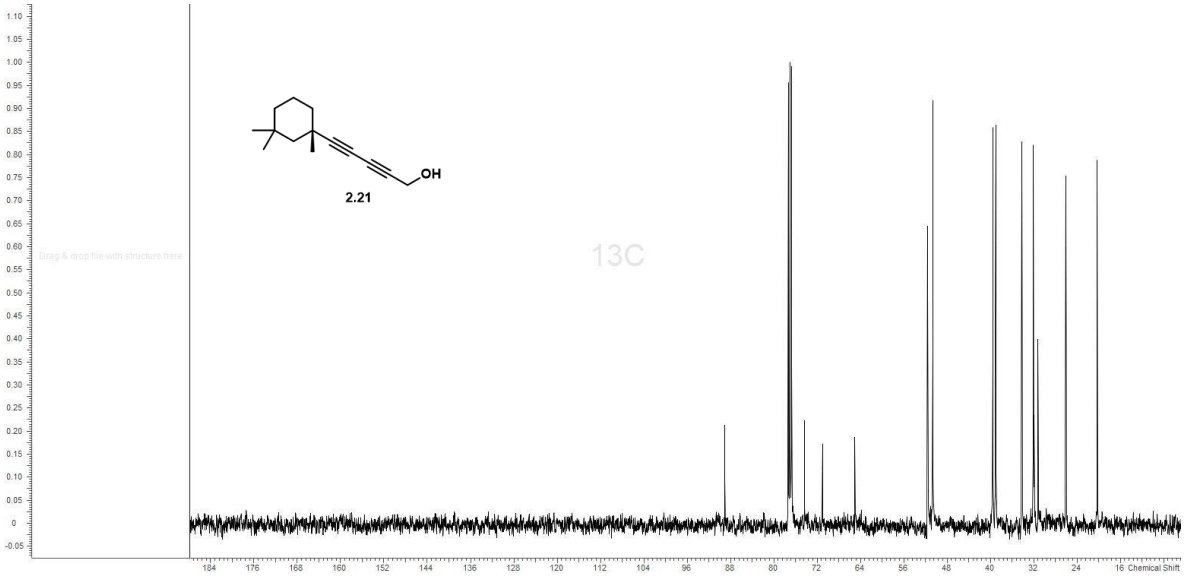
OH
2.21
13C
Chemical Shift

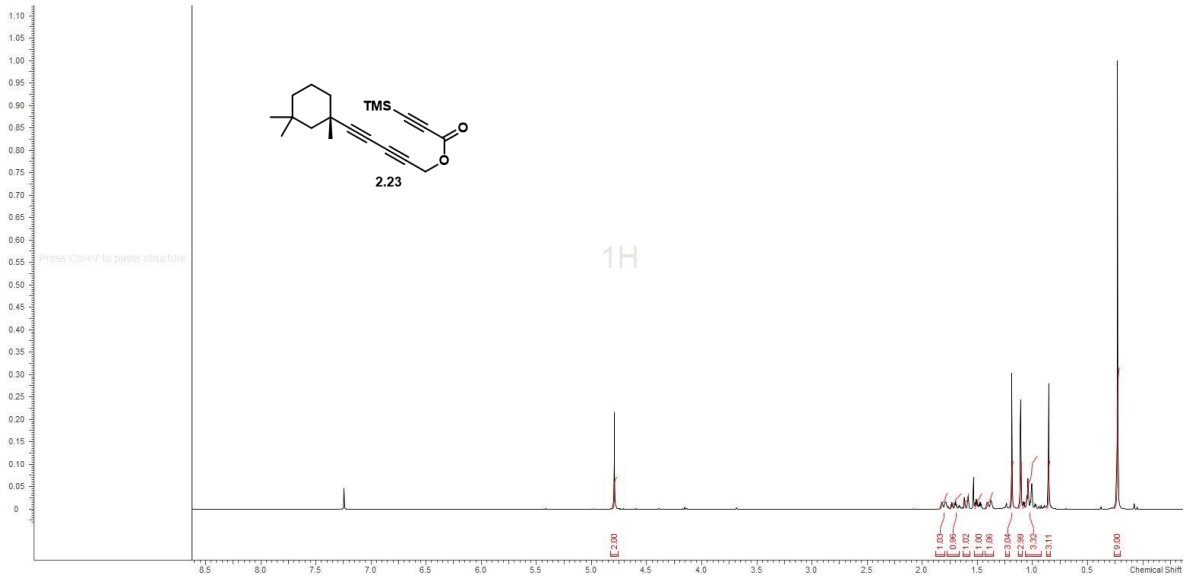
TMS
O
O
2.23
1H
Chemical Shift

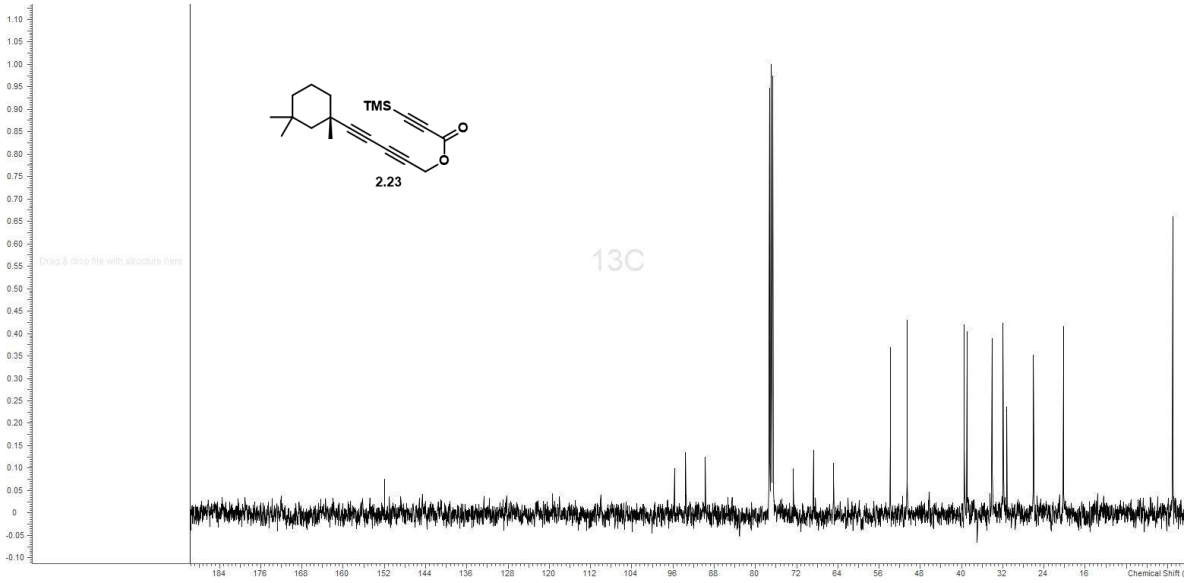
TMS
O
O
2.23
13C
Chemical Shift

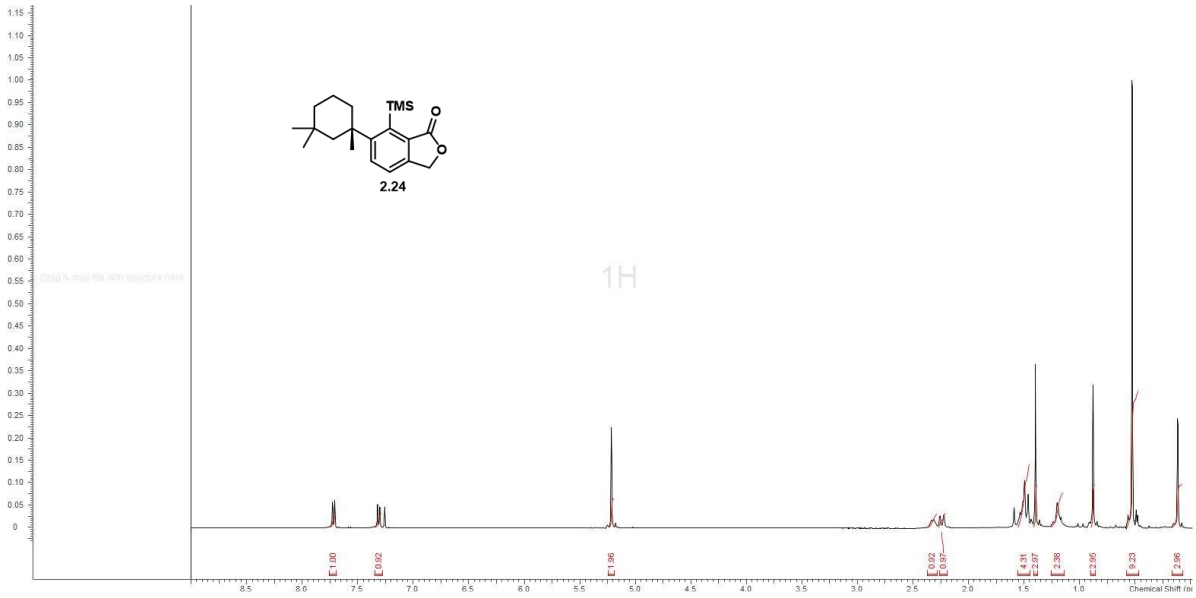
TMS
2.24
1H
Drag & drop file with structure here
Chemical Shift (pp

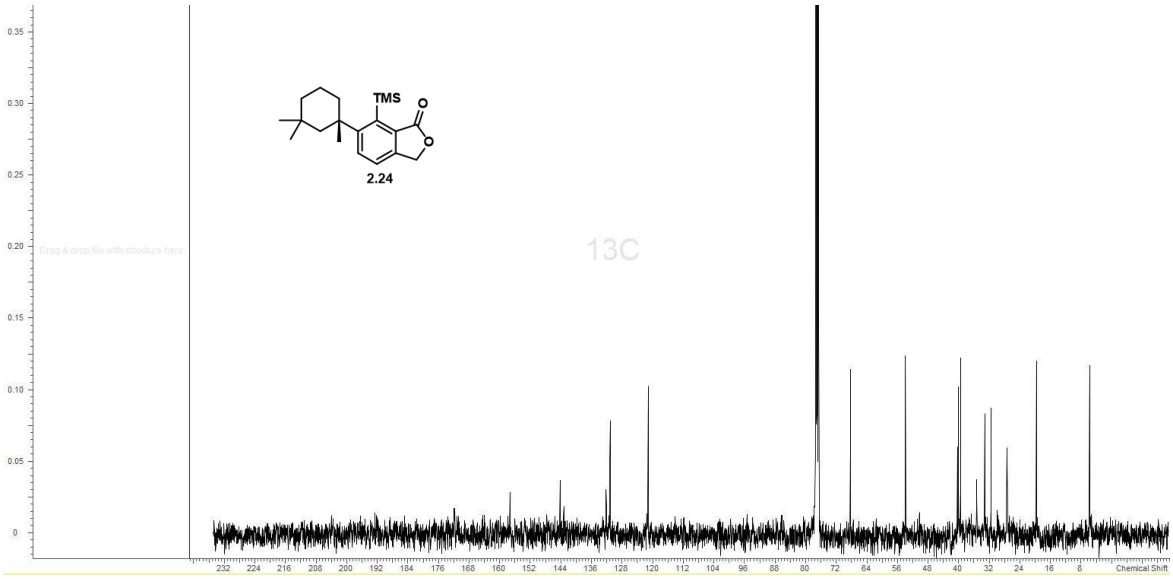
TMS
2.24
13C
Drag & drop file with structure here
Chemical Shift

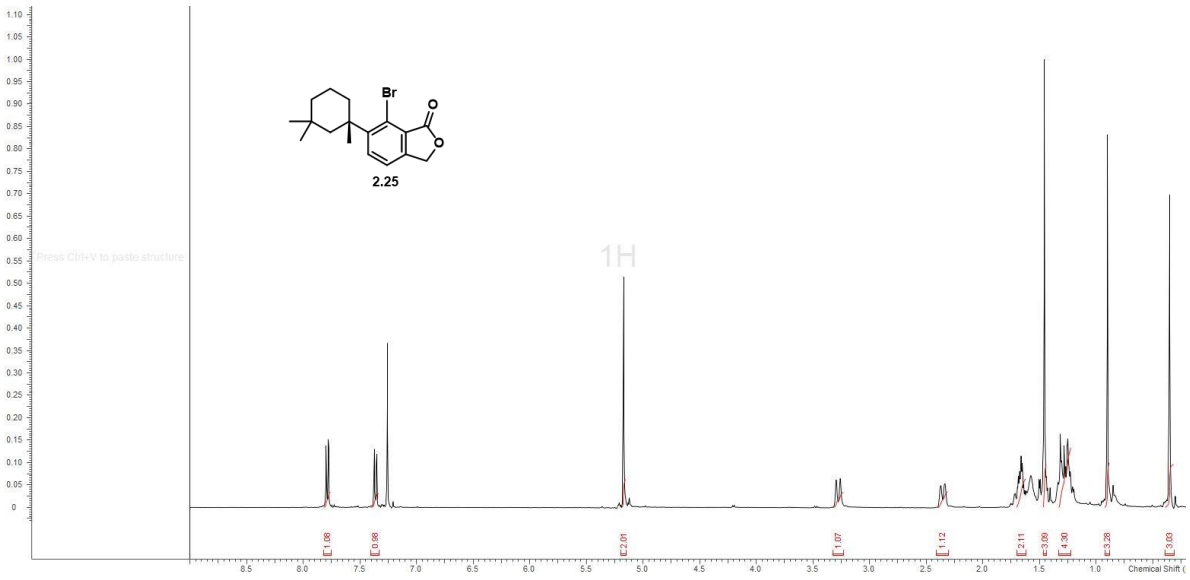
Br
O
O
2.25
1H
Press Ctrl+V to paste structure
1.88
0.88
2.01
1.07
1.12
2.11
3.09
4.30
3.28
3.03
Chemical Shift

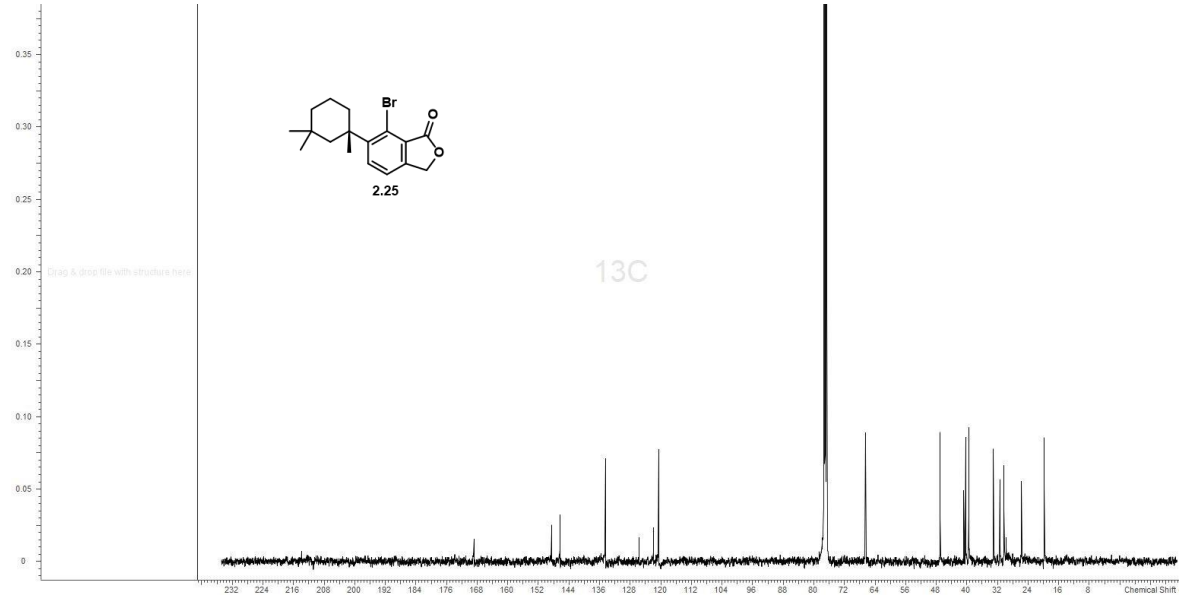
Br
O
O
2.25
13C
Drag & drop file with structure here
Chemical Shift

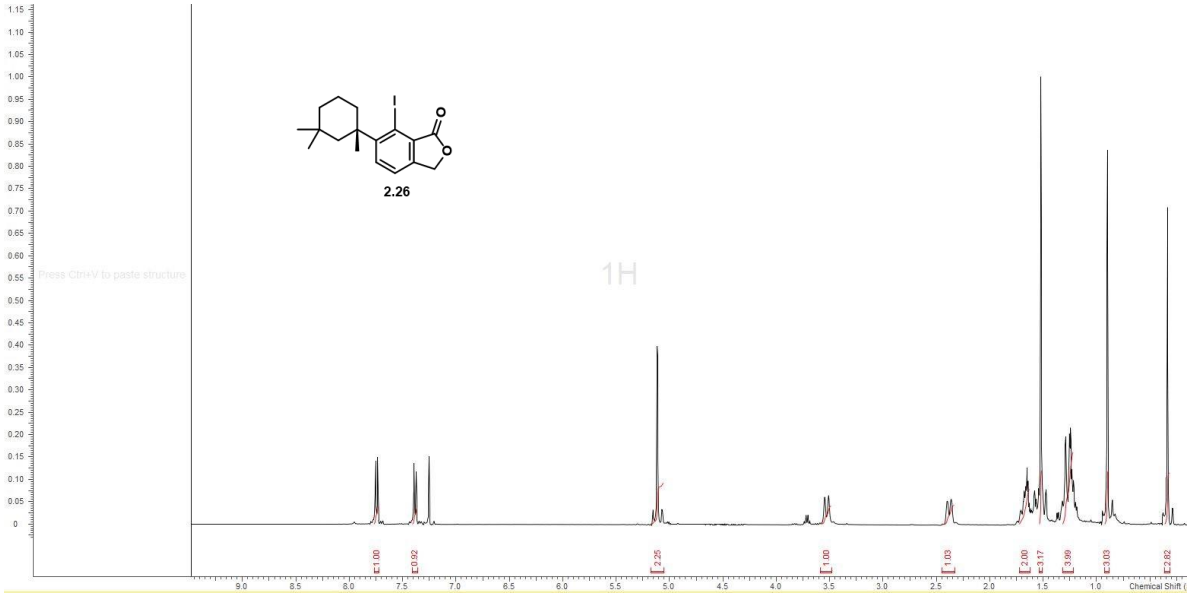
2.26
1H
Press Ctrl+V to paste structure
Chemical Shift

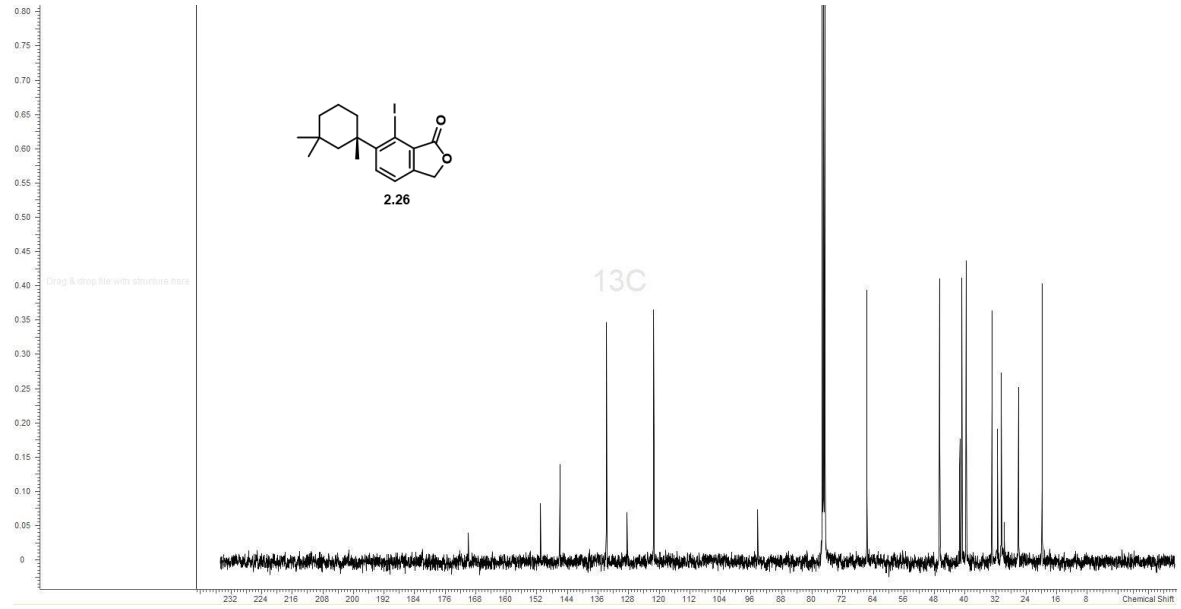
2.26
13C
Drag & drop file with structure here
Chemical Shift

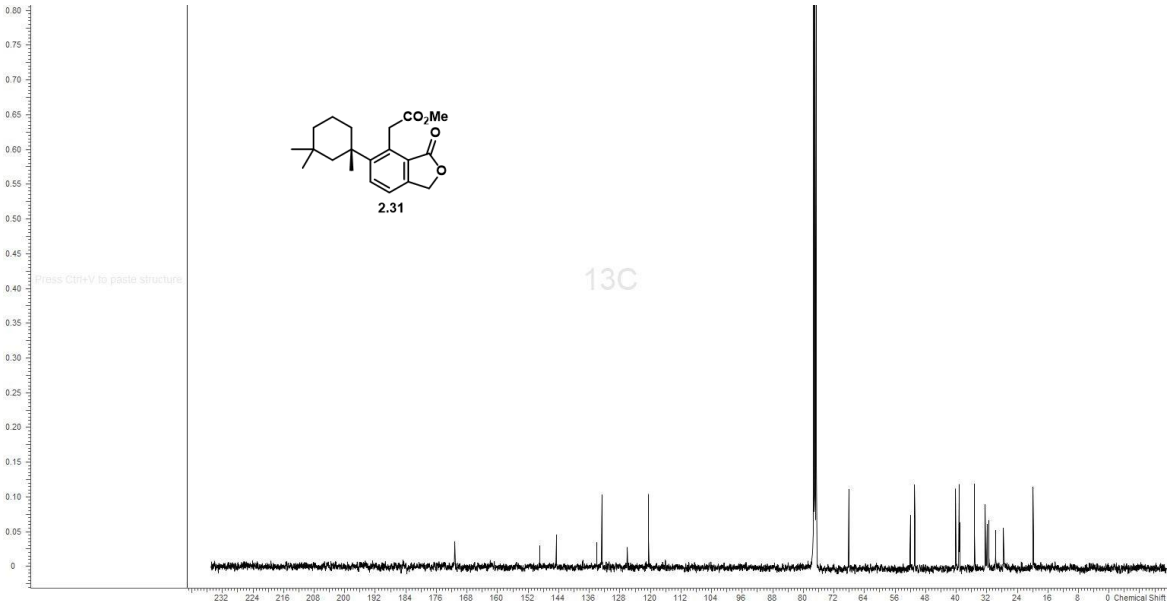
CO2Me
O
O
2.31
13C
Chemical Shift

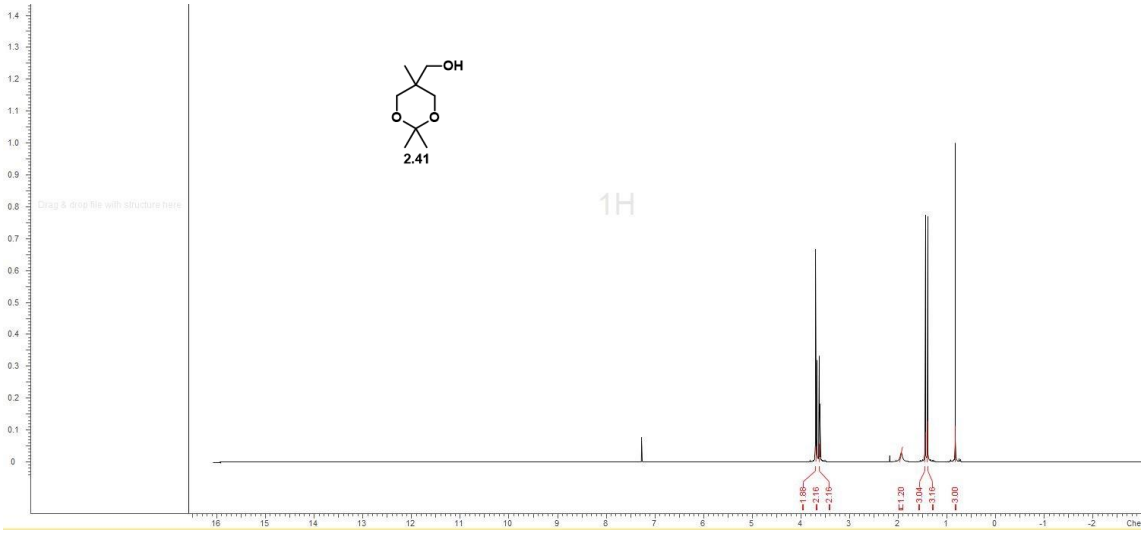
OH
O
O
2.41
1H
1.88
2.16
2.16
1.20
3.04
3.16
3.00

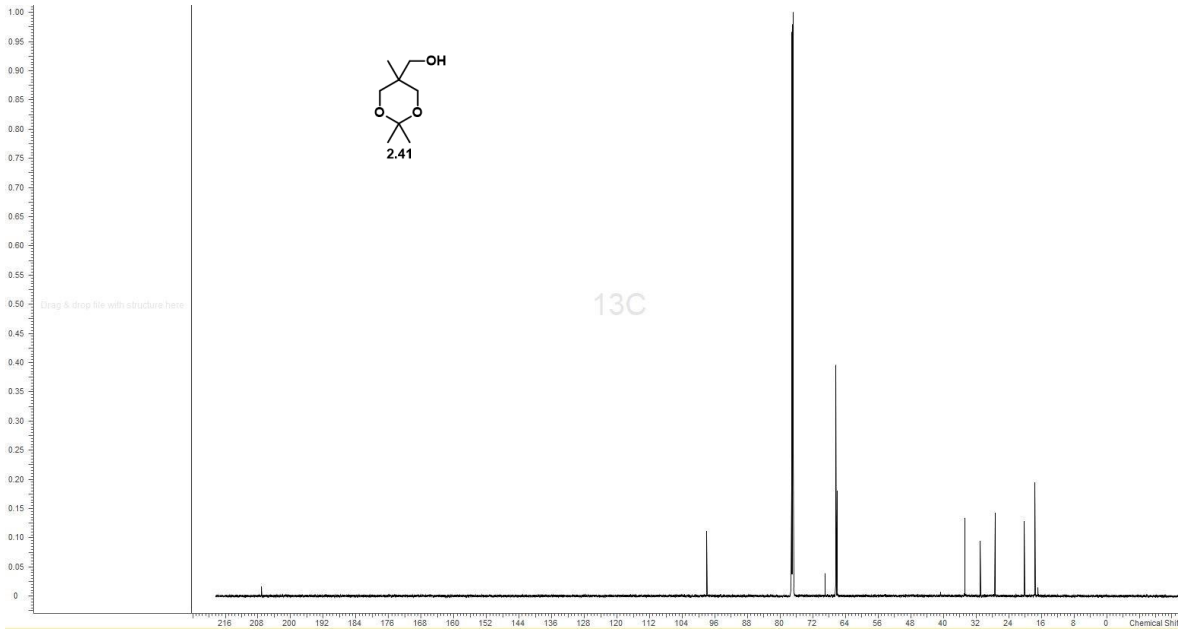
OH
2.41
13C
Drag & drop file with structure here
Chemical Shif

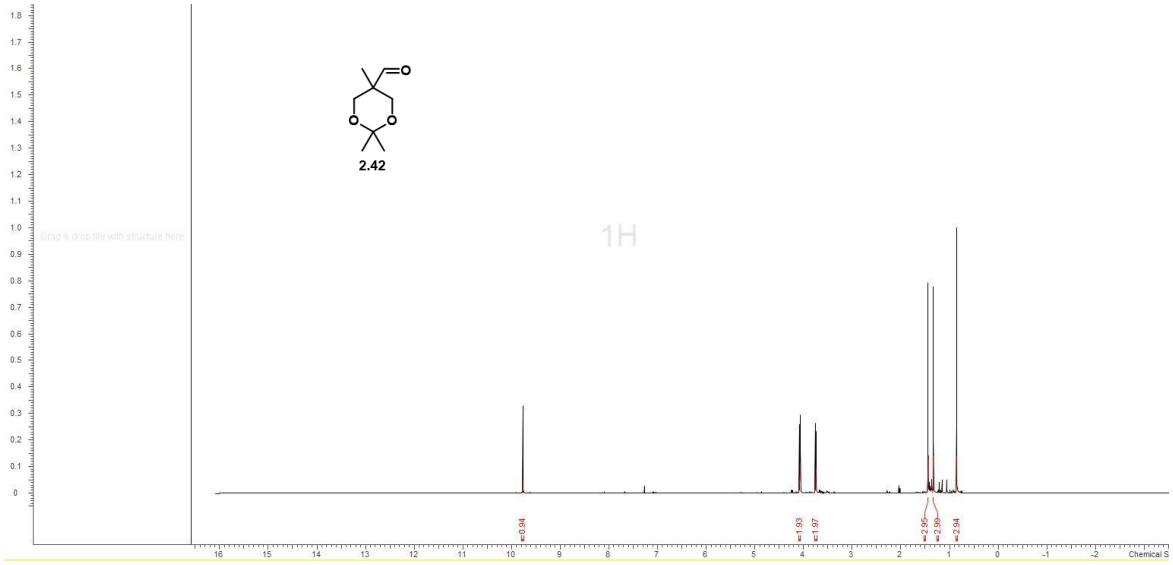
O
2.42
1H
Drag & drop file with structure here
Chemical S

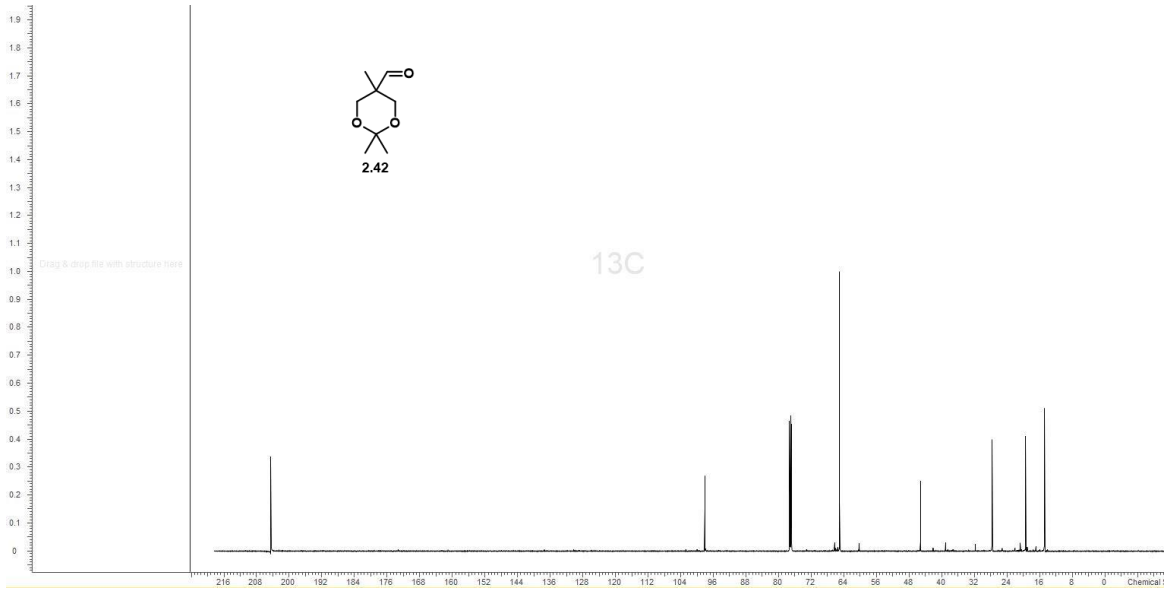
2.42
13C
Drag & drop file with structure here

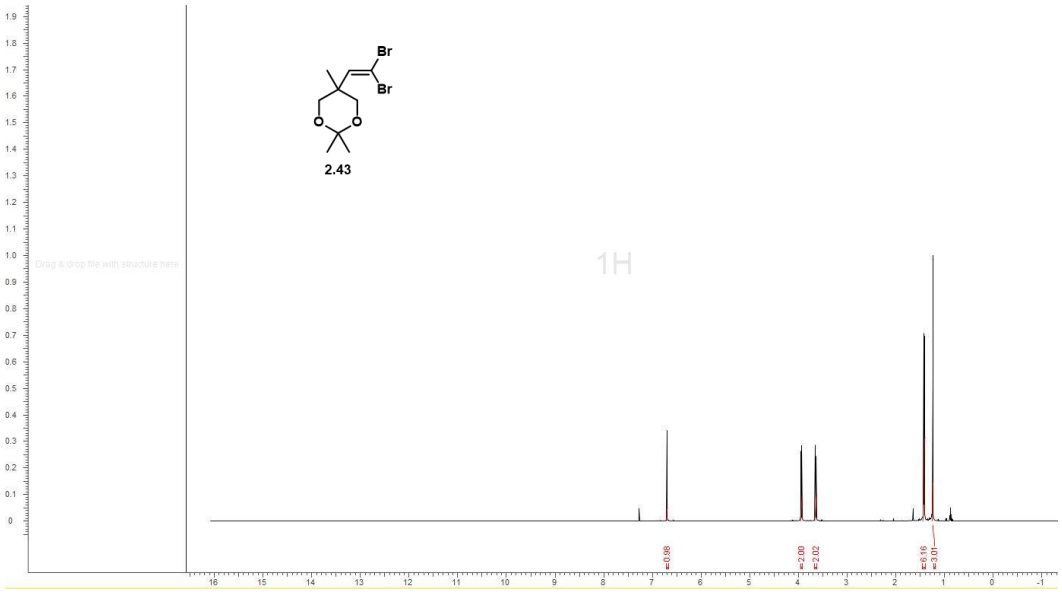
Br
Br
2.43
1H
Drag & drop file with structure here
0.98
2.00
2.02
6.16
3.01

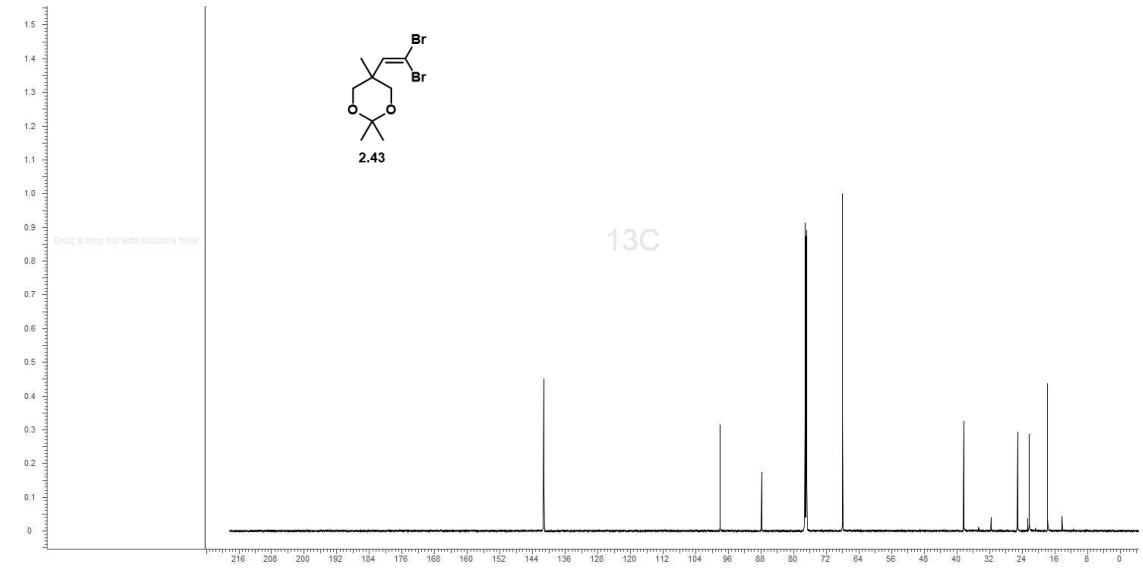
Br
Br
2.43
13C

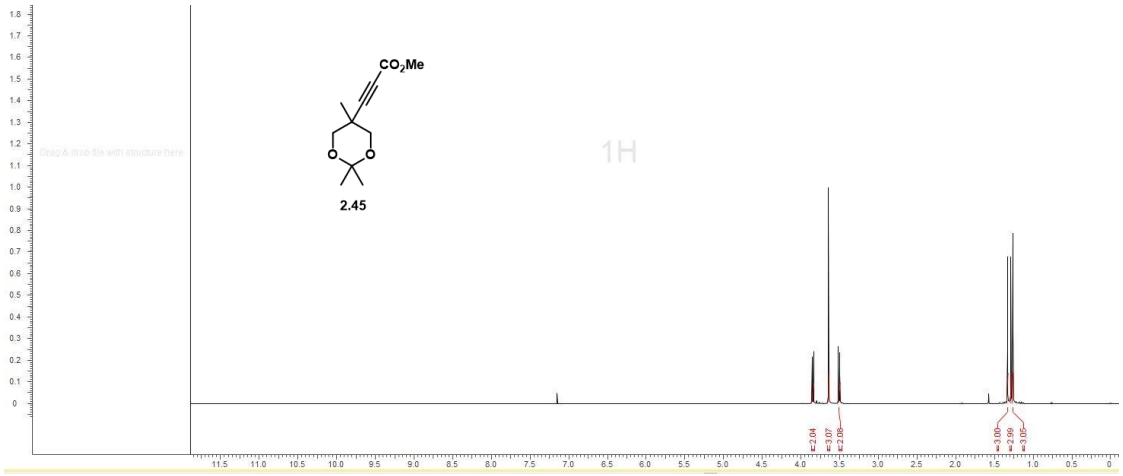
CO2Me
2.45
1H

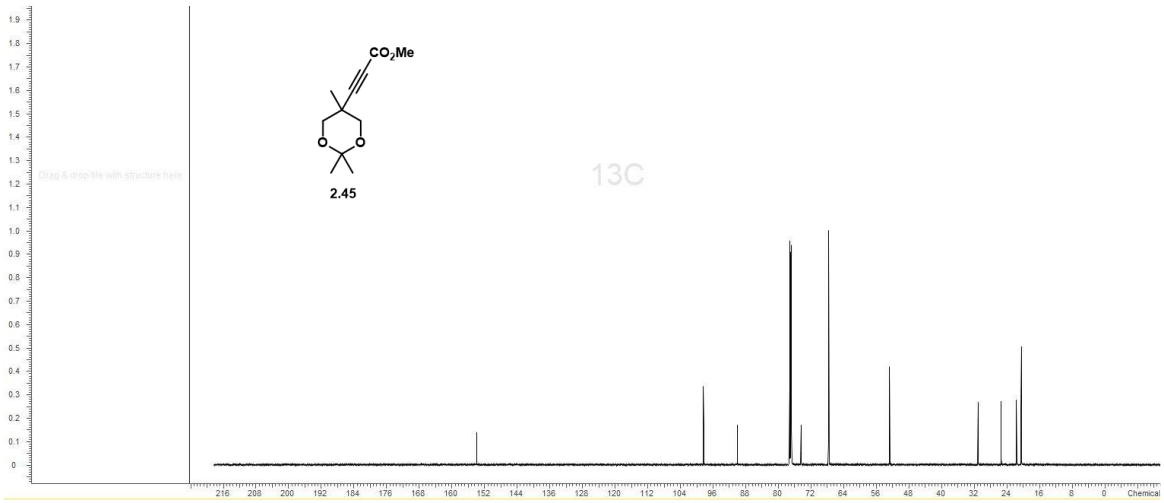
CO2Me
2.45
13C

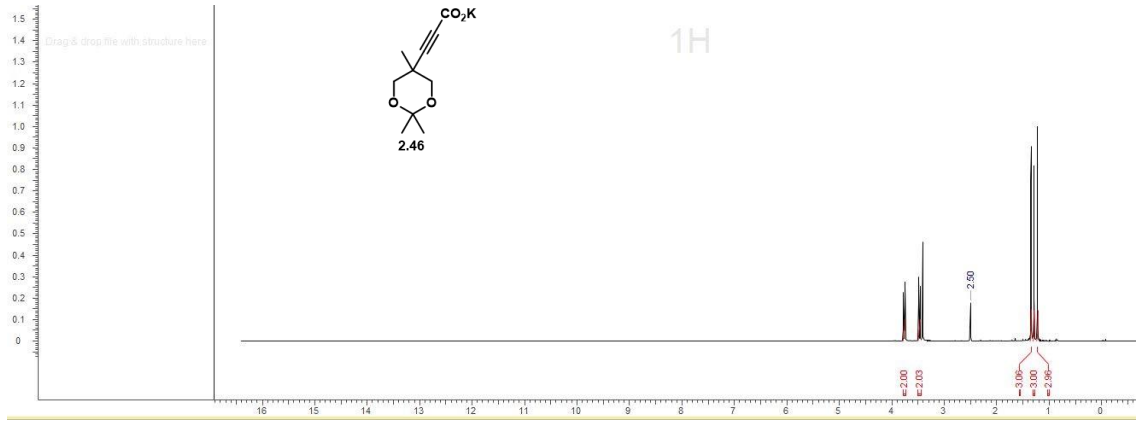
CO2K
2.46
1H
2.50
2.00
2.03
3.09
3.00
2.99

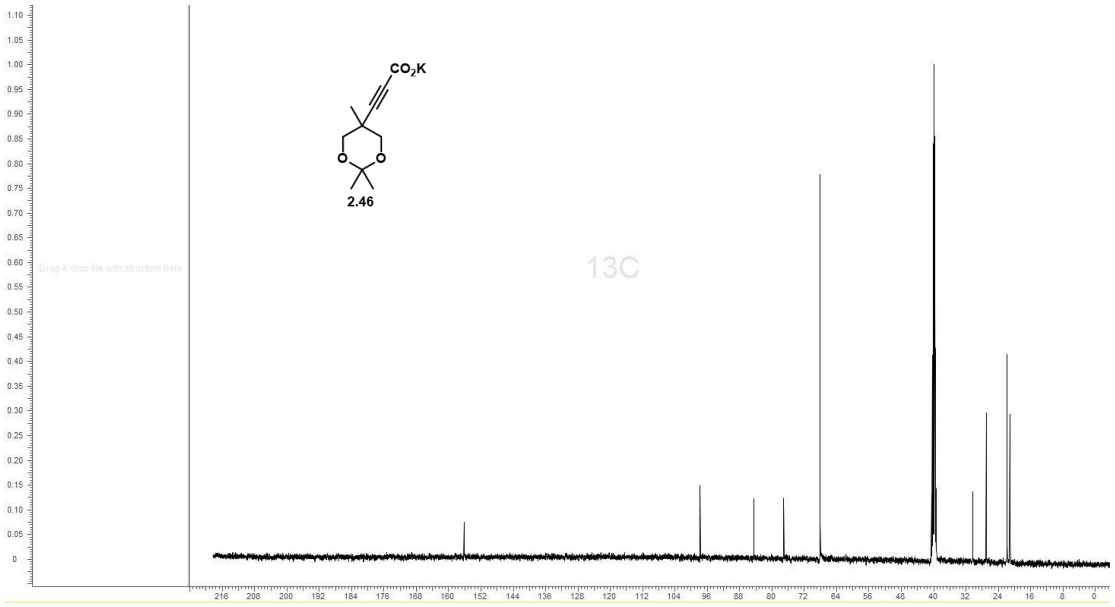
CO2K
2.46
13C

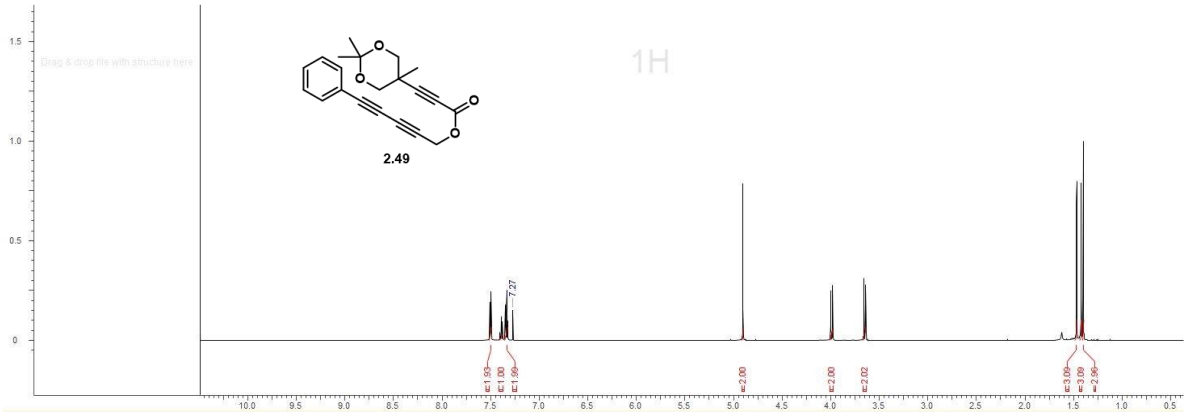
2.49
1H

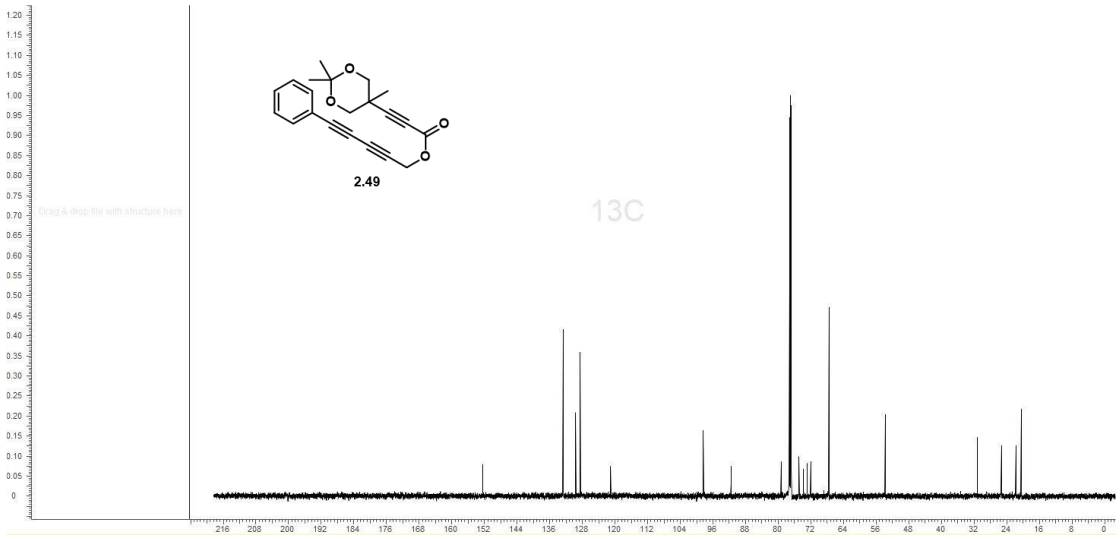
2.49
13C

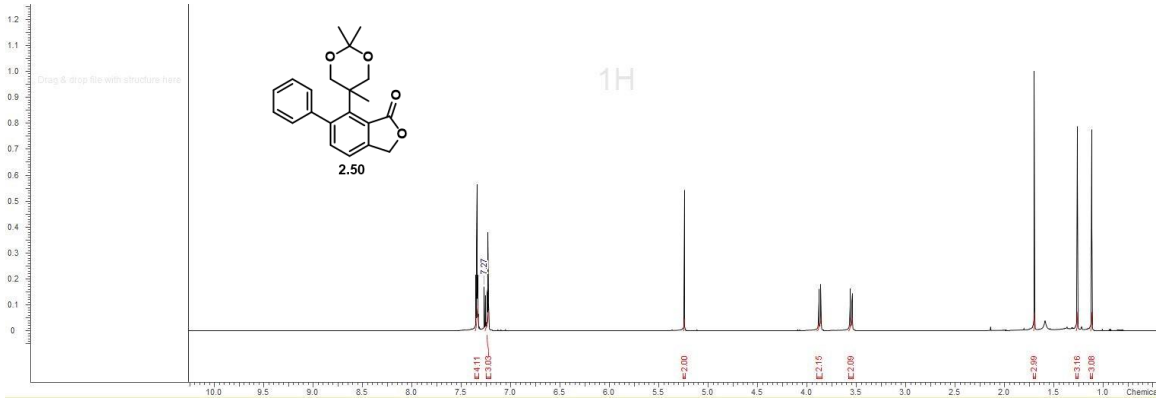
2.50
1H

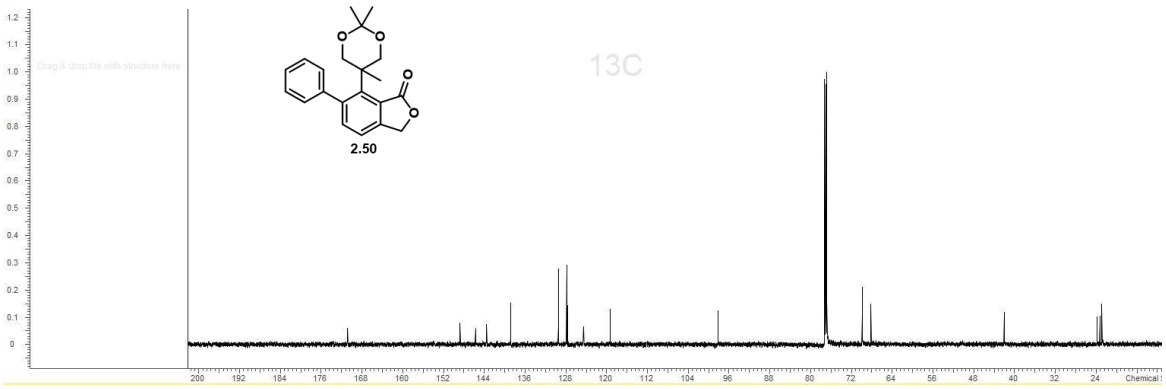
13C
2.50

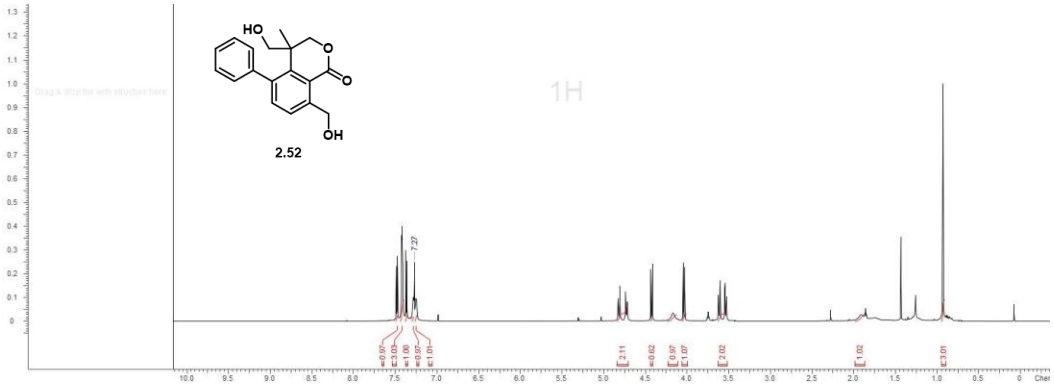
1H
HO
OH
2.52

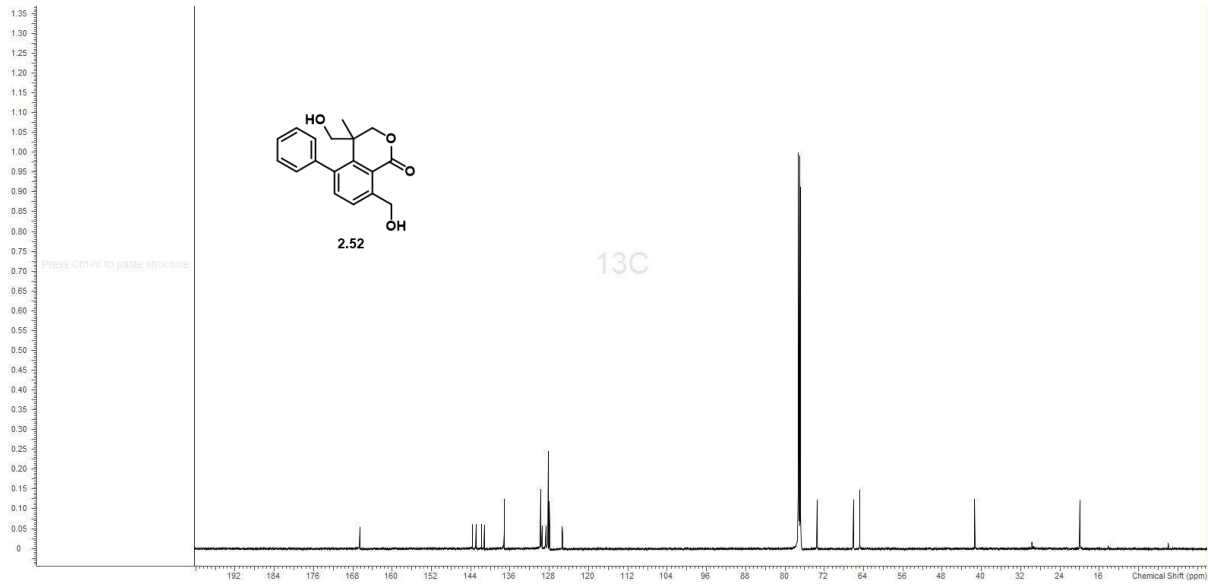
HO
O
O
OH
2.52
Press Ctrl+V to paste structure
13C
Chemical Shift (ppm)

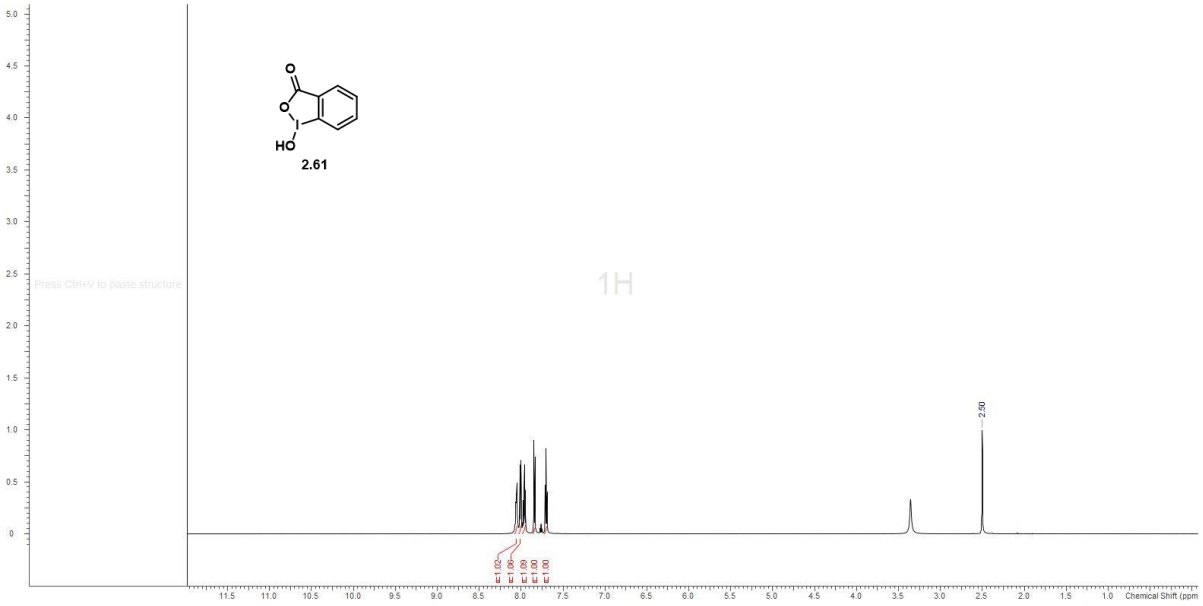
O
O
I
HO
2.61
Press Ctrl+V to paste structure
1H
2.50
Chemical Shift (ppm)

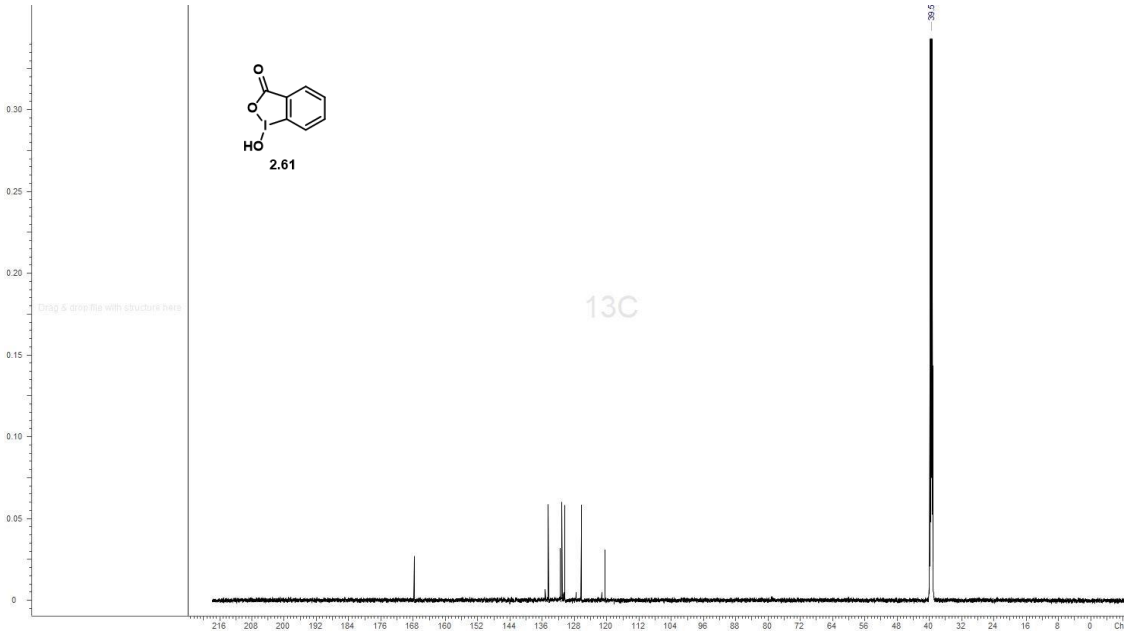
2.61
39.5
13C

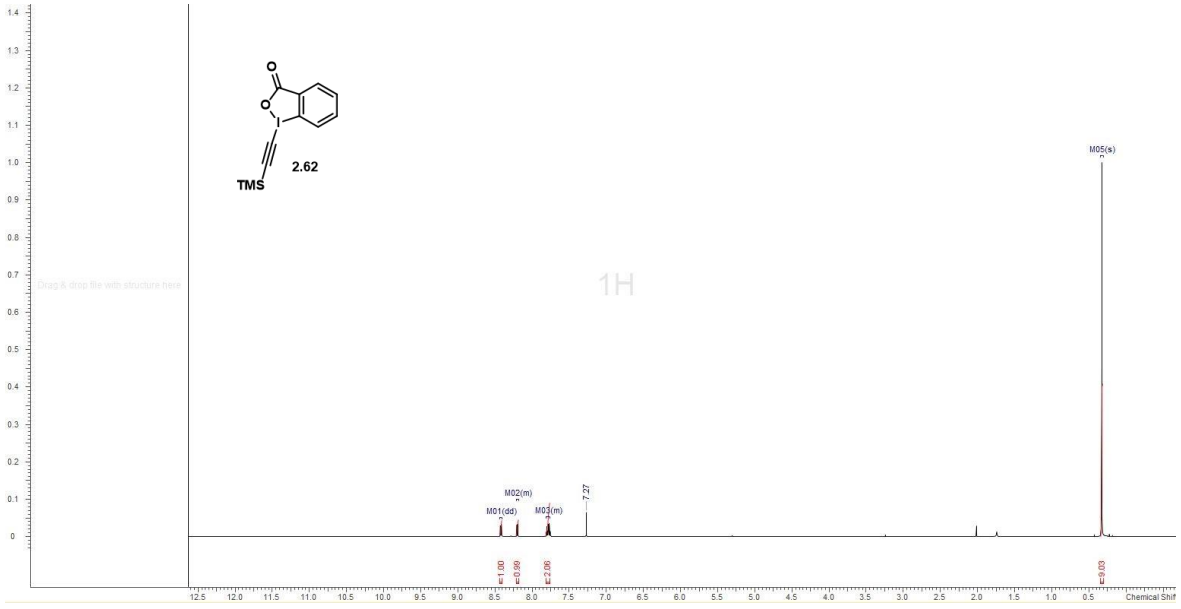
2.62
TMS
M05(s)
M02(m)
M01(dd)
M03(m)
7.27
1H

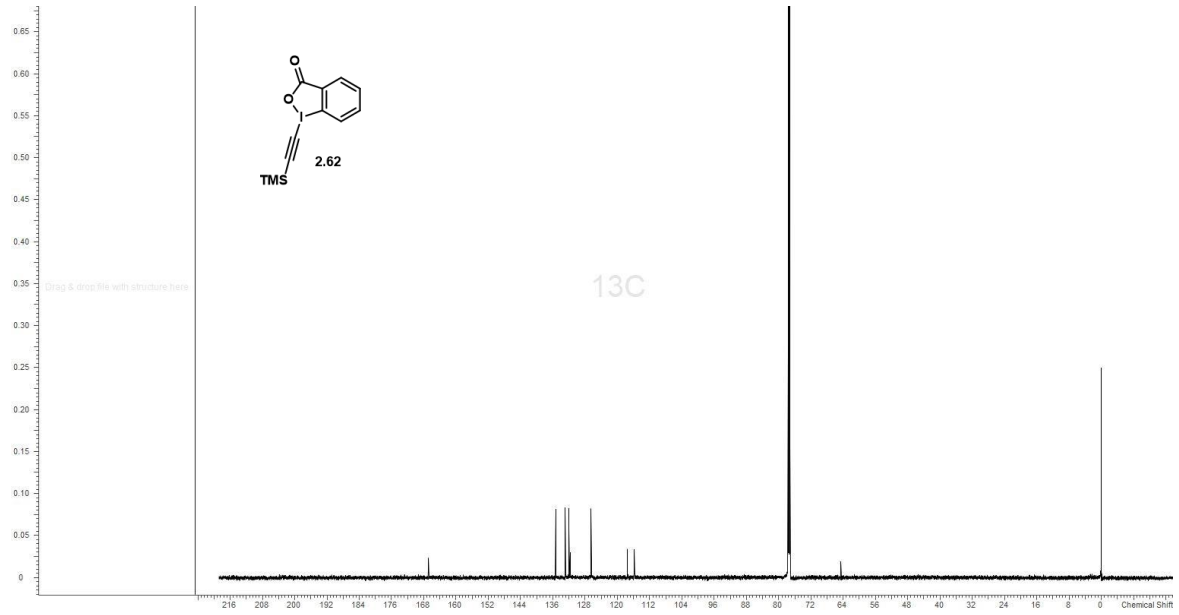
2.62
TMS
13C
Chemical Shift

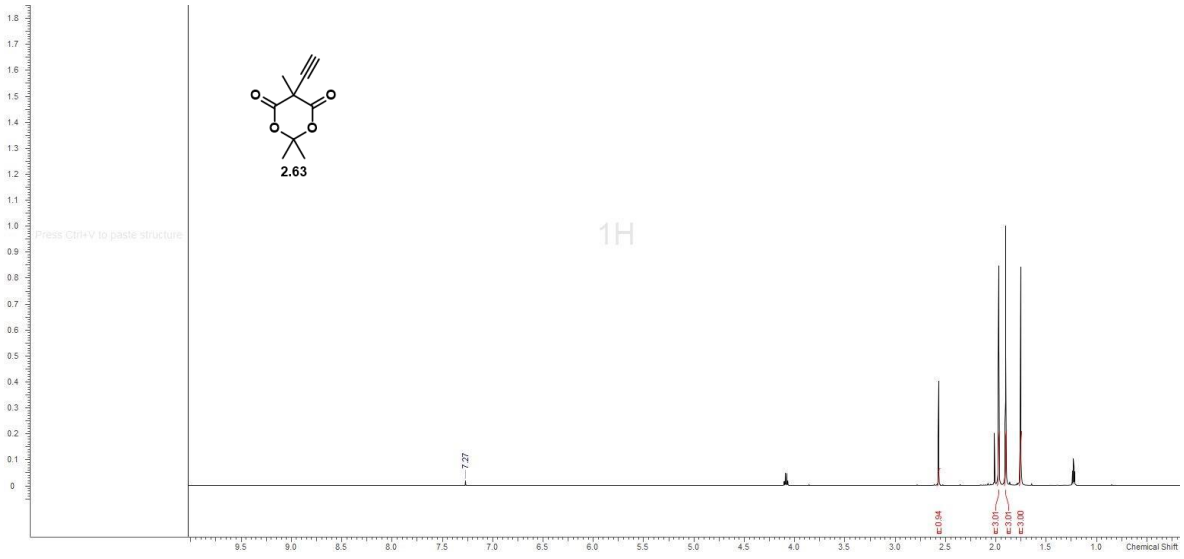
2.63
1H
7.27
0.94
3.01
3.01
3.00
Chemical Shift

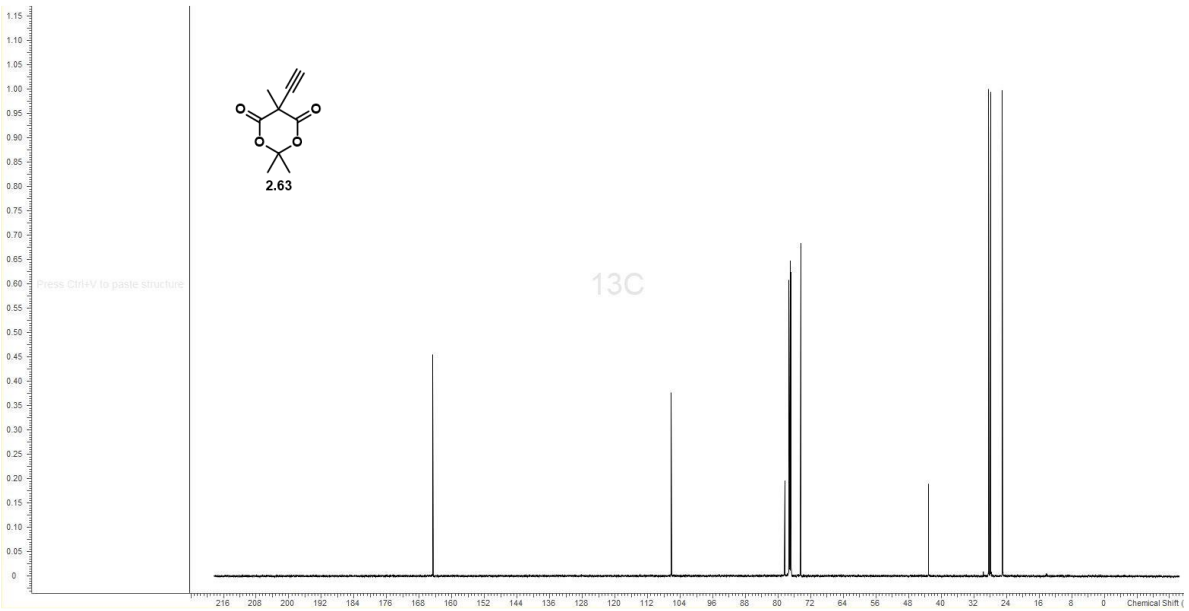
2.63
13C
Chemical Shift

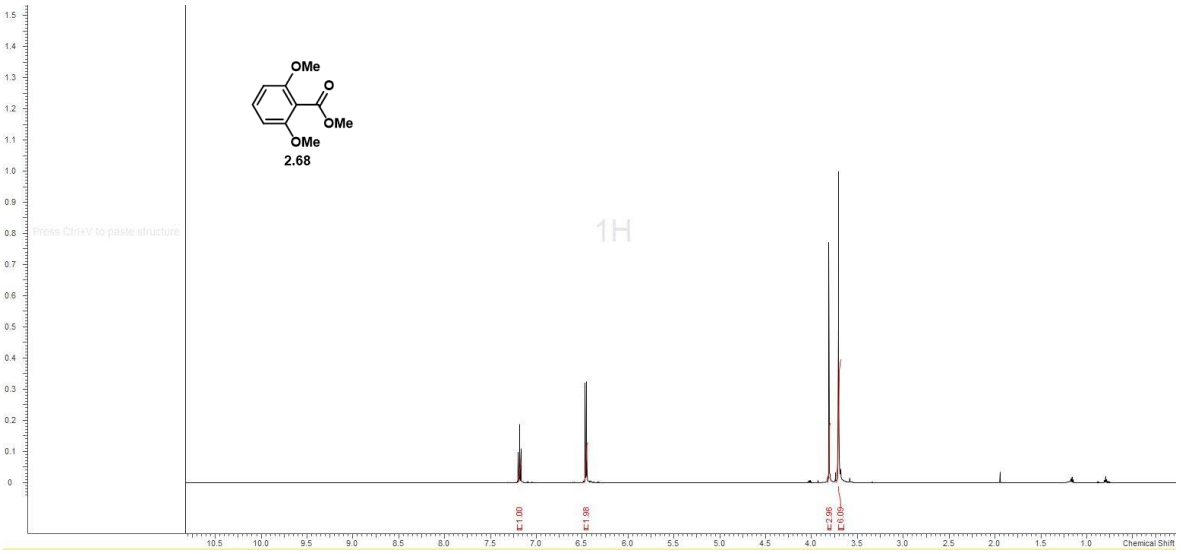
OMe
OMe
OMe
2.68
1H
Chemical Shift

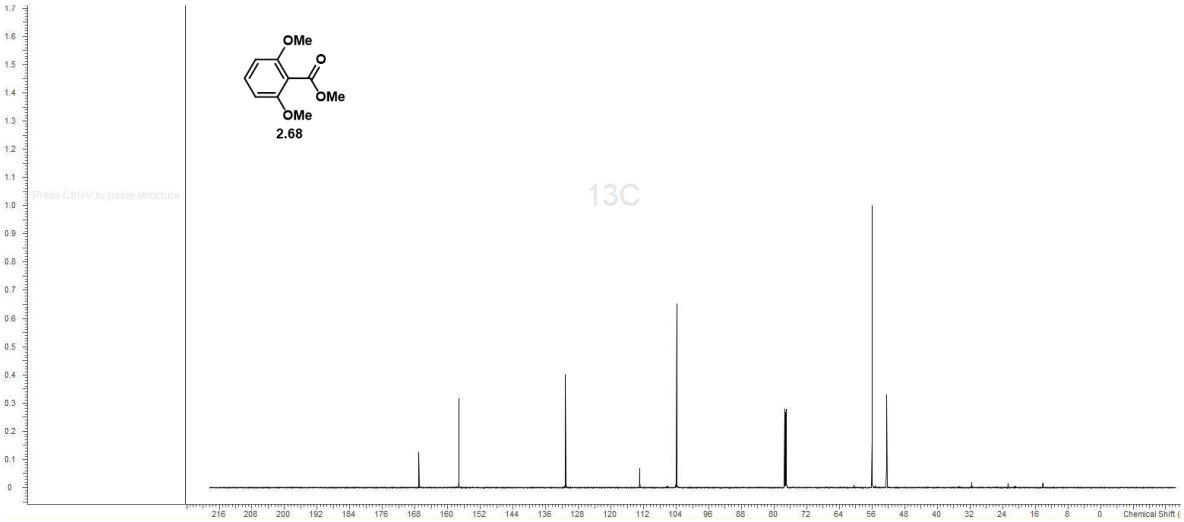
OMe
O
OMe
OMe
2.68
13C
Chemical Shift

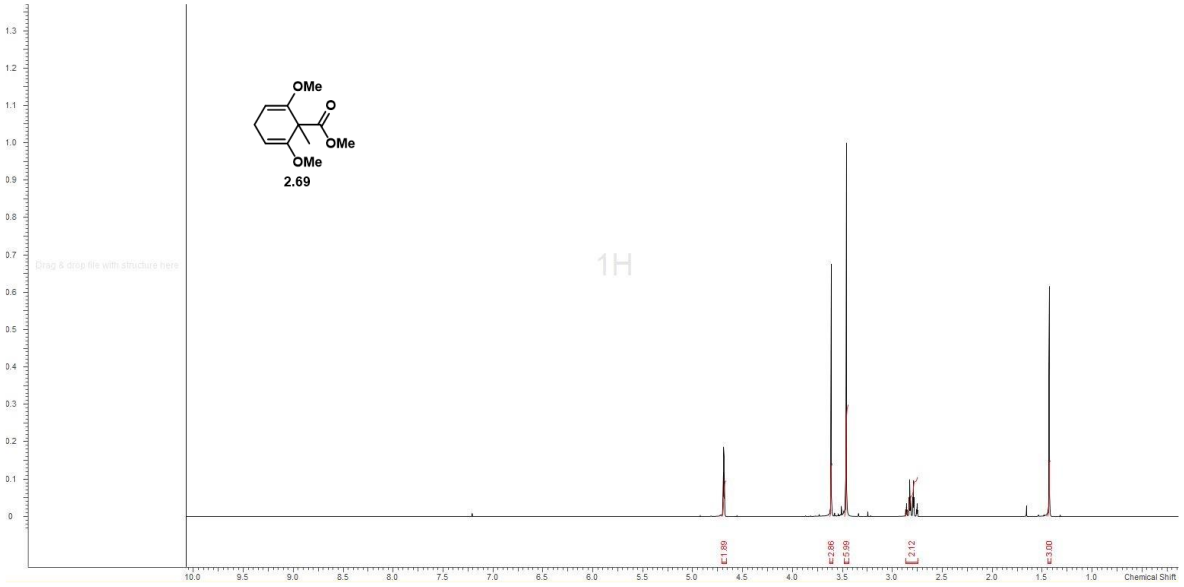
OMe
O
OMe
OMe
2.69
1H
1.89
2.86
5.99
2.12
3.00
Chemical Shift

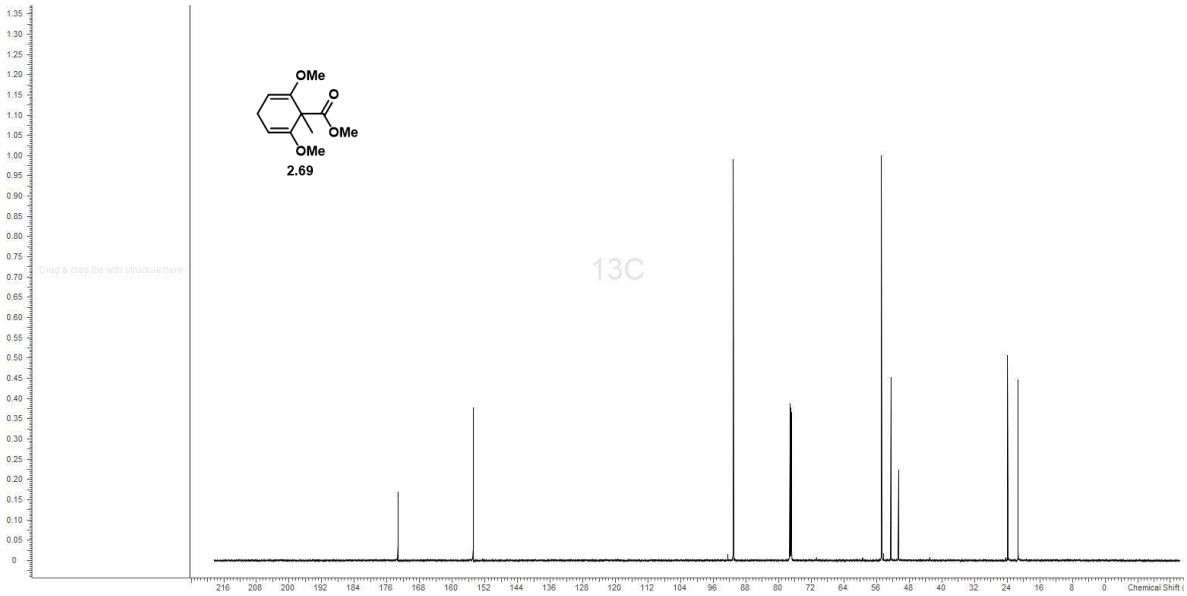
OMe
O
OMe
OMe
2.69
13C
Drag & drop file with structure here
Chemical Shift

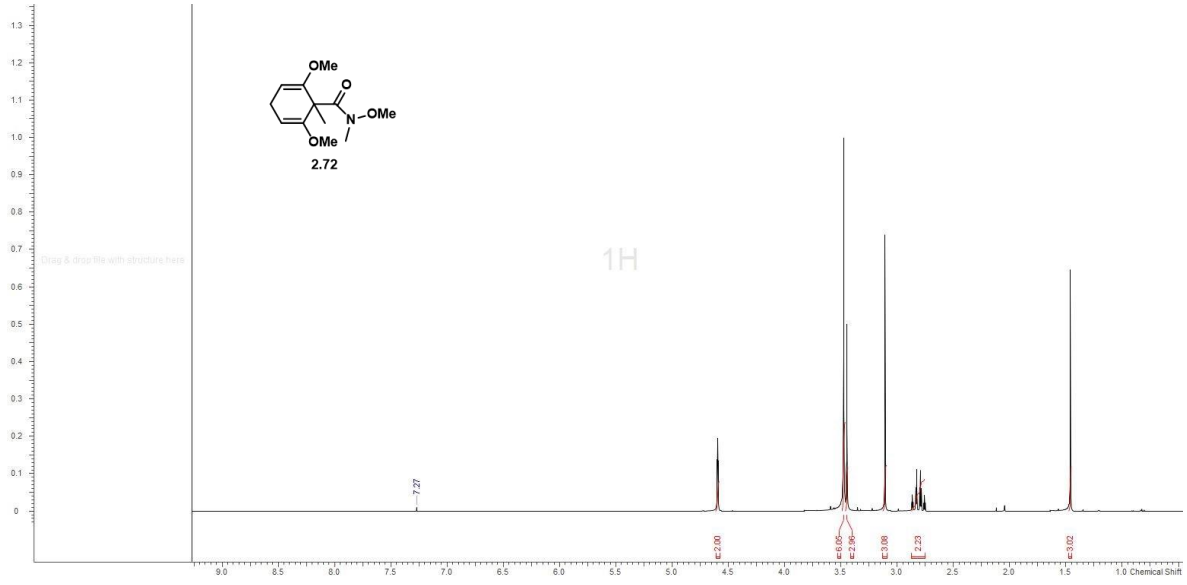
OMe
O
N
OMe
OMe
2.72
1H
Drag & drop file with structure here
7.27
2.00
6.05
2.99
3.08
2.23
3.02
Chemical Shift

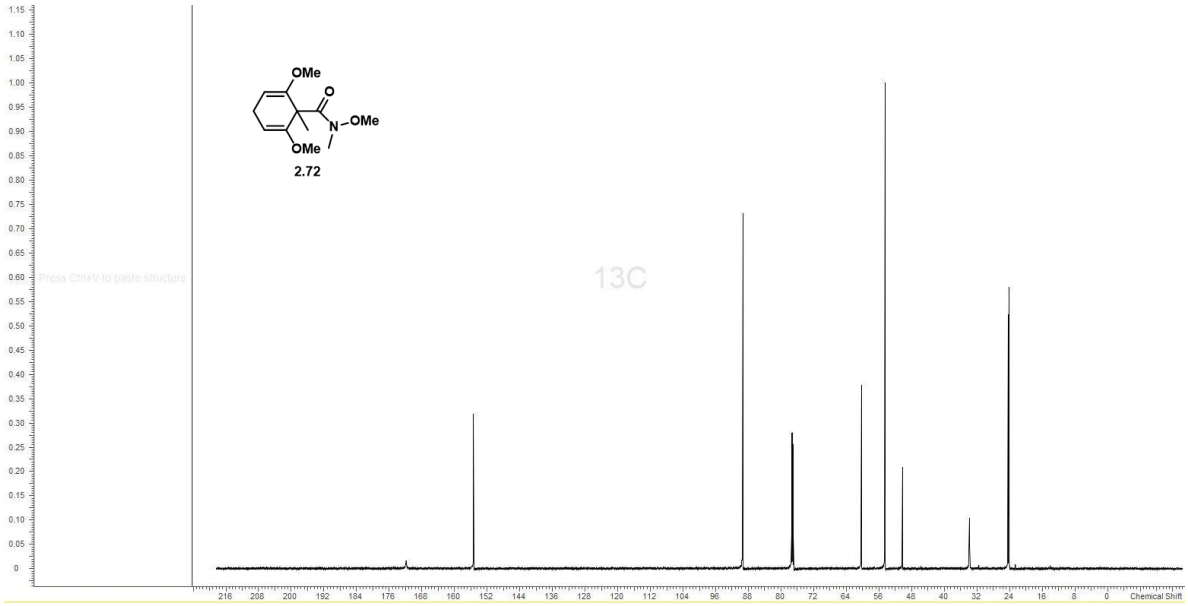
OMe
O
N
OMe
OMe
2.72
13C
Chemical Shift

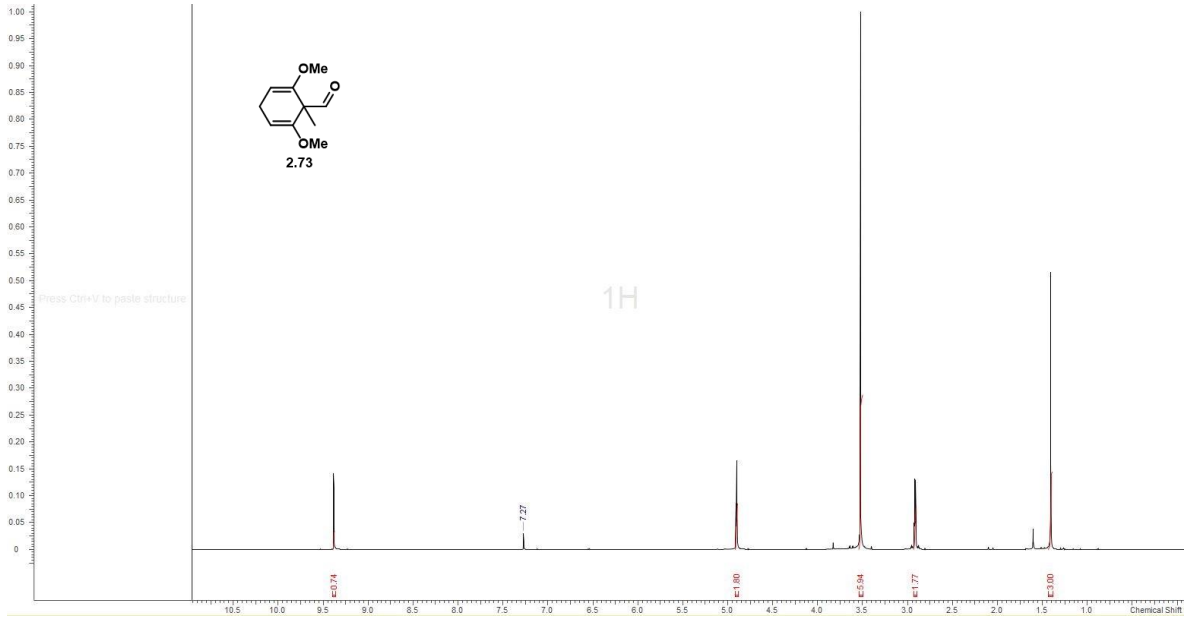
OMe
O
OMe
2.73
1H
7.27
0.74
1.80
5.94
1.77
3.00
Chemical Shift

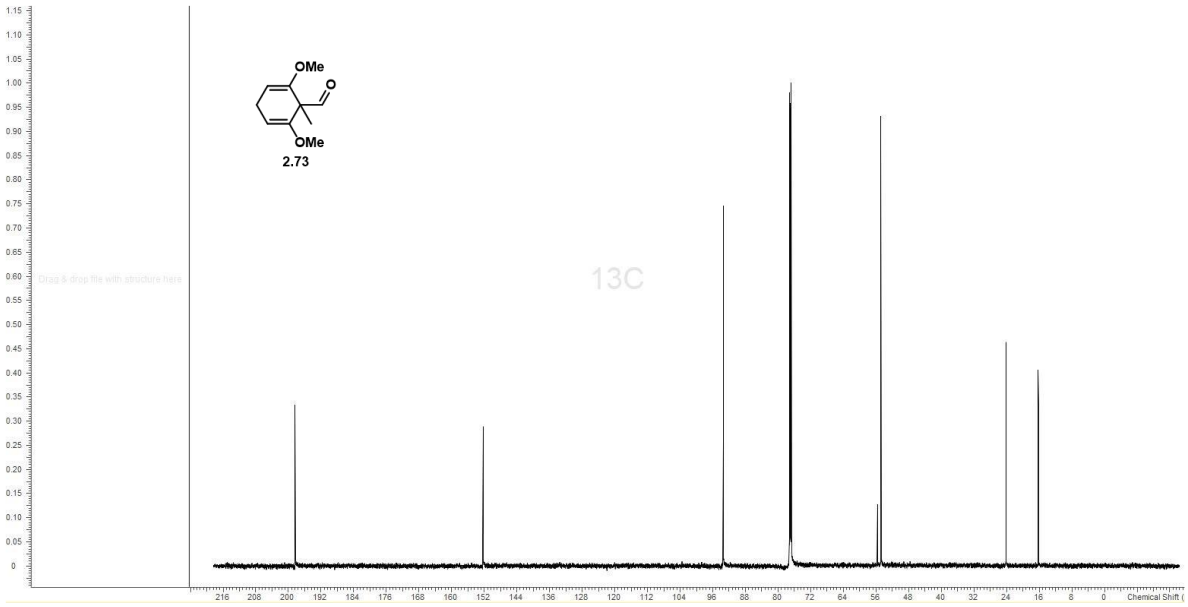
OMe
O
OMe
2.73
13C
Chemical Shift (

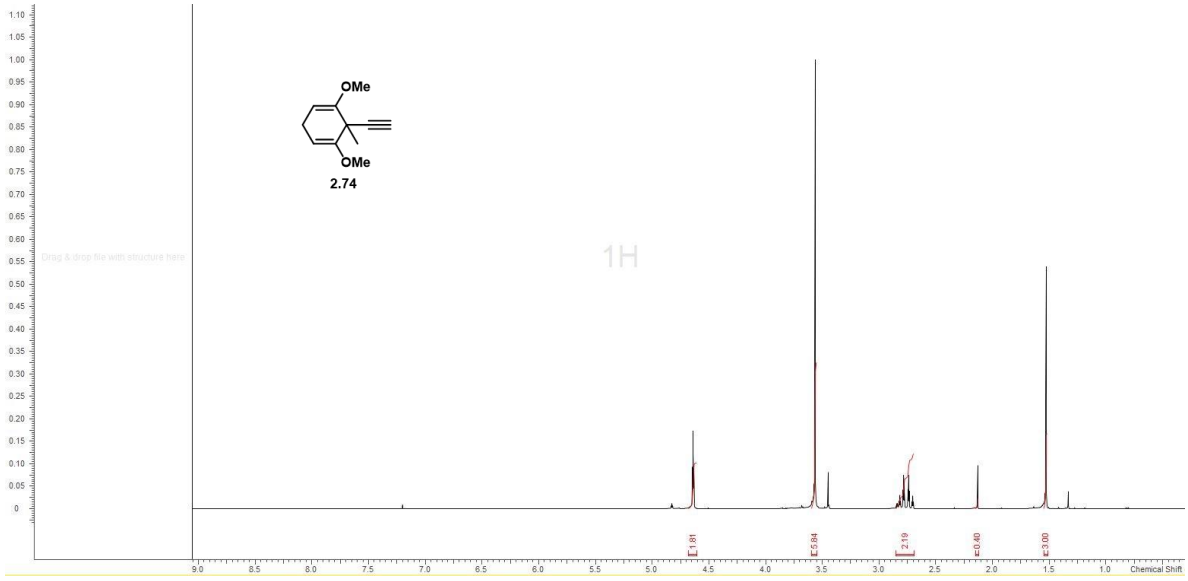
OMe
OMe
2.74
1H
1.81
5.84
2.19
0.40
3.00
Chemical Shift

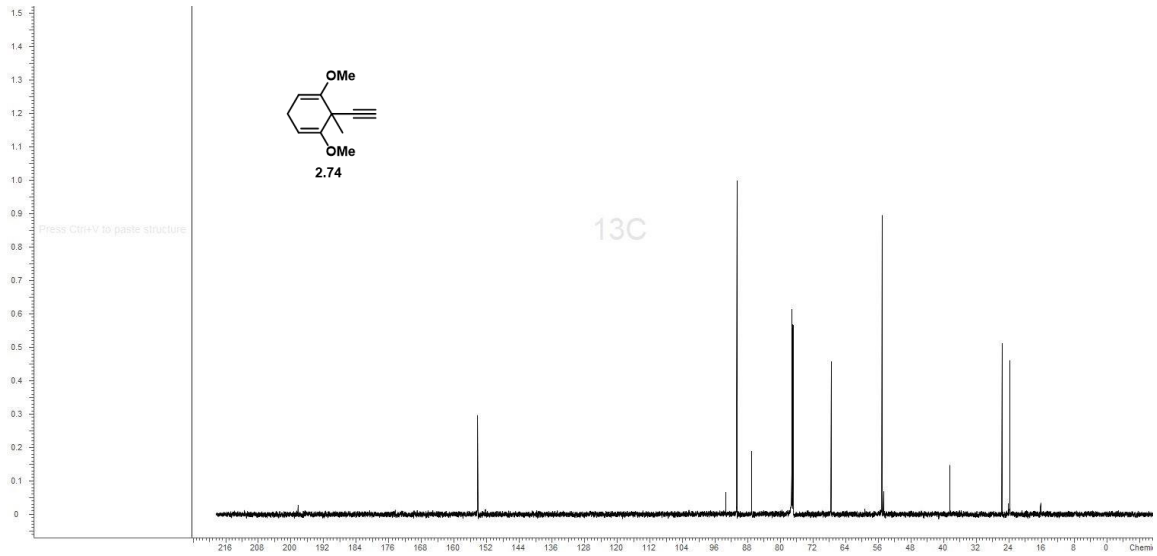
OMe
OMe
2.74
13C

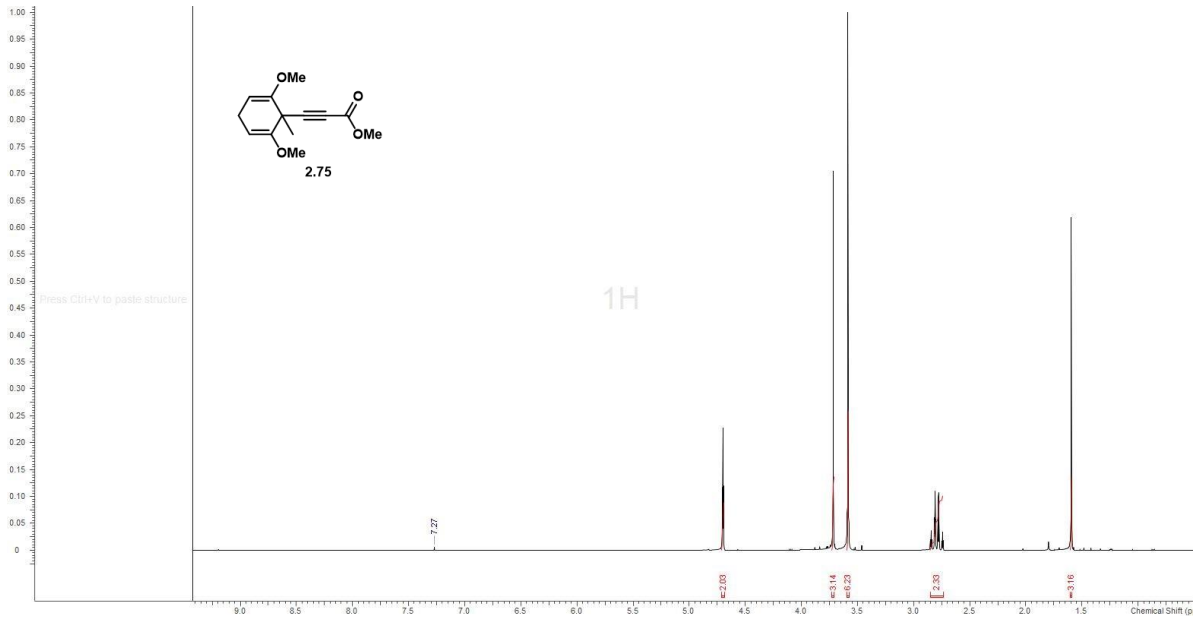
OMe
O
OMe
OMe
2.75
1H
7.27
2.83
3.14
6.23
2.33
3.16
Chemical Shift (p

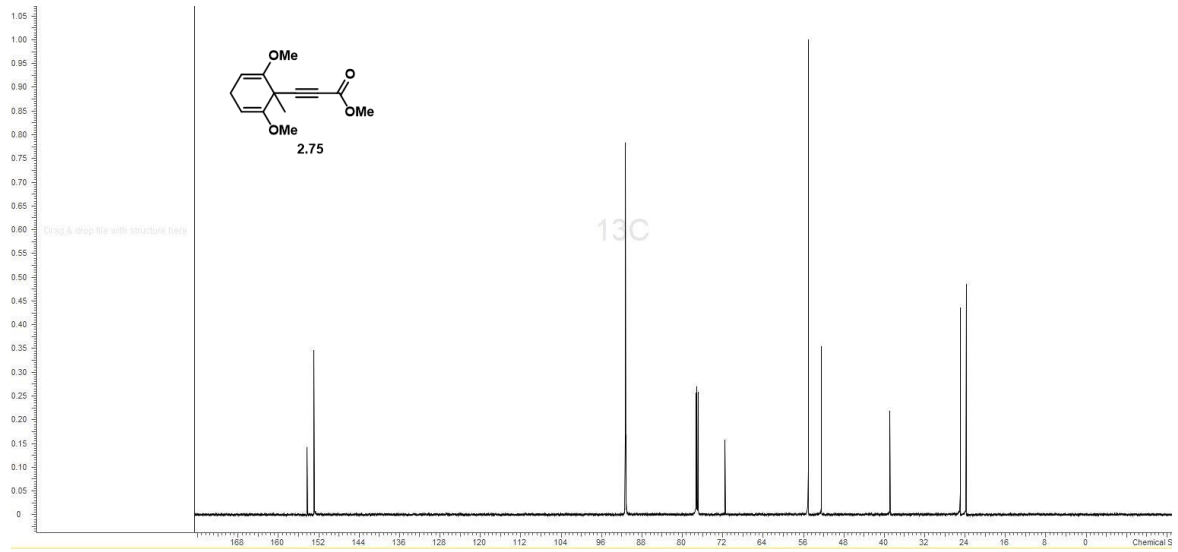
OMe
O
OMe
OMe
2.75
13C
Drag & drop file with structure here
Chemical S

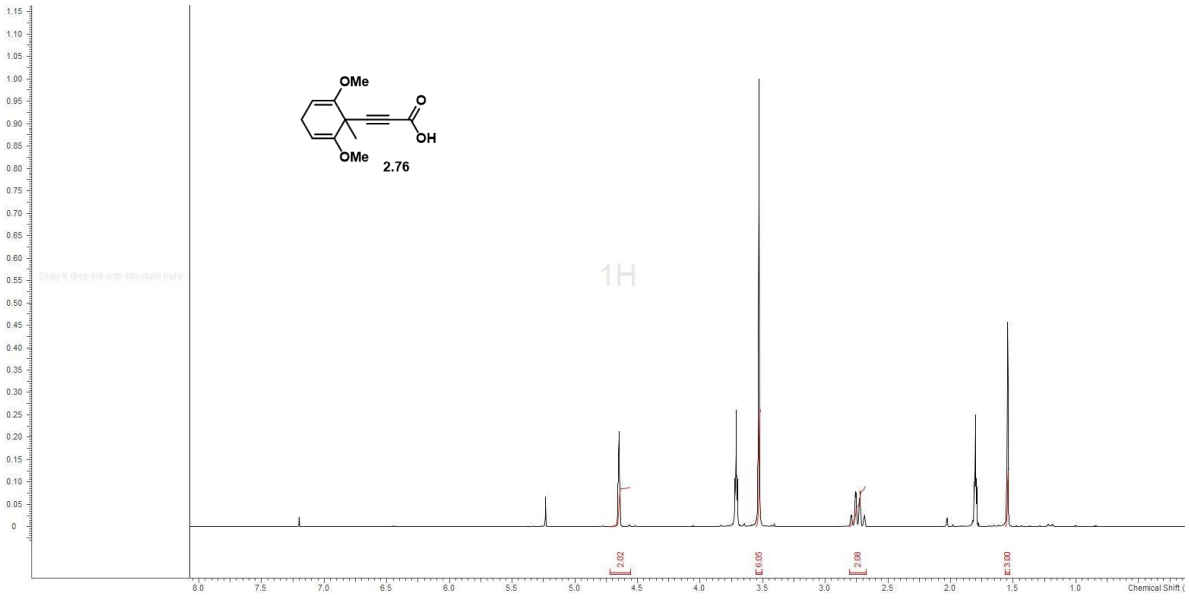
OMe
O
OH
OMe
2.76
1H
Drag & drop file with structure here
2.02
6.05
2.08
3.00
Chemical Shift (

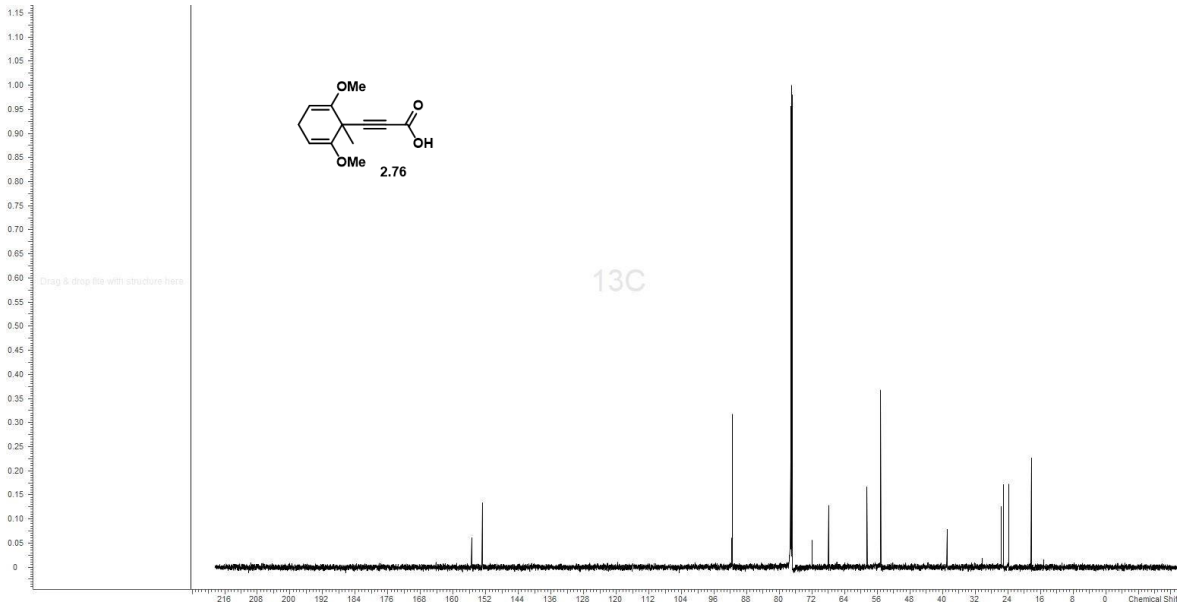
OMe
O
OH
OMe
2.76
13C
Chemical Shift

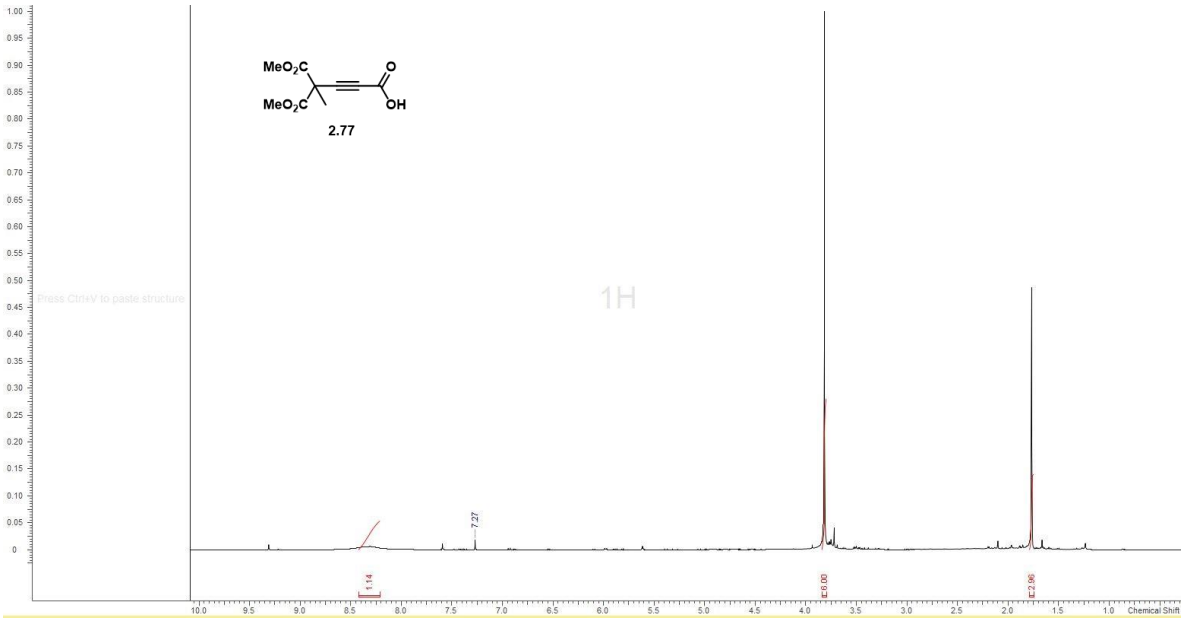
MeO2C
O
MeO2C
OH
2.77
1H
7.27
1.14
6.00
2.96
Chemical Shift

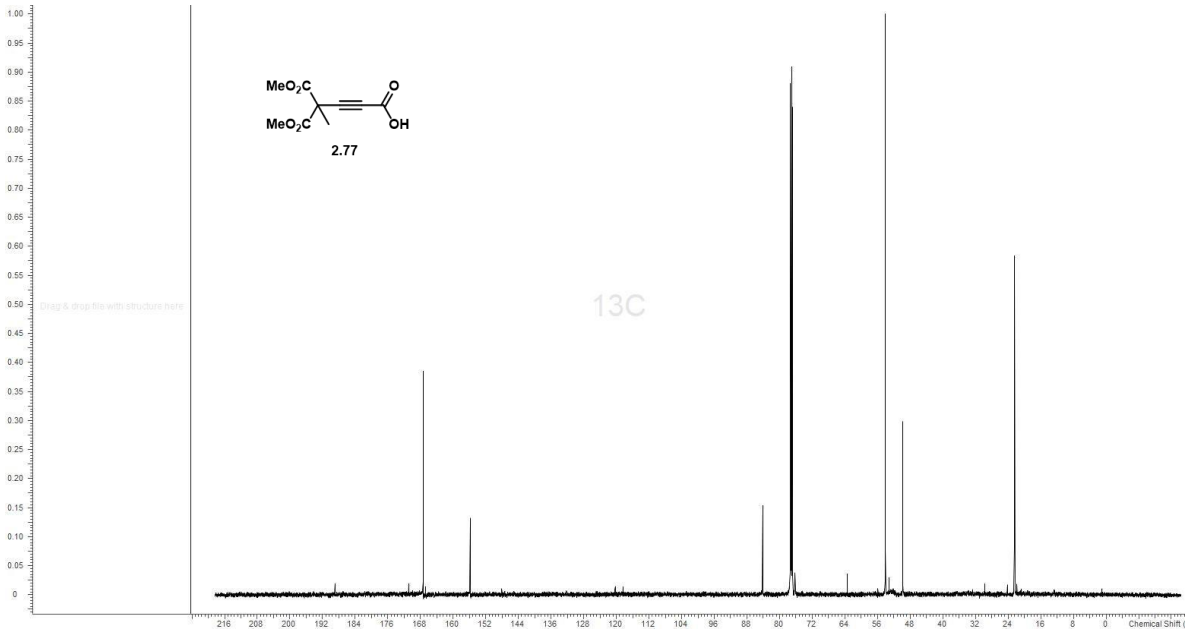
MeO2C
MeO2C
O
OH
2.77
13C
Chemical Shift

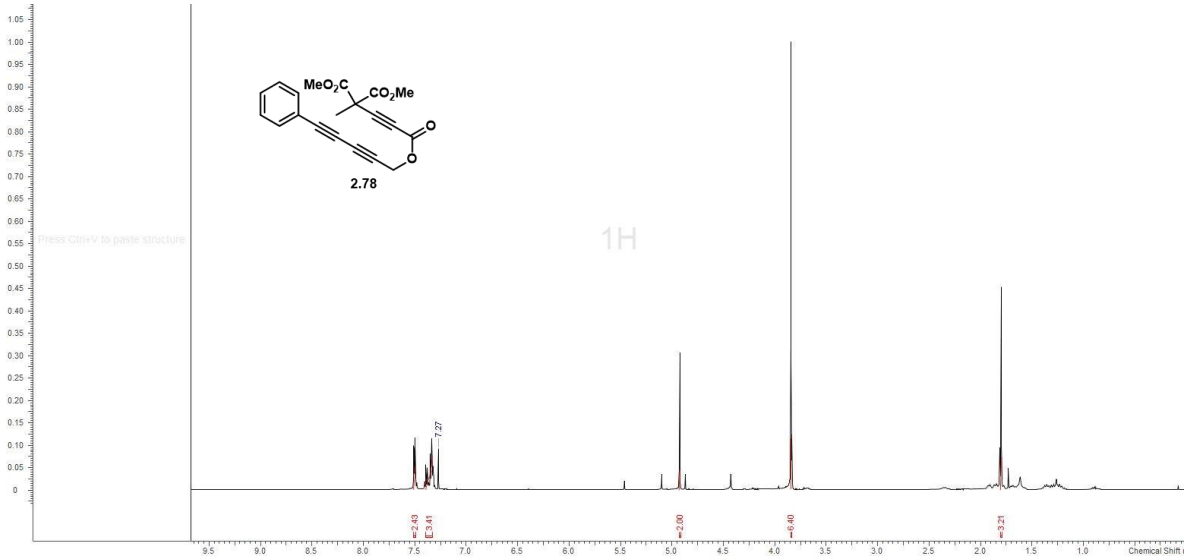
MeO2C
CO2Me
O
O
2.78
1H
7.27
2.43
3.41
2.00
6.40
3.21
Chemical Shift

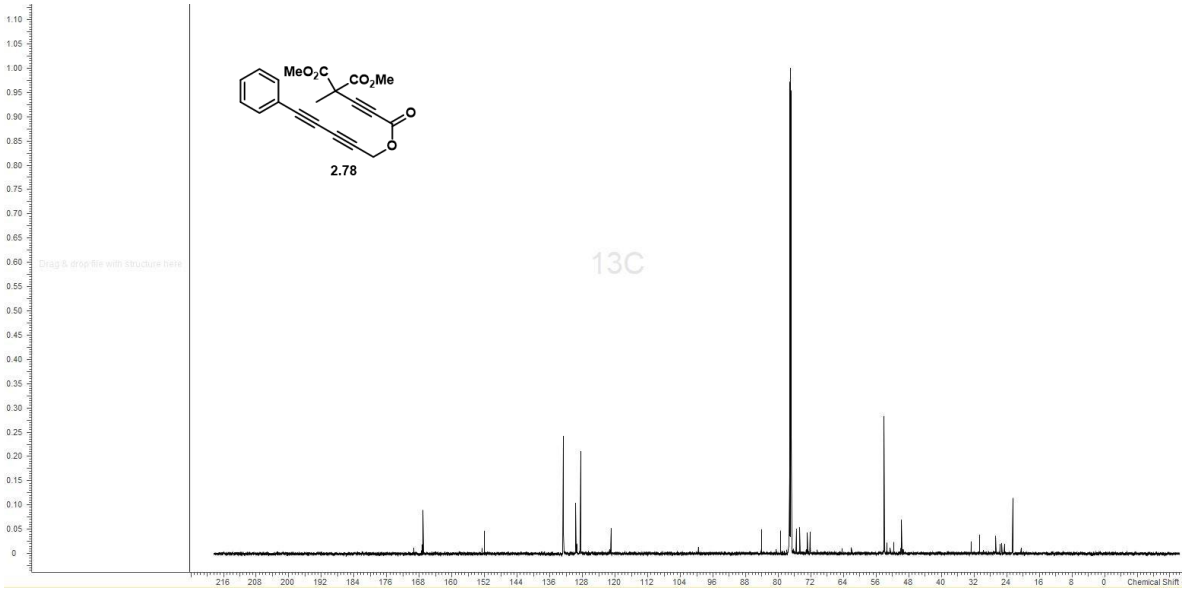
MeO2C
CO2Me
O
O
2.78
13C
Chemical Shift

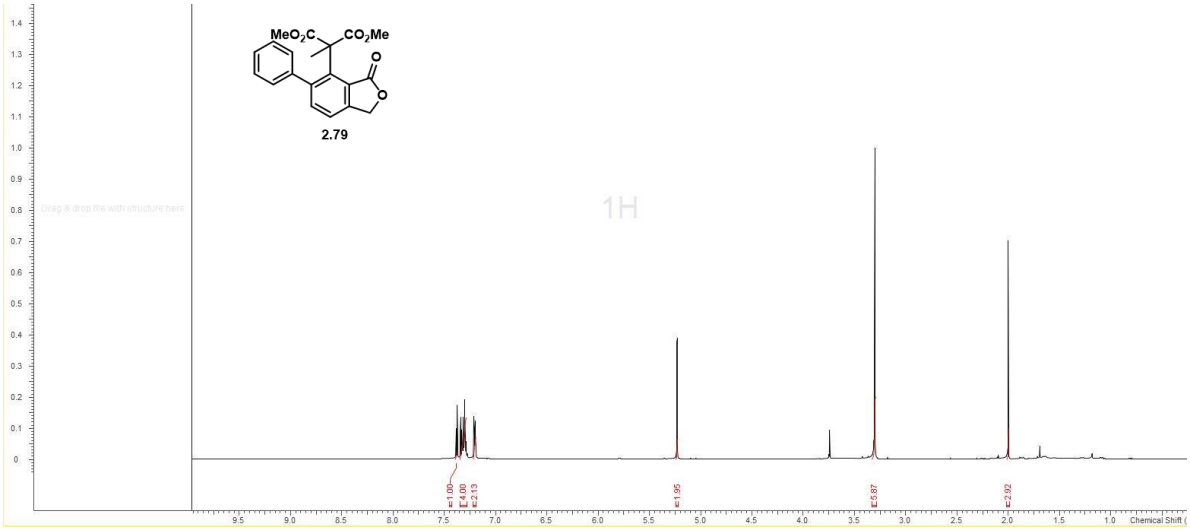
MeO2C
CO2Me
O
O
2.79
1H
Chemical Shift

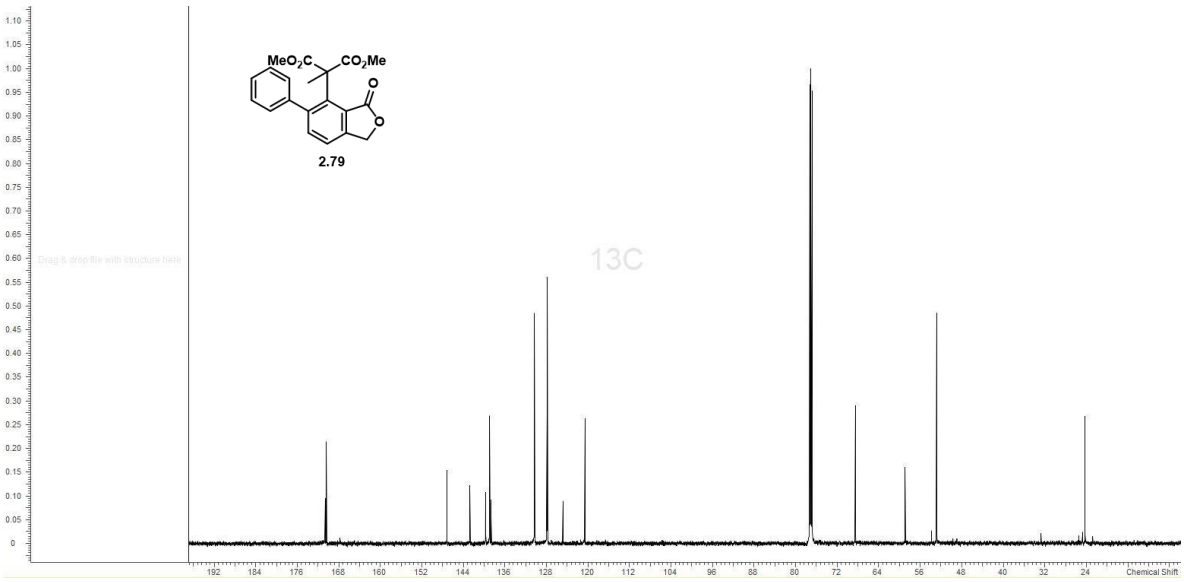
MeO2C
CO2Me
O
O
2.79
13C
Chemical Shift

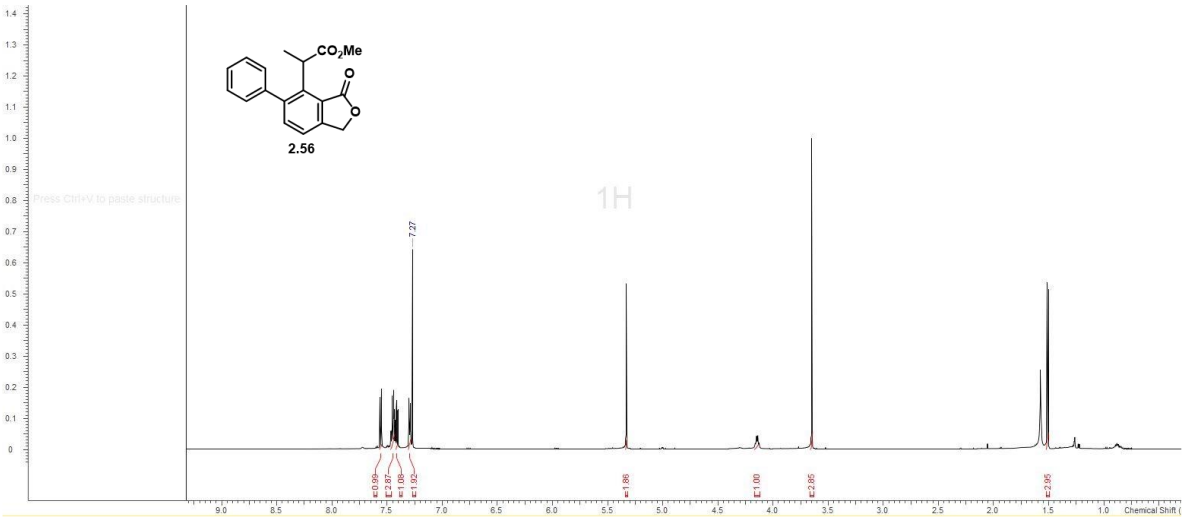
CO2Me
O
O
2.56
1H
7.27
Chemical Shift

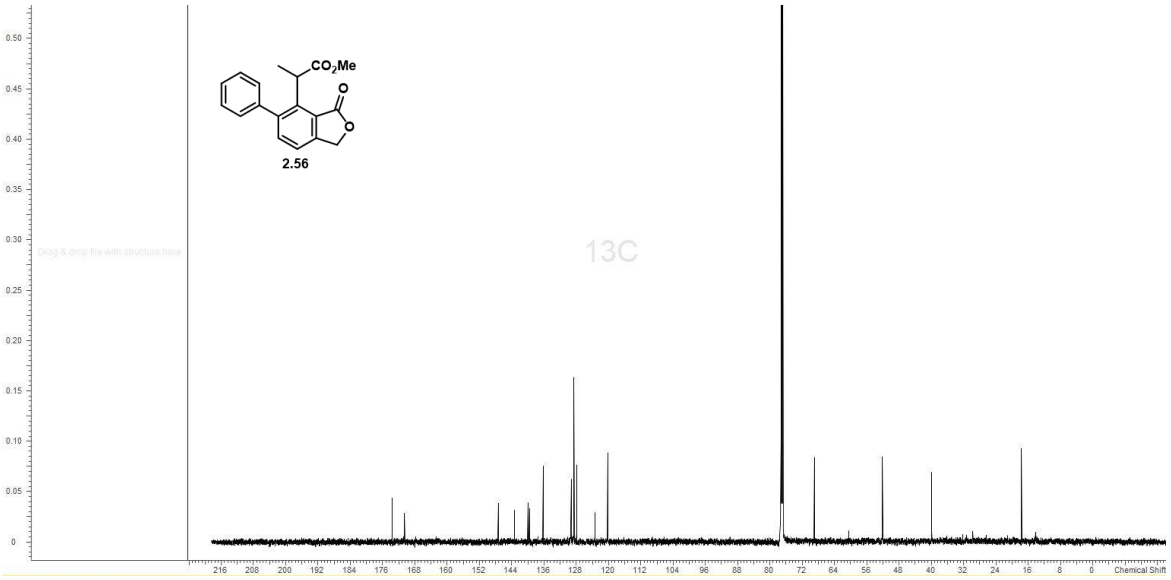
CO2Me
O
O
2.56
13C
Chemical Shift

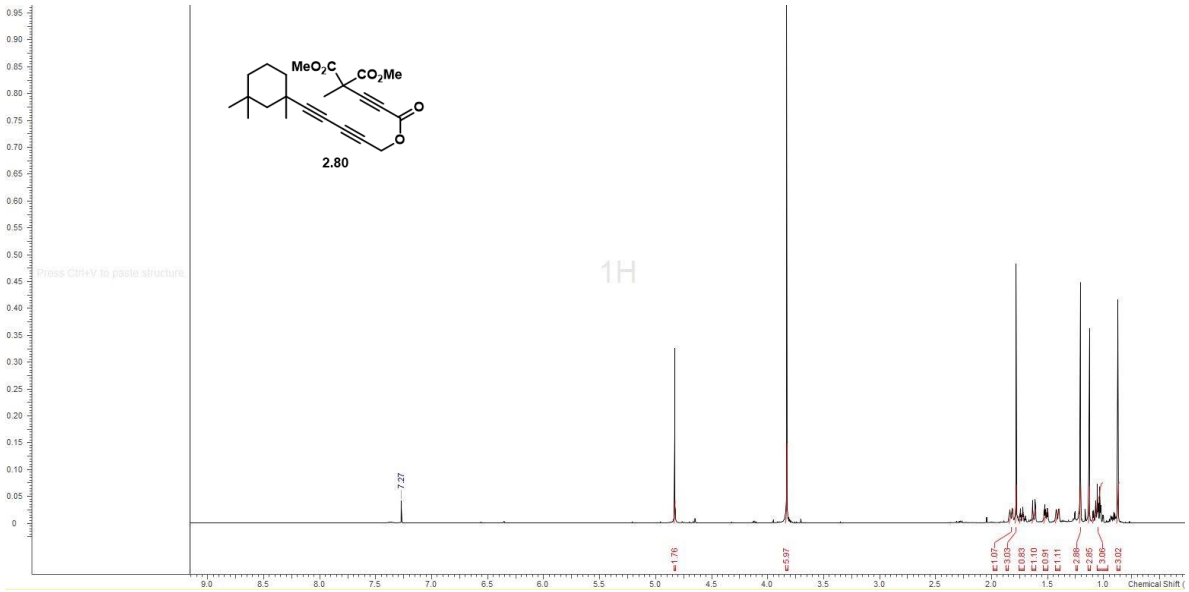
MeO2C
CO2Me
O
O
2.80
1H
7.27
1.76
5.97
1.07
3.09
0.83
1.10
0.91
1.11
2.88
2.85
3.06
3.02
Chemical Shift

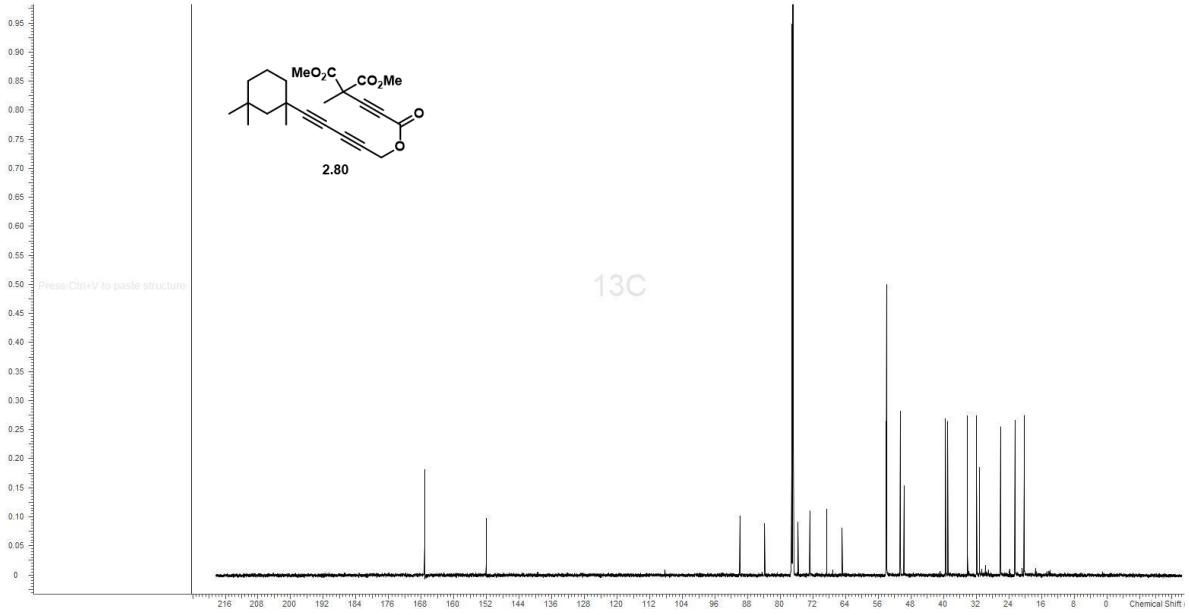
MeO2C
CO2Me
O
O
2.80
13C
Press Ctrl+V to paste structure
Chemical Shift

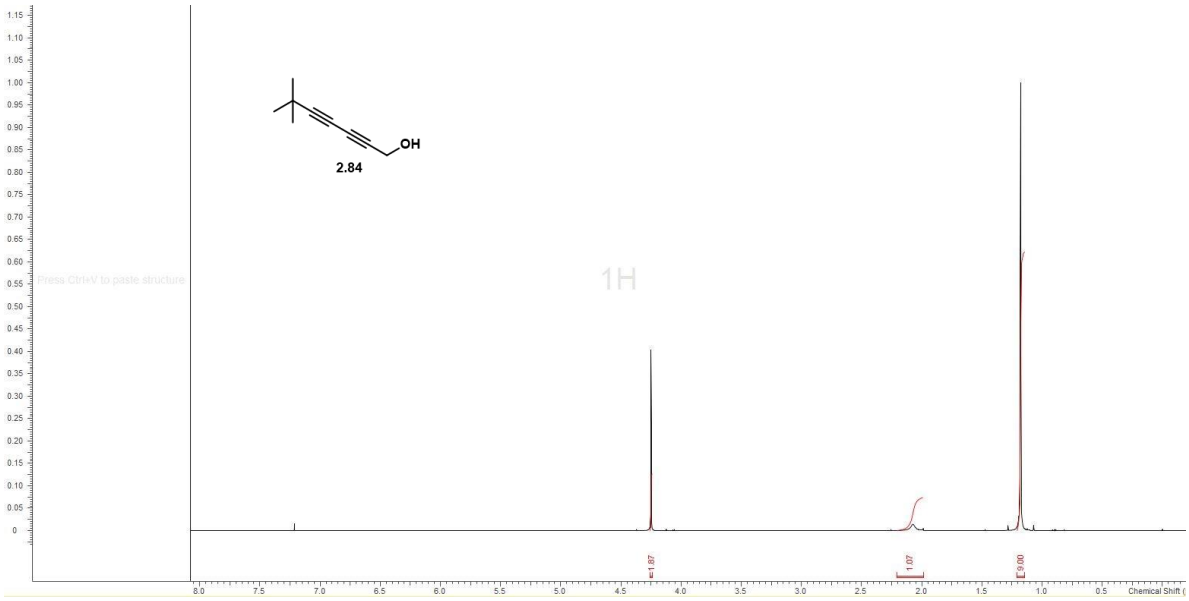
OH
2.84
1H
Press Ctrl+V to paste structure
1.87
1.07
9.00
Chemical Shift

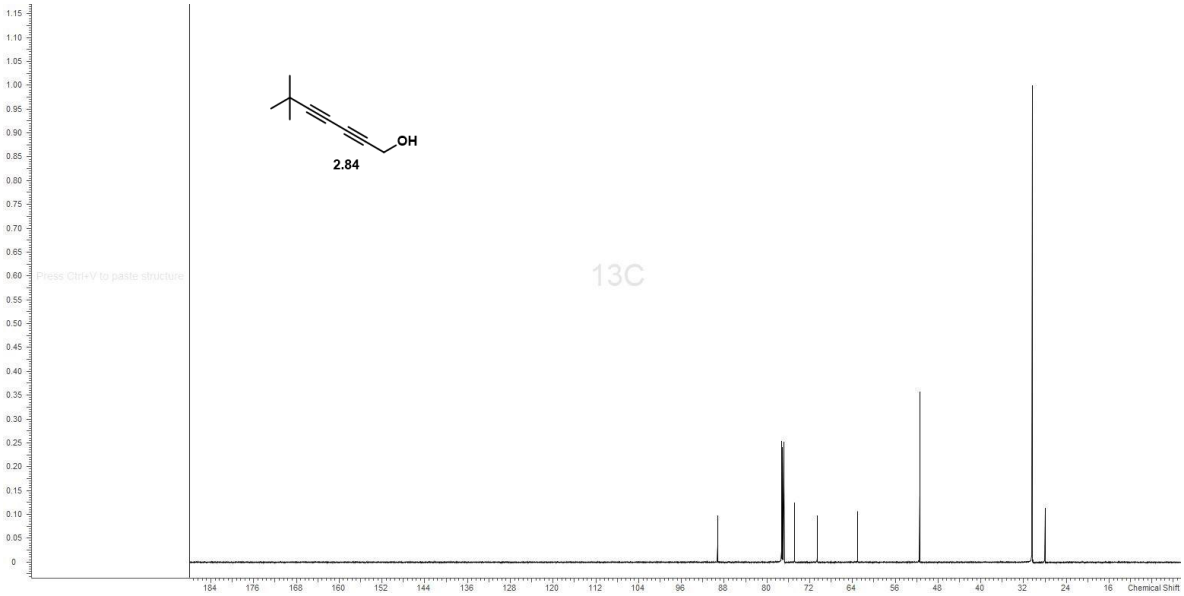
OH
2.84
13C
Chemical Shift

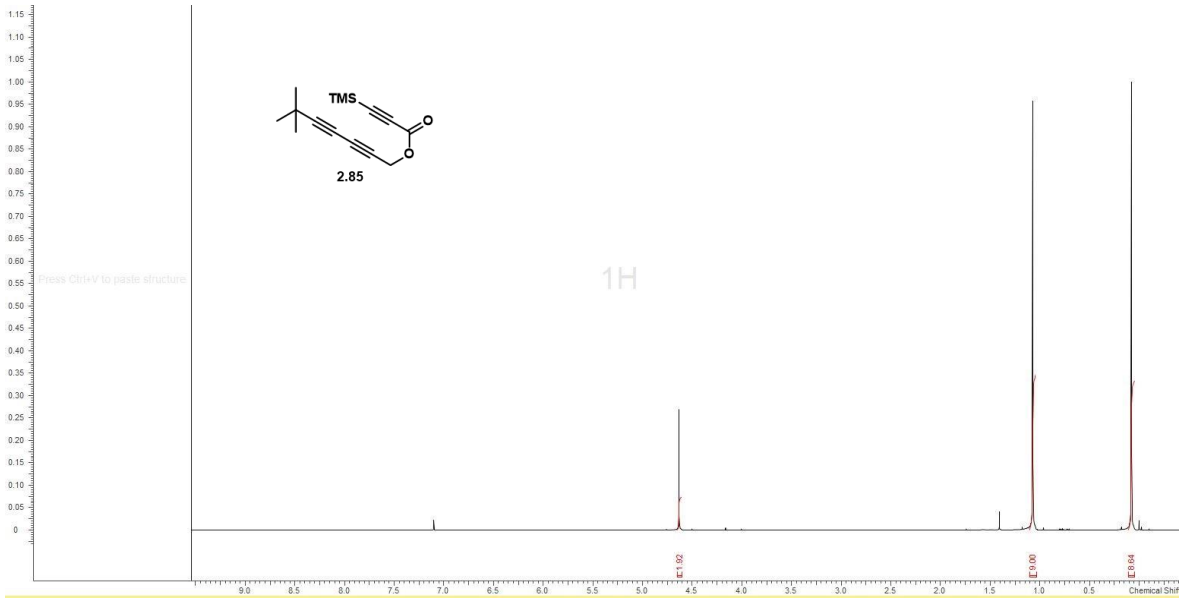
TMS
O
O
2.85
1H
1.92
9.00
8.64
Chemical Shif

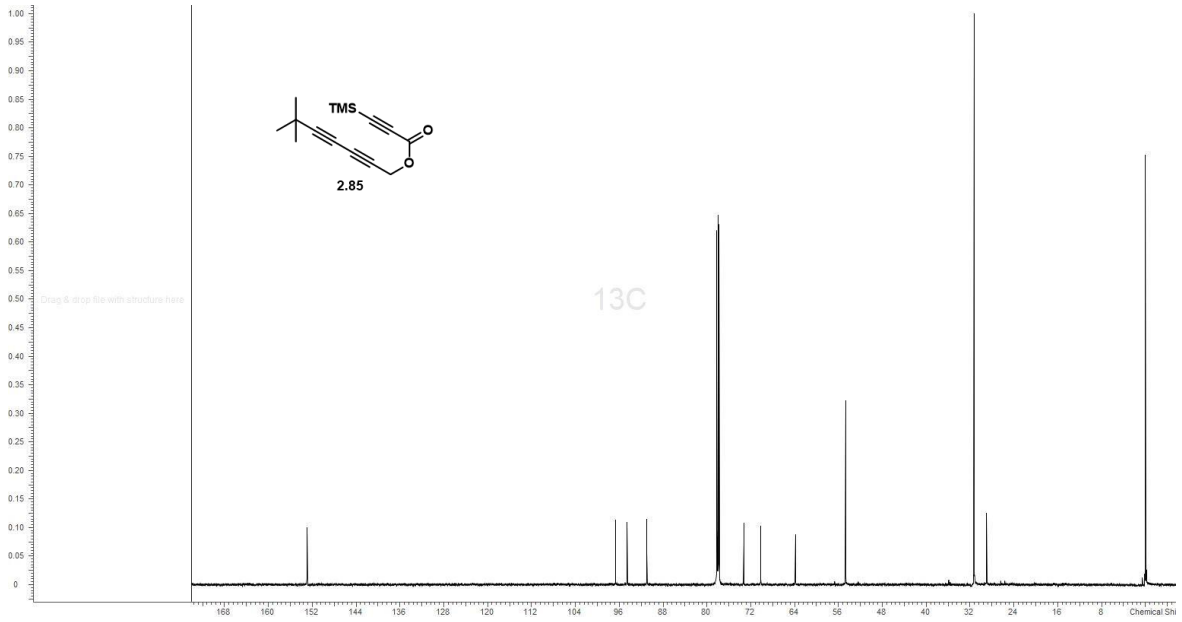
TMS
2.85
13C

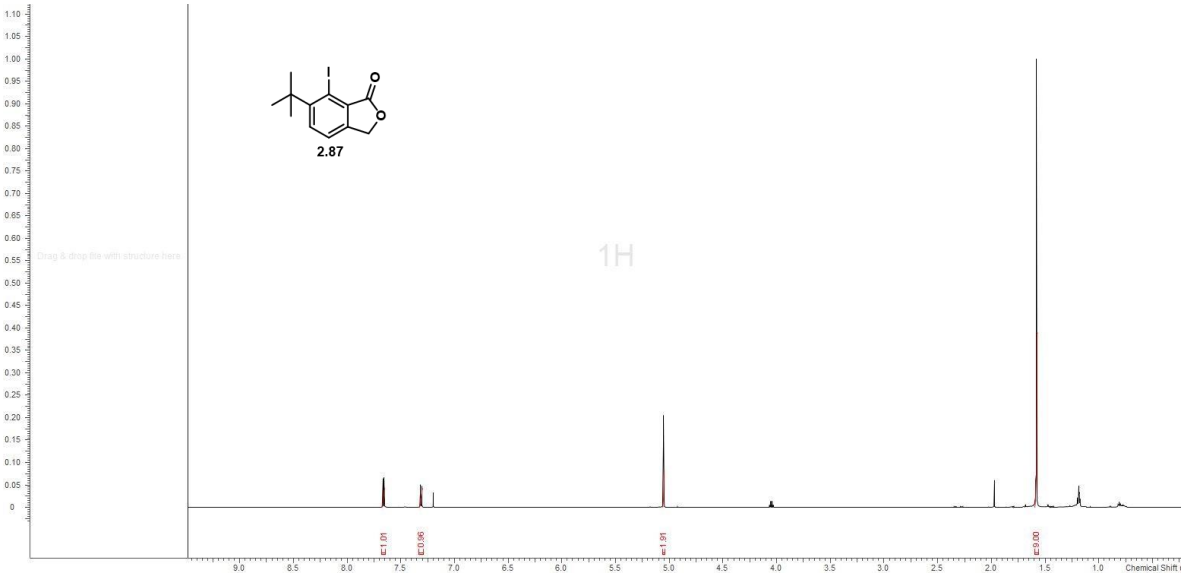
2.87
1H

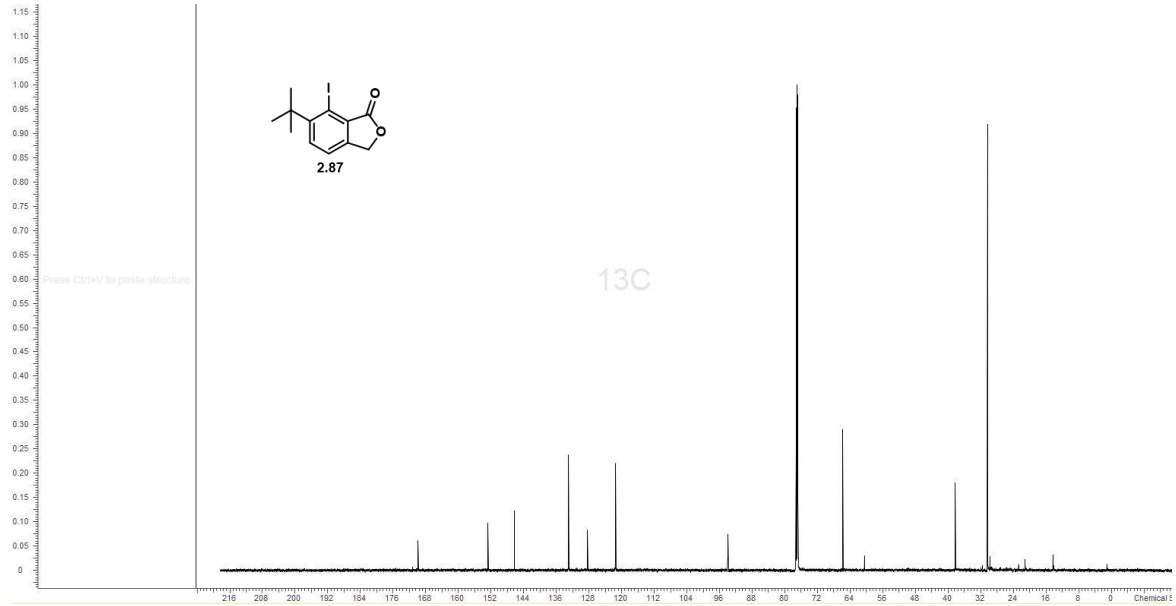
2.87
13C
Chemical S

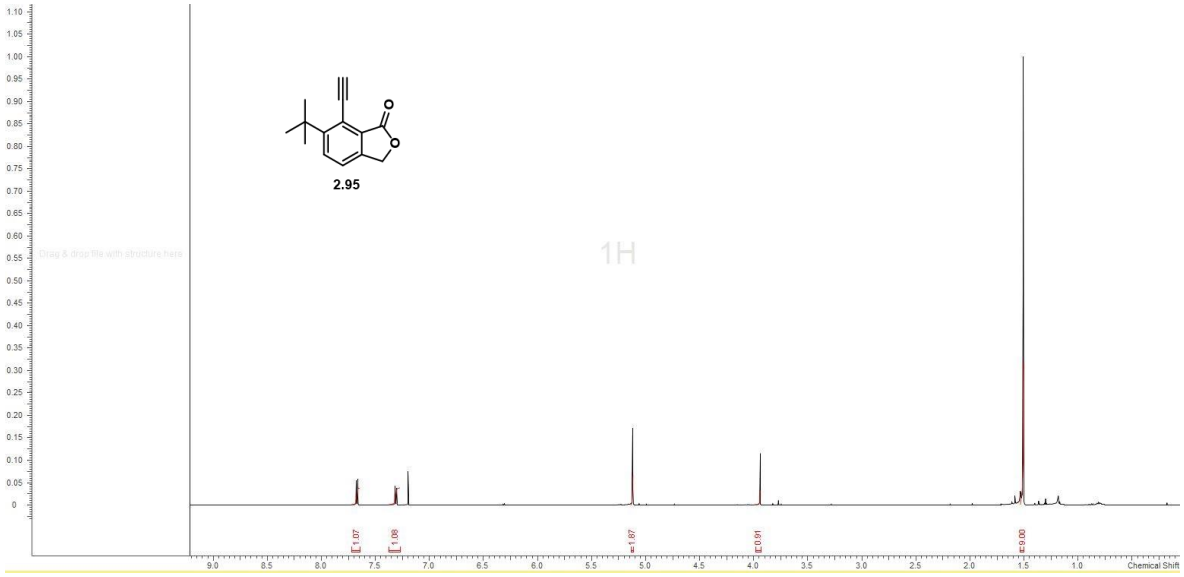
2.95
1H
1.07
1.08
1.97
0.91
3.00
Chemical Shift

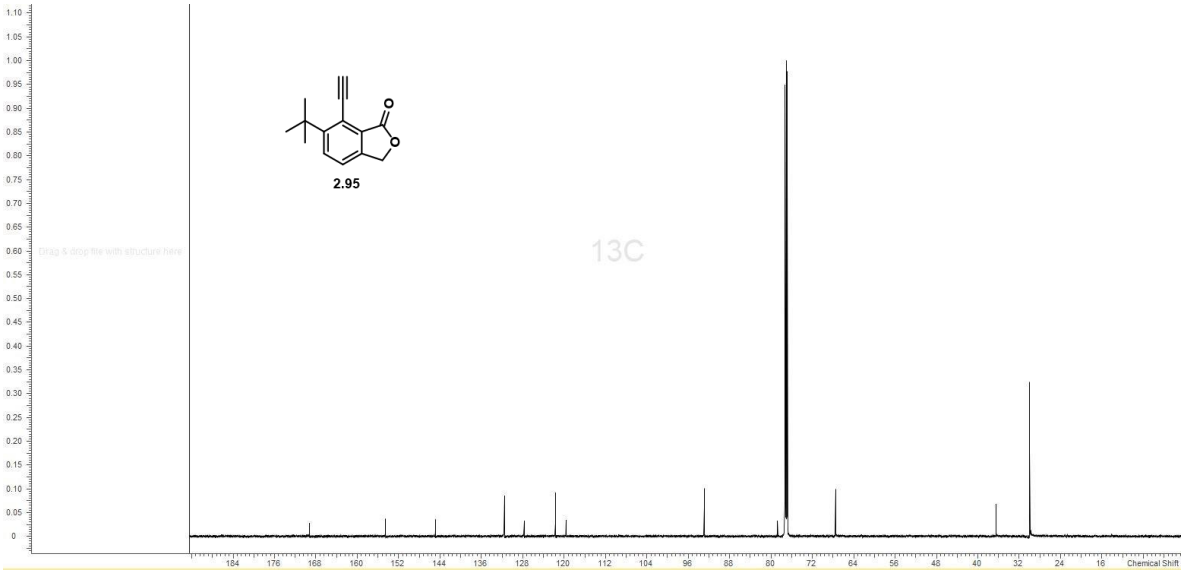
2.95
13C
Chemical Shift

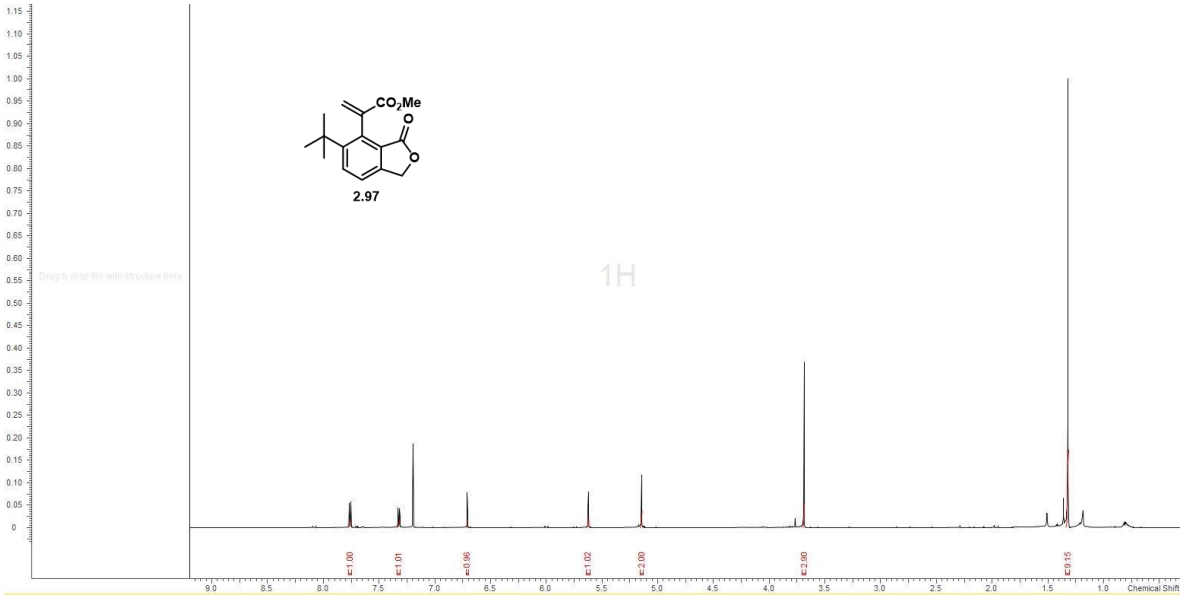
CO2Me
2.97
1H
Chemical Shift

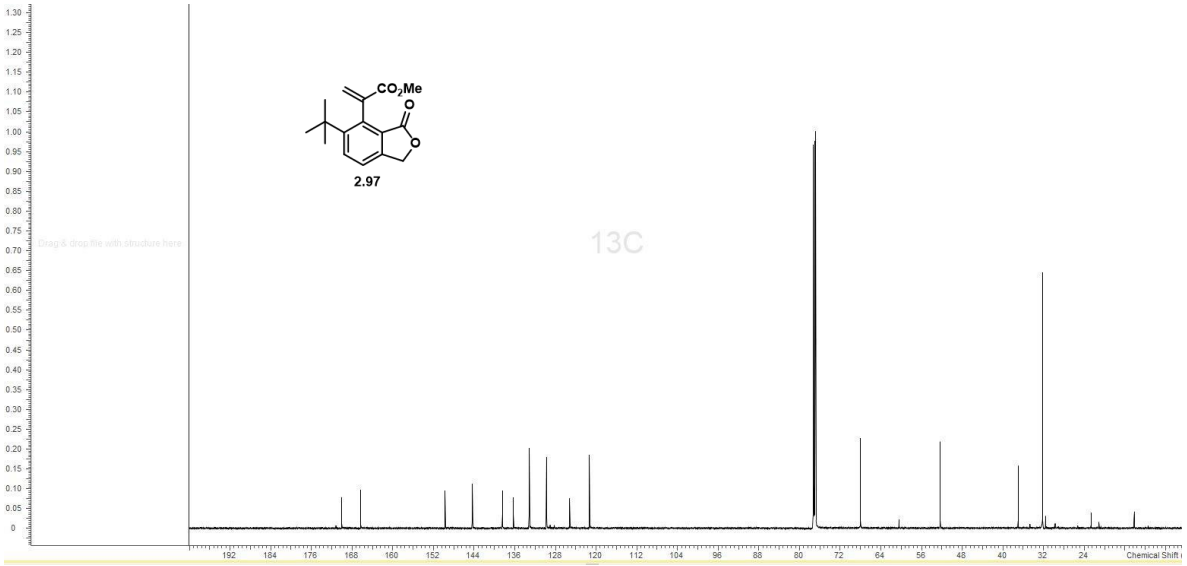
CO2Me
O
O
2.97
13C
Chemical Shift

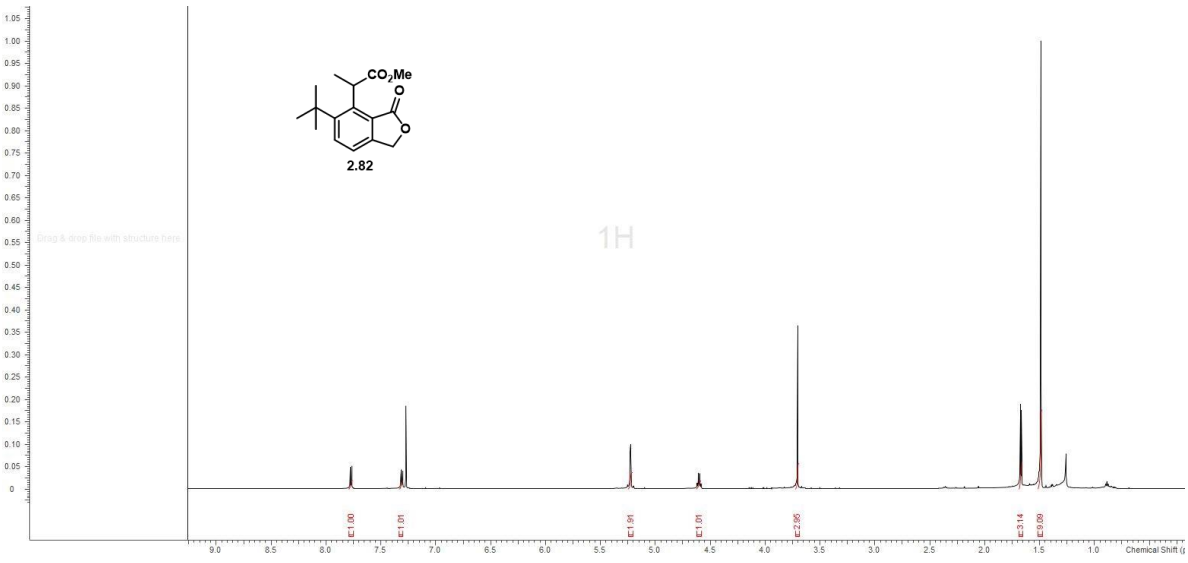
CO2Me
O
O
2.82
1H
I:1.00
I:1.01
I:1.91
I:1.01
I:2.95
I:3.14
I:9.09
Chemical Shift

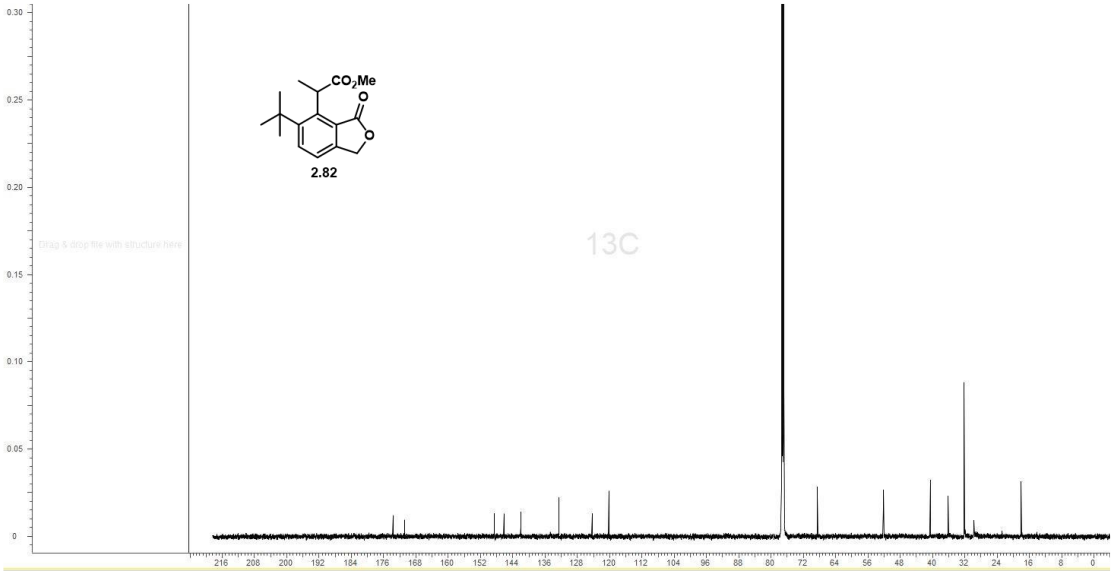
CO2Me
O
O
2.82
13C

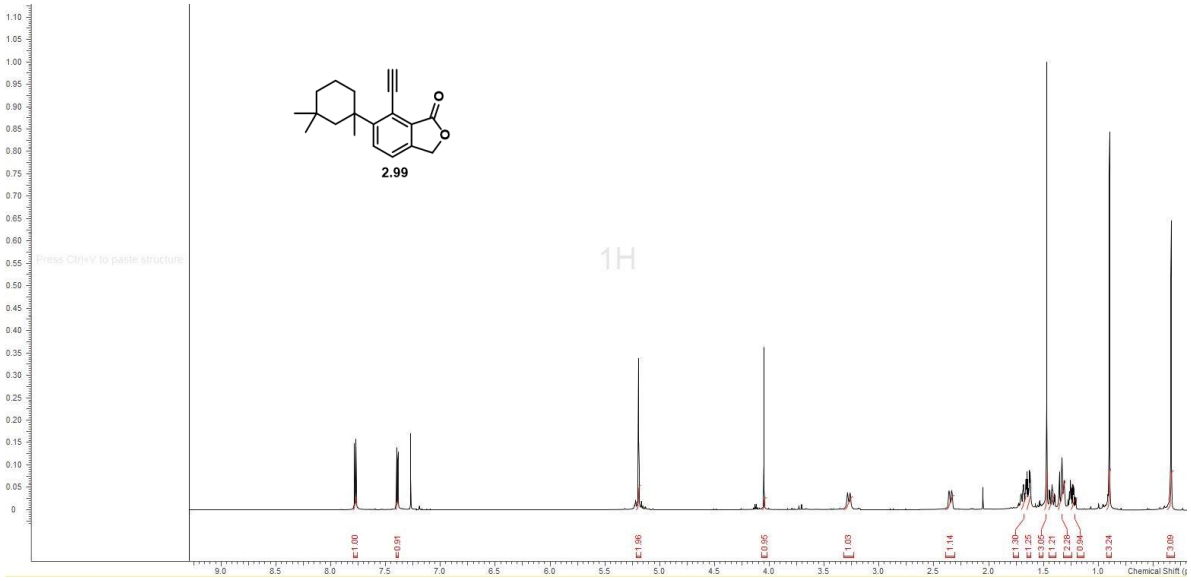
O
O
2.99
1H
Chemical Shift (p

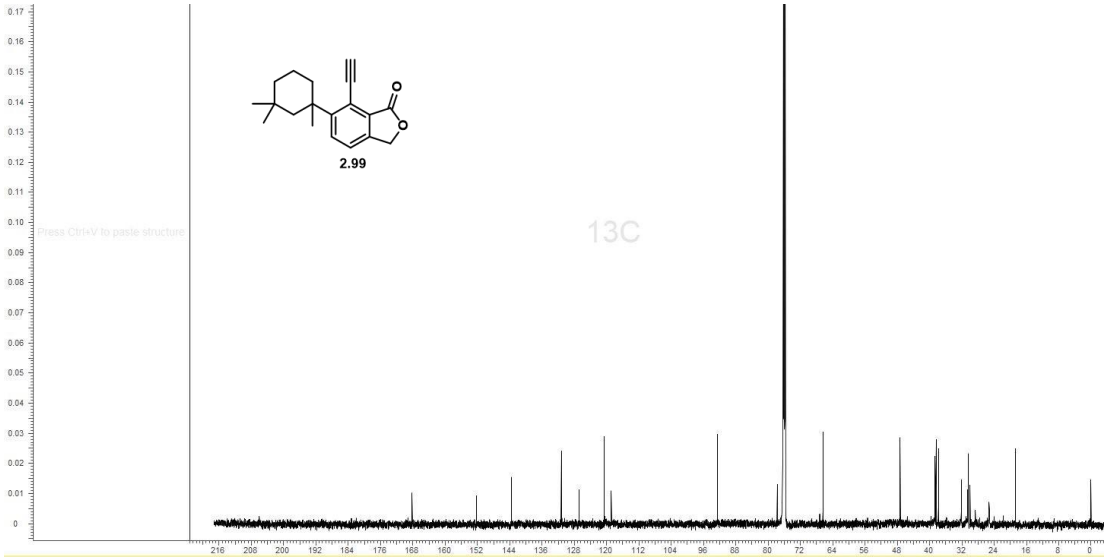
2.99
13C

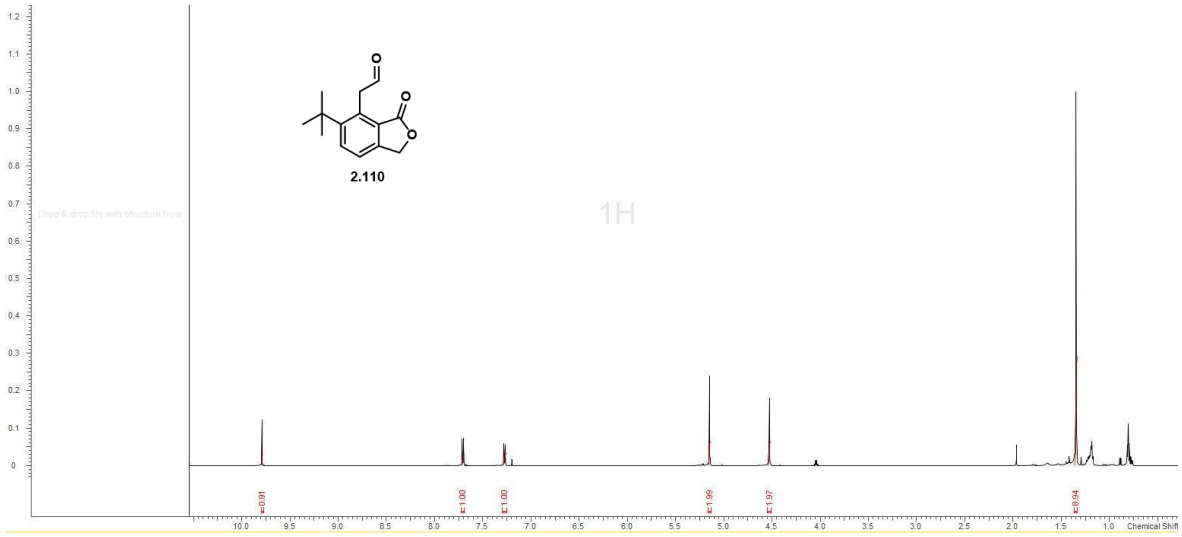
2.110
1H
Chemical Shift

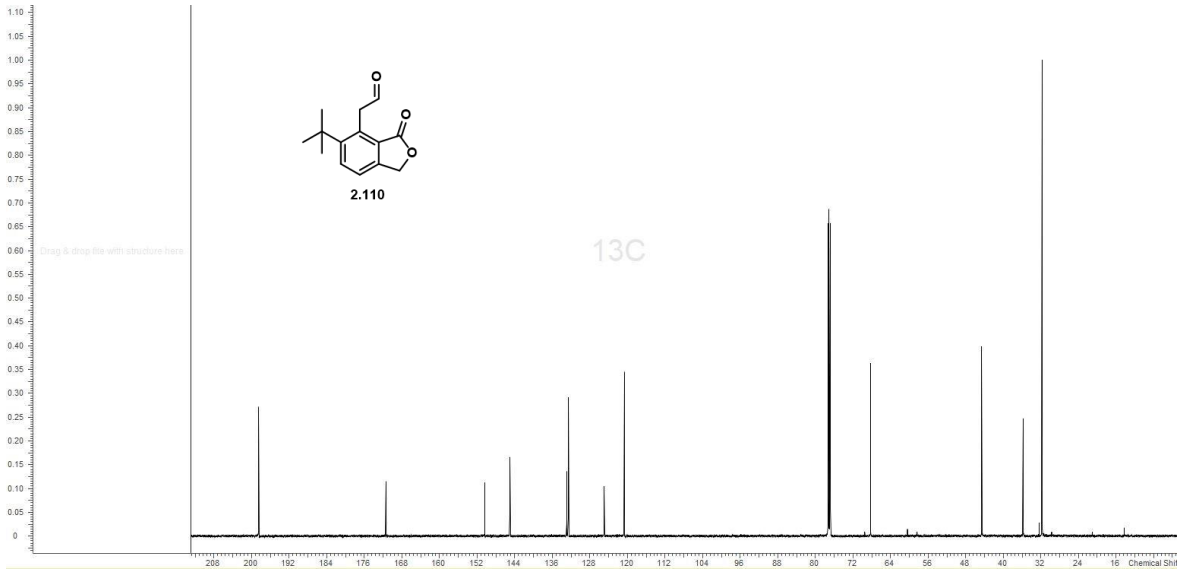
2.110
13C
Drag & drop file with structure here
Chemical Shift

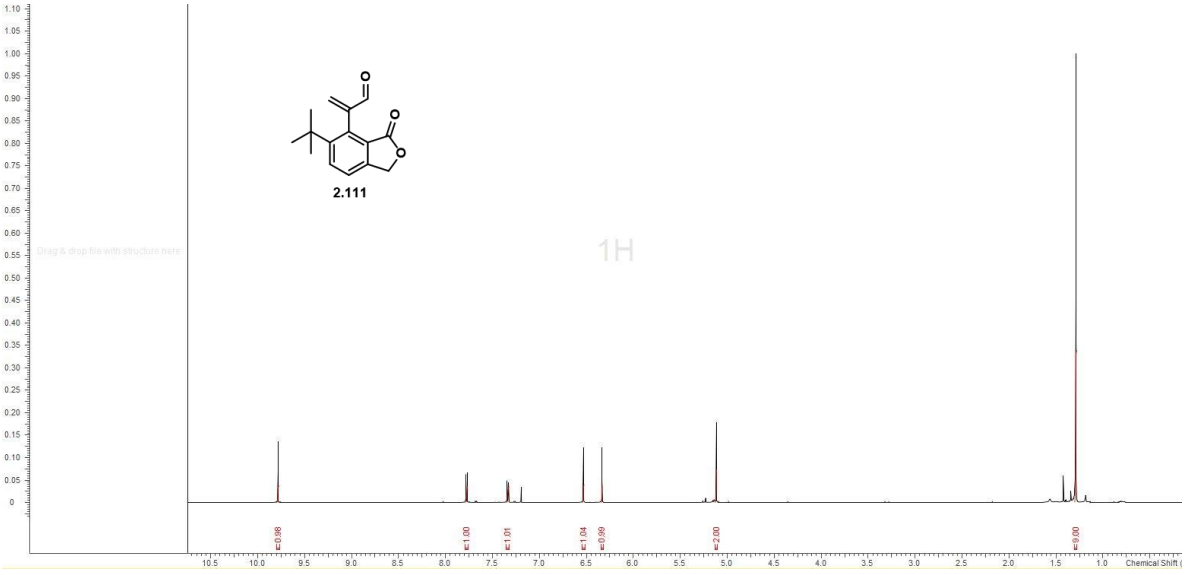
2.111
1H
Drag & drop file with structure here
Chemical Shift

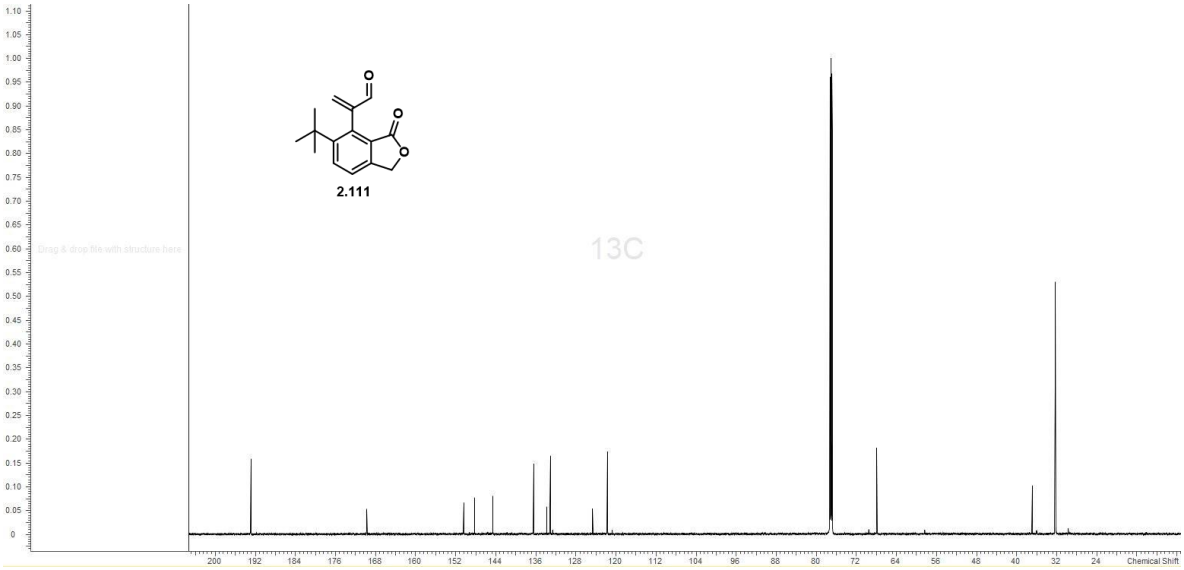
2.111
13C
Chemical Shift

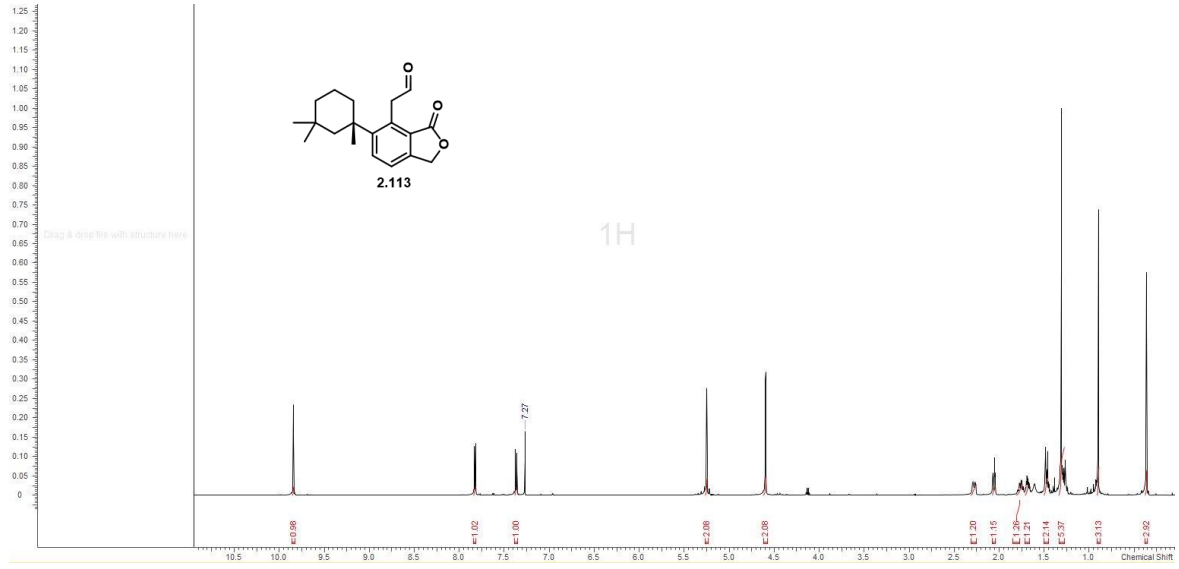
2.113
1H
7.27
Chemical Shift

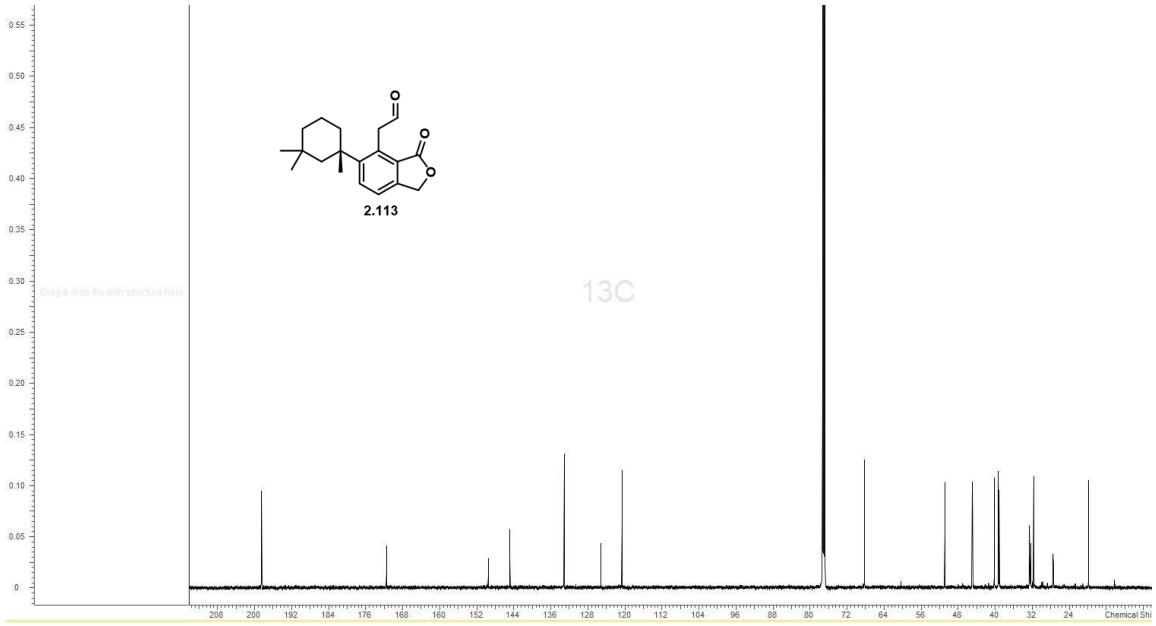
2.113
13C
Drag & drop file with structure here
Chemical Shi

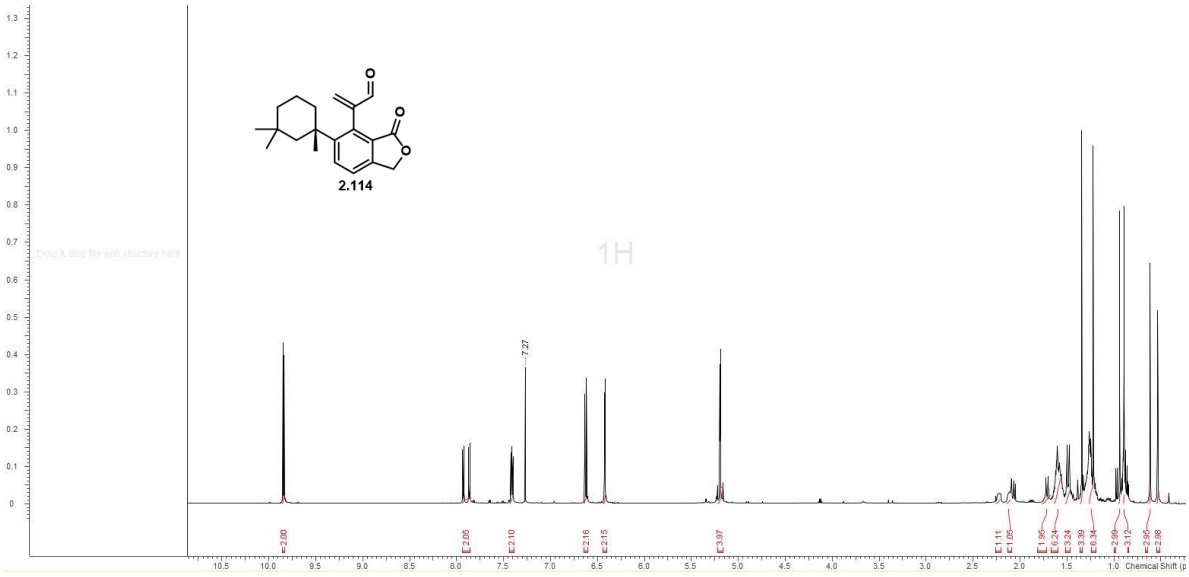
2.114
1H
Drag & drop file with structure here
7.27
Chemical Shift (p

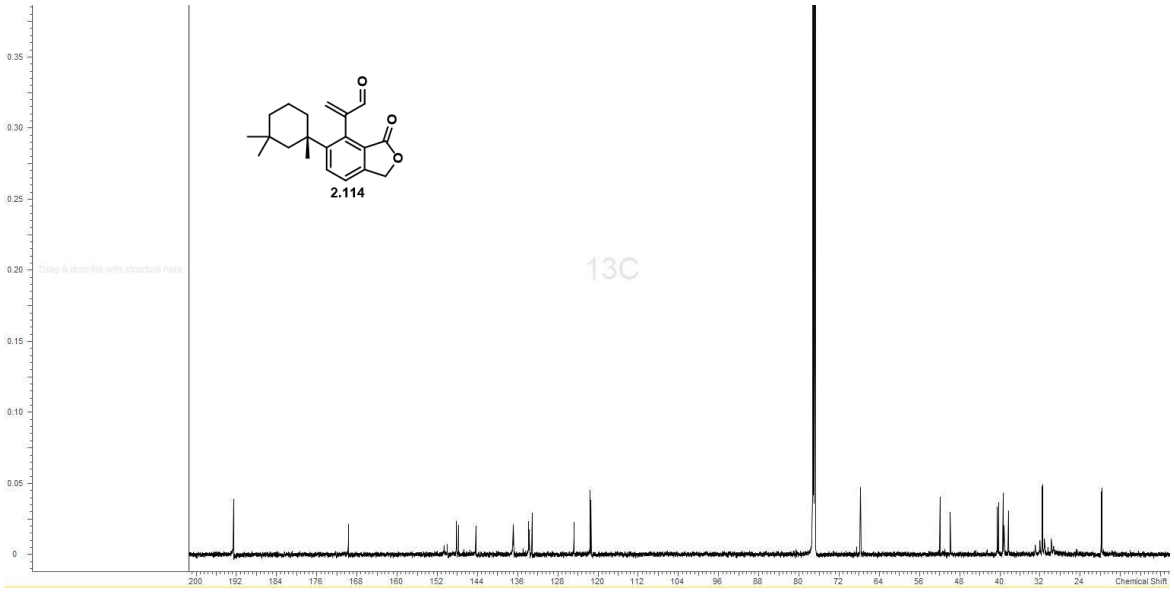
2.114
13C
Chemical Shift

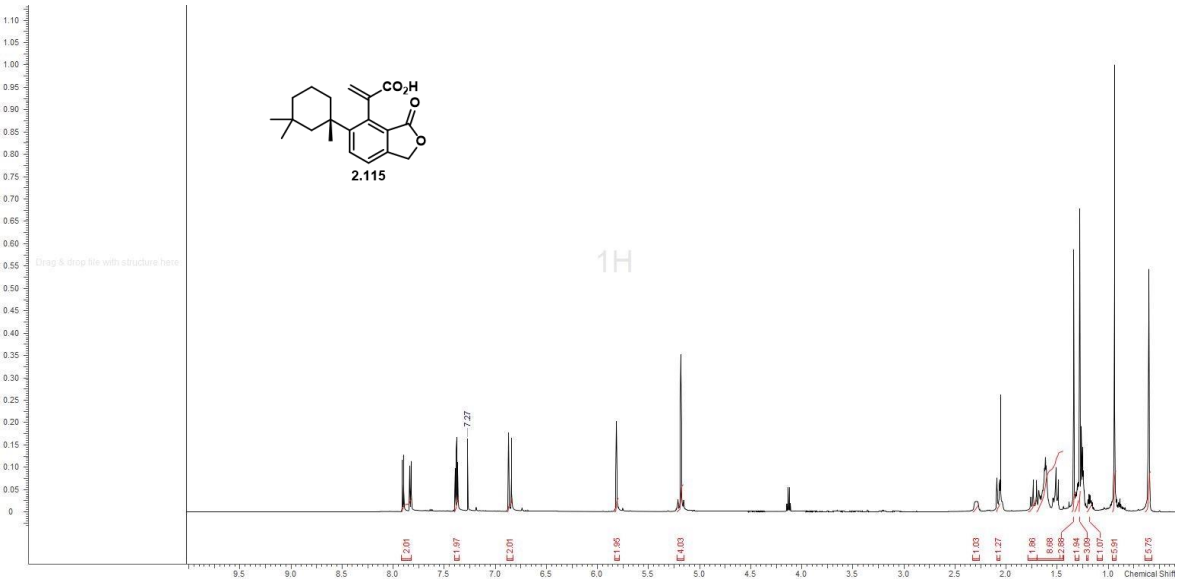
2.115
1H
7.27
Chemical Shift

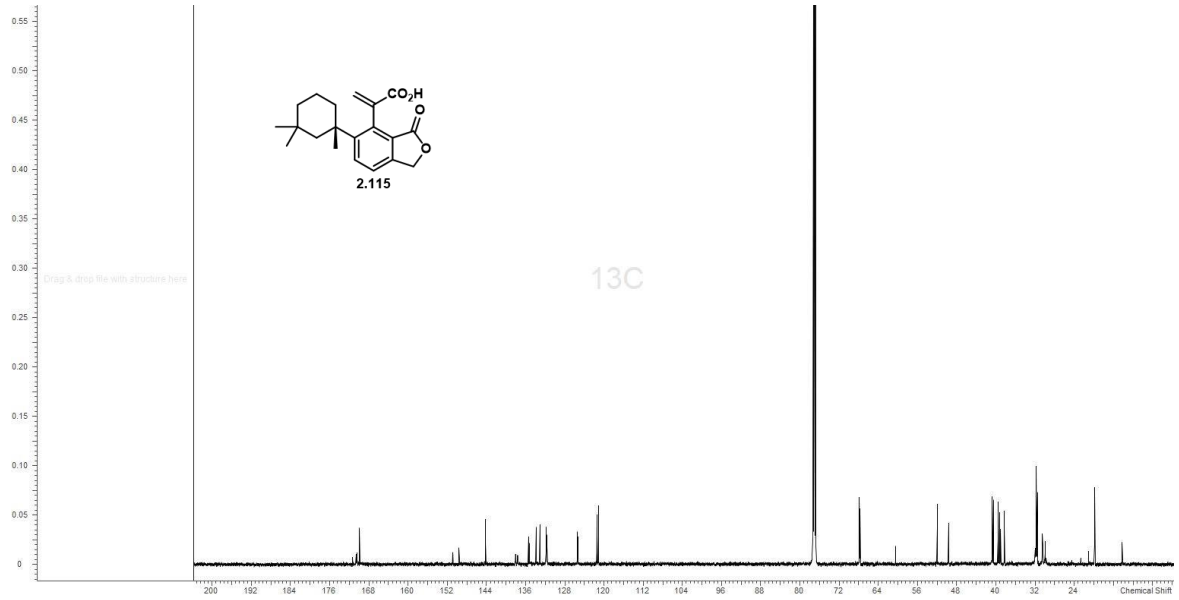
CO2H
O
O
2.115
13C
Chemical Shift

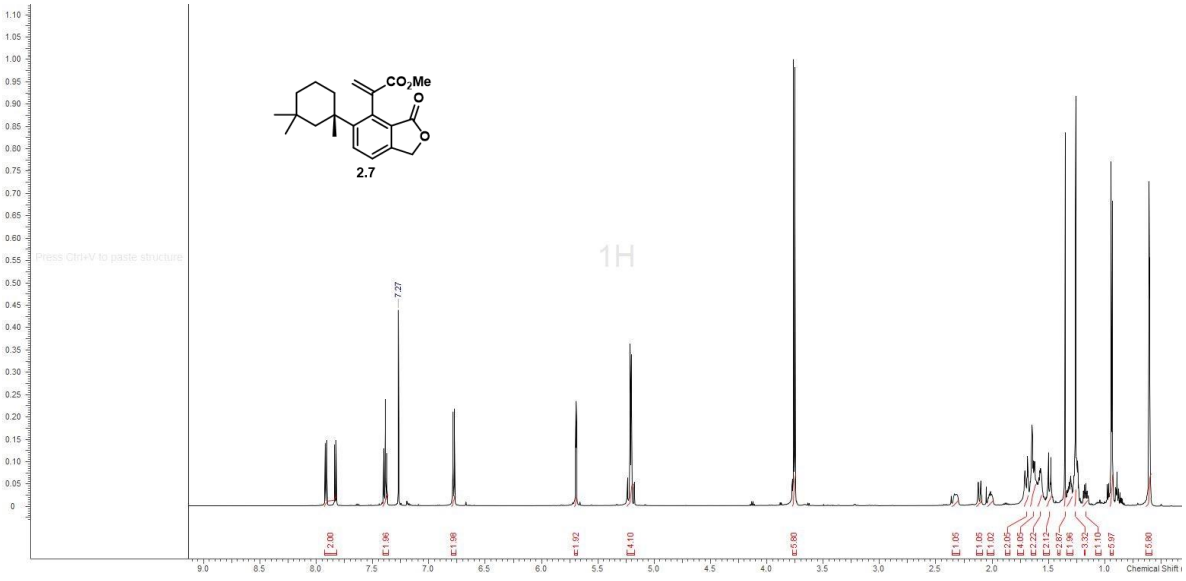
CO2Me
O
O
2.7
1H
7.27
Chemical Shift

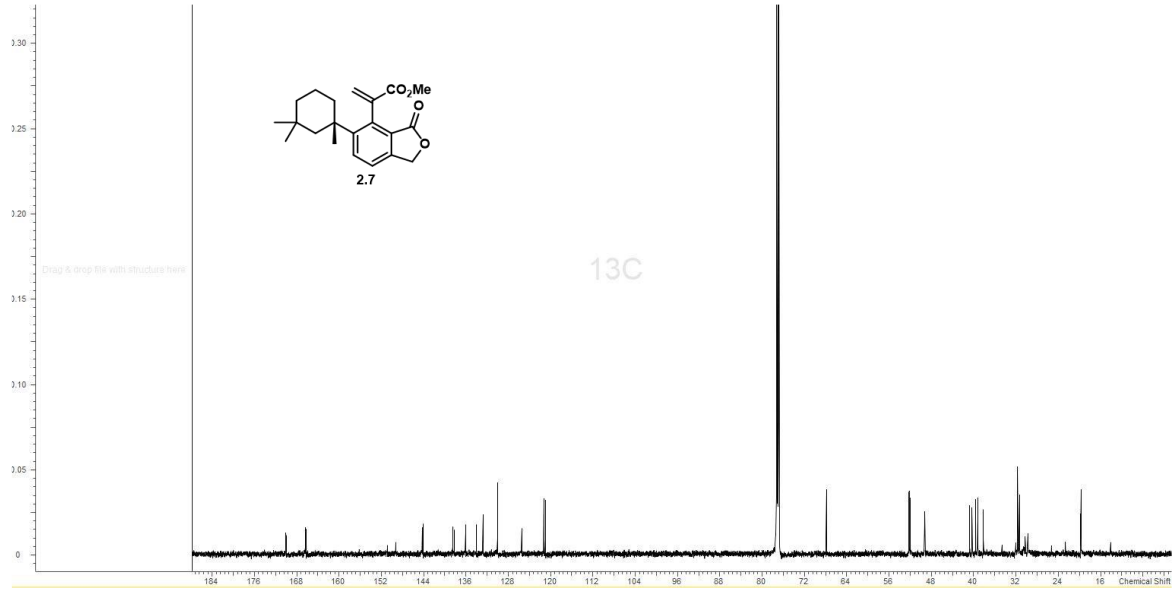
CO2Me
O
O
2.7
13C
Chemical Shift

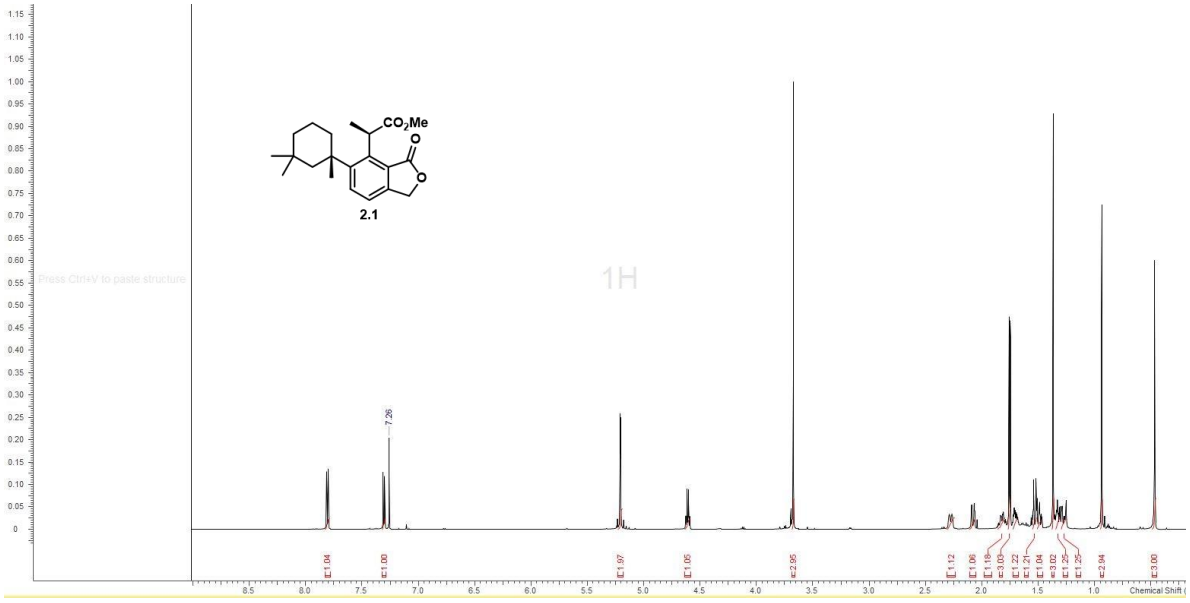
CO2Me
O
O
2.1
1H
7.26
Chemical Shift

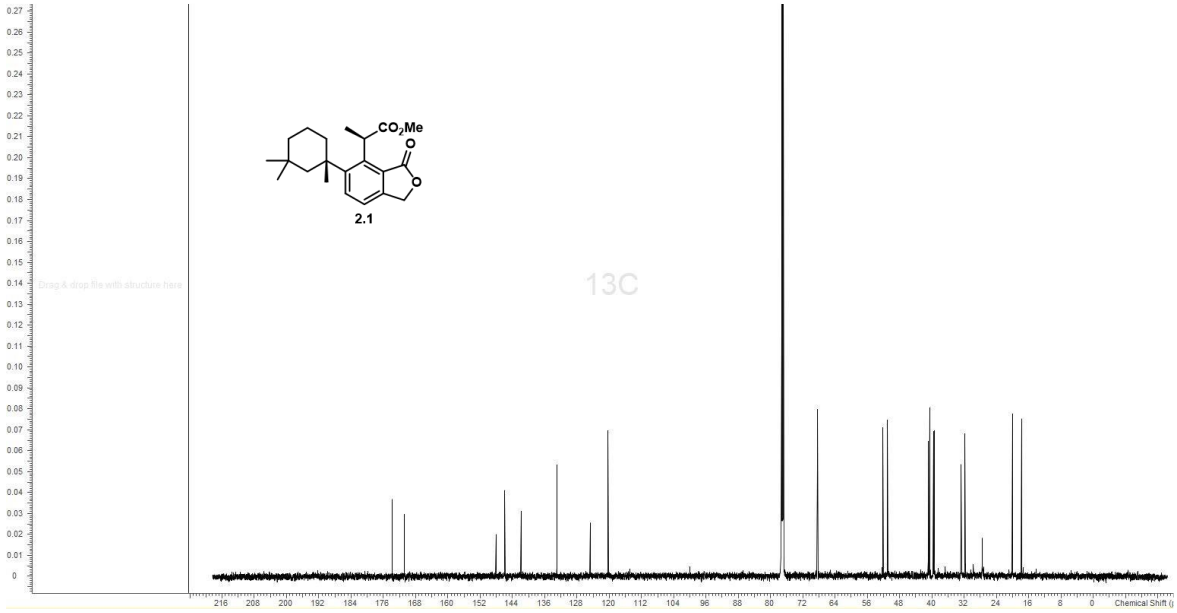
CO2Me
O
O
2.1
13C
Chemical Shift (

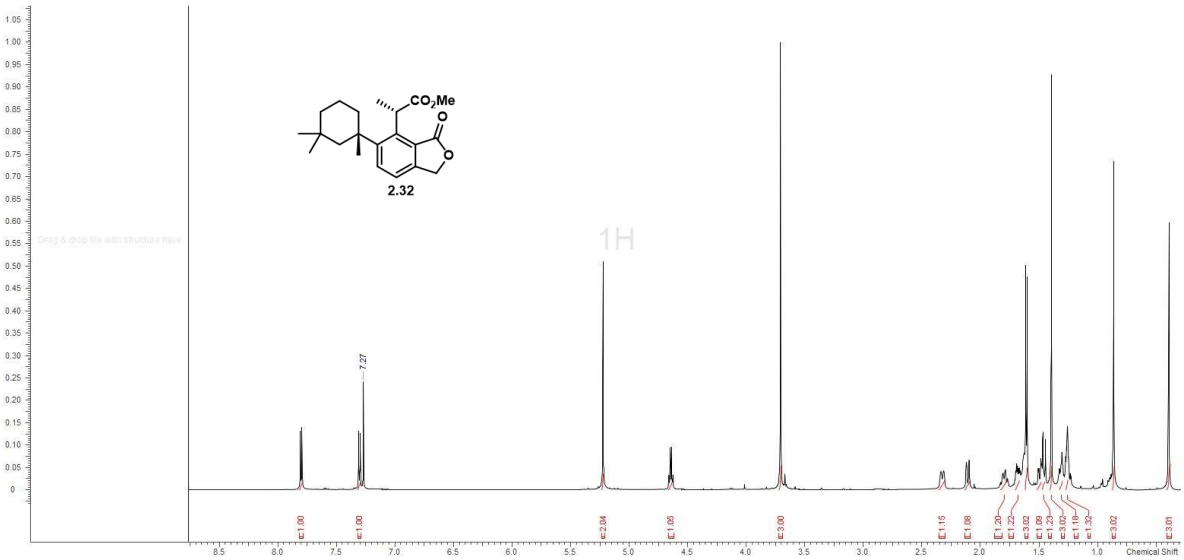
CO2Me
O
O
2.32
1H
7.27
Chemical Shift

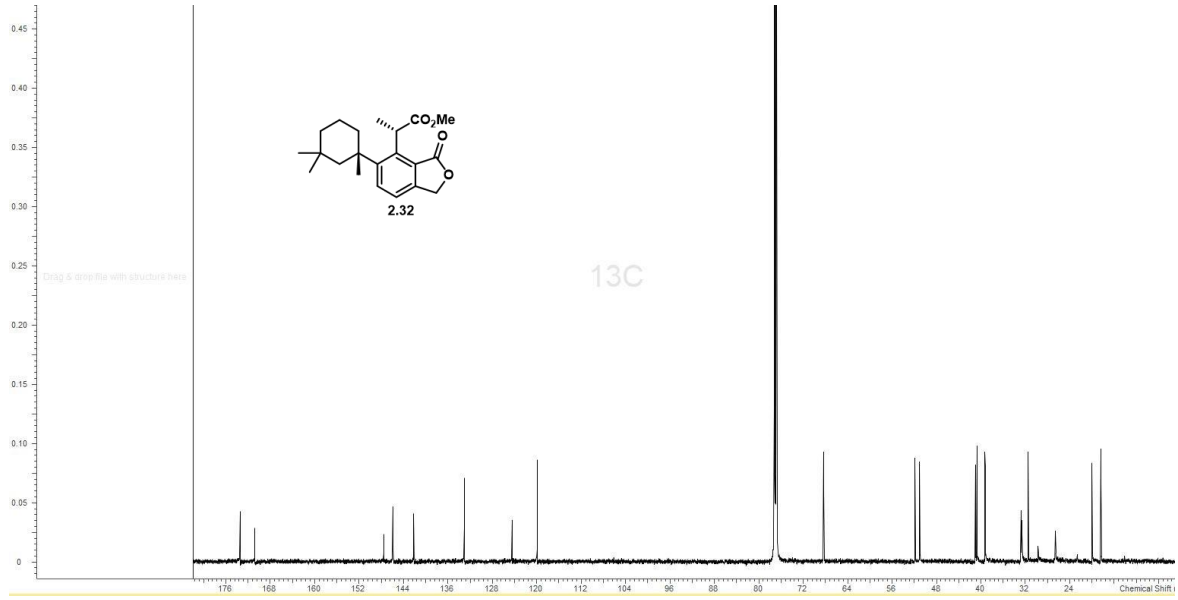
CO2Me
O
O
2.32
13C
Chemical Shift

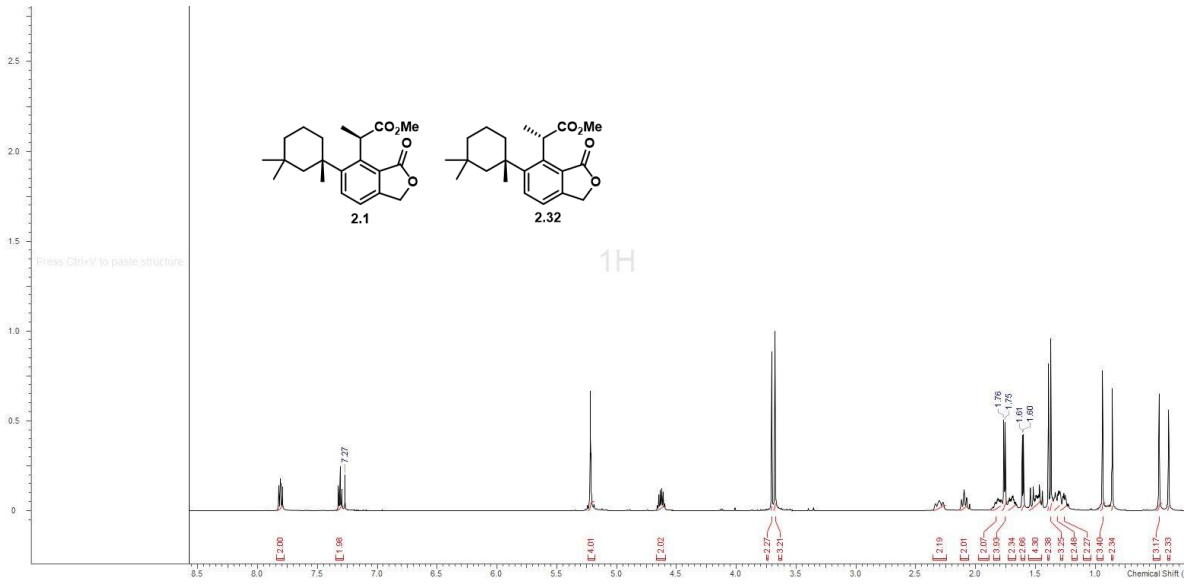
CO2Me
O
O
2.1
CO2Me
O
O
2.32
1H
7.27
1.76
1.75
1.61
1.60
2.00
1.98
4.01
2.02
2.27
3.21
2.19
2.01
2.07
3.95
2.34
2.66
4.30
2.38
3.25
2.48
2.27
3.40
2.34
3.17
2.33
Chemical Shift (

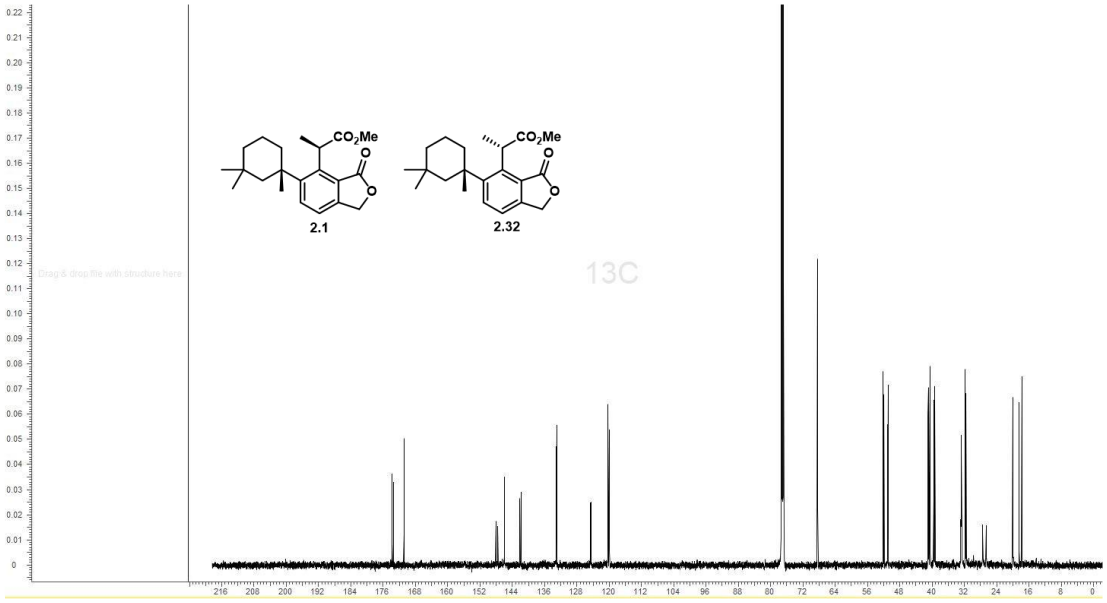
CO2Me
O
O
2.1
CO2Me
O
O
2.32
13C

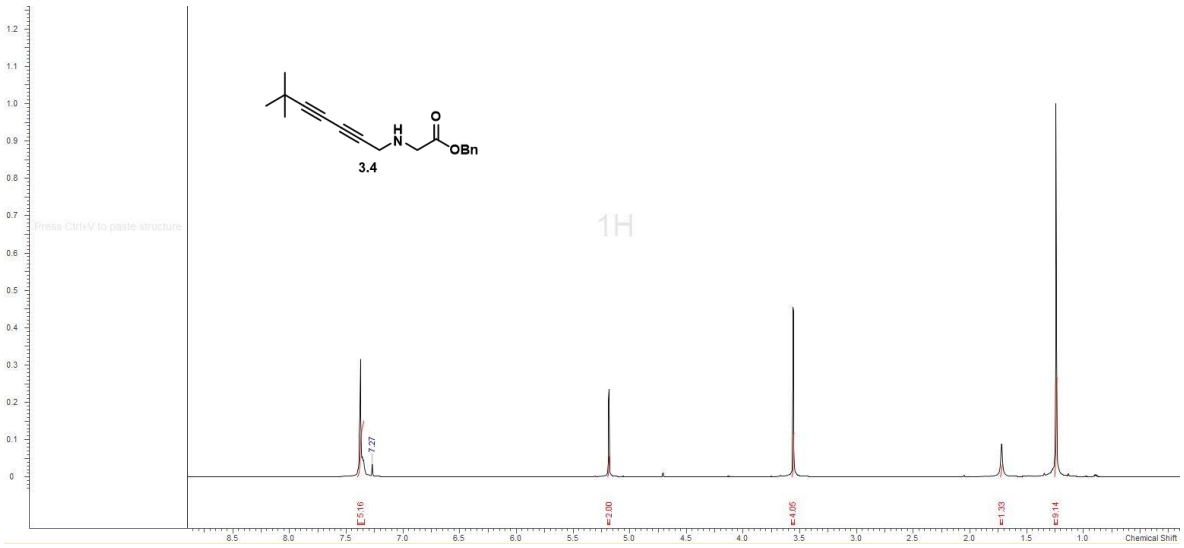
3.4
1H
Chemical Shift

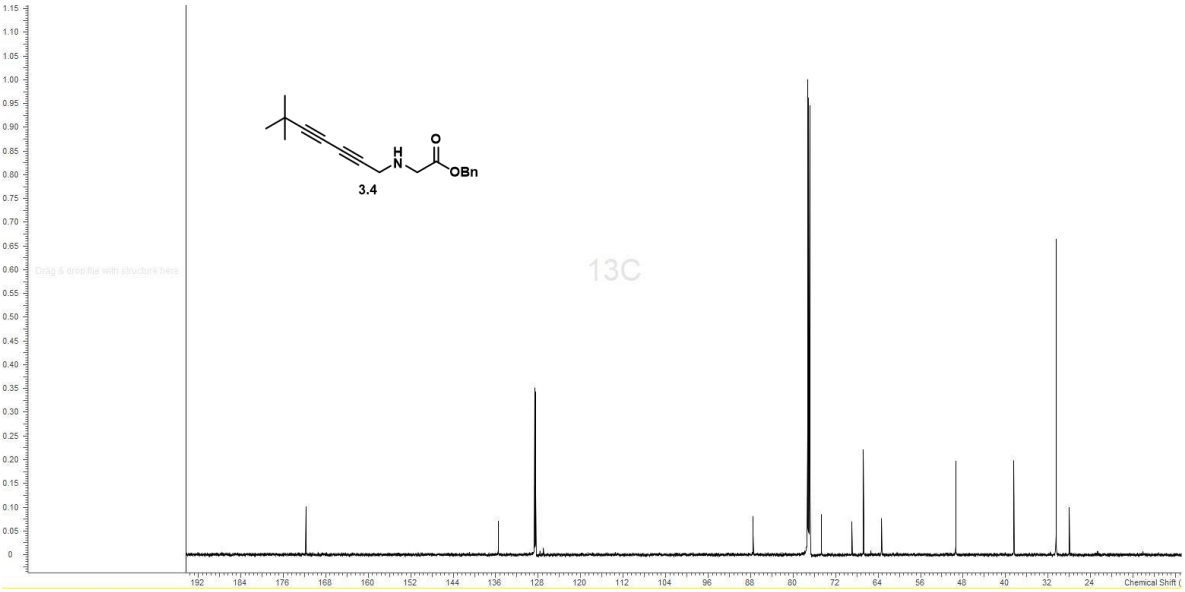
3.4
13C
Chemical Shift

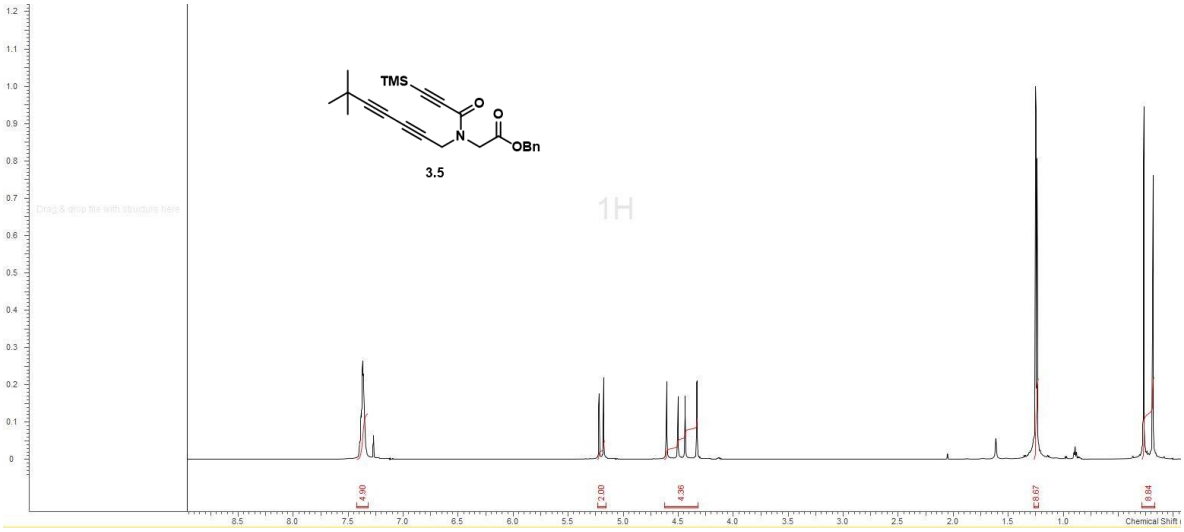
TMS
O
O
N
OBn
3.5
1H
4.90
2.00
4.36
6.67
6.84
Chemical Shift

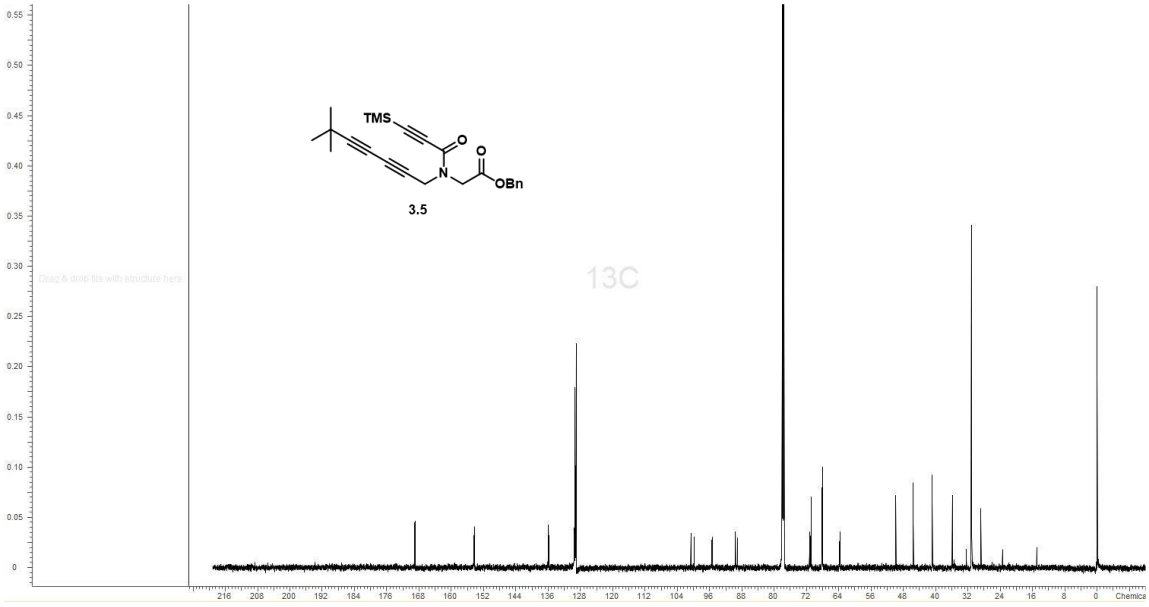
TMS
O
O
N
OBn
3.5
13C

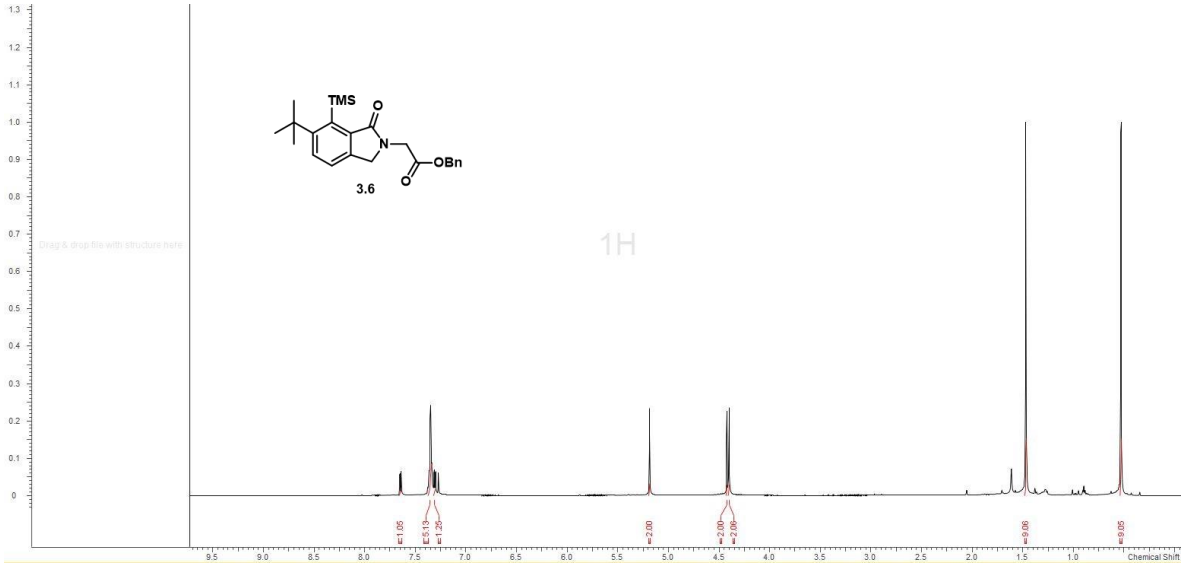
TMS
O
N
OBn
O
3.6
1H
Chemical Shift

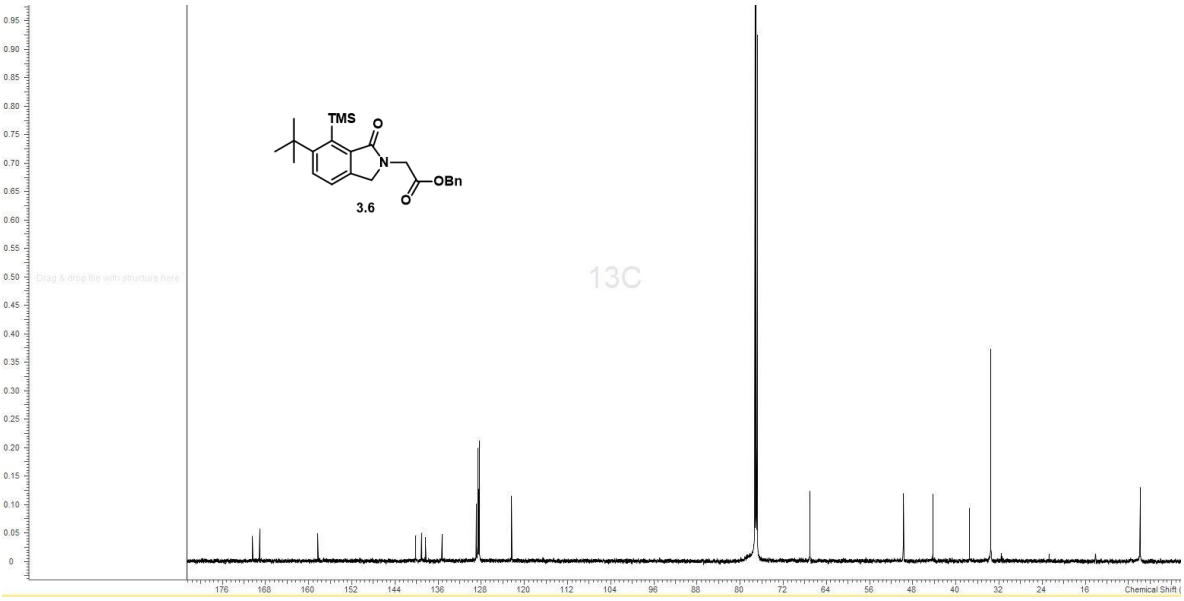
TMS
O
N
OBn
O
3.6
13C
Chemical Shift

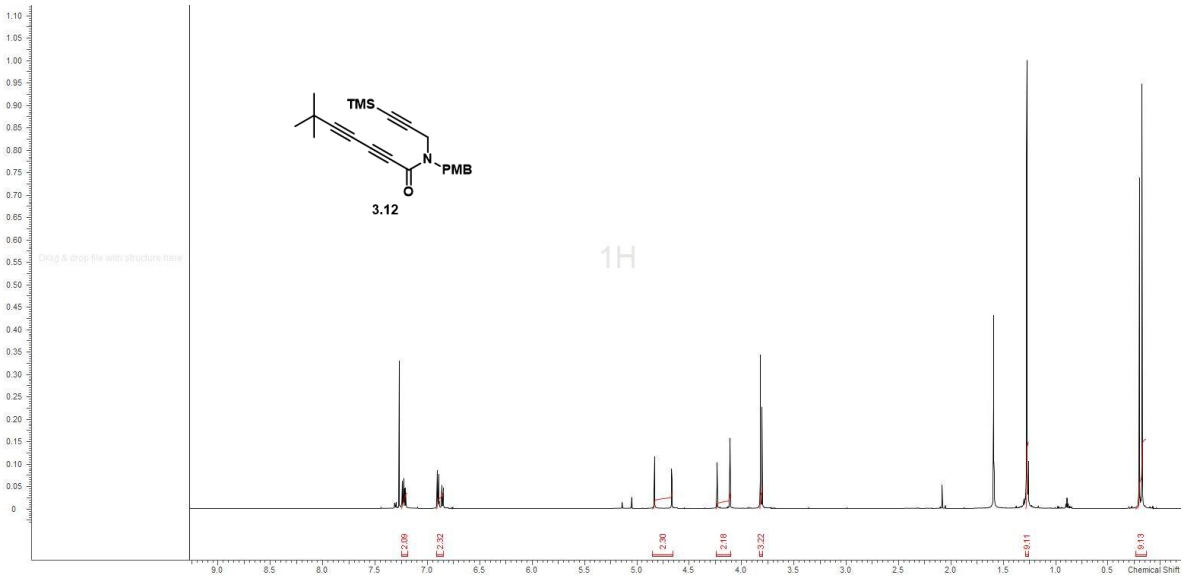
TMS
N
PMB
O
3.12
1H
2.09
2.32
2.30
2.16
3.22
9.11
9.13
Chemical Shift

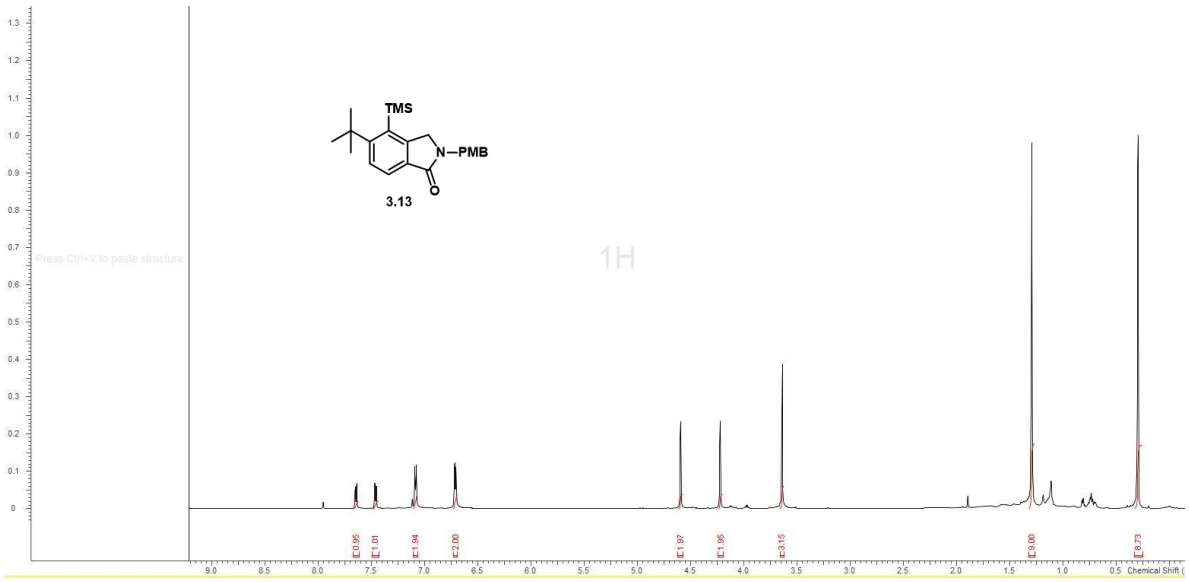
TMS
N—PMB
O
3.13
1H
Press Ctrl+V to paste structure
0.95
1.01
1.94
2.00
1.97
1.95
3.15
9.00
8.73
Chemical Shift

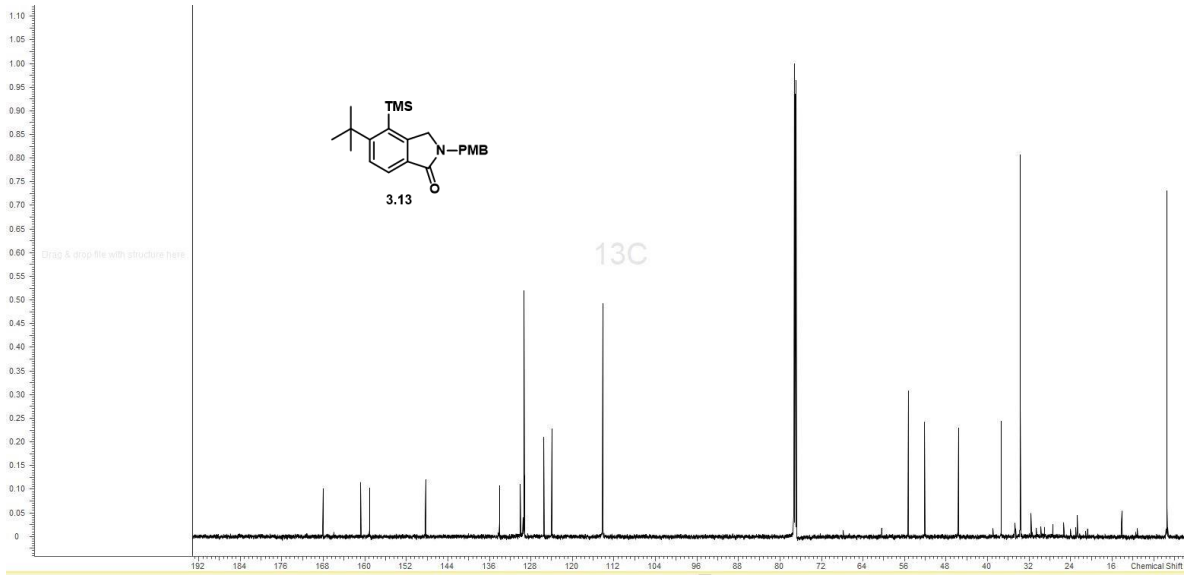
TMS
N—PMB
O
3.13
13C
Drag & drop file with structure here
Chemical Shift

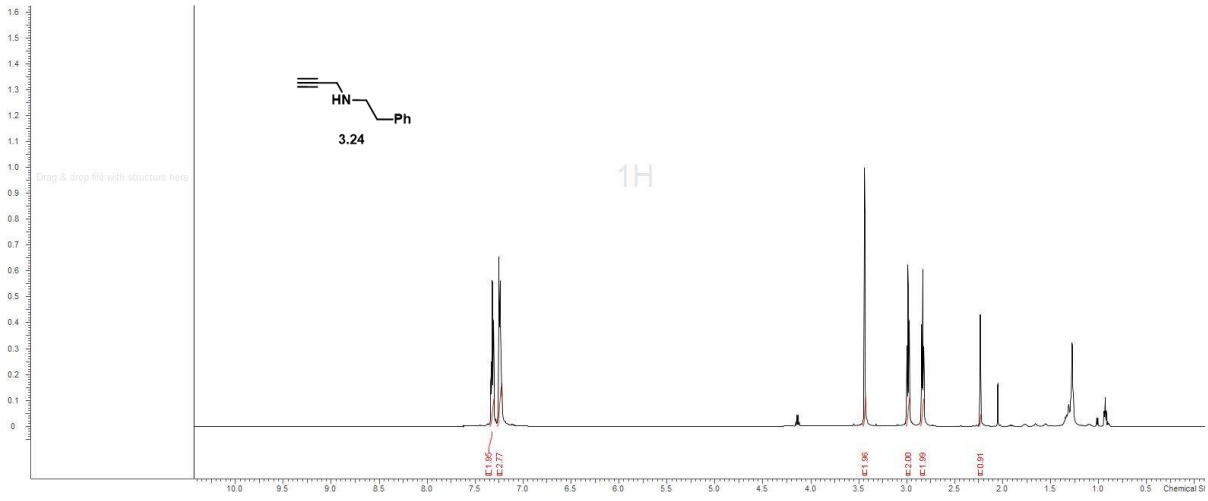
HN
Ph
3.24
1H
Drag & drop file with structure here
1.95
2.77
1.96
2.00
1.99
0.91

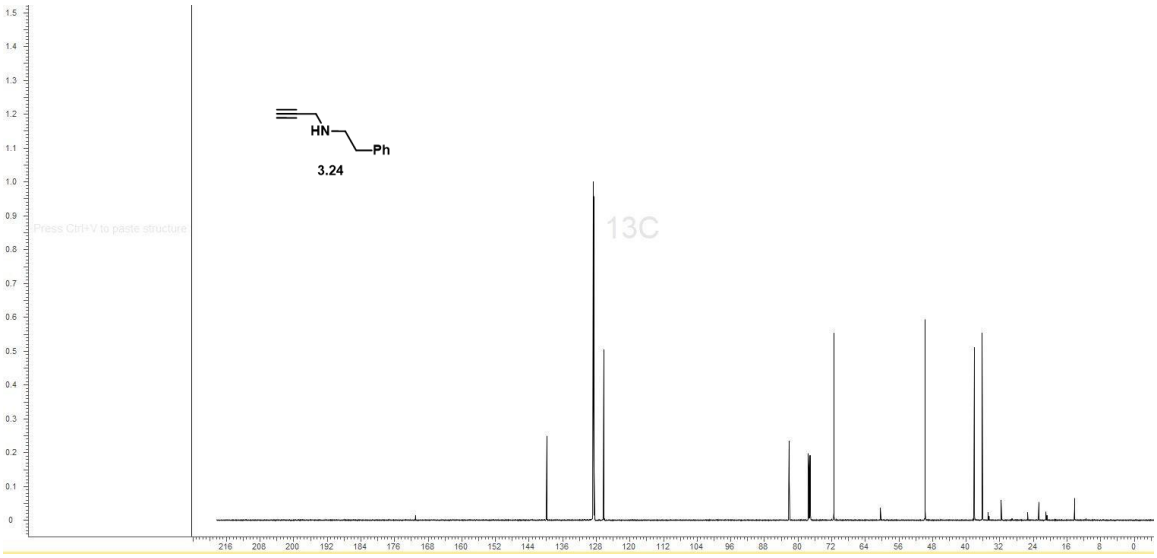
HN
Ph
3.24
13C
Press Ctrl+V to paste structure


TMS
N
Ph
O
3.16
1H

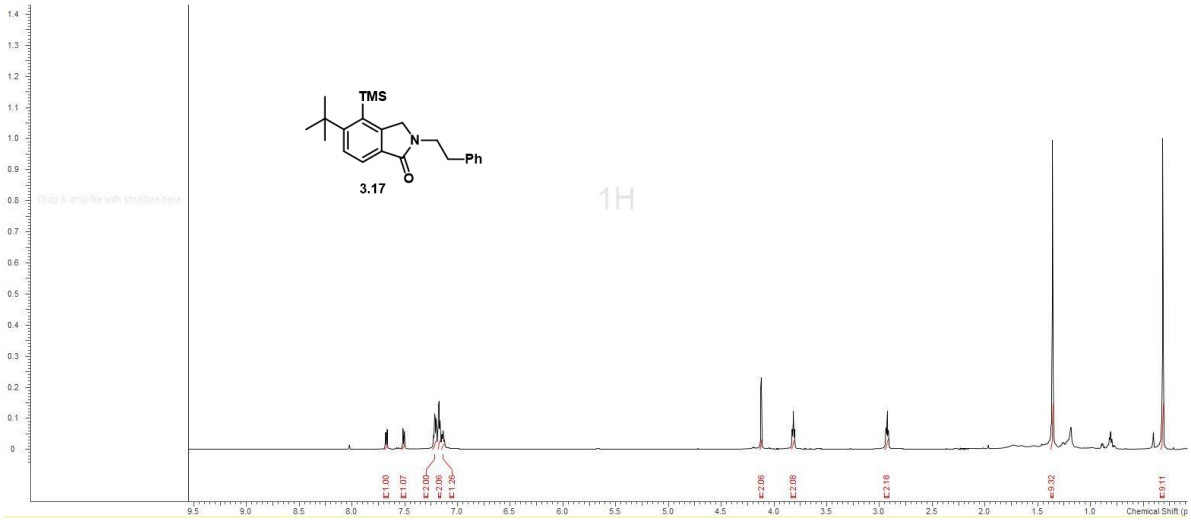
TMS
N
Ph
O
3.17
1H

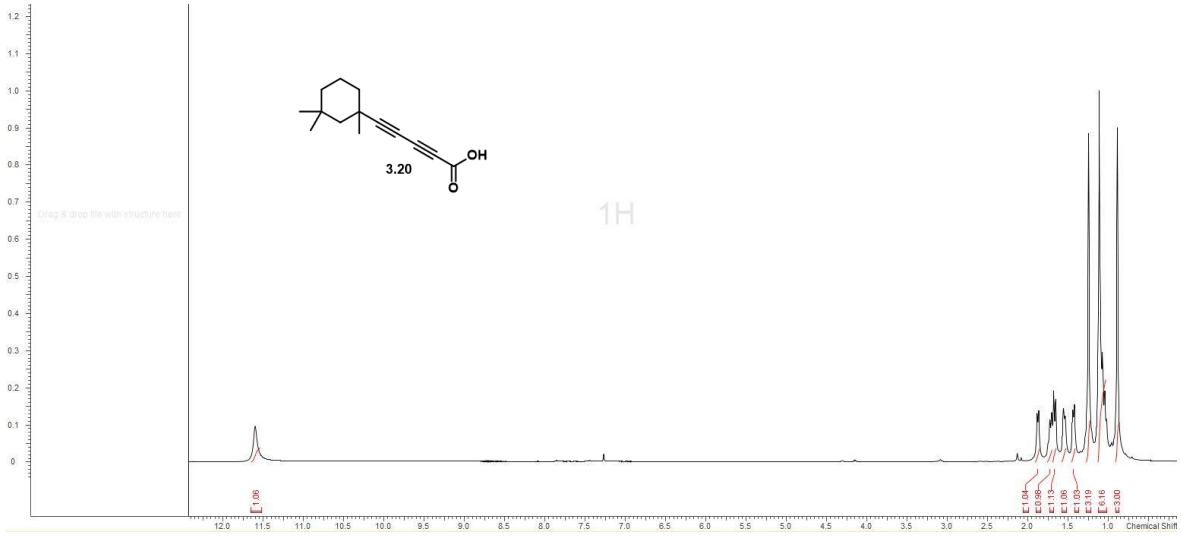
3.20
OH
O
1H
Chemical Shift

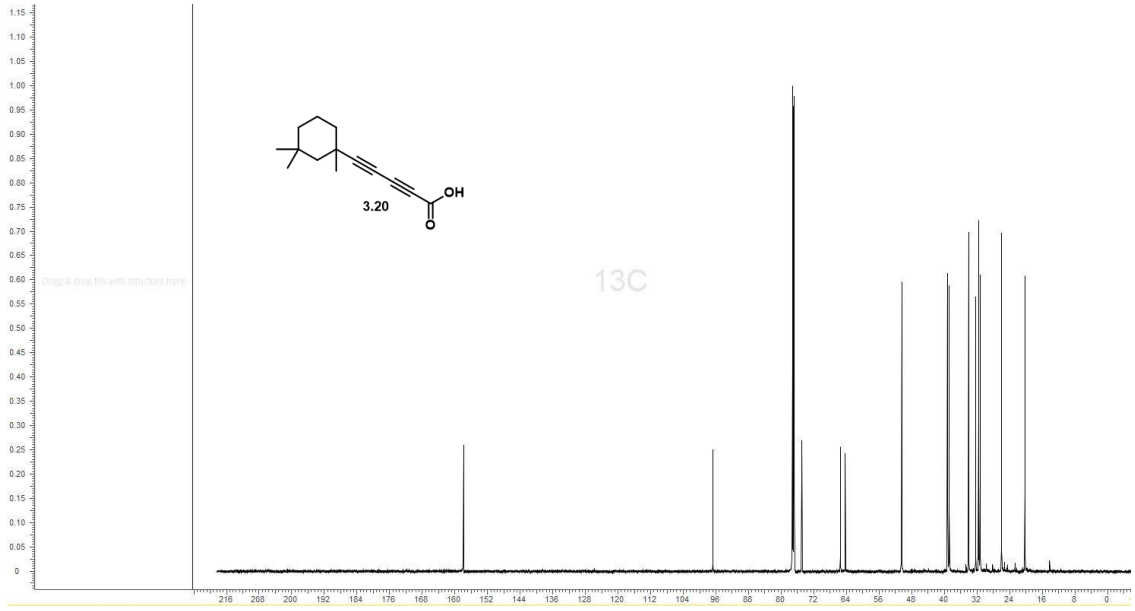
3.20
OH
O
13C

Appendix 3: Chiral GC/MS Chromatogram of 2.8

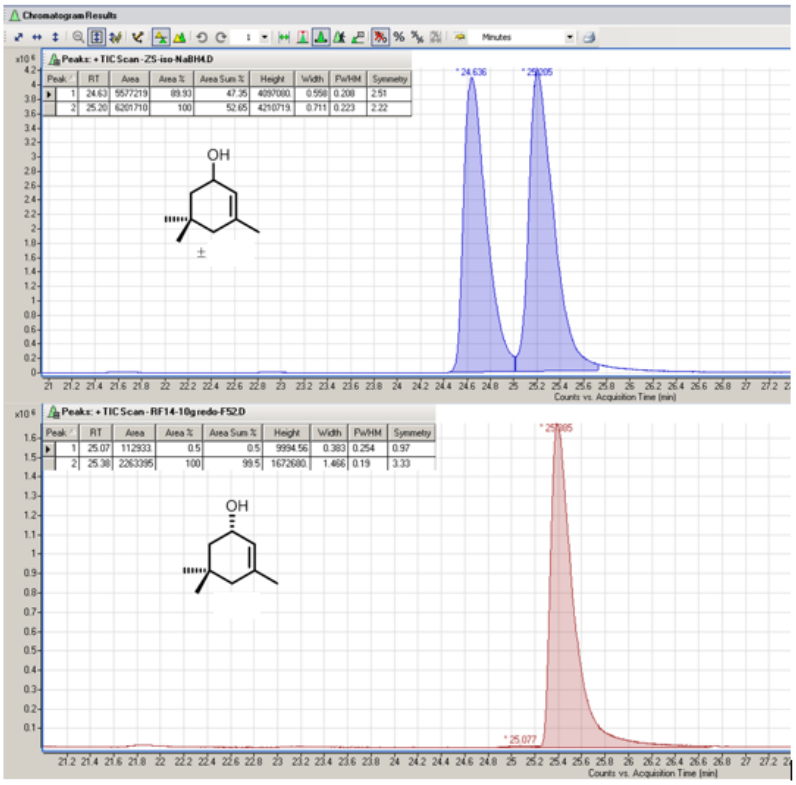

Appendix 4: Copyright Permissions

Open Access Review

A Review of Biofilm Formation of *Staphylococcus aureus* and Its Regulation Mechanism

by Qi Peng [1], Xiaohua Tang [1], Wanyang Dong [1], Ning Sun [2,*] and Wenchang Yuan [1,*]

[1] Guangzhou Key Laboratory for Clinical Rapid Diagnosis and Early Warning of Infectious Diseases, KingMed School of Laboratory Medicine, Guangzhou Medical University, Guangzhou 510180, China

[2] Guangzhou First People's Hospital, School of Medicine, South China University of Technology, Guangzhou 510180, China

[*] Authors to whom correspondence should be addressed.

Antibiotics **2023**, *12*(1), 12; **https://doi.org/10.3390/antibiotics12010012**

Submission received: 15 October 2022 / Revised: 23 November 2022 / Accepted: 25 November 2022 / Published: 22 December 2022

(This article belongs to the Collection **Antimicrobial Resistance and Anti-Biofilms**)

Editorial guidance

Proper citation

It is considered a good practice, both academically and editorially, to properly credit the source of any materials not authored by you. Subject to other terms described on this page, you may cite materials obtained from USPTO.gov websites using any or all of the following:

- The United States Patent and Trademark Office
- www.uspto.gov
- [system ID].uspto.gov/[specific web page address]; for example, patentcenter.uspto.gov/search or www.uspto.gov/about-us/events

Patent information

Patents are published as part of the terms of granting the patent to the inventor. Subject to limited exceptions reflected in 37 CFR 1.71(d) & (e) and 1.84(s), the text and drawings of a patent are typically not subject to copyright restrictions. The inventors' rights to exclude others from making, using, offering for sale, or selling the invention throughout the United States or importing the invention into the United States for a limited time is not compromised by the publication of the description of the invention. In other words, the fact that a patent's description may have been published without copyright restrictions does not give you permission to manufacture or use the invention without permission from the inventor during the active life of the patent. See MPEP § 600 - 608.01(v) regarding the right to include a copyright or mask work notice in patents.

Trademark information

Trademark images are published by the USPTO for public information dissemination purposes in accordance with the law. If you wish to use a trademark obtained from our records, you must do so in accordance with the individual licensing policies of the marks' owners. The USPTO will not assist in contacting trademark owners or arranging and managing licensing agreements.